SIMULATION OF STRUCTURAL AND SOLVENT EFFECTS ON ELECTRONIC AND NONLINEAR OPTICAL PROPERTIES OF PHENOTHIAZINE AND METHYLIDENE DERIVATIVES

BY

OLUWATOBA EMMANUEL OYENEYIN

B.Sc.(Ed.) Chemistry (Adeyemi), M.Sc. Physical Chemistry (Ibadan)

MATRIC. No.: 159867

A Thesis in the Department of Chemistry,
Submitted to the Faculty of Science
In Partial Fulfillment of the Requirement for the Degree of

DOCTOR OF PHILOSOPHY

of the

UNIVERSITY OF IBADAN

JUNE, 2019

ABSTRACT

Organic π-conjugated materials with Nonlinear Optical (NLO) properties have attracted interest because of their applications in optoelectronic devices. They are preferred to their inorganic/organometallic analogues owing to their lower cost of production. In previous works, the electronic and NLO properties of organic molecules based on phenothiazine and methylidene units have been reported. However, there is dearth of information on the structural and solvent effects on these properties. Therefore, this study was designed to investigate the structural and solvent effects on the electronic and NLO properties of literature experimental synthesised organic molecules and their modelled analogues.

Quantum mechanical calculations were employed to investigate the electronic band gap (E_g) and molecular first hyperpolarisability (β) of synthesised phenothiazine and methylidene derivatives and their modelled analogues using the density functional theory. Pure Becke Lee Yang Parr (BLYP) and hybrid Becke Three Lee Yang Parr (B3LYP) correlations were used for optimisation with 6-31G (d) basis set in vacuum and tetrahydrofuran. Both correlations were chosen in order to validate available literature experimental results. Time-dependent density functional theory was employed to calculate the maximum absorption wavelength (λ_{max}). Their values were compared with that of urea, a standard for organic NLO materials.

The calculated E_g of the synthesised phenothiazine, methylidene, modelled phenothiazine and methylidene analogues in vacuum were 3.90, 3.85, 2.57–3.84 and 3.30-3.58 eV, respectively with B3LYP while those for BLYP were 2.46, 2.47, 1.38-2.36 and 2.03-2.28 eV. The available literature experimental E_g for synthesised methylidene derivative was 2.27 eV. The BLYP ($\sigma = 0.20$ eV) correlation predicted E_g more accurately than B3LYP ($\sigma = 1.58$ eV). All values were lower than that of urea (literature experimental = 6.21 eV; calculated = 8.20 and 5.76 eV for B3LYP and BLYP, respectively) and decreased in tetrahydrofuran. The calculated β in vacuum were 1.49 $x10^{-30}$, 2.44 $x10^{-30}$, 1.71-5.13 $x10^{-30}$ and 3.84-9.67 $x10^{-30}$ esu, respectively with B3LYP while they were 1.51 $x10^{-30}$, 2.61 $x10^{-30}$, 1.74-5.76 $x10^{-30}$ and 4.03-10.09 $x10^{-30}$ esu with BLYP. The SHG efficiency of synthesised

methylidene derivative was 4.13 times that of urea. All modelled analogues had higher β than urea's (0.65 x 10^{-30} esu). The BLYP (4.02 times urea's, 97.3 %) correlation predicted SHG efficiency more accurately than B3LYP (3.75 times urea's, 90.8 %) and increased in tetrahydrofuran. The calculated λ_{max} in vacuum were 293, 344, 276-378 and 369-399 nm, respectively with B3LYP while those for BLYP were 362, 412, 346-470 and 496-517 nm. Literature synthesised phenothiazine derivative absorbed at 294 nm while the modelled phenothiazine absorbed at 294 nm and 362 nm for B3LYP and BLYP, respectively. The B3LYP predicted the λ_{max} accurately. All λ_{max} values were higher than urea's (< 200 nm) and increased in tetrahydrofuran.

The electronic and nonlinear optical properties of modelled phenothiazine as well as methylidene analogues were sterically enhanced by substituents groups and were altered by the inclusion of tetrahydrofuran solvent.

Keywords: π-conjugated materials, Organic nonlinear optical materials, nonlinear optical properties, Optoelectronic properties, Second harmonic generation

Word count: 470

DEDICATION

I dedicate this work to the glory of God Almighty, the giver of life and strength, the lover of my soul, my refuge and rock, who has been my source of power from birth till now. I successfully carried out this project by His grace.

ACKNOWLEDGEMENTS

I acknowledge the Almighty God, the Alpha and the Omega for providing me with a sound health and sustaining my life till now.

I appreciate my supervisor, Dr. I. A. Adejoro, for guidance, unlimited support, motivation, advice, encouragement, prayers and his keen interest in me and in the research I undertook under him. I also thank Professor B.B. Adeleke for his support and suggestions. I am grateful to the Head of Chemistry Department; Prof. T. I. Odiaka and all the staff of the Department for creating an enabling atmosphere for this research work. Special appreciation goes to Prof. G. O. Adewuyi, Prof. O. Olu-Olowolabi, Dr. B. O. Ogunsile and Dr. A. R. Ipeaiyeda who all took time to engage me in some intellectual discourse in this project.

Sincere gratitude goes to my parents Late S. O. Oyeneyin and my mum Mrs. F. A. Oyeneyin. I also show appreciation to my brother, Mr. Bamidele Oyeneyin and my sister, Miss Kemisola Oyeneyin. You are greatly appreciated. I also thank the following people who contributed to this work in a way or the other. Prof. N. O. Mimiko, Prof. C. O. Aboluwoye, Prof. N. A. Oladoja, HRH (Prof.) S. A. Amuseghan, Dr. T. A. Akinnifesi, Dr. O. Olonisakin Dr. B. T. Ogunyemi, Mr. and Mrs Emah, Mr. Eric Babatunde, Mr. Eric Akintemi, Mr. Taiwo Omomule, Mr. Segun Orimoloye, Mr. Akinlolu Akinkoye, Mr. Timothy Esan, Mr. Francis Ojo, Dr. Kayode Sanusi, Dr. Mutolib Bankole, Mr. Damilohun Metibemu, Mrs. Abosede Kolawole, Dr. A. G. Olaremu, Dr. (Mrs) A. N. Laleye, Dr. Segun Olaseni, Revd. Michael O. Otun, Pastor Yinka Adesoji and Prophet S. A. Aluko.

Special thanks to Dr. Jubril Oyeneyin, Mr. Habeeb Oyeneyin, Mr. Kamar Niyi Oyeneyin, Mr. Tajudeen Oyeneyin and Alh. Raufu Oyeneyin for the fatherly roles they played so far in my academic pursuits. God bless you all.

To my wife, Mrs Damilola Oyeneyin, and daughter, Miss. Treasure Oyeneyin, I say a big thank you for your patience, support and prayers.

Finally, I appreciate Tertiary Education Trust Fund (TETFund) and Adekunle Ajasin University, especially the staff in the Departments of Science Education and Chemical Sciences for the opportunity granted me to embark on this research work.

CERTIFICATION

I certify that this work was carried out by Oluwatoba Emmanuel **OYENEYIN**, in the Department of Chemistry, University of Ibadan, Nigeria.

.....

Supervisor
I. A. Adejoro
B.Sc, M.Sc. Ph.D. (Ibadan)
Reader, Department of Chemistry
University of Ibadan, Nigeria

TABLE OF CONTENTS

CHAPTER TWO

CHAPTER THREE

CHAPTER FOUR

LIST OF TABLES

LIST OF FIGURES

LIST OF ABBREVIATIONS

10-MTBP	10-Methyl thiophene based phenothiazine
10-OTBP	10-Octyl thiophene based phenothiazine
10-MP*m*SB	10-MethylPhenothiazine *mono* Schiff base
AQT	Aromatic Quinonoid Transition
AM1	Austin Model 1
B3LYP	Becke Three Lee Yang Parr
BLA	Bond Length Alternation
CB	Conduction Band CB
CI	Configuration Interaction CI
DFT	Density Functional Theory
D-A	Donor-Acceptor
ECL	Effective Conjugation Length
EDF	Empirical Density Functional
E_{ex}	Excitation Energy
GTO	Guassian Type Orbital
HF	Hartree-Fock
HOMO	Highest Occupied Molecular Orbital
HOM-LUM	HOMO-LUMO transition
ICT	Intramolecular Charge Transfer
LEDs	Light Emitting Devices
LCAO	Linear Combination of Atomic Orbitals
LR-DFT	Linear-Response Density Functional Theory
LDA	Local Density Approximation
LUMO	Lowest Unoccupied Molecular Orbital

MMP	1-[4-({(E)-[4(methylsulfanyl)phenyl]methylidene}amino)phenyl] ethanone
MP	Moller Plesset
NLO	Nonlinear Optics
OS	Oscillator Strength
PM3	Parameterization Method 3
PM6	Parameterization Method 6
PA	Polyacetylene
QR-DFT	Quadratic Response Density Functional Theory
QSPR	Quatitative Structure Property Relationship
SHG	Second Harmonic Generation
SCF	Self Consistent Field
SE	Semi Empirical
STO	Slater Type Orbital
TD-DFT	Time Dependent Density Functional Theory
2PA	Two-Photon Absorption
VB	Valence Band

CHAPTER ONE
INTRODUCTION

1.1 π-conjugated organic molecules

Different classes of organic π-conjugated materials possess large nonlinear optical (NLO) activities according to past investigations and reports (Tuutila *et al.,* 2009). Examples of such responses are the two-photon absorption, 2PA (Drobizhev *et al.,* 2006), second harmonic generation (SHG), sum frequency generation (SFG) etc. π-conjugated organic D-π-A type molecules (one part a donor and the other part an acceptor) have become a focus because of their applications in optoelectronic and optical limiting technologies (Sanusi *et al.,* 2014; Bankole and Nkoyong, 2015). They protect the human eyes and other sensors like the skin, body cell etc from intense laser light owing to their optical limiting potentials (Sanusi *et al.,* 2014). A lot of organic, inorganic and/or organometallic molecules have been investigated for their NLO activities (Adhikari and Kar, 2012; Sanusi *et al.,* 2014; Bankole and Nkoyong, 2015). Organic molecular materials are preferred to their inorganic and organometallic analogues in that apart from the extended π-conjugation they exhibit, they possess faster optical responses (Adhikari and Kar, 2012), excellent chemical and thermal stabilities (Ravindra *et al.,* 2009), high resistance to optical/laser damage i.e. high damage threshold (Adhikari and Kar, 2012; Ravindra *et al.,* 2009), easier to fabricate and integrated into devices (Jordon *et al.,* 2003), high hyperpolarizability (β), (Sanusi *et al.,* 2014; Bankole and Nkoyong, 2015), possess faster polarization because their π-electrons spread over a large distance and their crystals are more responsive to an external electric field as they are relatively weakly bonded to the nucleus, with entire molecule possessing delocalized orbitals all through it (Prasad and Williams, 1991), high electro-optic coefficients (Adhikari and Kar, 2012). They can also be tuned by varying either the ratio of various constituents or the manner by which these are chemically attached, for the purpose of altering their properties- the basis for this study.

Material scientists design materials that can be used for a number applications. The design of materials that are better than existing ones is important, for advancement and improvement. Hence, the need to search for molecules with better NLO activities. The properties of existing systems can be tuned by introducing electron donating (push) and electron withdrawing (pull) groups around them (Wade *et al.,* 2012). Polarizability, α, (a measure of how the electron cloud of a molecule is distorted by an electric field), asymmetric charge distribution (introduction of donor and acceptor groups leading to a charge transfer), non-centrosymmetry, energies of the highest occupied molecular orbital and lowest unoccupied molecular orbital gap, (HOMO-LUMO gap), ground state dipole moment, μ_{gs}, excited state dipole moment, μ_{ex}, bond length alternation (BLA), UV/Vis absorption, λ_{max} and the first hyperpolarizability (β), a measure of SHG efficiency, are just the basic properties to consider for an NLO molecule (D'Silva *et al.*, 2012; Sanusi *et al.*, 2014). These NLO molecules can be incorporated into devices useful in lasers, optical switches, electronics, and photonics especially in the field of high speed data transmission, processing and storage (Prasad and Williams, 1991).

A key phenomenon in studying nonlinear optical molecules is the concept of the donor-acceptor (D-A). D-A systems are investigated to establish the relationship between the molecular structure and nonlinear responses. Asymmetry polarization is the basis for designing organic materials for NLO applications (Cui *et al.,* 2005). This is to say that if the D-A capability of the substituents attached to the π-conjugated systems is increased, nonlinearity can be improved upon. Electron donor and acceptor groups on the π-conjugated systems leads to the movement of electron cloud, which is caused by intramolecular charge transfer (ICT) and therefore, a large value of β (Hadji and Rahmouni, 2015).

A lot of reports have been given on the NLO activity of π-conjugated organic molecular systems (Cui *et al.,* 2005; Sunitha *et al.,* 2012; Adhikari and Kar, 2012). However, with the advent of quantum mechanics theories, it has been proven that they are successful and efficient in studying, investigating and finding suiTable NLO materials (Adhikari and Kar, 2012; Hadji and Rahmouni, 2015).

This work seeks to extend the study on some D-A molecules based on phenothiazine units and 1-[4-({(E)-[4-(methylsulfanyl)phenyl]methylidene}amino)phenyl]ethanone, MMP

which have been synthesized and characterized by previous workers (Zebiao, 2015; D'Silva, 2012). The approach is to predict theoretically, the NLO activity of already synthesized molecules and design new derivatives by introducing some donor and acceptor groups into the molecular backbone and predict if they have better NLO responses than the already synthesized ones- the aim of computational chemistry (Young, 2001). The theoretical methods used in replicating experimental findings could be used as predictive tools to study the properties of new, hypothetical molecules. Such hypothetical molecules can be recommended for synthesis and further analysis if their properties were enhanced.

1.2 Statement of the Problem

Many of the optical equipment used for observation and navigation e. g. compact disk players (CD), super-market barcode readers etc contain lasers, which are dangerous to the human eyes, skin and other sensors under exposure. The military use these lasers on battlefield for range finding, detection and guidance. Blocking, scattering, diffracting, or absorbing the incoming laser light could be used to protect optical systems as well but these do not come without degrading the mission effectiveness to some level. In order to protect sensors and the human eyes from the damaging laser radiation without reducing or degrading mission effectiveness, NLO materials that limit the energy output of an incident light are used (Bankole and Nkoyong, 2015; Sanusi *et al.*, 2014), this is why they are sometimes referred to as optical limiters. They are also used to monitor the output of lasers in the laboratory for specific experiments.

1.3 Justification and Purpose of the Study

The structure of molecules can provide the necessary information that determines their chemical and physical properties. Therefore, the structure-property relationship can be established from molecular structures. The quantitative structure-property relationship (QSPR) can help to predict the behaviour of materials from which scientists can select and subject them to further experimental investigations.

The goal of researchers is to create or discover materials with optimal properties to meet certain applications. In some cases, scientists get disappointing results at the late-stage of

organic synthesis, therefore, the original physical properties of pi-conjugated organic materials at molecular level need to be critically investigated and understood, prior synthesis. Apart from cost and time consumption, the synthesis and test of these new materials for certain applications including NLO processes involves a large degree of trial-and-error. To overcome this bottleneck, a prior and fundamental understanding of the properties of existing materials or well-known systems is first established. This is best done by the state-of-the-art computational methods because researchers discovered that they are less costly and faster (Adhikari and Kar, 2012; Hadji and Rahmouni, 2015). Theoretical method(s) that can replicate experimental findings is first determined, and then the same method(s) could serve as predictive tools for properties of yet to be synthesized molecules. These modelled molecules could be synthesized for further studies. For example, drug design is a difficult area in science because of the cost and risks involved, therefore computer-aided drug design has been employed to determine if a molecule will bind to a target and if possible, how strongly. Findings from this will determine if the drugs should be synthesized and subjected to further studies like *in vitro* assay, animal testing and clinical trials.

1.4 Aim of the Study

Some phenothiazine *mono*-Schiff bases have been synthesized, characterized (Emese, 2010), some D-A type molecules based on phenothiazine units were also synthesized, characterized and reported as light-emitting materials (Zebiao *et al.,* 2015) and MMP (D'Silva *et al.,* 2012) have been synthesized, characterized and reported as a NLO crystal. However, it is necessary to theoretically investigate the NLO properties of the synthesized molecules and find a means of designing their derivatives that could possess better NLO properties than the already synthesized ones. It is necessary to look into the structures of the molecules in relation to reactivity and make recommendations as to whether the modeled, hypothetical molecules are going to be better NLO candidates. It is also necessary to look at the way the molecules will behave in a solvent environment and determine if solvent alters NLO processes.

This study sought to tune the properties of some π-conjugated organic molecules by introducing some substituents into their backbones. Therefore this research will focus on

studying the molecular and electronic properties of organic molecules, introduce electron donor and/or acceptor groups and critically investigate how these groups affect their reactivities, electronic and NLO properties in gas phase and in solution.

1.5 General Objectives

The target here is to determine the molecular structures, electronic and optical properties of the molecules under investigation and design a range of molecular systems similar to the synthesized ones by introducing substituents and study their NLO activities. This is based on the concept of ICT between the donor and acceptor groups on the molecular backbone. Properties calculated include the HOMO and LUMO energies (**E_{HOMO}** and **E_{LUMO}**), energy gap (E_g), polarizability (**α**), dipole moment (**μ**), first hyperpolarizabilty (**β**), Bond lengths with BLA**s** in vacuum and in Tetrahydrofuran, THF (ε = 7.58). The results obtained provide a giant step towards understanding the structure-property-relationship, solvent effects on the NLO properties of these materials.

1.5.1 Specific Objectives

The study will specifically be focused on:

i. Studying the various properties of π-conjugated organic molecules,
ii. Introducing substituents that will alter the properties of the systems,
iii. Investigating the effects of these substituents on other properties of the systems
iv. establishing the relationships between **μ, α, θ, BLA, energy gap** and **β**
v. investigating the effect of solvent on the properties above, especially the properties involving tensor components like **μ** and **β**,
vi. from the results obtained, the best material(s) with the best NLO activity will be identified, and
vii. recommending such material(s) for synthesis

CHAPTER TWO

LITERATURE REVIEW

2.1 Chemistry of Phenothiazines

Phenothiazine is an organic compound that is related to the thiazine class of heterocyclic compounds. It was used as insecticides before being waned out by better insecticides (Metcalf, 1948). Some of its derivatives like methyl blue were used as an antimalarial drug, others were used as anthelminthic drugs, and some have been studied for their potential use in advanced batteries and fuel cells (Ohlow and Moosmann, 2011). Some other of its derivatives like thionine and methyl green can be electro-polymerized into conductive polymers (Sokic-Lazic and Minteer, 2008). Owing to the donor nature of phenothiazine, it can be used in forming donor acceptor systems (D-π-A), which can be useful for light emitting applications.

2.2 Chemistry of Schiff bases

Schiff bases play significant roles in chemical sciences. They are widely applicable in many areas. Their structures can be modified easily to meet desired demands. Structural modification can be achieved through the reaction with aldehydes, ketones etc (Fig. 2.1) (Suresh and Prakash, 2010). Furthermore, their biological activities have been reported, among these are their antibacterial, antifungal, anticancer and herbicidal activities (Jarrahpour and Rezaei, 2006; 2009). On the other hand, they are used as precursors in the synthesis of Schiff base ligands. Metal complex Schiff bases have also been used in oxidation reactions (Jarrahpour *et al.,* 2004), owing to their ability to coordinate (as ligands), with various metals and make them stable in different oxidation states (Raman *et al.,* 2009).

Other π-conjugated organic systems having a D-π-A conFiguration have also been studied and reported for their NLO behaviours. MMP and its substituted derivatives are examples of such systems.

2.3 Linear and Nonlinear Optical Phenomena

Optics studies the interaction of light with molecular materials (McGraw-Hill, 1993). Nonlinear optics (NLO) describes the behavior of light when in contact with nonlinear media. That is, the relationship between P and E is nonlinear. The polarization density, is a product of the individual dipole moment, Ƥ induced by the applied electric field E and the number density of dipole moments *N*, eq. 2.1 (Parker, 1994);

$$\text{Ƥ} = N\text{E} \qquad 2.1$$

Before lasers were invented, the optical phenomena that were experienced are linear (reflection, refraction, absorption, scattering etc), these phenomena never depended on the intensity of light. The field of NLO began in 1875 by Kerr, who discovered how refractive index of CS_2 changed when exposed to an external field- a process called the Kerr-effect. When a material is subjected to light of a given frequency, it will respond by oscillating its electrons. In a linear absorption (Figs. 2.2a and 2.3a), the oscillation of the electron will be in harmony with the incident light, the energy absorbed is emitted as a secondary light of similar frequency. However, in a nonlinear process (Figs. 2.2b and 2.3b), the electrons will become anharmonic and the re-emitted light may differ in frequency from the incident light. The response of a medium to an external field (light) is described in terms of polarization (Kennedy and Lytle, 1986).

$$P_i = \mu_i^0 + \alpha_{ij}E_j + \beta_{iik}E_jE_k + \gamma_{iikl}E_jE_kE_l + \ldots \qquad 2.2$$

where P_i is the molecular polarization, μ_i^0 is the permanent dipole moment of the molecule in the i-th direction, α_{ij} is the linear polarizability responsible for refraction or reflection, β_{ijk} is the second order hyperpolarizability while E_j, E_k, and E_l are the external electric field in the j, k and l directions in the coordinates respectively.

Polarization is caused in materials resulting from the presence of the field applied on them. The polarization can be linear polarization, P^L (Fig. 2.3a) or nonlinear polarization, P^{NL} (Fig. 2.3b).

Polarization then can be expressed as (in equations 2.3-2.5);

$$P = P^L + P^{NL} \quad 2.3$$

$$P^L = \chi^1.E \quad 2.4$$

$$P^{NL} = \chi^2.EE + \chi^3.EEE \quad 2.5$$

Eq. 2.4 is at low field, in which the emitted light is the same in energy as the input light (Fig. 2.2a) while 2.5 is at high field, in which the photons are excited to a higher energy level and emitted higher energy than the input energy (Fig. 2.2b). χ^n is the susceptibility tensor. Where χ^1 is the linear Polarizability while χ^2 is the second-order nonlinear Polarizability and χ^3 is the third-order nonlinear polarizability. β and γ are sometimes also referred to as the first and second hyperpolarizability respectively. χ^n are the weighted averages of the molecular values with χ^1 a combines α values linearly, χ^2 a linear combination of β values and χ^3 a linear combination of γ values. α is the tendency for charge distribution to occur, like the electron cloud. It is related to the dipole moment by the relation in equation 2.6 (Targema *et al.,* 2013).

$$\mu^* = \alpha\xi \quad 2.6$$

With μ* being the induced dipole moment and ξ, the strength of the external field. α is usually expressed as a volume amount, the polarizability volume, α^{vol} (Targema *et al.,* 2013):

$$\alpha^{vol} = \frac{\alpha}{4\pi\varepsilon_0} \quad 2.7$$

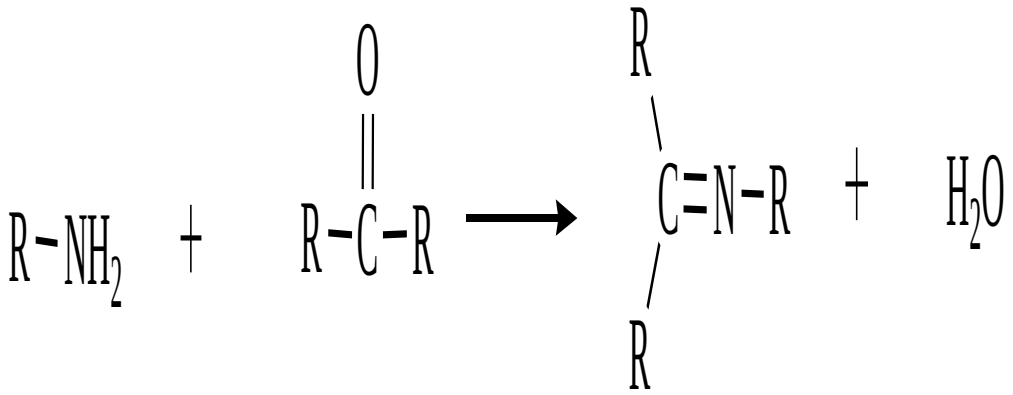

Where -R may be an alkyl or an aryl group.

Figure 2.1: Formation of Schiff base

If however, the applied electric field varies in molecules, the second-order perturbation theory is employed in getting their resultant polarizabilities (Targema *et al.*, 2013);

$$\alpha^{vol} = 2\sum_{n} \frac{\left|\mu_{0n}{}^{2}\right|}{E_{n}^{(0)}-E_{0}^{(0)}} \qquad 2.8$$

μ is also the product of the charge on a molecular system and R, the distance separating the charger on the system (molecular radius),

$$\mu = qR \qquad 2.9$$

$E_{n}^{(0)}-E_{0}^{(0)}$ can be approximated as the frontier energy gap ($E_{LUMO} - E_{HOMO}$), denoted by E_g, then eq. 2.8 becomes (Targema *et al.*, 2013);

$$\alpha = \frac{2(qR)^2}{E_g} \qquad 2.10$$

The polarizability increases as the size of the molecules increase and vice versa according to eq. 2.10. It also increases as E_g decreases. If a molecule has a low E_g value, the molecule has a high ICT, it is also termed a soft molecule as softness (S) of a molecule is inversely proportional to the chemical hardness (η), a property obtained directly by dividing the energy gap by 2, eq. 2.11. Such molecules could have high electro-optic responses if other pro

$$\eta = \frac{\Delta E}{2} \qquad 2.11$$

$$S = \frac{1}{\eta} \qquad 2.12$$

Inorganic and organometallic materials (Selah and Teich, 1991) like GaSe, SiO_2, lithium niobate crystal (LNB), potassium dihydrogen phosphate (KH_2PO_4) etc have been studied for their NLO applications but it is the organic counterparts that are preferred owing to some advantages earlier mentioned. NLO materials have been discovered to possess large NLO responses such as the two-photon absorption (2PA), second harmonic and third harmonic generation (SHG and THG) , high harmonic generation (HHG), reverse saturable absorption (RSA), nonlinear refraction (NLR) excited state absorption (ESA), nonlinear scattering

(NLS) etc. The materials may exhibit more than one of these responses (Bankole and Nkoyong, 2015). They have applications in photonics (Boyd, 2003), telecommunication and optical information processing.

Lasers are present in optical equipment like CD players, scanners, sensors, microscope, laser weapons, medical equipment etc (Fig. 2.4). They are used in the industry for cutting and welding, in the military for missile defense, range finding and targeting, in medicine for bloodless surgery, eyes surgery and dentistry, in research in areas like metrology, laser ablation, laser scattering etc and in cosmetic skin treatment like tattoo removing, and hair removal. They are also used by law enforcement agencies for fingerprint detection for forensics (Tripathi 2010). The essence of NLO materials is to protect optical elements, sensors, human eyes and skin from laser radiation. These optical limiting devices will allow the passage of or transmit light while they attenuate the output of high intense laser light to a constant in order to serve as protective shields (Fig. 2.5) to sensors and eyes (Sanusi *et al.*, 2014). That is, they exhibit decreased transmission of light as incident light intensity is increased.

2.4 Nonlinear Optical Phenomena

2.4.1 One- and Two- Photon Absorption

One photon absorption otherwise known as the single photon absorption (1PA) is a linear absorption process where one photon excites an atom or a molecule from a lower to a higher energy level, say, from the ground state (GS) to the first excited state (ES). Its rate is derived by the time-dependent perturbation theory (Boyd, 2003). The oscillator strength is used to determine the strength of the transition (Boyd, 2003). The ground state oscillator strength to the excited state, $g \rightarrow e$ (f_{eg}) transition is defined as (eq. 2.13);

$$f_{eg} = \frac{2m\omega_{eg} \sum_{\alpha}^{x,y,z} |\langle e|\mu_{\alpha}|g\rangle|^2}{3\hbar^2} \qquad 2.13$$

where μ_{α} is the dipole moment operator, $\hbar$ is the reduced Planck constant, m and ω are the mass and frequency of photon respectively. A typical nonlinear absorption process however, is a two-photon absorption process which simultaneously absorbs two photons of identical

or different frequencies under the interaction of light field resulting to the excitation of a molecule from a lower to a higher energy electronic state. The probability of a molecule to absorb two identical photons simultaneously is a function of the square of the light intensity. The relationship between the molecular structure and two-photon absorption (2PA) cross-section can also, like the 1PA be derived from time-dependent perturbation theory (Boyd, 2003). The 2PA cross-sections of systems (σ), according to are related to imaginary part of the second hyperpolarizability [Im(γ)].

$$\sigma = \frac{8\pi^2\hbar\omega^2}{n^2c^2} L^4 \mathrm{Im}(\gamma) \qquad 2.14$$

n, being the refractive index, ħ is the reduced Planck constant, ω is the frequency of photon, c is the speed of light and *L* is the local field factor.

The 2PA is an instantaneous nonlinearity which involves two photons causing a transition from the GS of the molecule to an ES through an intermediate (a virtual state) (Kershaw, 1998) in Fig. 2.6. The structure-property relationships of NLO materials can be fully explained by quantum mechanics and can provide adequate suggestions on molecular design and synthesis (Wang *et al*., 2003). Okuno and co-workers calculated the β values of three dimers in azobenzene dentrimers to ascertain why they have large β values using the *ab initio* calculations. It was observed that the large β values were smaller than those in solutions because of staggered conformations (Okuno *et al.,* 2001). Day and coworkers performed TD-DFT study of one and TPA properties for some non-centrosymmetric chromophores using the linear response DFT (LR-DFT) and they correlated well with the experimental results (Day *et al*., 2005). They also used the quadratic response DFT (QR-DFT) to predict the 2PA properties of other molecules Day *et al*., 2006, 2008). The 2PA spectra of some symmetrically substituted phtalocyanines in the excitation wavelength region from λ_{ex} = 800 – 1600 nm and observed that all molecules displayed strong but moderate 2PA band peaking between λ_{ex} = 870 – 1100 nm (Drobizhev *et al*., 2006). The 2PA spectra of metal-free tribenzo-tetraazachlorin (H_2TBTAC) and tetra-*tert*-butyl-phtalocyanine (H_2TtBuPc) were studied by Makarov and co-workers (Makarov *et al*., 2013).

An ideal optical limiting device exhibits a linear transmittance at low intensities and clamps or attenuates the output to a constant at high intensities (below and above a threshold). In

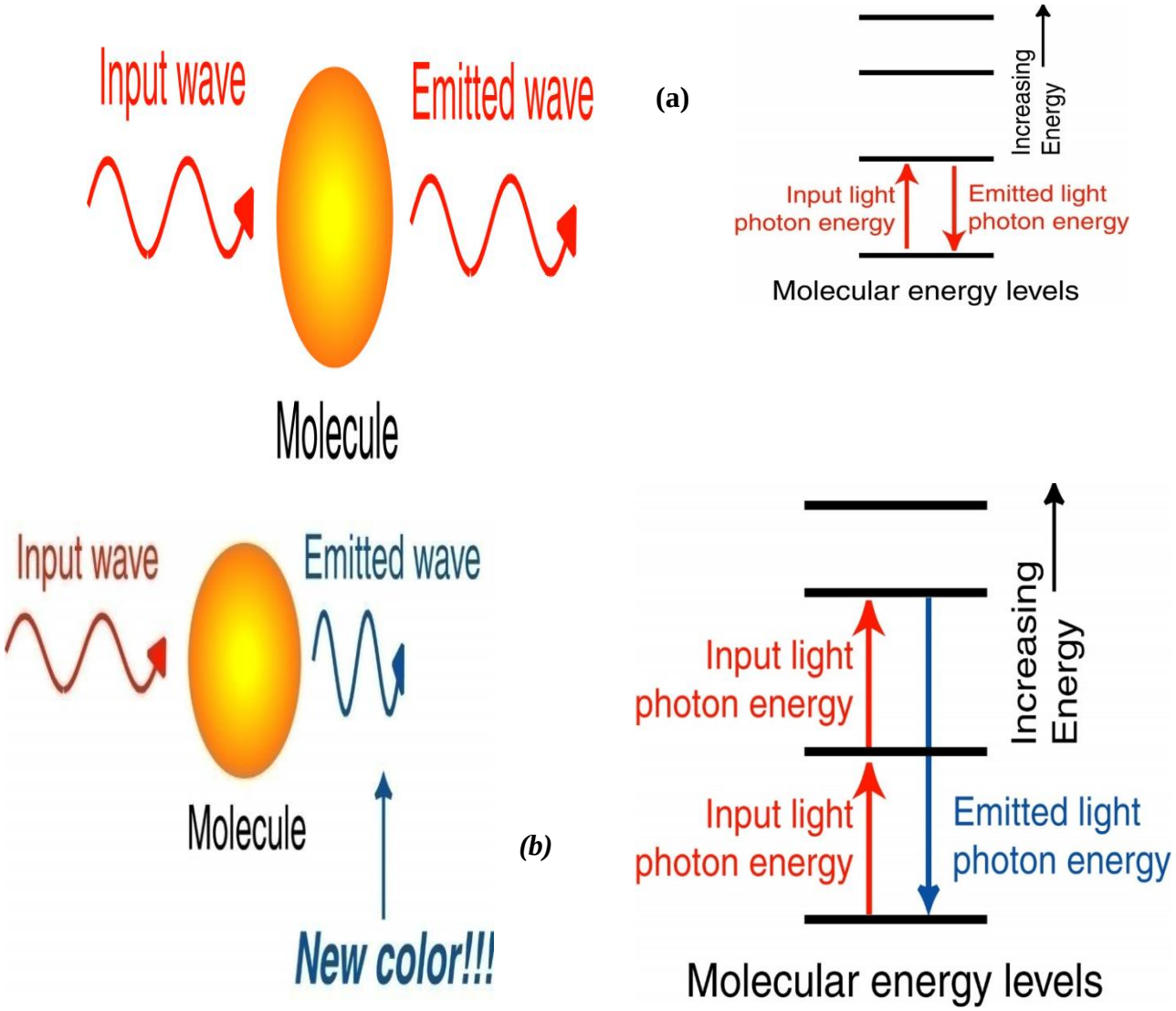

Figure 2.2 (a) The input wave is the same as the emitted wave in linear absorption (b) The input wave is different from the emitted wave in nonlinear absorption.

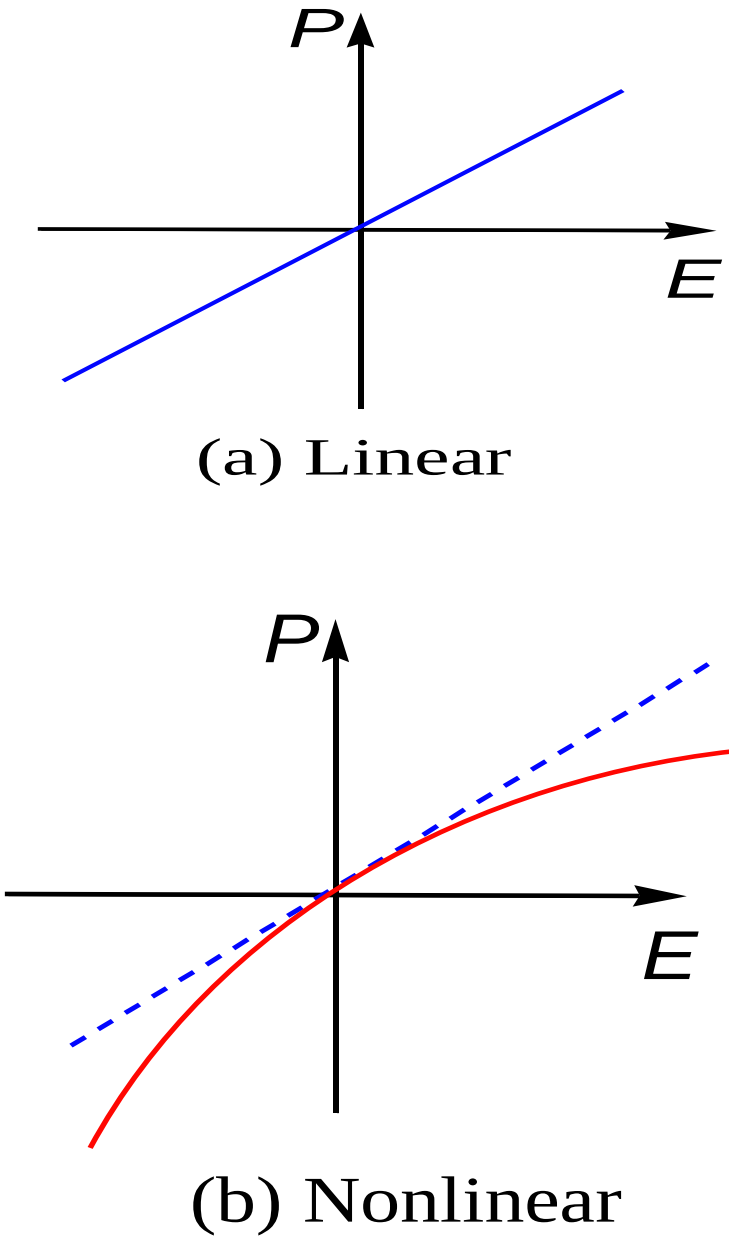

Figure 2.3: the P-E relation for (a) a linear dielectric medium and (b) a nonlinear medium

linear transition there is little or no ground state absorption at low intensities like in high intensities where two photons promote the molecule to an excited state. The beam intensity that passes through a material is (Bass, 1994) in eq. 2.15.

$$\frac{\partial I}{\partial z} = -[A + BI]I \qquad 2.15$$

Where A is the linear absorption coefficient and B is the 2PA coefficient, B was used in place of β so as not to confuse it with the second order hyperpolarizability tensor on the molecular level. Some materials have A values as zero, the change in intensity of the light propagating through them is therefore, given by eq. 2.16 (Bass, 1994).

$$I(L) = \frac{I_0}{1 + I_0 BL} \qquad 2.16$$

Where L is the length of the sample and I_0 is the incoming intensity. It can be seen from eq. 2.16, that the transmission decreases as the intensity, I_0 increases. Energy gap, E_g is a factor that influences the 2PA coefficient. According to eq. 2.17, E_g has a negative influence on B (Wherret, 1984).

$$B(\omega) = K\left(\frac{E_p^{\frac{1}{2}}}{n_0^2 E_g^{\ 3}}\right) F\left(\frac{2\hbar\omega}{E_g}\right) \qquad 2.17$$

Where K is the material independent constant, E_p is the Kane energy parameter of approximately 21 eV and E_g is the energy gap. However, only the 2PA is not enough to consider for a material investigated for NLO activities, other properties should be studied for confirmation of any observation. The 2PA properties have been studied theoretically by different authors with different models. The DFT methods have been employed in studying the 2PA cross-sections of molecules because it takes into account electron correlation. TD-DFT method was employed to study 1PA and 2PA properties of some Donor-π-acceptor non-centrosymmetric chromophores (Day *et al.,* 2005). They found out that the linear response DFT (LR-DFT) replicated the experimental findings closely. Zein and co-workers used the TD-DFT to predict the 2PA properties of fluorine and its derivatives (Zein *et al.,* 2009). They discovered that the 2PA cross-section increased in chloroform. 2PA studies

were done on phosphorus-based *tris*-hydrazone ligand and its metal complexes, some of which were found to possess large 2PA cross-sections at 770 nm (Chandrasekhar *et al.*, 2010).

2.4.2 Reverse Saturable Absorption (RSA)

Reverse saturable absorption (RSA) is a property of a material whose excited state absorption cross section at wavelength λ, σ_{ex} (λ), is more than that of the ground state, σ_{gs} (λ). This process occurs mainly in materials that absorb more in the ES than in the GS like dyes. It is a property of materials where the absorption and transmission of light decreases with increasing light intensity. Here, a material gets excited into a higher energy state as quickly as possible that there is no time for it to decay back into its ground state before the ground state becomes empty, leading to the saturation of the absorption (Band, 1986). A material exhibiting RSA properties should possess an efficient intersystem crossing (S_1-T_1), T_1 should be long lived and large absorption T_1-T_2 transition. In Fig. 2.7a, the ground state cross-section is σ_1, while the excited state cross-section is σ_2. The first excited state, S_1 is populated as the material absorbs light. If σ_2 is smaller than σ_1, the material is transparent owing to the depletion of electrons, a process called bleaching. If the reverse case occurs, absorption increases as S_1 is populated and reversed bleaching occurs. However, the one of interest in the two mentioned cases is the latter, where the ratio of σ_2 to σ_1 is >> 1.

The nonlinear absorption of rhodamine B dye was investigated in methanol and water using z-scan technique with nanosecond pulse (Srinivas *et al.,* 2003). An RSA at 435 nm was observed in both solvents and there is a transition from reverse saturation to RSA with an increase in intensity. Also, RSA studies were carried out on some platinum ter/bipyridyl polyphenylacetylide complexes at 532 nm with nanopulses, it was observed that the RSA can be improved upon by structural modifications (Deng *et al.,* 1999).

2.4.3 Second Harmonic Generation (SHG)

This is also called frequency doubling; it is a NLO process that adds two identical photons, each with a frequency, ω interacting with a nonlinear material to generate new photons of double energy and frequency, 2ω or half the wavelength of the initial photons (Figs. 2.8). Materials without centre of inversion (non-centrosymmetric) exhibit this phenomenon.

(a)

(b)

(c)

(d)

(e)

Figure 2.4: (a) a CD player (b) a microscope (c) in medicine (d) military personnel with laser weapons (e) a DVD player; all are optical devices

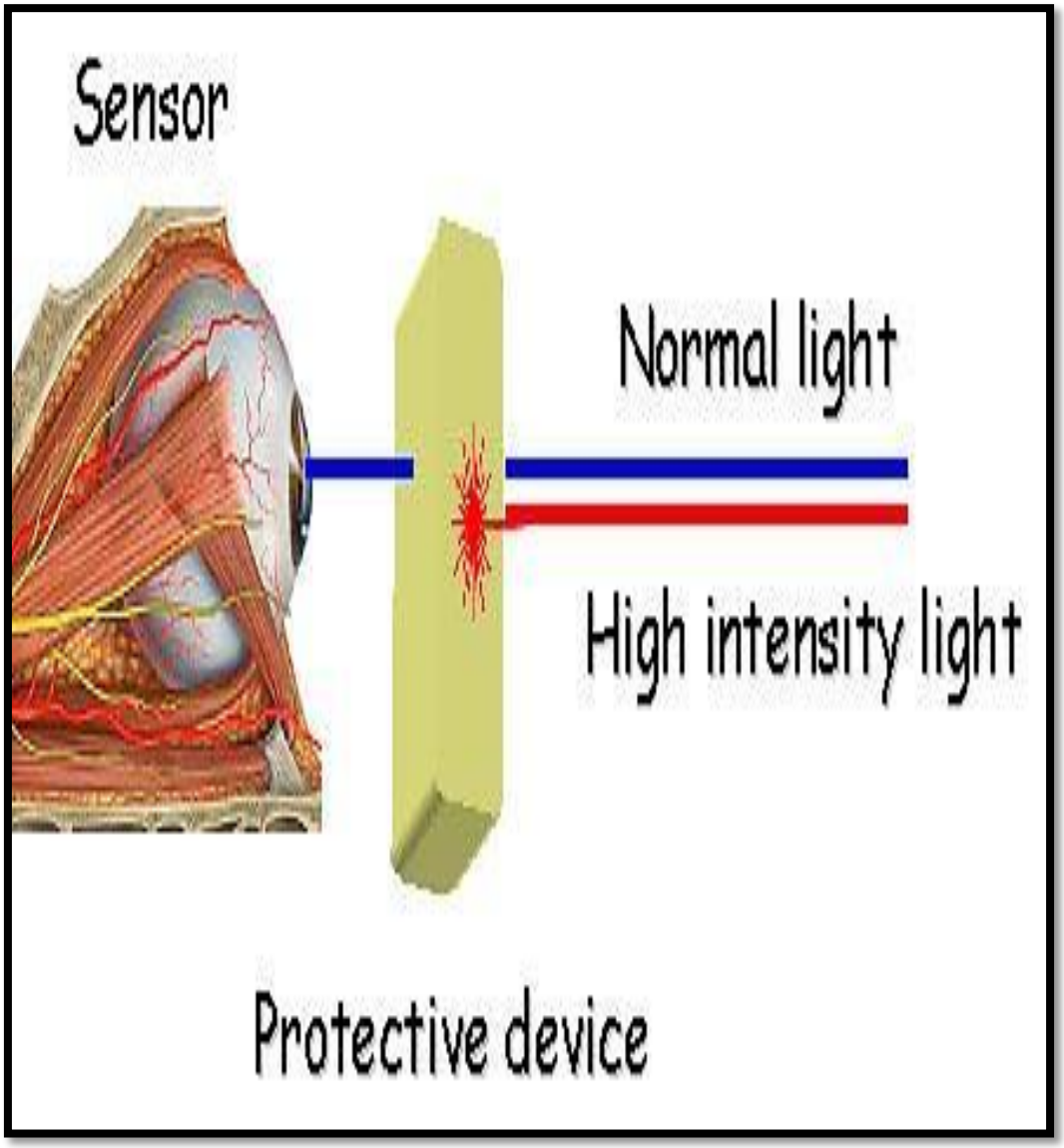

Figure 2.5: NLO materials shielding the human eyes **(**Sanusi et al., 2014**)**

Example of this is the sum-frequency generation. The magnitude of β and the molecule's orientation in a crystal lattice determine its SHG efficiency (Ravindra, 2009).If a molecule possesses a π-conjugation pathway, exhibits strong ICT and non-centrosymmetric, it is favoured to exhibit strong NLO activity (Targema *et al*., 2013). (Zhang and Cui, 2011) used a femtosecond high repetition rate laser system for measuring the SHG in some second-order NLO materials. The NLO susceptibilities of the thin films were also reported as promising NLO materials. An organic molecular crystal 3-methoxy-4-hydroxy-benzaldehyde (MHBA) was grown, its SHG is 30 times higher than that of urea and the cutoff wavelength was reported as 370 nm (Zhang *et al.,* 1992). Optical SHG coefficients have been measured for several organic molecular crystals. It has been established by different authors that SHG coefficients vary with differences in molecular structure. As_2S_3 and CdS nanoparticle aqueous solutions were investigated for their SHG efficiencies using the Z-scan technique and compared with each other (Ganeev *et al.,* 2003). They reported that the nonlinear refractive indices of As_2S_3 and CdS nanoparticles decreased with a growth in laser intensity and that high nonlinear optical susceptibility of such structures were attributed to size-related effects. Non-centrosymmetric N-(3,5-Ditert-butylsalicylidene)-2-aminopyridine was reported by (Sliwa *et al.,* 2008) to exhibit bulk second harmonic generation (SHG) activity. Experimental data were compared with theoretical calculations on the basis of the crystallographic data and were in good agreement. L-histidinium-2-nitrobenzoate (abbreviated as LH_2NB ($[C_6H_{10}N_3O_2]^+$ $[C_7H_4NO_4]^-$)), was synthesized and characterised via the X-ray diffraction method (Natarajan *et al.,* 2012). Its SHG efficiency is as twice as that of the standard potassium dihydrogen phosphate (KDB) crystals, a reference NLO material like urea.

2.5 Molecular Nonlinear Properties

2.5.1 Bond Length Alternation (BLA)

It is important for synthetic and material scientists to control the energy gap of molecular systems in order to get materials with enhanced properties. The BLA is used to decsribe the alternating single or double carbon-carbon bonds within a molecules architecture (Jacquemin and Adamo, 2013). Its reduction is achieved by reducing the energy gap of

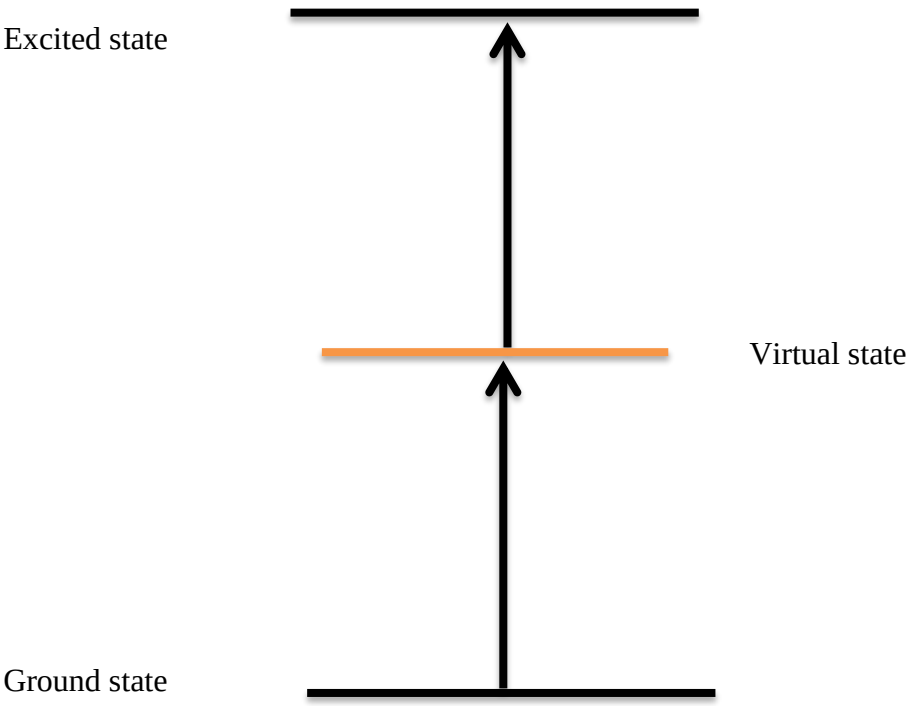

Figure 2.6: The molecule absorbs one photon to move an electron from its ground state to a virtual state before absorption to the excited state by a second photon.

molecules (Roncali, 1992). Heeger and co-workers successfully reduced the energy gap through the minimization of the δr in poly(isothianaphthene) (Heeger *et al*, 1988). Roncali also reduced the energy gap of poly(thiophene) from 2.0-2.2 eV to 1.1eV through the minimization of the δr arising from the fusing of the benzene and thiophene rings and increasing the quinonoid character of the poly(thiophene) backbone (Roncali, 1992). It is a structural parameter, which is to be tuned or manipuated for NLO responses as it directly gives a measure of the ground state polarization (Marder, 2006). Recent methods include the introduction of donor or acceptor groups at selected positions of the π-conjugated backbone or altering the conjugation length (Marder *et al.,* 1993).

The BLA was calculated using:

$$BLA = \frac{\sum|d_i - đ|}{N} \qquad 2.18$$

The relatonships between the BLA and the molecular NLO properties have been used till now to study and predict the effects of geometric parameters with NLO responses. So the BLA will be used to explain the NLO properties of the systems under study as a small change in them can lead to major changes in the size of the β and γ values as described by Marder (Marder *et al.,* 1994). An instance was reported by Torre and coworkers that distortion in the geometries of the nuclei owing to the presence of solvent media brought about changes in the electronic and NLO properties (Torre *et al*., 2004). Solvent effects on the BLA were reported by Gao and Alhambra, they observed that BLA decreased with the introduction of solvents, accompanied by a reduction in bang gap and red-shifts in absorption (Gao and Alhambra, 1997).

2.5.2 Polarizability (α)

This is defined as the ease with which a molecule or an atom is distorted. That is, it allows an originally nonpolar molecule to become polar by acquiring a dipole moment owing to the the electron clouds being distorted by an external electric field. Dipole polarizabilities, like dielectric constants, optical rotatory dispersion and some other optical properties, and Raman scattering explain the tendency of an external field to polarize a molecule. It explains better the interactions between nonpolar atoms and molecules. It is a quantum chemical

parameter used in determining the electronic properties of an organic molecule and how it can inhibit corrosion of metals in aggressive media. It is closely related to the dipole moment and is represented by the formula (eq. 2.6). However, all models of polarizability begin by calculating the dipole moment as a function of the electric field. Polarizability of a molecule is dependent on molecular size and frontier orbitals of the molecule Fig. 2.9. It increases with an increase in molecular size and a decrease in energy gap (Wang *et al*., 2003). It is directly proportional to the volume occupied by electrons (Targema *et al.*, 2013).

A molecule with a low E_g is more polarizable and it often highly reactive, its kinetic stability is low, and high electro-optic response. It is to note that the amount of electrons present in a species influences the polarizability of that species. Atoms and molecules with lesser electrons will have smaller, denser electron clouds owing to the strong interactions between the scanty electrons in the atomic orbitals and the nucleus. These types of atoms can not be polarized with ease by external fields. In contrast, atoms with large number of electrons are easily polarized because they have high atomic radii and very diffuse electron clouds.

2.5.3 Dipole Moment (μ)

To understand better about the interaction between atoms, the intermolecular forces needs to be studied. Dipole moment, μ**,** measures the polarity of a polar covalent bond. It is measured by the charge on the atoms in a molecule times the distance between the bonded atoms. Only the global polarity of a molecule however is described by the total dipole moment. The total molecular dipole moment for a molecular system may be approximated as the vector sum of individual bond dipole moments eq. 2.9.

The higher the dipole moment, the stronger is the intermolecular interactions. This quantity has been found to increase with a decrease in E_g of molecular systems.

2.5.4 Energy gap (E_g)

The energy gap (E_g) is the difference between the HOMO and LUMO energies and determine how reactive a molecule is. I is the negative of the HOMO energy value while A is the negative of the LUMO value, according to Koopman (1934) in eqs. 2.19-2.22.

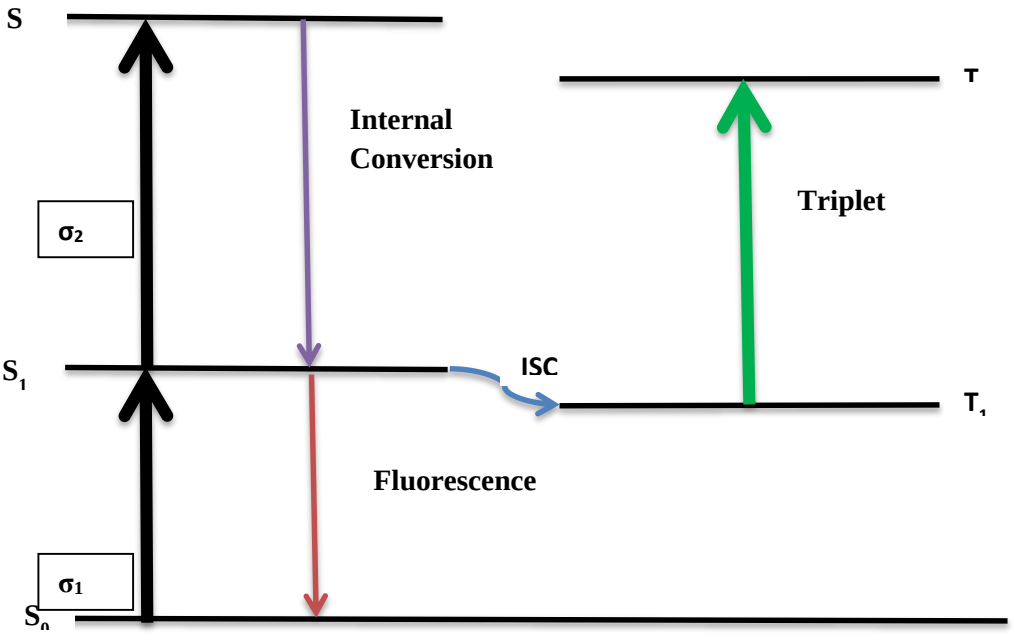

(a)

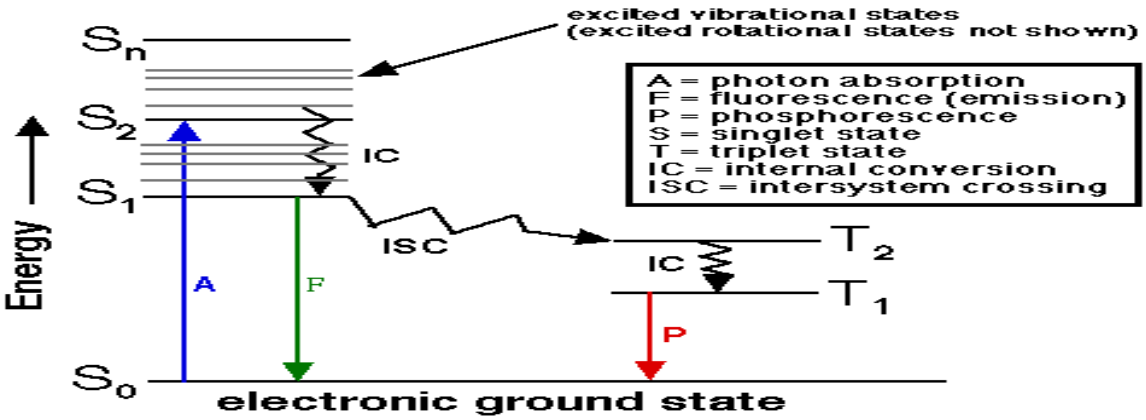

(b)

Figure 2.7: (a) RSA in molecules: The excited state cross section, σ_2 is larger than the ground state cross section, σ_1 (b) Jablonski diagram explaining electronic transitions.

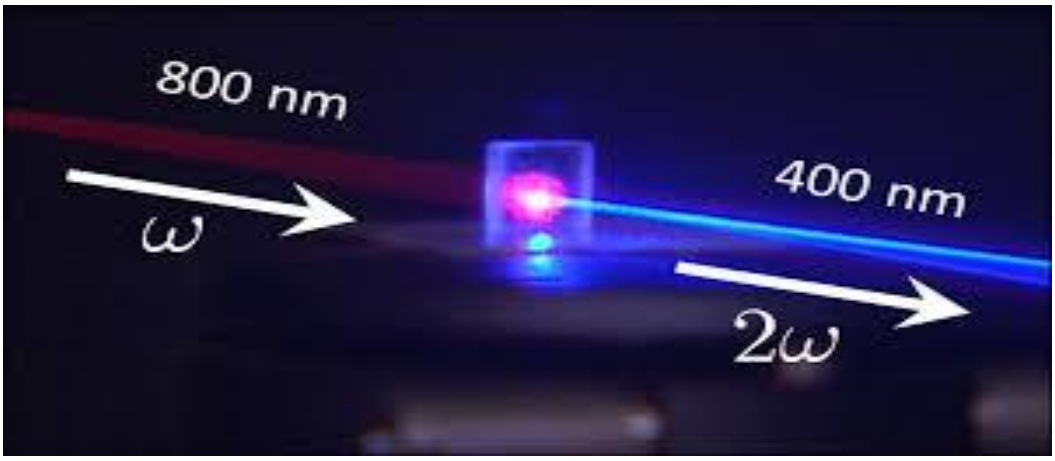

(a)

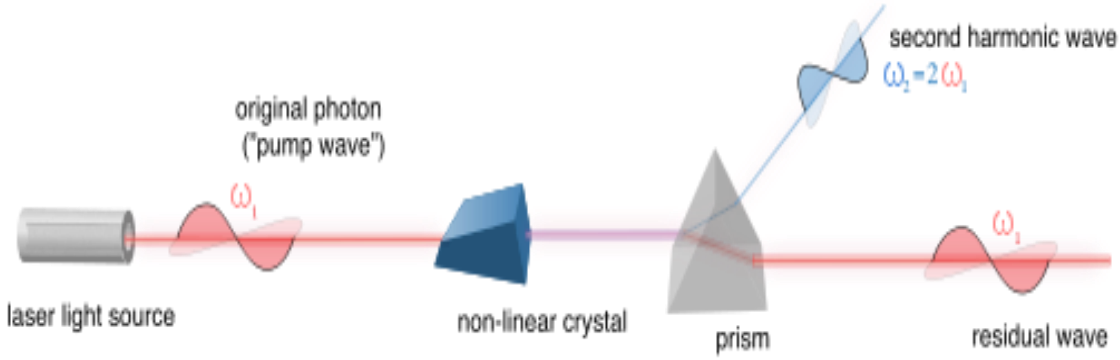

(b)

Figure 2.8: a and b: systematic presentations of SHG process

$$E_g = E_{LUMO} - E_{HOMO} \quad 2.19$$

$$I = -E_{HOMO} \quad 2.20$$

$$A = -E_{LUMO} \quad 2.21$$

$$E_g = I - A \quad 2.22$$

It is a leading property to consider when trying manipulating the physical properties of materials. Energy gap, according to the electronic band theory of solids, is the energy gap separating the VB (π) and CB (π*) bands of the solid materials. Materials with low energy gap are very useful in optoelectronic applications such as light emitting devices (LEDs) and solar cells (Bernier *et al.*, 1999). With the introduction of various elements or groups, the conductive properties of organic molecules could be enhanced due to the changes in energy gap, dipole moment, polarizability, hardness, global eletrophilicity etc. It implies that if we have a compound whose energy gap and other nonlinear optical properties are known, we can build derivatives using different electron donor or acceptor groups in some positions in the compound and study the effects they have on these properties. This is a diagnostic means to synthesizing compounds having similar or better nonlinear optical properties than the synthesized or already studied compounds. That is the summary of what will be done in this research. Although many other properties will be accounted for, it is important, however, that emphasis will be made on the electronic and spectroscopic properties, being the basis of this research. This research will therefore, be focused mainly on altering the energy gap of some Phenothiazine based organic molecules using various substituents and solvents and investigate which of such substituents alter the electronic properties in such a way to meet desired applicabilities.

Insulators have high energy gaps (> 2.0 eV), semiconductors have smaller energy gaps (0.2-2.0 eV), while conductors either have very low energy gaps or none (metals), owing to the overlap of the valence and conduction bands. The E_g obtained from band structure calculations for solids are similar to HOMO - LUMO energy differences in molecules (Alguno *et al.*, 2001). The energy gap required for NLO applications should not necessarily

be close to zero (0), crystals that are insulators at room temperature have been reported to exhibit NLO activities (D'Silva *et al.,* 2012; Zebiao *et al.,* 2015). This is because some other properties like α, β, μ, BLA and UV/vis λ_{max}.

A decrease of energy gap causes red shift in the absorption λ_{max} of materials. The red shift can be so pronounced to the extent of being very transparent in the visible spectrum and they might be used as IR sensors or detectors (Havinga, 1993). According to Roncali (2007), for a molecule to switch from an aromatic form to a quinoid form, energy is needed and it depends directly on the aromatic stabilization resonance energy of the aromatic unit. This resonance effect which tries to reduce the ambit with which the π-electrons move to aromatic ring and thus prevent their movement along the whole conjugated chain, contributes to the magnitude of E_g by a quantity (E_{Res}). A mean dihedral angle, (θ), between successive units therefore tends to confine the delocalization of π-electrons along the conjugated backbone and hence to increase E_g by a quantity (E_θ). Introducing electron-withdrawing or electron-donating groups is the easiest way to modify the HOMO and LUMO levels of a conjugated system. This of course modifies the energy gap, E_g and is represented by a term (E_{Sub}). These four structural factors can be used by synthetic scientists while engineering molecular HOMO-LUMO gap, E_g, of an isolated conjugated system. There is a fifth contribution when molecules/polymers are being assembled into a material, this contribution is (E_{Int}) related to intermolecular interactions, which sometimes can affect the magnitude of E_g (Figure 2.9). A linear p-conjugated system gives the energy gap expressed by the sum of all these contributions:

$$E_g = E_{BLA} + E_{Res} + E_{Sub} + E_\theta + E_{Int} \qquad 2.23$$

EMw is the dependence of the energy gap on the molecular weight of the organic materials (Gierschner *et al.*, 2007). π-conjugated molecules possess semiconductor properties because of the alternating single-double bond in their structures Their HOMO and LUMO levels are built from the overlapping P-z orbitals and, therefore, the HOMO is filled with the π-electrons. While the molecular structures are preserved by the σ-bonds via the chemical bonding, the π-system then undergo different optical and electronic transitions and interactions. From the π-orbitals emerges the valence band (HOMO), while the π* -orbitals

form the conduction band (LUMO). There exists an energy gap between the HOMO and the LUMO, also called the energy gap of the material. This zone is absent for metallic conductors, leading to half-filled bands and hence to intrinsic conduction (Kroon *et al.*, 2008) as in Fig 2.10.

So, for (Kroon *et al.*, 2008), the energy gap can be described as:

$$E_g = E_{BLA} + E_{Res} + E_{Sub} + E_{\theta} + E_{Int} + E_{EMw}. \quad 2.24$$

Several researchers agreed with Kroon's work in that it has been observed that as materials increase in size and conjugation the energy gap reduces. (Stefan *et al*, 2011 Cornil *et al.*, 2003).

However, the optical absorption spectrum of a conjugated polymer measures energy gap of the polymer. A maximum value is reached for the optical absorption in conjugated polymers, this is the effective conjugation length, ECL (Meier, 1998). The ECL of conjugated polymers can be improved to an extent desirous to the researcher by translating the non-classical quinonoid character to the repeat units.

2.5.5 Energy gap Engineering

Energy gap can as well be altered through a process called band engineering. It is the process of introducing elements in order to change the electronic and optical properties of the polymer. With the introduction of various elements, enhanced conductive properties due to the changes in energy gap can result in the design of novel materials useful in applications as sensors, molecular switches, organic light emitting diodes, photovoltaics and optical limiters (Andriotis and Menon, 2015).

Shikarawa and co-workers discovered that polyacetylene (PA) film can be made more conductive by exposing the polymer to chlorine, bromine or iodine vapour. The conductivity increases noticeably (over 10^7 in the case of iodine) as the halogens were taken up (Shikarawa *et al.*, 1977). This halogenation process was called 'doping' and the doped PA had a better conductivity than the previously known polymer. The use of nitrogen-containing heterocycles as efficient electron acceptors resulted in small energy gaps for electropolymerized donor-acceptor polymers (Mullekom *et al.*, 2001). Electrons in a

conjugated system are loosely packed; there is always a possibility for electron flow. Each bond contains a strong 'sigma' (σ) bond and a weaker 'pi' (π) bond, leading to delocalization of electrons over the whole system and can also be shared by many atoms. The movement of such delocalized electrons makes the system conductive. Conjugation, however, may not be enough to get the desired energy gap. The polymer, with its conjugation, needs to be doped for electron flow to occur. Doping can be done either by adding electrophiles (electron deficient) or nucleophiles (electron rich) substituents. An oxidation doping is the addition of an electrophilic (electron withdrawing) substituent e. g. iodine. Such substituent withdraws electrons from the polymer from one of the π bonds. The electrons are able to jump around the polymer chain once doping has occurred. For better conductivity, polymers can be tuned by chemical manipulation of the polymer backbone, by the nature of the polymer and by blending with other polymers (Angelopoulos, 2001). One can increase the energy level of the frontier orbilals by introducing different substituents. For instance, adding electron donating groups (EDGs) e.g thiophene and pyrrole to the molecule can increase the HOMO energy level. Similarly, electron withdrawing groups (EWGs) e. g thiadiazole, nitrile and pyrazine can lower the the energy level of the LUMO of the molecule. This improves the donor and acceptor units, and consequently lowers the energy gap of the material (Oyeneyin, 2017). Also, the π-conjugation length is of great importance since torsion in the polymer back bone causes a decrease in the conjugation length and the energy gap increases. Therefore, a high π-conjugation length results in a low energy gap polymer (Winder and Sariciftci, 2004).

Sunitha *et al.,* (2012) synthesized a D-A type conjugated polymer units. The calculated energy gap of the polymer was 2.39 eV. Stefan and coworkers prepared a family of donor-acceptor-donor (D-A-D) oligomers and the relationship between their spectral, structural and electrochemical properties were investigated and they have energy gaps ranging from 1.05 to 1.95eV with the oligomers having the narrowest energy gap (Stefan *et al.,* 2011). The optical absorption spectra of oligomers of PPV, and their methoxy-substituted derivatives were calculated by (Cornil *et al.,* 2003) on the basis of geometries optimized by semi-empirical AM1 method synergized with the conFiguration interaction (CI) technique. The results were in conformity with experimental, measured by UV-Vis absorption spectra. In 2003, the properties of the polyfluorenes were investigated via quantum chemical

calculations and were compared with copolymers of fluorene and ethylenedioxythiophene units in alternating form.

2.5.5.1 Global Reactivity Descriptors

2.5.5.1.1 Hardness (η) and Softness (S) determination

The resistance of a compound to change its electronic conFiguration is measured by its hardness and it is an indicator of chemical reactivity and electronegativity. According to Pearson acid-base concept, a molecule is hard if it is weakly polarizable and have high charge state (Jolly, 1984). It is used to explain the concept of orbital overlap, which is the concentration of orbitals on adjacent atoms in similar region of space, leading to bond formation and used to explain the molecular bond angle and orbital hybridization. (Pearson, 1997). A measure of orbital overlap is given by eq. 2.25

$$S_{AB} = \int \psi_A^* \psi_B dV \qquad 2.25$$

The integration extends over all space and the * on the first wavefunction indicates a complex conjugate. Hardness is measured empirically by, E_g, from eq. 2.11, where *I and A* are the ionization energy and the electron affinity, respectively. The energy of the reaction of the species is said to be proportional to the hardness. The chemical hardness, according to (Parr and Pearson, 1983), given by eq. 2.26;

$$\eta = \frac{1}{2}\left(\frac{\partial^2 E}{\partial N^2}\right)_z = \frac{1}{2}\left(\frac{\partial \mu}{\partial N}\right)_z = \frac{1}{2}(I\text{-}A) \qquad 2.26$$

The higher the energy gap, the harder the molecule is, the lower its reactivity, and low electro-optic response, this is because the high gap between the HOMO and LUMO orbitals makes it difficult for electrons to be transferred. It is therefore, expected that this property should increase with decreasing energy gap and vice versa, according to eq. 2.11. A molecule is soft if it has a very low hardness value, i.e. it is inversely proportional to hardness according to the relation in eq. 2.11.

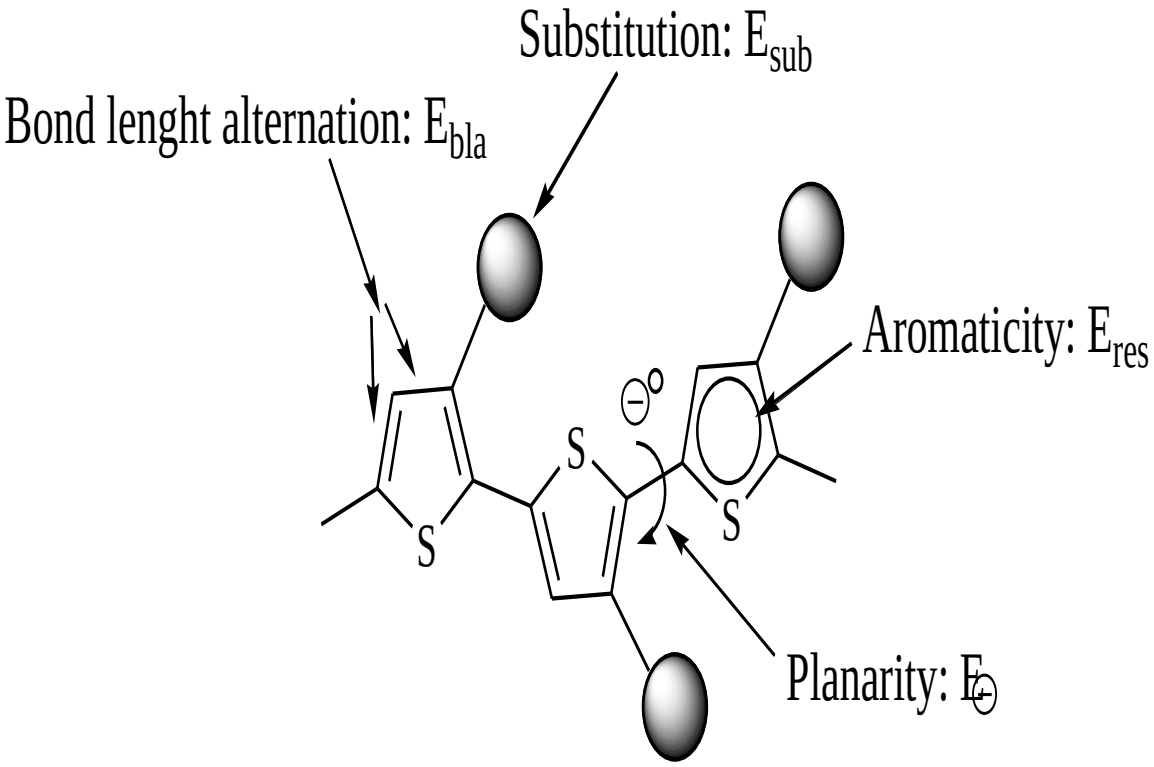

Figure 2.9: Structural factors determining the energy gap of materials derived from linear p-conjugated systems (Roncali, 2007)

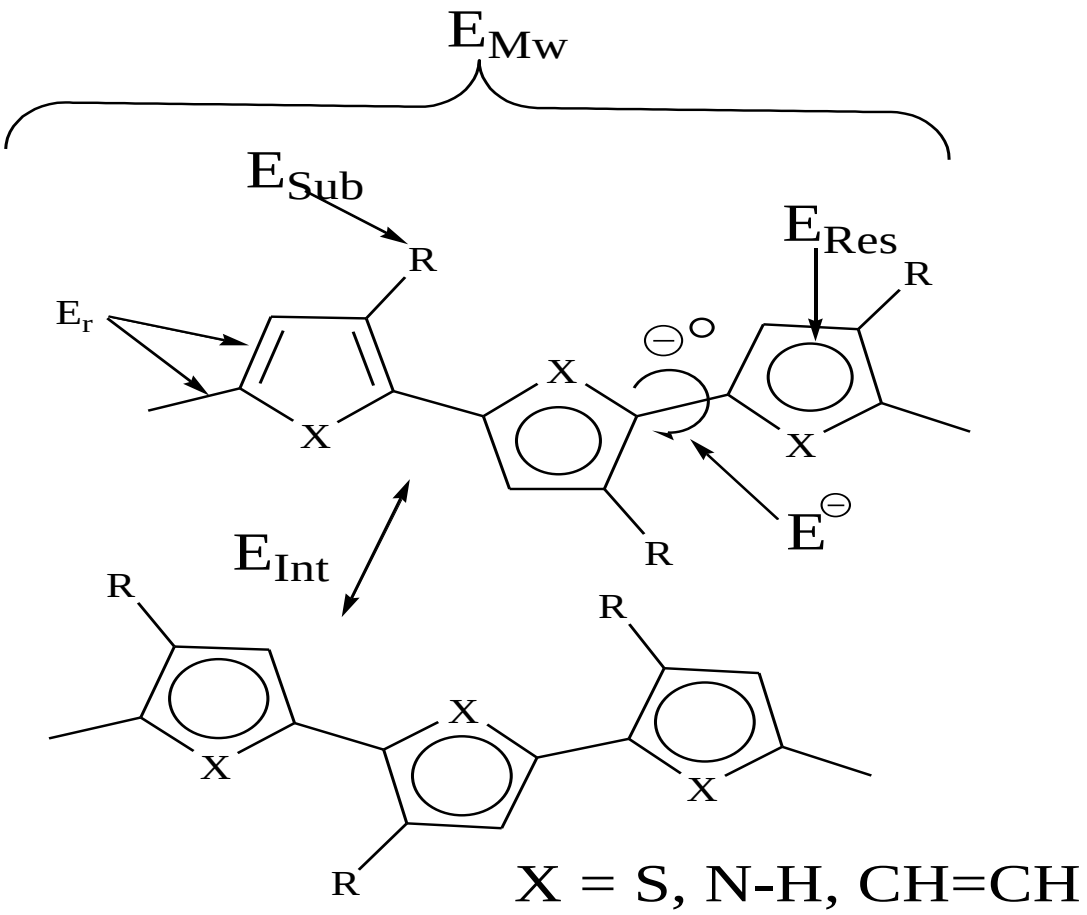

Figure 2.10: Parameters influencing the energy gap (Eg): molecular weight (Mw), bond length alternation (r), resonance energy (Res), substituents (R), torsion angle (u), and interchain effects (Int) (Kroon et al., 2008).

2.5.5.1.2 Chemical Potential (C^P) and Global Electrophilicity (ω)

Chemical potential is defined as a measure of how favourable it is, energetically for a system to accept electrons. It is closely related to the electronegativity in that, electrons move towards molecular moieties with high electronegativity from ones with low electronegativity until the electronegativity is equalized. It is given by eqs. 2.27 and 2.28.

$$C^P = -\left(\frac{I+A}{2}\right) \qquad 2.27$$

$$C^P = -\chi_{Mulliken} \qquad 2.28$$

That is, it is the negative of the absolute electronegativity. $\chi_{Mulliken}$ is the Mulliken's definition of electronegativity. Optical electronegativity is important in understanding the nature of chemical bonding and it can be used to predict other important chemical parameters. According to Mulliken, the electronegativity of a molecule is the negative value of its chemical potential as seen in eq. 2.28. It describes the ability of an atom/functional group to attract electrons to itself.

The global electrophilicity index (ω) is a quantity that measures the energy stabilization of a system which acquires an additional electronic charge from the environment (Parr *et al.*, 1999). It is calculated from the chemical potential and chemical hardness using the relation,

$$\omega = \frac{(C^p)^2}{2\eta} \qquad 2.29$$

A good and more reactive nucleophile is defined by a low value of C^P and ω, while a good electrophile has a high value of C^P and ω.

2.5.5.1.3 Molecular First Hyperpolarizability (β)

The first hyperpolarizability (β) of a molecule is an important parameter to investigate while studying any system for its nonlinear optical behaviours. Recent researches in nonlinear optics involve manipulation and engineering of a system backbone in order to maximize β as the value of the second order susceptibility χ^2 depends greatly on the value of β. Large value of β is one of the advantages organic materials have over inorganic analogues

(Adhikari and Kar, 2012). The process by which chemical substitutions affect the β is the basis of this study having established how chemical substitutions affect the energy gap.

In the presence of a static uniform electric field (F), the perturbed energy (E) of a molecule is given by:

$$E(F) = E_0 - \sum_i \mu_i F_i - \frac{1}{2!}\sum_{ij} \alpha_{ij} F_i F_j - \frac{1}{3!}\sum_{ijk} \beta_{ijk} F_i F_j F_k - \ldots \quad 2.30$$

where E_0 is the molecular energy without an electric field and μ_i are the permanent dipole moment components, α_{ij} are the dipole polarizability components and β_{ijk} are the first hyperpolarizability components. Therefore, the average linear polarizability is defined by:

$$\alpha = (\alpha_{xx} + \alpha_{yy} + \alpha_{zz})/3 \quad 2.31$$

The first hyperpolarizability has a vector component along the dipole moment direction β_{vec} abd it is defined by equation 2.32;

$$\beta_{vec} = \frac{\sum_i \beta_i \mu_i}{|\mu|} \quad [i = x,y,z] \quad 2.32$$

where μ is the dipole moment of the ground state and β_i is given by;

$$\beta_i = \sum_k \beta_{ikk} \qquad [i,k = x,y,z] \quad 2.33$$

β_{vec} is frequency dependent while the one obtained from DFT calculations is the static value. These static values, which have been reduced from the 27 components to 10 components of the 3D matrix owing to Kleinman symmetry (Kleinman, 1962) gives rise to a 3 x 3 x 3 matrix from the 10 components.

The first static hyperpolarizability (β_{ijk}) of 3 x 3 x 3 matrix with ten components was therefore calculated using the BLYP/6-31G* and B3LYP/6-31G*. The value of the resultant effective hyperpolarizability (β_{eff}**)** was determined from β_{ijk} using the following equation:

$$\beta_{eff} = [(\beta_{xxx} + \beta_{xyy} + \beta_{xzz})^2 + (\beta_{yyy} + \beta_{yzz} + \beta_{yxx})^2 + (\beta_{zzz} + \beta_{zxx} + \beta_{zyy})^2]^{1/2} \quad 2.34$$

The values were recorded in Debye $Å^2$ and in electrostatic units (esu) as (1 Debye $Å^2$ = 1 x 10^{-30} esu).

2.5.5.1.4 Electronic Transition Properties

The wavelength of maximum absorption and emission are shown for UV-Vis. The detailed electronic transitions which include the excitation energies, oscillator strength and the maximum absorptions in UV-vis (λ_{max}) were all determined using the TD-DFT calculations and with B3LYP/6-31G* and BLYP/6-31G* and presented. The equations were solved for 6 excited states.

2.6 Theoretical Background

Computational chemistry is an interesting area in chemistry which models and simulates systems like polymers, inorganic and organic molecules, biomolecules, drugs etc (Ramachandran *et al.*, 2008). Computational chemistry methods range from highly accurate (*Ab initio* and DFT methods) to less accurate (semi-empirical (SE) method), to very approximate (molecular mechanics methods), and can be used on systems with single molecule, or group of molecules. It is useful in calculating properties like structure, relative energies, dipole and multipole moments, reactivity, charge distribution, thermodynamic parameters, spectroscopic properties etc. (Ribeiro and Greca, 2003).

Quantum chemistry describes how electrons behave mathematically. Since molecules are characherized by electrons, we can say that quantum chemistry describes the behaviour of chemistry. The state of a system is described by a wavefunction in quantum mechanics and not by particle characteristics. Because quantum mechanics describes molecules in terms of their interaction between electrons and nuclei and molecular geometries in terms of the minimum energy arrangement of nuclei, it is therefore, the goal of all quantum chemical method to solve the time-independent Schrödinger equation using approximations (McQuarrie, 1997).

For a single particle, one dimensional equation can be represented as follows:

$$-\frac{\hbar^2}{2m}\frac{\delta^2\Psi(x)}{dx^2}+V(x)\Psi(x)=E\Psi(x) \qquad 2.35$$

This can be more generally written as:

$$\hat{H}\Psi=E\Psi \qquad 2.36$$

Where $\hat{H}$ is the Hamiltonian, E is the energy and Ψis the wave function which does not contain terms for spin of the electron but rather a probabilistic description of electron behaviour, as a wave (Young, 2001). It implies that the wave functions obtained from the Schrödinger equation are used to express the properties of a system.

2.7 The Shrödinger Equation

Quantum mechanics explain how the wave-particle properties are possessed by (dual nature of electron). The Schrödinger equation simplifies the wavefunction of a particle (Henre, 2003).

$$\left(-\frac{\hbar^2}{2m}\nabla^2+V\right)\Psi(\check{r},t)=i\hbar\frac{\partial\Psi(\check{r},t)}{\partial t} \qquad 2.37$$

In the equation 2.37 (time dependent Schrödinger equation), Ψ is the wavefunction, which describes the probability that an electron is in space but cannot predict the actual location, ħ is the planck's constant over 2π, m is the mass of the particle and V is the potential field in which the particle is moving. In order to find the probability distribution of the particle, we find the product of Ψ with its conjugate ($\Psi * \Psi$), often written as $/\Psi/^2$. This is to ensure that the solutions to this problem is made real and gives no chance for any imaginary situation. That is why the wave function is regarded as the probability amplitude.

2.7.1 The Molecular Hamiltonian

An isolated molecular system does not use the complete Hamiltonian in practice. The complete Hamiltonian includes nuclear and electronic kinetic energy operators, electrostatic

interaction among all charged particles and interaction among all magnetic moments due to spin and orbital motion of nuclei and electrons. Included in the complete Hamiltonian is a moving particle experiencing a change in mass due to relativistic effects. The Hamiltonian, $\hat{H}$, is written generally as:

$$\hat{H} = -\sum_{i}^{particles} \frac{\nabla_i^2}{2m_i} + \sum_{i<j}^{particles} \sum \frac{q_i q_j}{r_{ij}} \qquad 2.38$$

Where ∇_i^2 is the Laplacian operator acting on particle *i*. m_i and q_i are the mass and charge of particles*i*,and r_{ij} is the distance between the particles (electrons and nuclei). Equation 2.38 is the time-independent Schrödinger equation. The above Hamiltonian does not take into account the additional terms arising from relativity and interactions with electromagnetic radiation. This problem is then made simple by the Born-Oppenheimer approximation.

2.7.2 Born Oppenheimer Approximation (BOA)

The mathematical complexities used to describe chemical phenomena might be so too much that it is impossible to solve a problem exactly. It is possible to do part of the work if we are to obtain a quantitative result. Techniques applied in approximation are; to completely ignore the complex part of the calculation, variations, perturbations, simplified functions, and fitting parameters to reproduce experimental results.

BOA came to existence in early 1927, just after the birth of quantum mechanics by Born Oppenheimer. It assumes we can study behaviours of electrons in a field of frozen nuclei and also corrects $\hat{H}$ (Hamiltonian), it led to a way of simplifying the Schrödinger equation which is always complex for a molecule. The nuclei and electrons are attracted to each other with the same magnitude of electronic charge; hence, they exert some kind of force and momentum. B-O approximation takes advantage of this phenomenon and assumed that since nucleus is heavier in mass as compared with electron mass, its motion, kinetic energy can be ignored and the nuclei is assumed to be fixed while electrons revolve (Henre, 2003).

$$\hat{H}_{exact.} = T_{el} + V_{el\text{-}el} + T_{nuc} + V_{el\text{-}nuc} = H_{approx.} \qquad 2.39$$

Where T_{el} and T_{nuc} are the kinetic energy of the electron and nucleus respectively, $V_{el\text{-}el}$ is the potential energy of the electron to electron interaction, $V_{nuc\text{-}nuc}$ is the potential energy of

the nucleus to nucleus interaction, and $V_{el\text{-}nuc}$ is the potential energy of the electron-nuclear interaction or which is not separable, hence since nuclear positions are assumed to be fixed, we can neglect T_{nuc} and $V_{nuc\text{-}nuc}$ so we get $H_{elect.}$or $H_{approx.}$,

$$\hat{H}_{elect.} = T_{el} + V_{el\text{-}el} + V_{el\text{-}nuc} = H_{approx\ldots} \qquad 2.40$$

$$\hat{H}_{mol} = T_{elec} + V = \frac{-\hbar^2}{2m_e} \sum_{i}^{electrons} \nabla_i^2 + \frac{1}{4\pi\varepsilon_0} \sum_{j} \sum_{k>j} \frac{q_j q_j}{|r_k - r_j|} \qquad 2.41$$

This is called the B-O approximation but since $V_{el\text{-}el}$ is cannot be separated, it requires another approximation like the independent particle model which assumes each electron moves in its own orbital ignoring correlation of an electron with the others.

2.7.3 Hartree Fock Approximation (HF)

This method breaks down the many-electron Scrödinger equation into many simpler one-electron equations, each solved to obtain a single-electron wave function, an orbital, accompanied with an energy, the orbital energy. It is applied in the solution of Schrodinger equation for atoms, molecules, nanostructures, solids and in nuclear physics (Henre, 2003).

The HF method is a single electron approximation technique used in many-electron systems. The molecular Hamiltonian is divided into individual single electron Hamiltonians. Consider a molecular system with *N*-electrons, each with degrees of freedom r_i. The wavefunction (Hartree function) $\psi h(r1, r2, \ldots, rN)$ is given by the Hartree product as shown in equation 2.42:

$$\psi h(r1, r2, \ldots, rN) = \varphi 1\,(r1)\,.\varphi 2\,(r2)\ldots\varphi N\,(rN) \qquad 2.42$$

The Hamiltonian can be computed based on this premise. For the *n*-electron system, the Hamiltonian is given by;

$$H_e = T_e + V_{ne} + V_{ee} + V_{nn} \qquad 2.43$$

Where $T_e = \sum_{i=1}^{n} \frac{-\nabla_i^2}{2}$, $V_{ne} = \sum_i^n \sum_A^N \frac{-Z_A}{r_{iA}}$, $V_{ee} = \sum_i^n \sum_j^n \frac{1}{r_{ij}} = g_{ij}$ and $V_{nn} = \sum_A^N \sum_{B>A}^N \frac{Z_A Z_B}{R_{AB}}$.

Where A and B are for the representing nuclei, i and j are for the representing electrons, Z is the nuclear charge, T is the kinetic energy operator, V is the potential energy operator, or the Hamiltonian is written as;

$$H = \sum_{i=1}^{n} \frac{-\nabla_i^2}{2} + \sum_i^n \sum_A^N \frac{-Z_A}{r_{iA}} + \sum_i^n \sum_j^n \frac{1}{r_{ij}} + \sum_A^N \sum_{B>A}^N \frac{Z_A Z_B}{R_{AW}} \qquad 2.44$$

Here, V_{nn} is independent of electronic coordinators. T_e and V_{ne} depend upon one-electron coordinators.

$$T_e + V_{ne} = \sum_{i=1}^{n} \frac{-\nabla_i^2}{2} + \sum_i^n \sum_A^N \frac{-Z_A}{r_{iA}} = \sum_{i=1}^{n} \left(\frac{-\nabla_i^2}{2} + \sum_A^N \frac{-Z_A}{r_{iA}} \right) = \sum_{i=1}^{n} h_i \qquad 2.45$$

Finally, there is a term V_{ee}, which is the sum of sum of n(n-1)/2 two electron coordinators. Hence, the Hamiltonian becomes

$$H = \sum_A^N \sum_{B>A}^N \frac{Z_A Z_B}{R_{AB}} + \sum_{i=1}^{n} h_i + \sum_i^n \sum_{j>i}^n \frac{1}{r_{ij}} \qquad 2.46$$

Substituting the Hamiltonian expression into the energy equation

$$E = \int \Psi \left[\sum_A^N \sum_{B>A}^N \frac{Z_A Z_B}{R_{AB}} \right] \Psi dx + \int \Psi \left[\sum_{i=1}^{n} h_i \right] \Psi dx + \int \Psi \left[\sum_i^n \sum_{j>i}^n \frac{1}{r_{ij}} \right] \Psi dx \qquad 2.47$$

The first term of the integral stands for nuclear-nuclear repulsion and is the integral over a constant which is independent of coordinates. Hence,

$$V_{NN} = \int \Psi \left[\sum_A^N \sum_{B>A}^N \frac{Z_A Z_B}{R_{AB}} \right] \Psi dx = \left[\sum_A^N \sum_{B>A}^N \frac{Z_A Z_B}{R_{AB}} \right] \qquad 2.48$$

The second and third term can be written as;

$$\sum_{i=1}^{n} [\int \Psi h_i \Psi dx] = \sum_{i=1}^{n} [\int X_i \, dT] = \sum_{i=1}^{n} h_{ii} \quad 2.49$$

$$h_{ii} = \int \emptyset_i h_i \emptyset_i dT = \int \emptyset_i [\frac{-\nabla_i^2}{2} + \sum_A^N \frac{-Z_A}{r_{iA}}] \emptyset_i dT \quad 2.50$$

$$h_{ii} = \int \emptyset_i \left[\frac{-\nabla_i^2}{2}\right] \emptyset_i dT + \int \emptyset_i \left[\sum_A^N \frac{-Z_A}{r_{iA}}\right] \emptyset_i dT = \sum_{i=1}^{n} h_{ii} \quad 2.51$$

$$\sum_{i=1}^{n} h_{ii} = \sum_{i=1}^{n} \left[T_{e,i} + V_{Ne,i}\right] = T_e + V_{Ne} \quad 2.52$$

T_e is the electronic kinetic energy, and V_{Ne} is the potential energy due to nuclear-electronic Coulombic attraction. The third integral terms, and two electron terms are more complex. The molecular orbital is considered as a product of single electron orbitals in Hartree treatment. Thus:

$$\Psi(r_1, r_2, \ldots\ldots) = \emptyset(r_1)\emptyset(r_2) \quad 2.53$$

2.7.4 The Self-Consistent Field Method (SCF)

The SCF theory studies the behavior of large and stochastic models by studying that of a simpler model (Blinder, 1965). The models reduce the many-body problem to a one-body problem by reducing the single averaged effect of individual components interacting with each other. It was first used by Weiss to describe phase transitions (as in Weiss, 1907), and have applications in game theory (Lasry and Lions, 2007). That is, the n-body system is replaced by a 1-body problem with a chosen good external molecular field (Chaikin and Lubensky, 2000), which replaces the interaction of all other particles to an arbitrary particle. This makes it easy to study systems behaviour cheaply.

The basis used for the self-consistency field (SCF) theory is the Bogoliubov's inequality which states that the free energy of a system with Hamiltonian is,

$$H = H_0 + \Delta H \quad 2.54$$

Has the following upper bound;

$$F \leq F_0 \stackrel{\text{def}}{=} \langle H \rangle_0 - TS_0. \quad 2.55$$

Where S_0 is the entropy and H_0 is the Hamiltonian of the reference system. If the reference Hamiltonian is that of a non-interacting system, then it can be written as,

$$H_0 = \sum_{i=1}^{N} h_i(\varepsilon_i) \quad 2.56$$

Where ε_i, is the degrees of freedom of the individual components of the statistical systems.

2.7.5 The Variational Principle

This is an alternative method used in determining the state or dynamics of physical systems by identifying an extreme value (minimum, maximum or saddle point) of a function. It is a way of approximating the ground state and some excited states (Henre, 2003). Suppose we solve the time-independent Schrodinger equation (2.36). If ψ is a normalized solution of the above equation, the variational principle then states that the expected *H* value calculated with the trial wavefunction is always greater than or equal to the ground state energy, E_0. i.e.,

$$E_0 \leq \langle \psi | H | \psi \rangle \quad 2.57$$

The expectation valueof *H* is minimized if the value of ψ is varied. And the approximation of the wavefunction and energy of the ground state is obtained.

2.7.6 Linear Combination of Atomic Orbitals (LCAO)

Quantum mechanics describes the electron conFiguration of atoms as wavefunctions, which are the basis set of functions describing the electrons in an atom, mathematically. Chemically, orbital wavefunctions are adjusted in that the cloud shape of the electron is changed, depending on the type of atoms involving in the chemical bonds. The earlier postulate was that linearly, the number of molecular and atomic orbitals are equal. In actual sense, *n* atomic orbitals combine to form *n* molecular orbitals, which can be numbered *i* = 1 to *n* and may not always be the same. The linear expression for the ith molecular orbital would be;

$$\emptyset_i = C_{1i}\chi_1 + C_{2i}\chi_2 + C_{3i}\chi_3 + \ldots + C_{ni}\chi_n \quad 2.58$$

Or

$$\emptyset_i = \sum_r C_{ri}\chi_r \qquad 2.59$$

Where $\emptyset_i$ is the molecular orbital represented as the sum of n atomic orbitals, χ_r each multiplied by a corresponding coefficient C_{ri}, and r (numbered 1 to n) represents which atomic orbital is combined in the term. The coeeficients (which can be determined by the Hartree Fock method), being the weight of the contributions of the n atomic orbitals to the molecular orbital.

The orbitals are therefore, expressed as linear combinations of basis functions, which are one-electron functions centered on the nuclei of the component atoms of the molecule. Slater type orbitals (STOs) are used to describe the atomic orbitals used because they are like hydrogen atoms and can only be determined analytically while other choices are possible like Guassian functions from standard basis sets.

2.8 Quantum Mechanics

Quantum mechanics (QM) mathematically describes much of the wave-particle duality behaviours and interactions of energy and matter. It can theoretically predict exactly the properties of individual atoms or molecules exactly, though it has only been solved exactly for one electron systems, in practice (Young, 2001). That is what led to the various aforementioned approximations.

2.8.1 Semi-Empirical Methods (SE)

Some information such as two-electron integral are sometimes approximated or omitted in HF calculations. To correct for this, semi-empirical methods are parameterized (Pople and Beveridge, 1970). The methods are faster but less accurate and less predictive than the *Ab initio* methods. Examples of such methods include the extended Huckel method, Neglect of Differential Overlap (NDO), Neglect of Diatomic Differential Overlap (NDDO), Austin Model 1 (AM1), Parameterization method 3 (PM3), and Pariser-Parr-Pople (PPP).

Semi-empirical methods follow empirical methods where the two-electron part of the Hamiltonian is not explicitly included for π-electron system. This was Huckel method but

for all valence electron system, the extended Huckel method was proposed (Hoffman, 1963). Semi-empirical methods are useful in studying organic chemistry and also provide researchers with a quick way of studying the structure and behaviour of molecules especially as compared with ab-initio counterparts. These methods allow the user to obtain qualitative and quantitative results than ab-initio methods. Lipiński and Bartkowiak reported on how solvent affects molecular hyperpolarizabilites of some chromophores using the semi-empirical quantum mechanical calculations, it was observed that NLO responses were affected by the changes in geometry, conformation and solvent effects (Lipiński and Bartkowiak, 1999).

2.8.1.1 The Extended Hückel Method

This calculation neglects all interactions between electrons, making them fast but with less accuracy. Information about the shapes and energies of molecular orbitals are gotten from it. It also approximates the distribution of electron density in space. These models are good for chemical visualization and can be applied to frontier orbital treatments of chemical reactivity. It is chosen today because it is used for all the periodic Table elements and it also used for calculating band structures (Young, 2001).

2.8.1.2 Austin Method, Version 1 (AM1).

A reparameterised version of Modified neglect of diatomic orbitals (MNDO) which includes changes in nuclear repulsion terms, it is used for modeling organic compounds, predicts heat of formation (ΔH_f) (Young, 2001). AM1 and PM3 are most likely to give the best results possible for organic molecules (Young, 2001).

2.8.1.3 Parameterisation Model, Version 3 (PM3).

This is an improved method compared ti the AM1. Because it is recent, some of its defects may still be unknown or undiscovered.

2.8.2 Ab Initio Methods

This is a method used without the inclusion of experimental data. The approximations made are purely mathematical e.g., the HF approximation, DFT, Moller-Plesset perturbation (MP), conFiguration interaction (CI) etc.

2.8.2.1 Density Functional Theory (DFT)

DFT is a method in computational chemistry used to determine the electronic structure of molecules. DFT methods can be often considered an *ab-initio* method for determining molecular electronic structures despite many of the common functionals use parameters are derived from empirical data or from more complex calculations. In DFT methods, the total energy is expressed in terms of the total one-electron density rather than the wavefunction because electron density is an effective way of explaining the properties of systems in that is measurable. This method is particularly useful for high quality energy and property calculation including calculations on transition metals, inorganic and organic molecules and organometallic compounds (Henre, 2003).

The major postulate of DFT is that energy of a molecule can be represented as some mathematical form of the electron density as originated by Hoenburg and Kohn. The original theorem applied only to finding the electronic energy of the ground state of a molecule. A practical application of this theory was developed by Kohn and Sham who formulated a method similar in structure to the HF method. DFT dates back to Thomas (1927), Fermi (1927), and Dirac (1930). It is not a newcomer in the field of computational chemistry but has been less popular until recently.

The DFT methods have been used in studying molecular properties. Targema and co-workers used the *ab-initio* restricted HF-DFT self-consistent field method (B3LYP) with a polar 6-31G* basis set to study substituents and solvents effects on the geometric and electronic properties of some aniline derivatives. It was discovered that the properties vary with different substituents and solvents (Targema *et al.,* 2013). Zhang and co-workers reported the dipolar/octupolar contributions to the second-order NLO activity of some subtriazaporphyrin derivatives were studied using the DFT methods with B3LYP and a basis set of both polar and diffuse function, 6-31+G* and it was discovered that octupolar and dipolar contributions are theoretically separated in the molecules, leading to enhanced NLO acticity (Zhang *et al*., 2012). Some phthalocyanine-quantum dot nanocomposites were studied for the optical limiting performance by free-carrier absorption mechanism and verified with DFT calculations by Sanusi and co-workers. It was discovered that the DFT calculated properties were well within the range of experimental findings (Sanusi *et al.,*

2014). TD-DFT calculations were used to study the solvent effects on the geometric and electronic structures and 2PA properties of a D-π-A azobenzene dye (Chuan-Kui *et al.*, 2007). The DFT results are in good agreement with experimental discoveries. Nitrated L-leucine was studied theoretically by Adhikari and Kar (2012) using HF and DFT methods. Its crystal was deemed suiTable for NLO applications and also that the value of second order susceptibility χ^2 of a NLO material depends on the molecular hyperpolarizability, β. The electrostatic potential and the NLO properties of *m*-nitroacetanilide were investigated theoretically using HF and DFT methods and proved that the molecule exhibits NLO behavior (Boukabcha *et al.,* 2015). They also reported that the energy gap reduced with methanol solvent as compared with methanol. Islam and Lone studied the optoelectronic and nonlinear properties of octaphyrin derivatives computationally using the DFT and TDDFT and reported enhancement of NLO responses upon introduction of different electron donating groups into octaphyrin backbone (Islam and Lone, 2017).

2.8.2.2 The Kohn-Sham Molecular Orbital Theory

Hohenberg, Kohn and Sham (Hohenberg and Kohn, 1964; Kohn and Sham, 1965), developed the DFT based on Thomas-Fermi approximation (Thomas, 1927; Fermi, 1927). It can be applied to systems of interacting particles in an external potential. Using electronic density as a basic variable to describe the many-body system is the idea of DFT, that is, it simplifies the many-body Schrodinger equation. Two theorems were proposed by Hohenberg and Kohn in 1964:

i. For a system of interacting particles in an external potential, (V_{ext}(**r**), the external potential and the total energy is a unique functional of the ground state electron density n_0(**r**)
ii. We can obtain the ground state energy variationally. For any particular external potential, (V_{ext}(**r**), the ground state energy of the system is the global minimum of this functional. The exact ground state density, n_0(**r**) minimizes the total energy. The many-body problem is solved by replacing independent particles equation with interacting density.

$$E[n(r)]= T[n(r)]+ \frac{1}{2}\iint drdr' \frac{n(r)n(r')}{|r-r'|} + E_{xc}[n(r)] + \int drV_{ext}(r)n(r) \qquad 2.60$$

(V_{ext}(**r**) is the external potential, E_{xc}[n] is the exchange correlation functional of electronic density. The density is given by the sums of the squares of the simple particle orbitals.

$$n(r)= \sum_{i=1}^{N}\left|\varphi_i(r)\right|^2 \qquad 2.61$$

The independent particle kinetic energy T[n(**r**)] is given by;

$$T_0[n(r)] = \sum_{i=1}^{N} \int dr \varphi_i^*(r)\left(-\frac{-\hbar^2}{2m_e}\nabla^2\right)\varphi_i(r) \qquad 2.62$$

Applying the variational principle to Kohn Sham functional,

$$\frac{\delta\{E[n(r)]-\sum_{i=1}^{N}\varepsilon_i[\int dr\varphi_i^*(r)\varphi_i(r)-1]\}}{\delta\varphi_i(r)}=0 \qquad 2.63$$

The single particle Kohn Sham equation becomes,

$$\{-\frac{-\hbar^2}{2m_e}\nabla^2+ V_{ext}(r) + \int dr\ \frac{n(r)}{|r-r'|}+ \frac{\delta E_{xc}[n]}{\delta n}\}\varphi_i(r)= \varepsilon_i\varphi_1(r) \qquad 2.64$$

Which can be solved by iteration until a self-consistency is reached. Because of the inability to obtain the exact form of E_{xc}[n(r)], consistent approximations are needed to exchange correlation energy.

2.8.2.3 Local Density Approximation (LDA)

These are approximations made to the exchange correlation energy, E_{xc}[n(**r**)] functional in the DFT that depend solely upon the value of the electronic density at each point in space (as against the Kohn Sham orbital, which use the derivative of the density). The LDA is the same as functional based on homogeneous electron gas (HEG) approximation. For a spin-unpolarized system, a LDA for the exchange correlation is written as;

$$E_{xc}^{LDA}[\rho]= \int \rho(r)E_{xc}(\rho)dr \qquad 2.65$$

That is, the exchange correlation energy decomposes into exchange and correlation terms linearly, so that the expressions for Ex and Ec are to be found.

$$E_{xc} = E_x + E_c \quad 2.66$$

Ex is exactly known while Ec is not known exactly, leading to further numerous approximation. This method underestimates energy gap values and therefore, not a good predictive tool in analyzing the conductivity and magnetism of systems.

2.8.2.4 Basis Sets

The basis set most commonly used in quantum mechanical calculations are composed of atomic functions. The next approximation expresses the molecular orbitals as linear combinations of a pre-defined set of one-electron functions known as basis function. An individual molecular orbitals is defined as:

$$\phi_i = \sum_{\mu=1}^{N} c_{\mu i}\chi_\mu \quad 2.67$$

where the coefficients $c_{\mu i}$ are known as expansion coefficients for molecular orbitals. The basis function $\chi_1 ... \chi_N$ are also chosen to be normalized. Gaussian-type atomic functions were used as basis functions.

Quantum chemical calculations are performed in modern computational chemistry using a set of finite basis functions, representing the wavefunctions of the system as vectors, whose components corresponds to coefficient in a linear combination of the basis functions in the used basis set. Basis set composing of a finite number of atomic orbitals, centered at each atomic nucleus within the molecule is commonly used. These atomic orbitals are well described with Slater type orbitals (STOs), which decays exponentially with distance from the nuclei accurately describing the long-range overlap between atoms. Because of the computational difficulty, STOs were later discovered that these orbitals could be approximated as linear combination of Gaussian orbitals. It saves time and effort in that it is calculates with Gaussian basis functions the overlap and other integrals. Basis sets include the minimum basis set like the STO-3G which approximates Slater type orbitals with Gaussian functions, polarized basis set like 6-31G* which is used for medium-sized systems, diffuse basis set like 6-31+G* which allows orbitals to occupy a larger region of space, high angular basis set like 6-311++G* which adds multiple polarization function on many systems etc.

2.9 Solvent Models

A lot of theoretical works have been reported in vacuum/gas phase in past and even in recent times, however, in a bid to understand molecular behaviours properly, it is necessary to mimic the real experimental conditions before trying to use theory to corroborate experiments. The solvent continuum model was employed to consider the effects a solvent will have on molecular properties. It is reported that molecules change conformations in different solvent media, depending on the dielectric constants of the solvents under consideration. Researchers have reported that there are changes in molecular properties as solvents were introduced as compared to when the calculations were done in vacuum/gas phase (Targema *et al.,* 2013, Skyner *et al.,* 2015). To account for molecular behaviours via their properties, the solvent models are used (Skyner *et al.,* 2015). The implicit and explicit models have been developed and tested. Owing to computation cost and closeness to experimental results, the implicit model is preferred to the explicit models.

The implicit or continuum models assumes that a homogeneously polarizable medium can replace implicit solvent molecules in as much as the polarizable medium gives similar or equivalent properties (Skyner *et al.,* 2015), with the dielectric constant defining the extent of polarizability of the solvent. They are generally used in Hartree Fock (HF), Post-HF and DFT methods. The explicit model the solvent molecules explicitly. They are generally applied in molecular dynamics (MD), molecular mechanics (MM) or Monte Carlo (MC).

2.9.1 Polarizable Continuum Model and Discrete Model

The Polarizable Continuum Model (PCM) is used to model solvent effects in the field of computational chemistry. This method eradicated the disadvantage of high computational cost modeling of a chemical reaction in solvent media if it considered each solvent molecule as a separate molecule. It models the solvent as a polarizable continuum, rather than individually. The dielectric PCM (D-PCM) is employed, here the continuum is polarizable. This approach is represented by Onsager reaction field model (Onsager, 1936) or the polarizable continuum model, PCM (Fortunelli and Tomasi, 1994). This model views the solvent environment as a homogeneous dielectric continuum medium with its dielectric constant, ε. The solute molecule as described by quantum mechanics is assumed to be within the cavity immersed in the medium. There exists a solvent-solute interaction in which the

dielectric continuum is polarized by the solute, the dielectric continuum in return polarizes the solute charge distribution till an equilibrium is reached. It could be solved by an iterative procedure. The solvent effects can be regarded as a perturbation, H_1, to the Hamiltonian of an isolated solute molecule, H_0.

$$H = H_0 + H_1 \qquad 2.68$$

The charge distribution of the solute molecule in a dielectric continuum model induces polarization vector $\mathbf{P^{tot}}$ in solvent molecules (Mennucci *et al.,* 1998). An approximation is introduced to describe the solvent response, this approximation separates the polarization into two components; optical polarization vector, $\mathbf{P^{op}}$ and inertial/orientational polarization, $\mathbf{P^{in}}$.

$$P^{tot} = P^{op} + P^{in} \qquad 2.69$$

The discrete model assumes that the solute molecule and its surrounding solvents are altogether a giant molecule in which short-range inter-molecular interaction are explicitly treated. This model would have yielded more accurate results if used with the continuum model as semi-continuum model but for its high computational costs.

2.9.3 Solvent effects on NLO processes

Many researchers have reported changes in molecular conformations in solvent media, as a consequence, the molecular properties were altered. Nag and co-workers reported the solvent effects on the two-photon 2PA of non-centrosymmetric rhodamine dyes, they observed no exact correlation between the 2PA cross section and the dielectric constant of the solvent (Nag and Goswani, 2009). Solvents effects on the NLO properties of Z and E isomers of azo-enaminine derivatives were investigated (Machado *et al*, 2016). They observed that solvent have impact on the electronic properties and more pronouncedly on β values. The effects of solvents on the linear and NLO properties of D-A polyenes were investigated (Cammi *et al.,* 1998). Observable changes were seen in the linear and NLO responses. Solvent effects on NLO behaviours of silver nanoclusters were investigated, it was reported that the NLO properties were enhanced in solvent media (Bhavitha *et al.,* 2017). In the same way, solvent effects on NLO properties of some *p*-nitroaniline

derivatives were investigated, it was reported that the NLO properties were enhanced in solvent meida (Pegu, 2012). In light of this, optimizations will be carried out in both vacuum/gas phase and in a solvent, tetrahydrofuran (THF).

2.10 Description of what is to be done

OTBP and its –CHO substituted derivative have been synthesized by Zebiao and co-workers (Zebiao *et al.,* 2015). Their optical energy gaps and UV absorptions were reported in gas phase and in solution of THF. It was observed that these molecules are promising materials for NLO applications; however, their second order susceptibilities were not reported as well as their hyperpolarizability values. This work will use the DFT/B3LYP and BLYP methods to predict the optical energy gaps and UV absorptions vacuum and in solutions to ascertain if it can explain experimental observations and extend the investigation into the molecular first hyperpolarizabilities and the geometric parameters like the bond length alternation, BLA and dihedral angles that affect NLO properties. Other substituted derivatives were also investigated by same methods used in predicting and corroborating experimental findings. 10-MTBP and substituted derivatives, similar to the ones in 10-OTBP were investigated.

MP*m*SB were reported to be promising NLO chromophores by Emese (2010). Also, the molecular properties like molecular first hyperpolarizability which is a measure of second order susceptibility was not considered.

MMP was synthesized by D'Silva and co-workers (D'Silva *et al.,* 2012). They also reported the optical energy gap, UV absorption and the second harmonic generation efficiency and discovered that MMP is 4.13 times better than urea, a standard for organic NLO molecules. DFT methods will be used to determine if it could predicts/corroborates experimental discoveries. Urea is a standard for organic NLO materials, the molecular properties calculated will be compared to available experimental values of that of urea.

CHAPTER THREE

COMPUTATIONAL METHODS

3.1 Quantum Chemical Calculations

The electronic properties of the molecules under investigation done with Spartan 14 software package on intel®Core (TM) i5-3317U CPU @2.50GHz 2.50Hz computer using the *ab* initio restricted hybrid Density Functional Theory (DFT) and the time dependent Density Functional Theory (TDDFT) (Hohenberg and Kohn, 1964; Kohn and Sham, 1965) with the pure Becke (BLYP) and hybrid Becke Three Lee Yang Parr (B3LYP) exchange-correlation method (Becke, 1993). It has been shown that BLYP and B3LYP/6-31G (d) give proper ground state structures of conjugated polymers (Rughooputh *et al.*, 1987) and give accurate results when used to calculate the geometric and electronic properties due to their electron correlation effects. To obtain the lowest energy conformation at the initial point for further calculations, the molecules were submitted to a conformational search around the free rotation bonds using molecular mechanics/MMFF (Merck molecular force field) method. This gives us the local minima, from which the global minimum (lowest energy conformation from the local minima) is selected and subjected to calculations.

The ionization potentials (IPs) and electron affinities (EAs) were calculated from the results obtained from the energies of the HOMO and LUMO respectively. The energy gaps were calculated from the IPs and EAs obtained. The TDDFT at BLYP and B3LYP/6-31G* was used to calculate the UV-vis absorptions and excitation energies. The bond length and bond length alternation (BLA) was obtained to ascertain which of the studied compounds minimized the BLA most.

Two most well-known functionals are the Becke exchange functional $E_x[\rho]$ with 2 extra parameters β and γ (eq. 3.01). BLYP and B3LYP functionals were used to optimize the molecules.

The Lee-Yang-Parr correlation functional $E_c[\rho]$ (eq. 3.2);

$$E_X^B[\rho] = E_X^{LDA} - \beta \int \rho^{\frac{4}{3}} \frac{\chi^2}{1+\gamma\chi^2}, \chi = \frac{|\nabla\rho|^2}{\rho^{\frac{4}{3}}} \quad 3.1$$

Equations 3.1 and 3.2 combined together to form the BLYP functional (eq. 3.3);

The hybrid B3LYP is augmented with 20% HF exchange (eq. 3.4)

$$E_c^{LYP}[\rho] = -a\int \frac{1}{1+d\rho^{\frac{-1}{3}}} \left\{\rho + b\rho^{\frac{-2}{3}}\left[C_F\rho^{\frac{5}{3}} - 2t_w + \left(\frac{1}{9}t_w + \frac{1}{18}\nabla^2\rho\right)\right] e^{-c\rho^{\frac{1}{3}}}\right\} d\mathbf{r} \quad 3.2$$

$$E_{XC}^{BLYP} = E_X^B + E_C^{LYP} = \int \rho(\mathbf{r}) e_X^B(\rho, \nabla\rho) d\mathbf{r} + \int \rho(\mathbf{r}) e_C^{LYP}(\rho, \nabla\rho) d\mathbf{r} \quad 3.3$$

$$E_{XC}^{B3LYP} = aE_X^B + E_C^{LYP} + b\sum_{m,\, n-1}^{N} P_{mn} \sum_{k,l-1}^{N} P_{kl} \left\langle \frac{km}{nl} \right\rangle \quad 3.4$$

All calculations were carried out in isolated gaseous system and in THF at 298.15 K and 1atmosphere pressure.

3.2 Structures of the Studied Molecules

The geometries of 10-octyl-3,7-di(thiophen-2-yl)-*10H*-phenothiazine, named 10-octylthiophene based phenothiazine (10-OTBP), 10-methyl-3,7-di(thiophen-2-yl)-*10H*-phenothiazine, named *10*-methylthiophene based phenothiazine (10-MTBP), 10-methylphenothiazine *mono*-Schiff base (10-MP*m*SB) and 1-[4-({(E)-[4-(methylsulfanyl)phenyl] methylidene}amino)phenyl] ethanone, MMP, MMP are defined using the structure in Figs. 3. 1-3.4. In these structures, different substituent groups are put in place of –R in different positions.

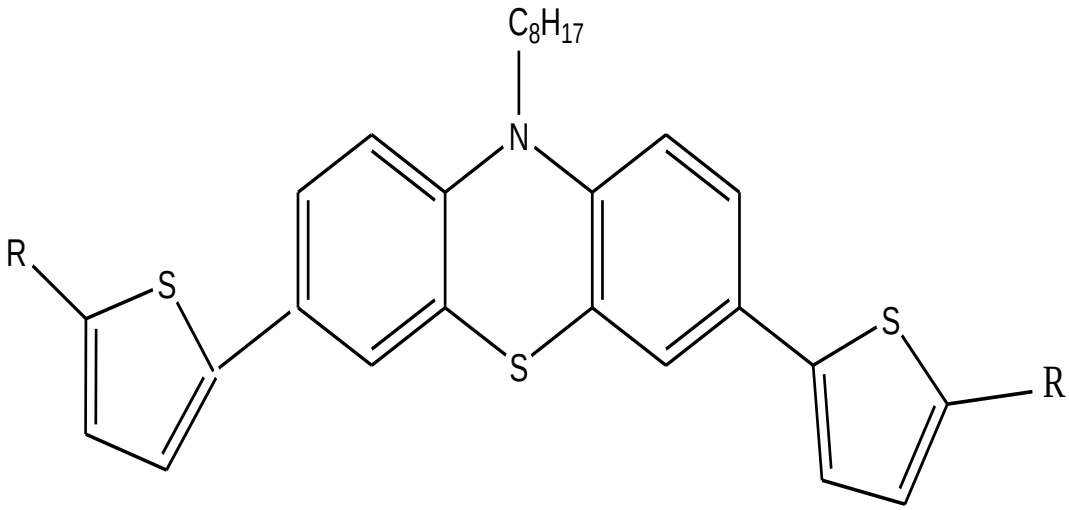

Figure 3.1: Structural representation of 10-OTBP

1a. R = H

1b. R = NO_2

1c. R= CN

1d. R= CHO

1e. R = CH=C(CN)COOH

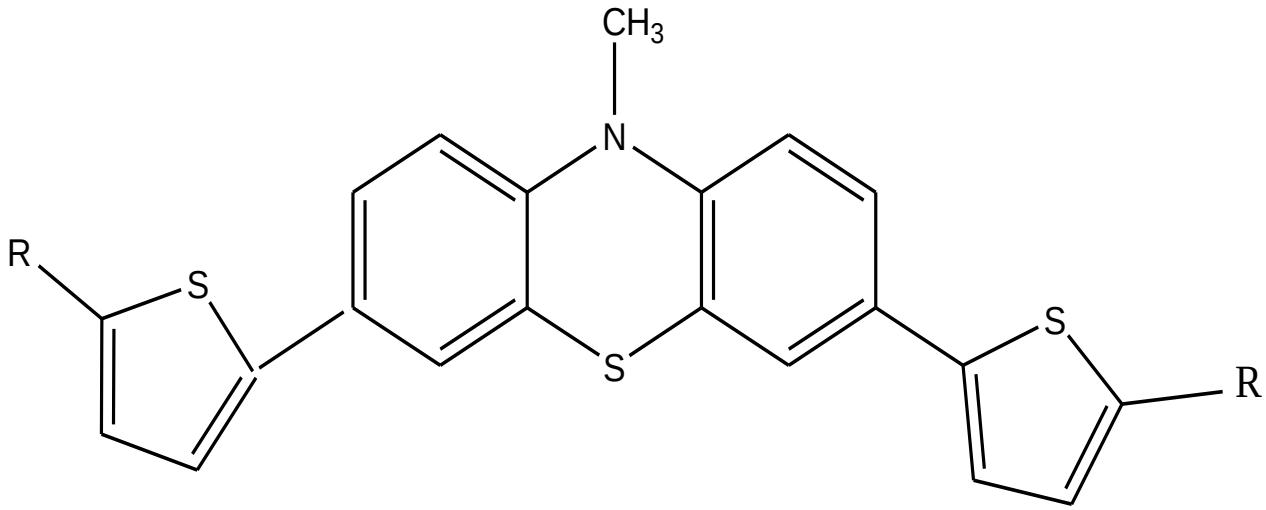

Figure 3.2: Structural representation of 10-MTBP

2a. R = H

2b. R= NO_2

2c. R= CN

2d. R= CHO

2e. R = CH=C(CN)COOH

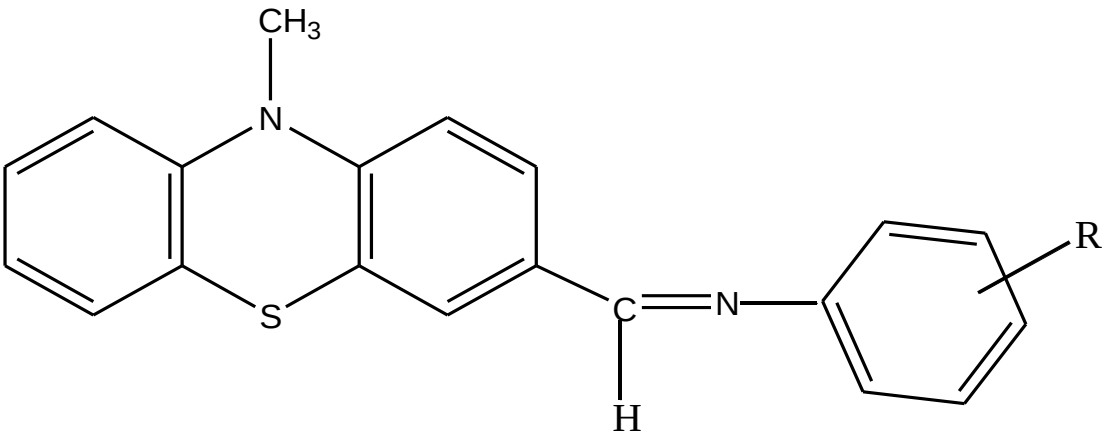

***Figure 3. 3: Structural representation of* 10-MP*m*SB**

3a. R = H

3b. R= *p*-CH=CH_2

3c. R=*m*-NO_2

3d. R= *m*-CN

3e. R= *m*-CHO

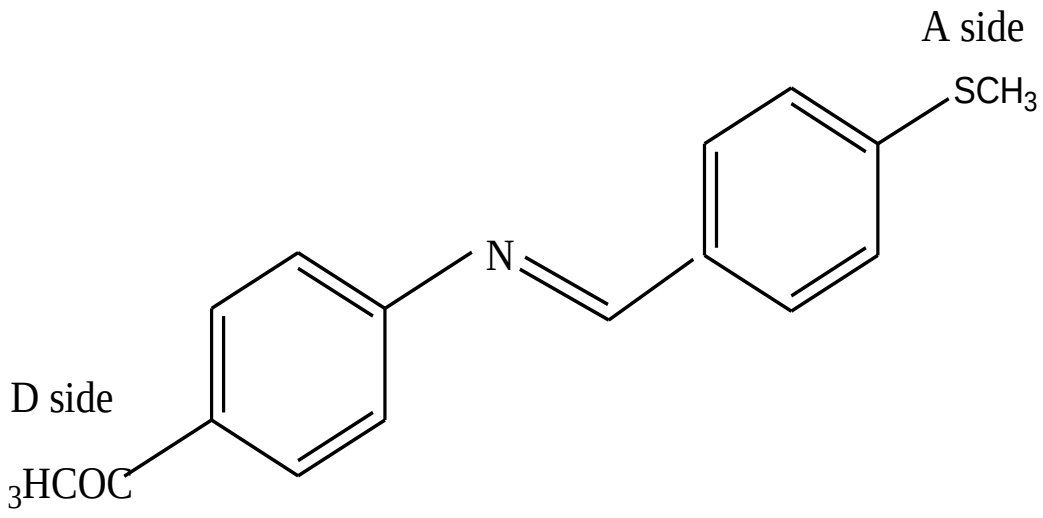

***Figure 3. 4: Structural representation of* MMP**

4a. *A*-$COCH_3$, D-SCH_3, MMP (MMP)

4b. *A*-NO_2, D-SCH_3 (MMPB)

4c. *A*-NO_2, D-NH_2 (MMPC)

4d. *A*-CH=C(CN)COOH, D-SCH_3 (MMPD)

4e. *A*-CH=C(CN)COOH, D-NH_2 (MMPE)

3.3 Geometry Optimization

It is a process of finding an arrangement of a collection of atoms in space where the net inter-atomic force on each atom is assumed to be close to zero and the position of the PES is assumed stationary. '***r***' describes the atomic positions, introducing the concept of the energy, a function of the positions, E(***r***). The problem at hand is to find the value of ***r*** for which E(***r***) is at local minimum, i. e the derivative of the energy with respect to the position of the atom, $\frac{\partial E}{\partial \boldsymbol{r}}$, is the zero vector and the second derivative matrix of the system, $\frac{\partial \partial E}{\partial ri \partial rj}$, which is the Hessian matrix, describes the curvature of the PES at ***r***. The optimization process is often started with an initial guess, with the absence of symmetry i.e. C1 symmetry. The local minimum yields the geometry with the lowest energy and this can be confirmed by subjecting the molecule to a vibrational frequencies calculation to ascertain if there is any imaginary frequency (Henre, 2003). The structural representations of the molecules are shown in Figs. 3.1 - 3.4 and the optimized geometries of the studied molecules are shown below in Figs. 3.5 - 3.8:

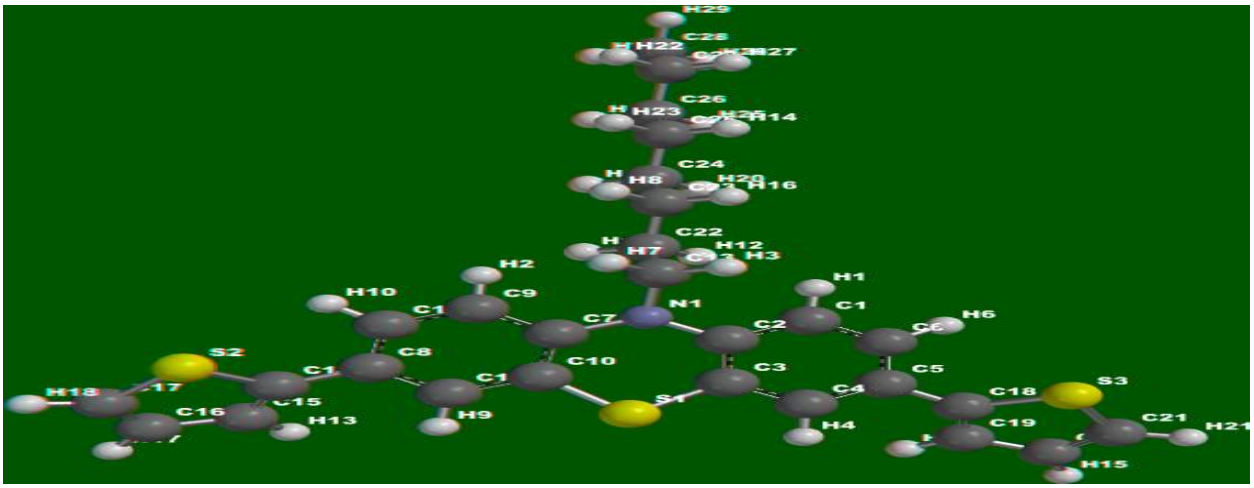

Figure 3.5: Optimized structure of 10-OTBP- ball and spoke model

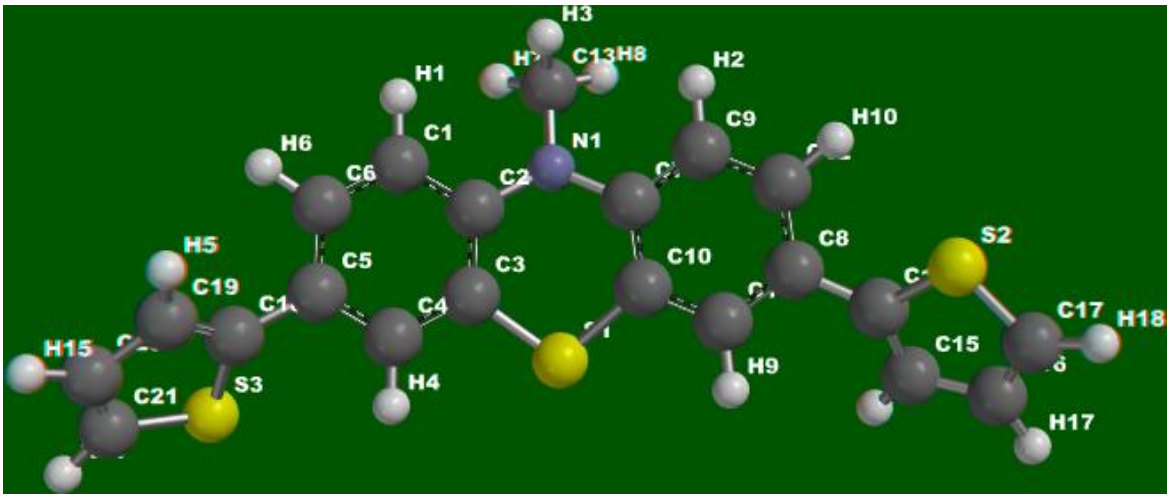

Figure 3.6: Optimized structure of 10-MTBP- ball and spoke model

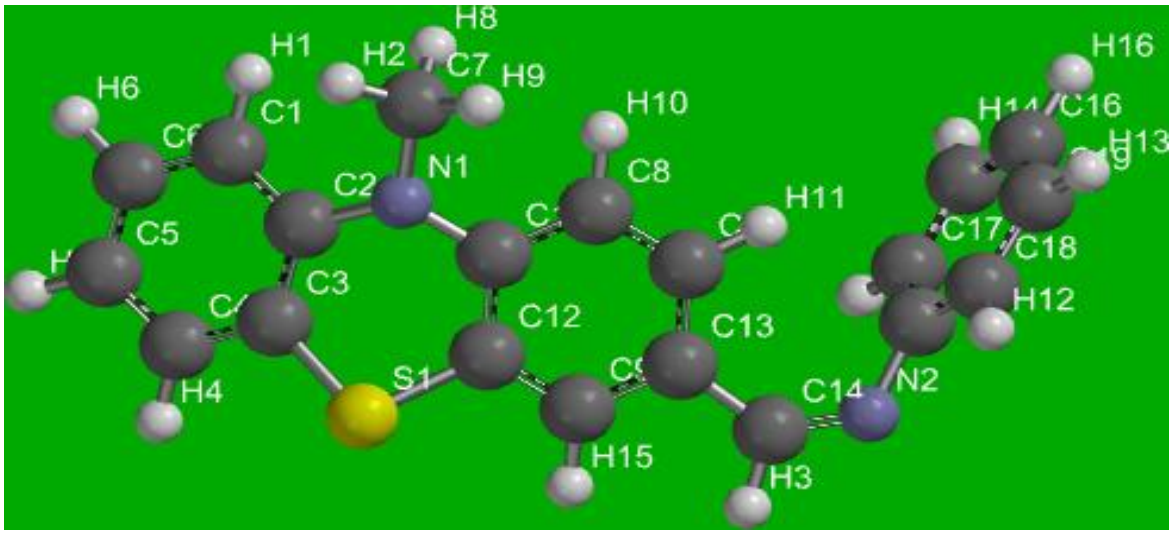

Figure 3.7: Optimized structure of 10-MPmSB- ball and spoke model

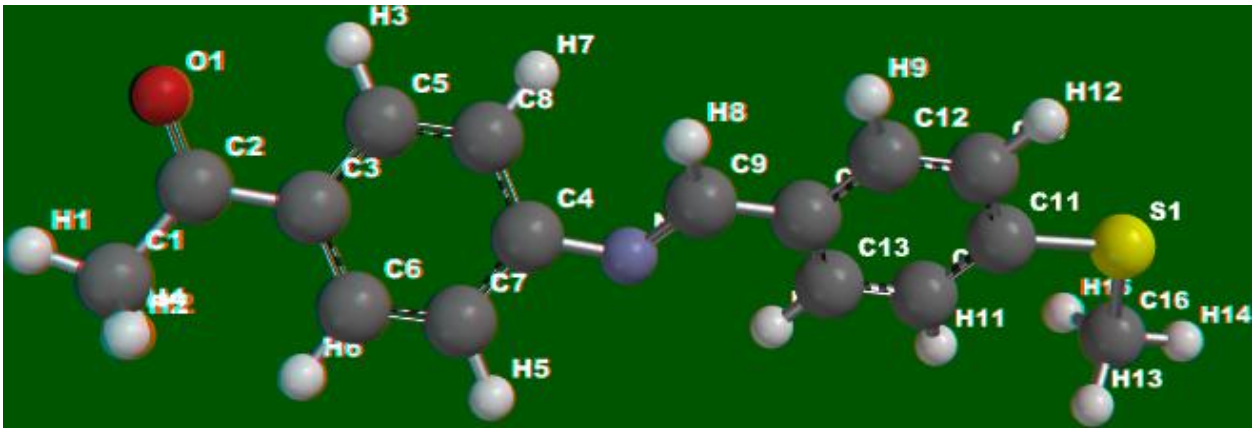

Figure 3.8: Optimized structure of MMP - ball and spoke model

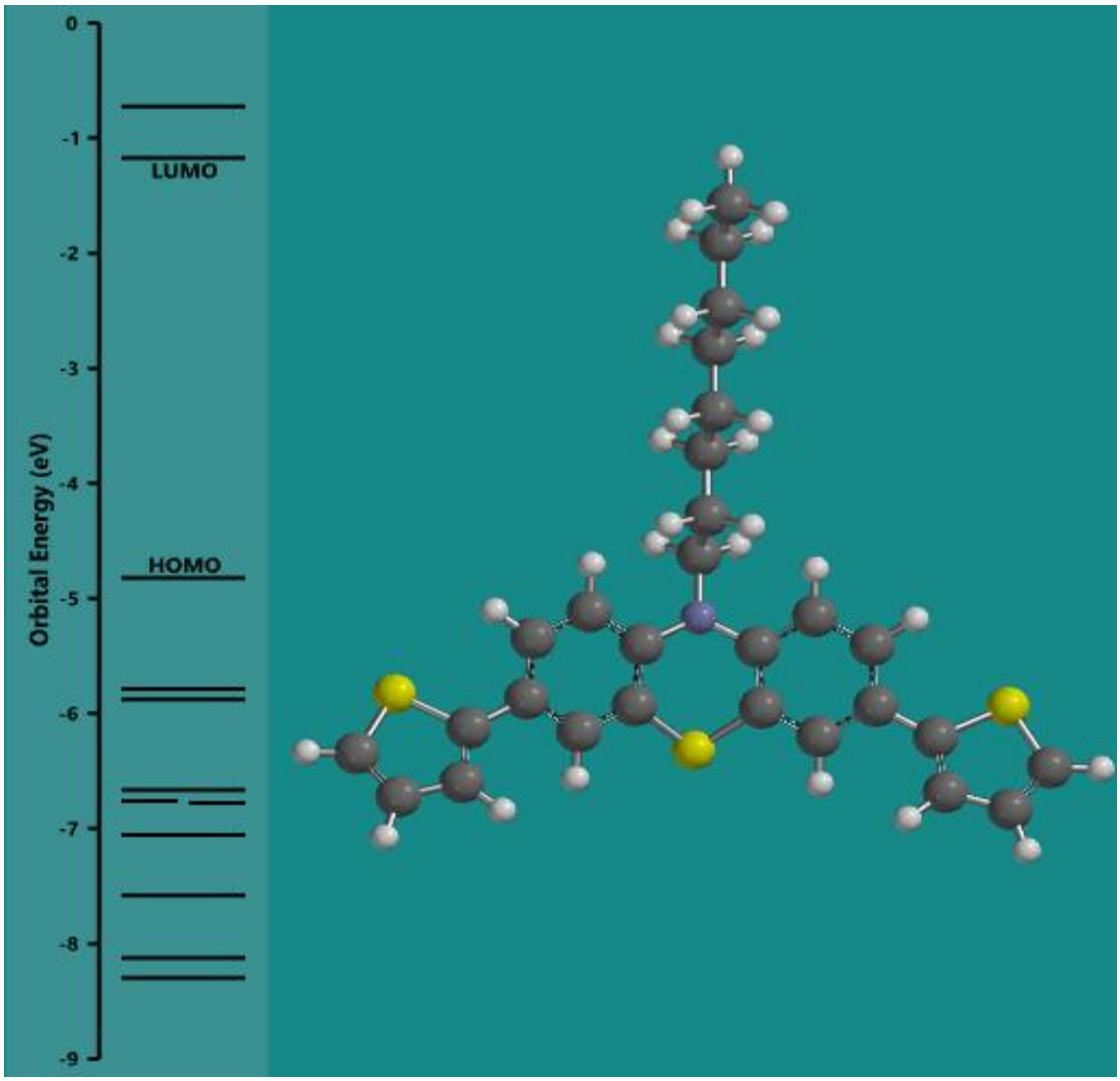

Figure 3.9: An illustration of the HOMO and LUMO energy levels molecules using that of 10-OTBP as example

3.4 Molecular Geometry

The bond lengths, bond angles and dihedral angles are the components of molecular geometry. Bond length, also known as bond distance measures the average distance between the centers of two atoms bonded together in a molecule. The bond angle on the other hand is the angle formed between three atoms across at least two bonds while the dihedral angle is a measure of the angle formed by two intersecting planes, one which contains the first three atoms and the other which contain the last three atom selected. The geometric properties analyzed for this work however, are the bond length because it is needed to determine the bond length alternation (BLA), which is one of the contributing factors that determine the energy gap of molecules and the dihedral angle which tells us about the planarity of the molecules and how it affects their conjugation. These were determined using the *ab* initio restricted DFT method at BLYP/6-31G* and B3LYP/6-31G*.

CHAPTER FOUR

RESULTS AND DISCUSSION

4.1 Geometries of the Studied Systems

The equilibrium geometries for the systems under investigation are presented, the geometric and electronic structures of 10-OTBP, 10-MTBP, 10-MP*m*SB and MMP were used as references to their substituted analogues (Fig. 3.1- 3.4). Their geometric parameters were obtained after total optimization. The Bond lengths with BLAs are recorded in Tables 4.1-4.8 for both BLYP and B3LYP in gas phase and in THF. Both correlations reproduced the same trends.

4.1.1 Structural and Solvent Dependence on the Bond Length and Bond Length Alternation (BLA)

For 10-OTBP and substituted derivatives, the calculated bond lengths of the reference molecule (i.e when R = H) are 1.401 Å for C_{12}-C_8, 1.406 Å for C_8-C_{11}, 1.466 Å for C_8-C_{14}, 1.377 Å for C_{14}-C_{15}, 1.425 Å for C_{15}-C_{16}, 1.367 Å for C_{16}-C_{17}, 1.735 Å for C_{17}-S_2 and 1.082 Å for C_{17}-H_{18}. For 10-MTBP and substituted derivatives, the calculated bond lengths of the reference molecule (i.e when R = H) are 1.402 Å for C_{12}-C_8, 1.407 Å for C_8-C_{11}, 1.467 Å for C_8-C_{14}, 1.377 Å for C_{14}-C_{15}, 1.425 Å for C_{15}-C_{16}, 1.367 Å for C_{16}-C_{17}, 1.735 Å for C_{17}-S_2 and 1.082 Å for C_{17}-H_{18}. Optimal NLO responses of molecules can be achieved by distorting the conjugation bridge to form a fully delocalized ionic cyanine-like structure from a polyenic-like structure (Thorley *et al.*, 2013). Solvents, as reported, greatly affect molecular NLO properties (Gao and Alhambra, 1997). It is therefore expected that molecular properties like BLA will be enhanced with substituents and in solutions. In a bid to take into account medium effects on these properties, optimizations were carried out in THF. The BLAs of the derivatized molecules were lower than those of the reference/unsubstituted ones. Molecular properties e.g dihedral angles, dipole moments,

polarizabilities, UV-vis absorptions, energy gaps, and hyperpolarizabilities were also investigated to compare the derivatized molecules with the reference ones. The global reactivity descriptors were also analyzed.

Donor and acceptor substituent groups altered the nonlinearity of molecules as seen in Tables 4.1-4.8 and Figures 4.1-4.4, the derivatized amolecules have lowered BLAs. This will definitely affect the molecules' NLO characters. The Bond lengths with BLAs of 10-MP*m*SB and its substituted analogues are presented on Tables 4.5 and 4.6 and Figures 4.1 – 4.4.

4.1.2 Structural and Solvent Dependence on Dihedral Angles (Ɵ)

The dihedral angle also known as the torsional angle, measures the angle formed by two intersecting planes, one with the first three atoms selected and the other which selected the last three atoms (Fig. 4.5). That is, between the donor and the acceptor, there are deviations from coplanarity and are observed to vary with different substituent groups, it is used to specify the molecular conformation. From Tables 4.9 – 4.16, all compounds studied are all planar. This is due to the delocalization of π-electrons and the lone pair on nitrogen.

Table 4.1: Bond lengths with BLAs (Å) of 10-OTBPs [B3LYP (vacuum) and THF (ε = 7.58)].

Molecules	C_{12}-C_8	C_8-C_{11}	C_8-C_{14}	C_{14}-C_{15}	C_{15}-C_{16}	C_{16}-C_{17}	C_{17}-S_2	C_{17}-H_{18}	BLA(Å)
				VACUUM					
R=H	1.401	1.406	1.466	1.377	1.425	1.367	1.735	1.082	0.269
2-NO_2	1.402	1.407	1.462	1.386	1.412	1.373	1.737	1.429	0.199
2-CN	1.401	1.406	1.464	1.382	1.414	1.380	1.752	1.414	0.209
2-CHO	1.401	1.406	1.463	1.386	1.411	1.380	1.750	1.460	0.201
2-CH=C(CN)COOH	1.402	1.407	1.460	1.389	1.405	1.392	1.769	1.429	0.210
				THF					
R=H	1.403	1.407	1.467	1.376	1.424	1.366	1.736	1.082	0.269
2-NO_2	1.404	1.408	1.461	1.389	1.407	1.377	1.740	1.417	0.200
2-CN	1.403	1.407	1.463	1.383	1.411	1.381	1.753	1.407	0.209
2-CHO	1.403	1.407	1.464	1.387	1.408	1.381	1.751	1.453	0.201
2-CH=C(CN)COOH	1.404	1.409	1.459	1.392	1.401	1.395	1.763	1.420	0.208

Table 4.2: Bond lengths with BLAs (Å) of 10-OTBPs [BLYP (vacuum) and THF (ε = 7.58)].

Molecules	C_{12}-C_8	C_8-C_{11}	C_8-C_{14}	C_{14}-C_{15}	C_{15}-C_{16}	C_{16}-C_{17}	C_{17}-S_2	C_{17}-H_{18}	BLA(Å)
				VACUUM					
R=H	1.413	1.419	1.470	1.390	1.431	1.379	1.753	1.089	0.267
2-NO_2	1.414	1.420	1.467	1.401	1.418	1.386	1.755	1.439	0.199
2-CN	1.413	1.421	1.469	1.394	1.420	1.393	1.774	1.416	0.212
2-CHO	1.415	1.420	1.468	1.400	1.416	1.393	1.773	1.466	0.203
2-CH=C(CN)COOH	1.416	1.421	1.465	1.403	1.411	1.405	1.785	1.430	0.212
				THF					
R=H	1.414	1.42	1.471	1.389	1.431	1.378	1.754	1.089	0.269
2-NO_2	1.416	1.421	1.463	1.403	1.412	1.391	1.76	1.424	0.200
2-CN	1.415	1.42	1.467	1.396	1.416	1.396	1.776	1.408	0.213
2-CHO	1.416	1.42	1.467	1.401	1.413	1.396	1.774	1.457	0.204
2-CH=C(CN)COOH	1.416	1.421	1.465	1.403	1.411	1.405	1.785	1.43	0.212

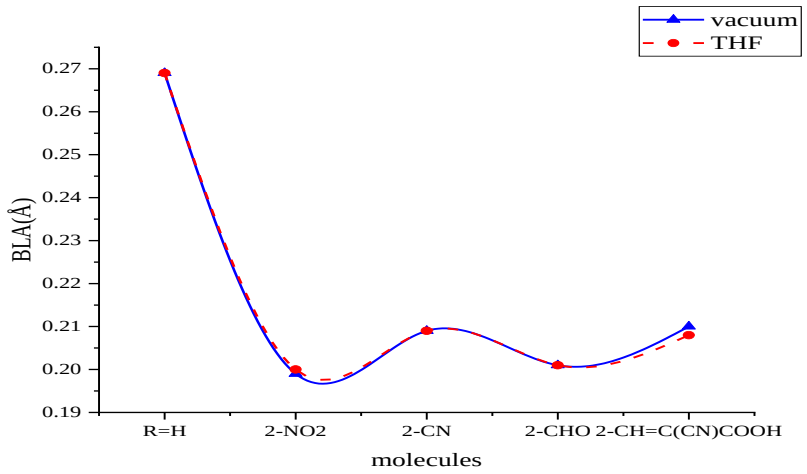

Figure 4.1a: BLAs for 10-OTBPs (B3LYP)

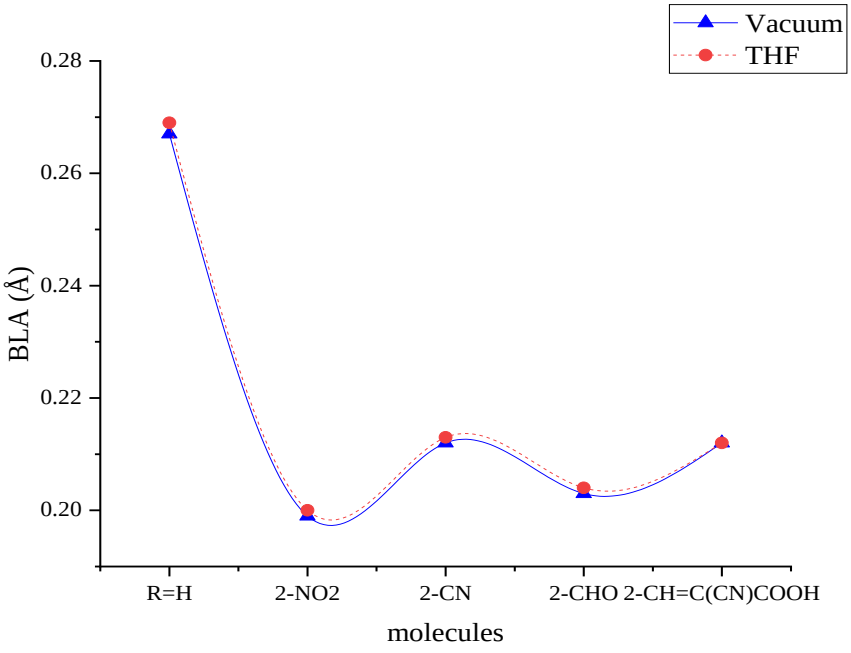

Figure 4.1b: BLAs for 10-OTBPs (BLYP)

Table 4.3: Bond lengths with BLAs (Å) of 10-MTBPs [B3LYP (vacuum) and THF (ε = 7.58)].

Molecules	C_{12}-C_8	C_8-C_{11}	C_8-C_{14}	C_{14}-C_{15}	C_{15}-C_{16}	C_{16}-C_{17}	C_{17}-S_2	C_{17}-H_{18}	BLA(Å)
				VACUUM					
R=H	1.402	1.407	1.467	1.377	1.425	1.367	1.735	1.082	0.269
2-NO_2	1.403	1.408	1.464	1.386	1.413	1.373	1.737	1.429	0.199
2-CN	1.403	1.407	1.465	1.381	1.415	1.379	1.751	1.414	0.208
2-CHO	1.403	1.408	1.465	1.386	1.411	1.380	1.750	1.461	0.201
2-CH=C(CN)COOH	1.404	1.408	1.462	1.388	1.406	1.391	1.762	1.428	0.208
				THF					
R=H	1.403	1.407	1.467	1.377	1.425	1.366	1.736	1.082	0.269
2-NO_2	1.404	1.408	1.461	1.389	1.407	1.377	1.740	1.417	0.200
2-CN	1.403	1.407	1.464	1.383	1.411	1.382	1.753	1.407	0.209
2-CHO	1.403	1.408	1.464	1.387	1.408	1.382	1.751	1.453	0.201
2-CH=C(CN)COOH	1.404	1.409	1.459	1.392	1.401	1.395	1.763	1.420	0.208

Table 4.4: Bond lengths with BLAs (Å) of 10-MTBPs [BLYP (vacuum) and THF (ε = 7.58)].

Molecules	C_{12}-C_8	C_8-C_{11}	C_8-C_{14}	C_{14}-C_{15}	C_{15}-C_{16}	C_{16}-C_{17}	C_{17}-S_2	C_{17}-H_{18}	BLA(Å)
				VACUUM					
R=H	1.414	1.419	1.471	1.390	1.431	1.379	1.753	1.089	0.267
2-NO_2	1.415	1.420	1.467	1.400	1.418	1.386	1.757	1.439	0.199
2-CN	1.415	1.420	1.469	1.395	1.420	1.393	1.774	1.416	0.212
2-CHO	1.415	1.420	1.468	1.400	1.416	1.393	1.773	1.466	0.203
2-CH=C(CN)COOH	1.416	1.421	1.465	1.403	1.411	1.405	1.785	1.430	0.212
				THF					
R=H	1.414	1.42	1.471	1.389	1.431	1.378	1.754	1.089	0.269
2-NO_2	1.416	1.421	1.463	1.403	1.412	1.391	1.76	1.424	0.200
2-CN	1.415	1.42	1.467	1.396	1.416	1.396	1.776	1.408	0.213
2-CHO	1.416	1.42	1.467	1.401	1.413	1.396	1.774	1.457	0.204
2-CH=C(CN)COOH	1.416	1.421	1.465	1.403	1.411	1.405	1.785	1.43	0.212

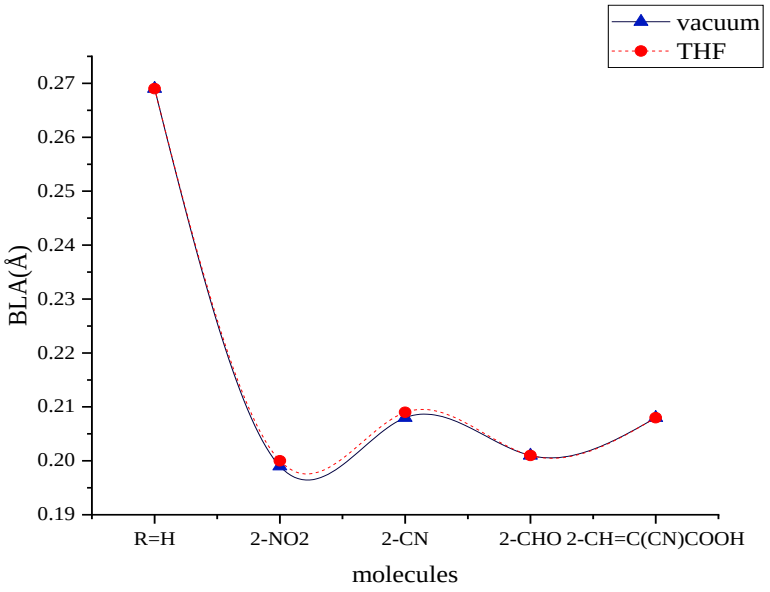

Figure 4.2a: BLAs of 10-MTBPs (B3LYP)

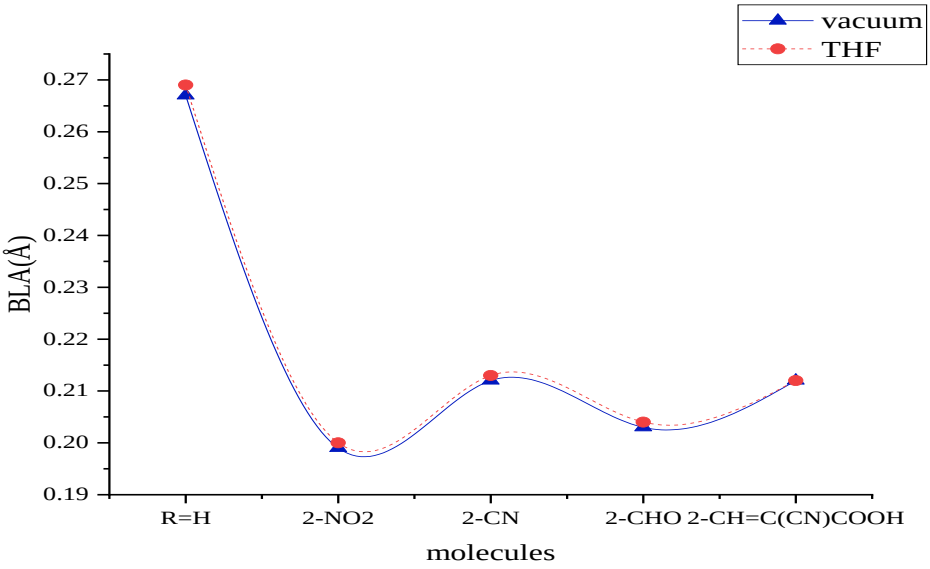

Figure 4.2b: BLAs of 10-MTBPs (BLYP)

Table 4.5: Bond lengths with BLAs (Å) of 10-MP*m*SBs [B3LYP (vacuum) and THF (ε = 7.58)].

Molecules	C_{12}-N_2	N_2-C_{15}	C_{15}-C_{18}	C_{18}-C_{19}	C_{19}-C_{16}	C_{16}-C_{20}	C_{20}-C_{17}	C_{16}-H_{16}	BLA(Å)
				VACUUM					
R=H	1.278	1.405	1.405	1.394	1.397	1.397	1.394	1.086	0.217
p-CH=CH_2	1.278	1.402	1.408	1.388	1.408	1.405	1.392	1.469	0.082
m-NO_2	1.280	1.400	1.407	1.394	1.394	1.393	1.391	1.474	0.075
m-CN	1.280	1.401	1.407	1.394	1.393	1.404	1.402	1.435	0.073
m-CHO	1.279	1.403	1.406	1.397	1.391	1.403	1.399	1.481	0.079
				THF					
R=H	1.283	1.406	1.406	1.394	1.396	1.396	1.394	1.085	0.215
p-CH=CH_2	1.284	1.402	1.408	1.388	1.408	1.406	1.391	1.47	0.081
m-NO_2	1.284	1.400	1.408	1.394	1.394	1.394	1.393	1.469	0.072
m-CN	1.284	1.400	1.408	1.393	1.393	1.405	1.404	1.432	0.071
m-CHO	1.283	1.403	1.406	1.397	1.391	1.403	1.400	1.478	0.078

Table 4.6: Bond lengths with BLAs (Å) of 10-MP*m*SBs [BLYP (vacuum) and THF (ε = 7.58)].

Molecules	C_{12}-N_2	N_2-C_{15}	C_{15}-C_{18}	C_{18}-C_{19}	C_{19}-C_{16}	C_{16}-C_{20}	C_{20}-C_{17}	C_{16}-H_{16}	BLA (Å)
VACUUM									
R=H	1.292	1.413	1.417	1.404	1.407	1.407	1.404	1.094	0.216
p-CH=CH_2	1.293	1.410	1.420	1.397	1.420	1.417	1.400	1.474	0.081
m-NO_2	1.294	1.408	1.420	1.404	1.404	1.404	1.401	1.491	0.074
m-CN	1.294	1.408	1.419	1.403	1.403	1.417	1.414	1.439	0.070
m-CHO	1.294	1.410	1.418	1.407	1.401	1.414	1.410	1.488	0.077
THF									
R=H	1.298	1.414	1.418	1.404	1.407	1.406	1.404	1.093	0.213
p-CH=CH_2	1.299	1.409	1.421	1.397	1.420	1.417	1.400	1.474	0.079
m-NO_2	1.299	1.407	1.421	1.403	1.404	1.405	1.404	1.484	0.069
m-CN	1.299	1.408	1.420	1.403	1.402	1.417	1.416	1.435	0.067
m-CHO	1.298	1.411	1.419	1.407	1.400	1.415	1.411	1.484	0.076

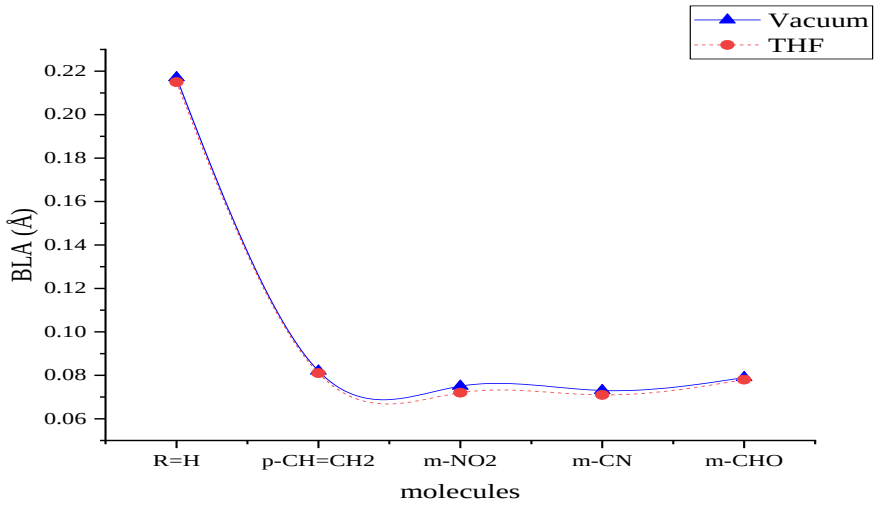

Figure 4.3a: BLAs of 10-MPmSBs (B3LYP)

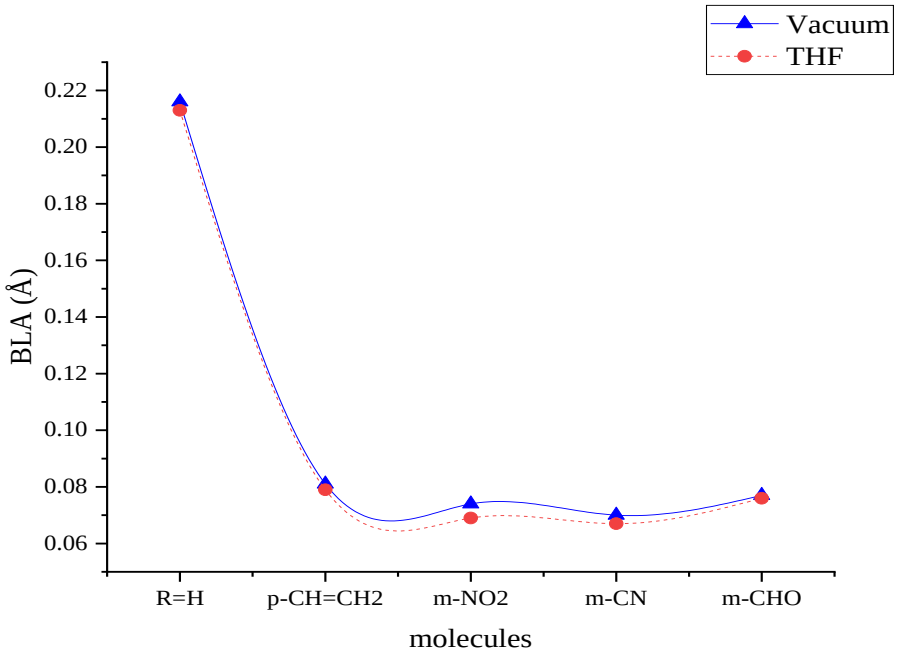

Figure 4.3b: BLAs of 10-MPmSBs (BLYP)

Table 4.7: Bond lengths with BLAs (Å) of 10-MMPs [B3LYP (vacuum) and THF (ε = 7.58)].

Molecules	C_3-C_2	C_3-C_5	C_3-C_6	N_1-C_9	C_{11}-S_1	C_{11}-C_{15}	C_{11}-C_{14}	BLA
			VACUUM					
A-$COCH_3$, D-SCH3, MMP	1.495	1.404	1.405	1.283	1.777	1.406	1.406	0.182
A-NO_2, D-SCH_3	1.465	1.397	1.395	1.284	1.776	1.406	1.406	0.174
A-NO_2, D-NH_2	1.463	1.397	1.395	1.287	1.383	1.408	1.413	0.057
A-CH=C(CN)COOH, D-SCH_3	1.462	1.411	1.413	1.285	1.755	1.407	1.406	0.160
A-CH=C(CN)COOH, D-NH_2	1.461	1.411	1.414	1.288	1.382	1.409	1.413	0.062
			THF					
A-$COCH_3$, D-SCH3, MMP	1.494	1.405	1.406	1.288	1.777	1.406	1.406	0.181
A-NO_2, D-SCH_3	1.457	1.399	1.397	1.289	1.776	1.406	1.407	0.169
A-NO_2, D-NH_2	1.454	1.398	1.398	1.288	1.367	1.412	1.417	0.063
A-CH=C(CN)COOH, D-SCH_3	1.467	1.400	1.399	1.296	1.784	1.400	1.399	0.176
A-CH=C(CN)COOH, D-NH_2	1.455	1.428	1.430	1.313	1.368	1.426	1.431	0.067

Table 4.8: Bond lengths with BLAs (Å) of 10-MMPs [BLYP (vacuum) and THF (ε = 7.58)].

Molecules	C_3-C_2	C_3-C_5	C_3-C_6	N_1-C_9	C_{11}-S_1	C_{11}-C_{15}	C_{11}-C_{14}	BLA
				VACUUM				
A-$COCH_3$, D-SCH3, MMP	1.503	1.416	1.417	1.299	1.792	1.417	1.417	0.182
A-NO_2, D-SCH_3	1.497	1.408	1.406	1.300	1.790	1.418	1.417	0.181
A-NO_2, D-NH_2	1.476	1.407	1.407	1.296	1.394	1.419	1.423	0.058
A-CH=C(CN)COOH, D-SCH_3	1.465	1.425	1.427	1.301	1.790	1.418	1.418	0.164
A-CH=C(CN)COOH, D-NH_2	1.464	1.425	1.427	1.304	1.391	1.42	1.424	0.060
				THF				
A-$COCH_3$, D-SCH3, MMP	1.501	1.416	1.417	1.304	1.792	1.417	1.418	0.180
A-NO_2, D-SCH_3	1.469	1.410	1.408	1.305	1.791	1.418	1.418	0.170
A-NO_2, D-NH_2	1.466	1.409	1.410	1.303	1.375	1.424	1.429	0.063
A-CH=C(CN)COOH, D-SCH_3	1.458	1.426	1.428	1.306	1.791	1.418	1.418	0.164
A-CH=C(CN)COOH, D-NH_2	1.455	1.428	1.430	1.313	1.368	1.426	1.431	0.067

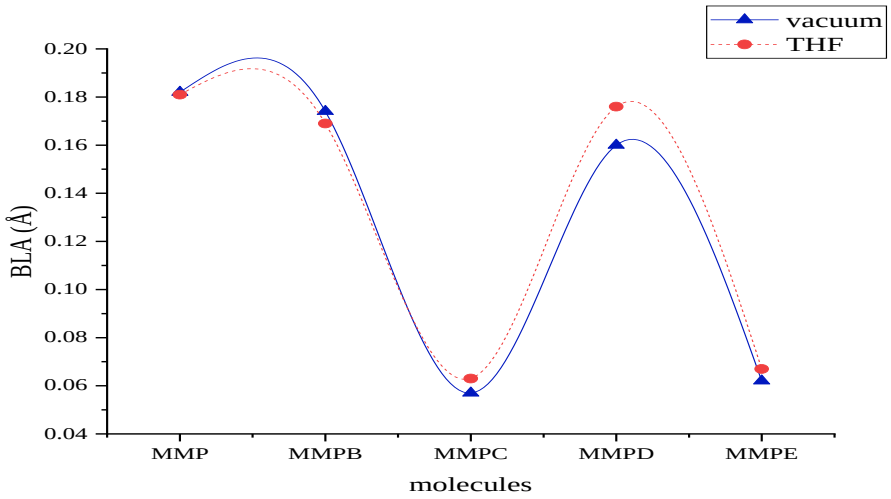

Figure 4.4a: BLAs of MMPs (B3LYP)

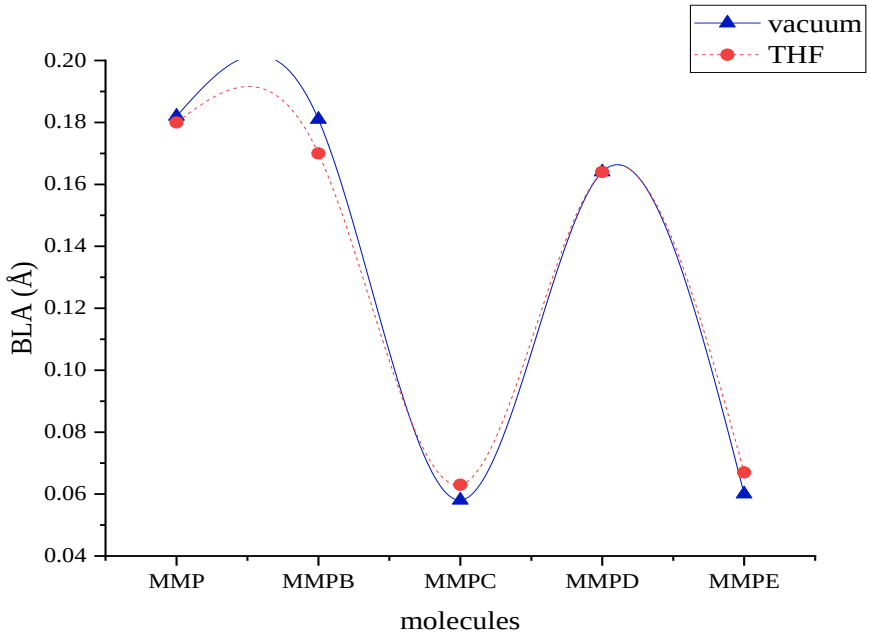

Figure 4.4b: BLAs of MMPs (BLYP/)

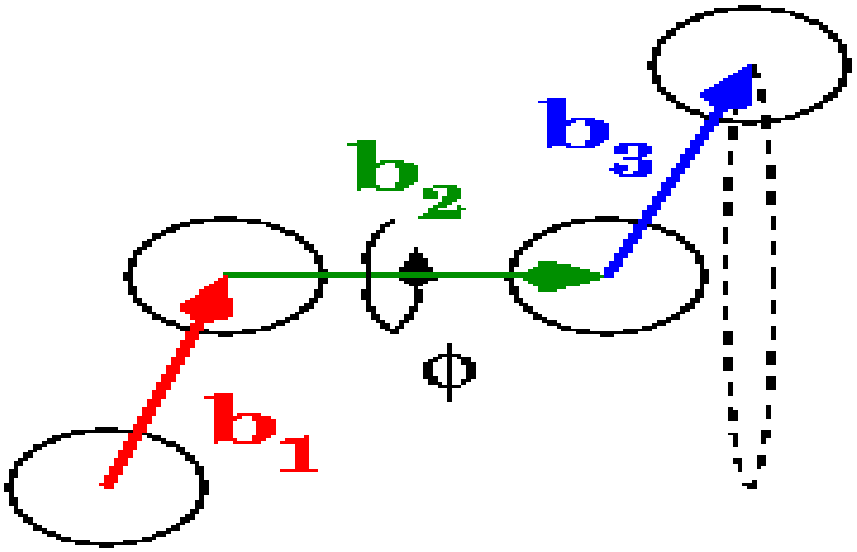

Figure 4.5: Illustrations of the dihedral angle

Table 4.9: Selected dihedral angles (°) of 10-OTBPs [B3LYP (vacuum) and THF (ε = 7.58)]

Molecules	C_{14}-C_{15}-C_{16}-C_{17}	C_{15}-C_{16}-C_{17}-S_2	C_{16}-C_{17}-S_2-C_{14}	C_{15}-C_{16}-C_{17}-H_{18}
		VACUUM		
R=H	0.04	-0.46	0.57	179.78
2-NO_2	-0.03	-0.53	0.72	179.52
2-CN	-0.02	-0.58	0.78	179.42
2-CHO	0.08	0.43	-0.63	-179.60
2-CH=C(CN)COOH	0.03	0.38	0.51	179.76
		THF		
R=H	-0.03	-0.40	-0.51	-179.65
2-NO_2	-0.04	0.49	-0.68	-179.56
2-CN	0.02	0.62	-0.84	-179.48
2-CHO	-0.03	-0.53	-0.73	179.53
2-CH=C(CN)COOH	0.02	0.39	-0.54	-179.89

Table 4.10: Selected dihedral angles (°) of 10-OTBPs [BLYP (vacuum) and THF (ε = 7.58)]

Molecules	C_{14}-C_{15}-C_{16}-C_{17}	C_{15}-C_{16}-C_{17}-S_2	C_{16}-C_{17}-S_2-C_{14}	C_{15}-C_{16}-C_{17}-H_{18}
		VACUUM		
R=H	0.02	0.30	-0.42	-179.65
2-NO_2	0.04	-0.45	-0.64	-179.61
2-CN	0.01	-0.49	-0.670	-179.68
2-CHO	0.01	0.43	-0.57	-179.68
2-CH=C(CN)COOH	-0.01	0.30	-0.42	-179.83
		THF		
R=H	-0.04	0.30	-0.43	-179.65
2-NO_2	0.13	-0.39	-0.61	-179.69
2-CN	0.06	-0.56	-0.76	-179.60
2-CHO	0.07	0.44	-0.63	-179.61
2-CH=C(CN)COOH	-0.07	0.49	-0.60	-179.59

Table 4.11: Selected dihedral angles (°) of 10-MTBPs [B3LYP (vacuum) and THF (ε = 7.58)]

Molecules	C_{14}-C_{15}-C_{16}-C_{17}	C_{15}-C_{16}-C_{17}-S_2	C_{16}-C_{17}-S_2-C_{14}	C_{15}-C_{16}-C_{17}-H_{18}
		VACUUM		
R=H	0.00	0.32	-0.43	-179.68
2-NO_2	0.02	0.50	-0.67	-179.64
2-CN	-0.00	0.56	-0.74	-179.56
2-CHO	-0.01	0.50	-0.65	-179.66
2-CH=C(CN)COOH	0.01	0.38	-0.51	-179.80
		THF		
R=H	-0.04	0.40	-0.51	-179.65
2-NO_2	0.06	0.49	-0.68	-179.59
2-CN	0.04	0.62	-0.84	-179.50
2-CHO	-0.03	0.57	-0.73	-179.59
2-CH=C(CN)COOH	0.02	0.39	-0.54	-179.89

Table 4.12: Selected dihedral angles (°) of 10-MTBPs [BLYP (vacuum) and THF (ε = 7.58)]

Molecules	C_{14}-C_{15}-C_{16}-C_{17}	C_{15}-C_{16}-C_{17}-S_2	C_{16}-C_{17}-S_2-C_{14}	C_{15}-C_{16}-C_{17}-H_{18}
		VACUUM		
R=H	0.03	0.31	-0.42	-179.66
2-NO_2	0.05	0.45	-0.62	-179.62
2-CN	0.01	0.52	-0.69	-179.70
2-CHO	0.03	0.43	-0.59	-179.68
2-CH=C(CN)COOH	0.01	0.33	-0.44	-179.85
		THF		
R=H	0.06	0.30	-0.43	-179.65
2-NO_2	0.15	0.39	-0.61	-179.69
2-CN	0.07	0.56	-0.78	-179.60
2-CHO	0.07	0.44	-0.63	-179.61
2-CH=C(CN)COOH	-0.07	0.49	-0.60	-179.59

Table 4.13: Selected dihedral angles (°) of 10-MP*m*SBs [B3LYP (vacuum) and THF (ε = 7.58)]

Molecules	C_{15}-C_{18}-C_{19}-C_{16}	H_{12}-C_{18}-C_{19}-C_{16}	C_{18}-C_{19}-C_{16}-C_{20}	H_{16}-C_{16}-C_{19}-C_{18}
		VACUUM		
R=H	-1.11	179.08	-0.12	-179.46
***p*-CH=CH$_2$**	-1.33	179.96	-0.12	-179.87
***m*-NO$_2$**	0.03	-179.59	0.63	179.57
***m*-CN**	-1.44	178.72	0.09	-179.33
***m*-CHO**	0.06	-179.67	0.73	-179.92
		THF		
R=H	-0.36	179.42	-0.24	-179.82
***p*-CH=CH$_2$**	-0.91	179.55	-0.08	-179.95
***m*-NO$_2$**	-0.03	-179.93	0.49	-179.93
***m*-CN**	-0.75	179.30	-0.13	-179.74
***m*-CHO**	0.19	-179.61	0.44	-180.00

Table 4.14: Selected dihedral angles (°) of 10-MP*m*SBs [BLYP (vacuum) and THF (ε = 7.58)]

Molecules	C_{15}-C_{18}-C_{19}-C_{16}	H_{12}-C_{18}-C_{19}-C_{16}	C_{18}-C_{19}-C_{16}-C_{20}	H_{16}-C_{16}-C_{19}-C_{18}
		VACUUM		
Standard	-1.12	179.11	-0.04	-179.36
***p*-CH=CH$_2$**	-1.48	178.93	0.08	-179.71
***m*-NO$_2$**	-0.02	-179.45	0.59	-179.93
***m*-CN**	-1.44	178.69	0.15	-179.28
***m*-CHO**	0.04	-179.60	0.69	-179.90
		THF		
Standard	-0.39	179.37	-0.20	-179.80
***p*-CH=CH$_2$**	-1.03	179.48	-0.09	179.98
***m*-NO$_2$**	-0.11	-179.64	0.39	179.99
***m*-CN**	-0.69	179.26	-0.11	-179.71
***m*-CHO**	0.34	-179.64	0.36	179.91

Table 4.15: Selected dihedral angles (°) of MMPs [B3LYP (vacuum) and THF (ε = 7.58)]

Molecules	H_5-C_4-C_{10}-H_{11}	H_6-C_4-C_{10}-H_{10}	N_1-C_9- C_{10}-C_{13}	C_5-C_8- C_4-N_1
		VACUUM		
A-$COCH_3$, D-SCH3, MMP	44.29(52.09)	60.51(52.44)	1.93	178.72
A-NO_2, D-SCH_3	133.59	144.32	-1.23	179.10
A-NO_2, D-NH_2	133.91	145.03	-1.07	179.15
A-CH=C(CN)COOH, D-SCH_3	44.43	58.14	2.02	178.24
A-CH=C(CN)COOH, D-NH_2	43.02	57.28	1.58	178.65
		THF		
A-$COCH_3$, D-SCH3, MMP	43.44	59.17	1.87	178.69
A-NO_2, D-SCH_3	134.58	144.98	-1.18	178.94
A-NO_2, D-NH_2	136.97	147.55	0.06	176.90
A-CH=C(CN)COOH, D-SCH_3	78.67	101.29	-0.58	179.10
A-CH=C(CN)COOH, D-NH_2	40.19	52.80	1.48	178.85

Experimental results in brackets (D'Silva et al., 2012).

Table 4.16: Selected dihedral angles (°) of MMPs [BLYP (vacuum) and THF (ε = 7.58)]

Molecules	H_5-C_4-C_{10}-H_{11}	H_6-C_4-C_{10}-H_{10}	N_1-C_9- C_{10}-C_{13}	C_5-C_8- C_4-N_1
		VACUUM		
A-$COCH_3$, D-SCH3, MMP	44.15(52.09)	59.20(52.44)	1.98	178.31
A-NO_2, D-SCH_3	134.57	144.68	-0.78	176.68
A-NO_2, D-NH_2	90.45	107.79	-0.56	176.71
A-CH=C(CN)COOH, D-SCH_3	45.10	60.60	2.21	178.72
A-CH=C(CN)COOH, D-NH_2	43.02	57.28	1.58	178.65
		THF		
A-$COCH_3$, D-SCH3, MMP	43.39	57.94	2.08	178.25
A-NO_2, D-SCH_3	135.26	144.97	-0.99	178.58
A-NO_2, D-NH_2	90.18	106.83	0.08	176.37
A-CH=C(CN)COOH, D-SCH_3	44.41	57.51	2.03	178.30
A-CH=C(CN)COOH, D-NH_2	38.51	48.07	1.27	178.42

Experimental results in brackets (D'Silva *et al.*, 2012).

In describing the NLO responses of non-centrosymmetric molecules, intramolecular charge transfer excitations are important (Sanusi *et al.*, 2014). It has been established from the reports of previous researchers that the polarizabilities, hyperpolarizabilities and dipole moments of molecules increase with decreasing HOMO-LUMO energy gaps (Da Silva *et al.*, 2006). E_g increases with increasing angle twists, from the Tables (4.9 - 4.16), as substitution occurs, the substituted derivatives curved from their positions. This is also also observed in THF. That is, the internal rotations of the molecules were enhanced both with substitution and in solution. This is because the steric and inductive effects are increased by hyper conjugation which is a consequence of the substituent group(s). The derivatized molecules are expected to form instantaneous dipoles more readily.

4.2 Electronic Properties

4.2.1 Structural and Solvent Dependence on Energy gap (E_g)

The E_g values of the substituted molecules should differ in order to ascertain a difference in their ICT. Both methods (B3LYP and BLYP) allow comparison between the results obtained and the ones available in experiments. From Tables 4.17 - 4.24 and Figures 4.6-4.9. E_g value for unsubstituted 10-OTBP in the experiments by Zebiao and coworkers was 2.89 eV and 2.86 eV (vacuum and THF respectively). It gave 3.65 eV and 3.53 eV (vacuum and THF respectively) with B3LYP and was 2.29 eV and 2.42 eV (vacuum and THF respectively) with BLYP. The substituted derivatives are expected to have different values than unsubstituted 10-OTBP. For instance, *2*-CHO derivative has 2.48 eV in vacuum and 2.46 eV in THF in experiments (Zebiao *et al.*, 2015), the calculated value was 3.06 eV (vacuum) and 2.89 eV (THF) with B3LYP and was 1.76 eV (vacuum) and 1.59 eV (THF). E_g values reduced with different substituents. The E_g values were also reduced in THF.

For 10-OTBP, the B3LYP E_g values ranged from 2.57 - 3.65 eV with 1e having the least value (2.57 eV) while the unsubstituted system has a value of 3.65 eV, followed by 1b also have a low energy gap of 2.64 eV. The values ranged from 2.21 – 3.54 eV, with 1e having the least value (2.21 eV), 1b also has a low energy gap (2.28 eV) while the unsubstituted system has a value of 3.54 eV in THF. That is, the E_g also decreased in THF. The E_g ranged from 1.38 eV– 2.29 eV (BLYP) with 1e being the least (1.38 eV) while the unsubstituted

system has a value of 2.29 eV, 1e was followed by 1b (1.48 eV). The values ranged from 1.20 – 2.42 eV, with 1e being the least (1.20 eV), 1b also have a low energy gap (1.25 eV) while the unsubstituted system has a value of 2.42 eV in THF. That is, the E_g values also decreased in THF. E_g values decreased with different substituents because the molecular weights are increased and conjugation length becomes stretched. 1e and 1b have the least E_g values because $–NO_2$ is a stronger than others in its electron withdrawing ability, the nitro group increased mesomeric effects while cyano acrylic acid group is the longest and with the highest molecular weight. It is expected for example, that the –CN substituted derivative of 10-OTBP, 1c (exp. = 2.48 eV, calculated = (B3LYP) 3.06 eV and (BLYP) 1.76 eV) should have E_g value lower than 1a (exp. = 2.89 eV, calculated = (B3LYP) 3.65 eV and (BLYP) 2.29 eV), this is exactly what was observed both in experiment and in theory. This is due to the fact that the electron-withdrawing aldehyde groups is taking part in the conjugation. Also, just as the experimental E_g value decreased in THF, there is also a decrease in the theoretical E_g value in THF as well.

E_g for 10-MTBP ranged from 2.71 – 3.87 eV, with 2e having the least (2.71 eV) while the unsubstituted system has a value of 3.87 eV, 2b also has a low energy gap of 2.90 eV, the lowest after 2e. The values ranged from 2.40 – 3.81 eV, with 2e having the least (2.4 eV), 2b also have low E_g (2.47 eV), the lowest after 2e. The values ranged from 2.44 – 3.81 eV, with 2e the lowest (2.44 eV), 2b also has a low energy gap of 2.53 eV while the unsubstituted system has a value of 3.81 eV in THF. The BLYP results ranged from 1.51 – 2.46 eV, with 2e the lowest (1.51 eV), followed by 2b (1.59 eV) while the unsubstituted system has a value of 2.46 eV. All substituted molecules, however, reduced the energy gap as compared to the unsubstituted system in vacuum. The values ranged from 1.29 – 2.42 eV, with 2b and 2e having the lowest value of 1.29 eV while the unsubstituted system has a value of 2.42 eV in THF, all on Tables 4.19 and 4.20.

The B3LYP results for 10-MP*m*SB ranged from 3.23 – 3.90 eV (Tables 4.21 and 4.22), with 3c the lowest (3.23 eV) while the unsubstituted system has a value of 3.90 eV. The values ranged from 2.81 – 3.78 eV, with 3c the lowest value (2.81 eV) while the unsubstituted system has a value of 3.78 eV in THF. The BLYP results ranged from 1.79 – 2.44 eV, with 3c the lowest (1.79 eV) while the unsubstituted system has a value of 2.44 eV. All

substituted molecules, however, reduced the energy gap as compared to the unsubstituted system in vacuum. The values ranged from 1.34 – 2.33 eV, with 3c the lowest (1.34 eV) while the unsubstituted system has a value of 2.33 eV in THF.

The B3LYP results for MMPs ranged from 3.30 – 3.85 eV (4.23 and 4.24), with 4d and 4e with the lowest values (3.36 eV and 3.30 eV respectively) while MMP has a value of 3.85 eV. The values ranged from 3.73 – 3.64 eV. That is, the E_g values decreased in THF. The BLYP results ranged from 2.03 – 2.47 eV, with 4d and 4e with the lowest values (2.06 eV and 2.03 eV respectively) while MMP has a value of 2.47 eV. The values ranged from 1.66 – 2.36 eV in THF.

The experimental E_g for MMP (*A*-$COCH_3$, D-SCH_3, MMP) was found to be 2.27 eV, 2.80 eV and 2.94 eV, the values were obtained from three different experimental methods, from $\varepsilon_2^{1/2}/\lambda$ versus $(1/\lambda)$ in Tauc's expression (Tauc *et al.,* 1966; D'Silva *et al.,* 2012), direct and indirect energy gap methods. The B3LYP E_g value of MMP is 3.85 eV with 6-31G* basis set while its BLYP value is 2.47 eV with 6-31G*. The E_g in BLYP method (2.47 eV) is closer to Tauc's $\varepsilon_2^{1/2}/\lambda$ versus $(1/\lambda)$ method value of 2.27 eV and underestimated the direct and indirect energy gap values of 2.80 eV and 2.94 eV, while being 3.85 eV with B3LYP. The substituted derivatives have different E_g values from MMP, as expected owing to different effects like the inductive and mesomeric effects from substituent groups, -NO_2 acceptor group and -CH=C(CN)COOH, which is a larger group. It is expected as E_g values tend to decrease with higher molecular weight. This trend is repeated even in both methods. The substituted molecules are expected to be softer than their unsubstituted analogues. The substituted molecules should therefore, have higher ability to form instantaneous dipoles than MMP. The dipole moments of the derivatized molecules are therefore expected to be of higher values compared to unsubstituted analogues.

The overall observation is that the HOMO and LUMO orbitals are stabilized with substituents and solvent, sometimes due to minimization of hyperconjugation, due to increase in mesomeric effect e.g for –NO_2 substituents or due to larger size or longer conjugation length e.g for -CH=C(CN)COOH or due to the nature of the acceptor or donor group like in MMP in which the from donor (SCH_3) transfers charge to acceptor ($COCH_3$) group via the methylidene backbone (D'Silva *et al.,* 2012); these consequently lead to

decrease in the optical energy gap, E_g. As a result of this, the reactivities of the molecules are enhanced owing to the notion that whenever there is low E_g value, there is optimal amount of electron density (charge) transfer.

4.2.2 Chemical Hardness (η)

The chemical hardness is directly proportional to the energy gap (tables 4.17-4.24 and figs. 4.10-4.13). The B3LYP results for η of 10-OTBP ranged from 1.29 – 1.83 eV, 1e being of the lowest value (1.29 eV) while the unsubstituted system has a value of 1.83 eV. That is, all substituted molecules reduced η as compared to the unsubstituted system in vacuum. The values ranged from 1.11 – 1.77 eV, with 1e being of the lowest value (1.11 eV) while the unsubstituted system has a value of 1.77 eV in THF. That is, the η values decreased in THF. The BLYP results ranged from 0.69 – 1.15 eV, with 1e being of the lowest value (0.69 eV) while the unsubstituted system has a value of 1.15 eV, a trend similar to the B3LYP results in vacuum. The values ranged from 0.60 – 1.21 eV, with 1b and 1e being of the lowest value (0.60 eV) while the unsubstituted system has a value of 1.21 eV in THF. That is, η values also decreased in THF. The trend observed here is similar to that of the energy energy gap in that it is calculated directly from it, eq. 2.25.

The B3LYP results for η of 10-MTBP ranged from 1.36 – 1.94 eV, 2e the lowest (1.36 eV) while the unsubstituted system has a value of 1.94 eV. That is, all substituted molecules reduced η as compared to the unsubstituted system in vacuum. The values ranged from 1.22 – 1.91 eV, 2e the lowest (1.22 eV) while the unsubstituted system has a value of 1.91 eV in THF. That is, the η values decreased in THF. The BLYP results ranged from 0.76 – 1.23 eV, 2e the lowest (0.76 eV) while the unsubstituted system has a value of 1.23 eV, a trend similar to the B3LYP results in vacuum. The values are ranged from 0.65 – 1.21 eV, 2b and 2e the lowest (1.36 eV) while the unsubstituted system has a value of 1.21 eV in THF.

The B3LYP results for 10-MP*m*SB ranged from 1.62– 1.95 eV, 3c the lowest (1.62 eV), while the unsubstituted system has a value of 1.95 eV. That is, all substituted molecules reduced η as compared to the unsubstituted system in vacuum. The values ranged from 1.41 – 1.89 eV, 3c the lowest (1.41 eV) while the unsubstituted system has a value of 1.89 eV in THF. The BLYP results ranged from 0.89 – 1.22 eV, 3c the lowest (0.89 eV) while the

unsubstituted system has a value of 1.22 eV, the same as in B3LYP results. The values ranged from 0.67 – 1.17 eV, 3c the lowest (0.67 eV) while the unsubstituted system has a value of 1.17 eV in THF.

The B3LYP results for MMPs ranged from 1.65 – 1.93 eV, with 4d and 4e being the lowest (1.68 eV and 1.65 eV respectively) while MMP has a value of 3.85 eV. The values ranged from 1.62 – 1.87 eV in THF. The BLYP results ranged from 1.02 – 1.24 eV, with 4d and 4e being the lowest (1.03 eV and 1.02 eV respectively) while MMP has 1.24 eV. The values ranged from 0.83 – 1.18 eV in THF.

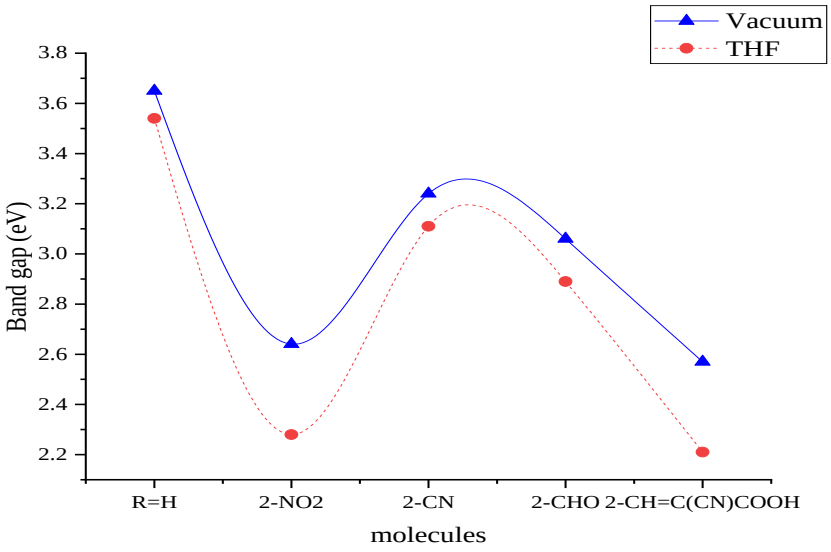

Figure 4.6a: Energy gaps of 10-OTBPs (B3LYP)

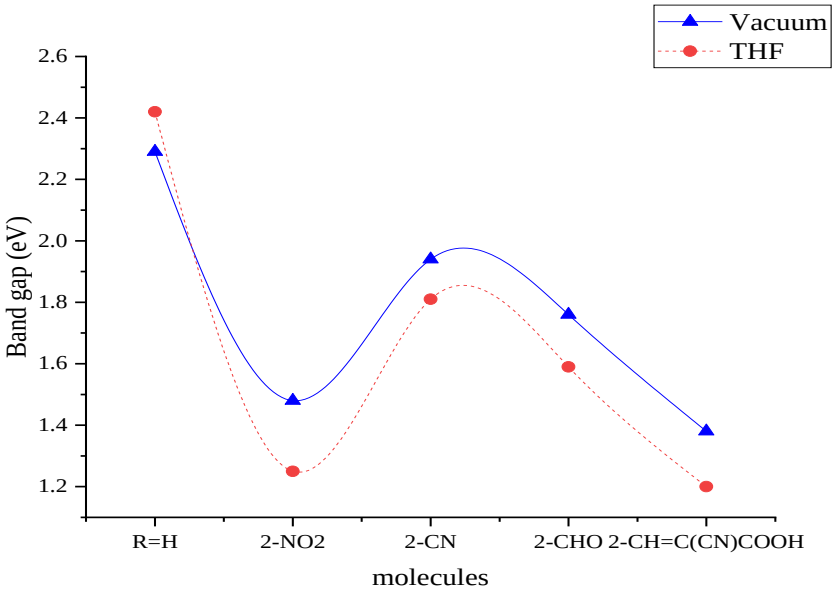

Figure 4.6b: Energy gaps of 10-OTBPs (BLYP)

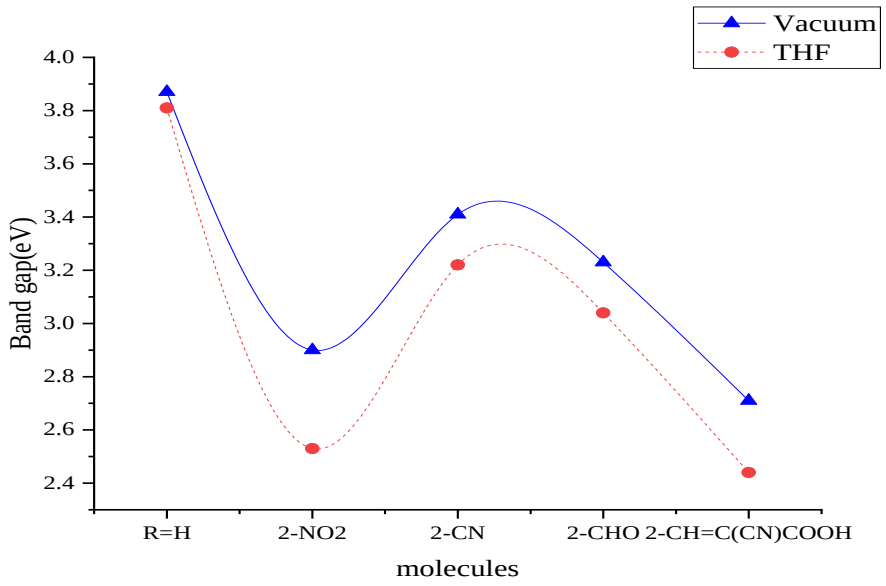

Figure 4.7a: Energy gaps of 10-MTBPs (B3LYP)

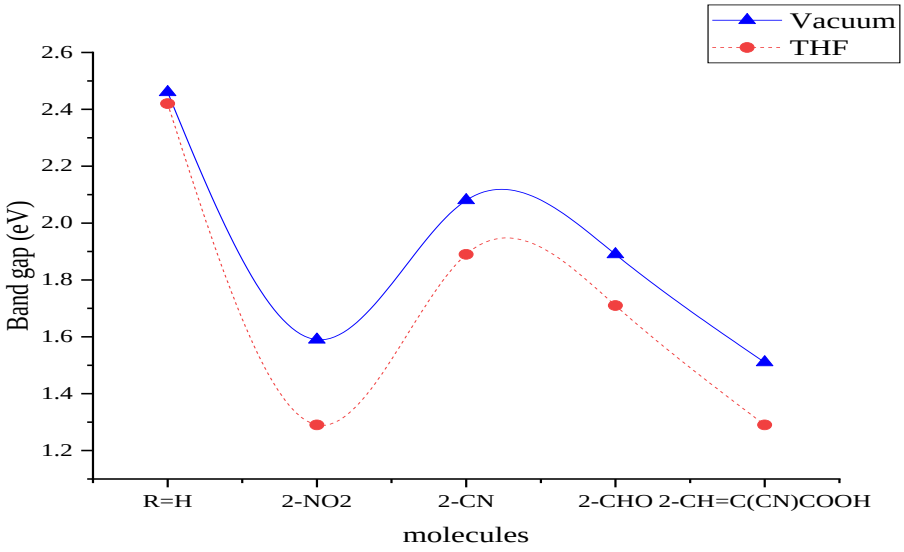

Figure 4.7b: Energy gaps of 10-MTBPs (BLYP)

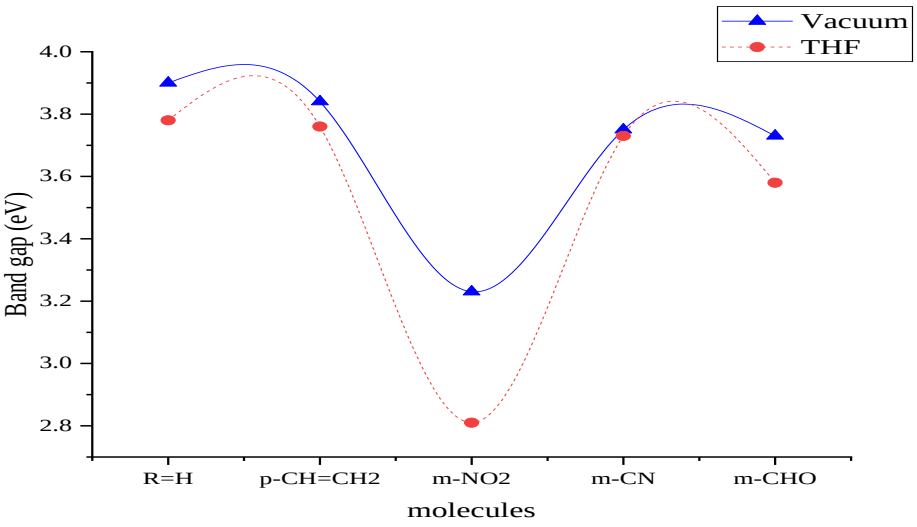

Figure 4.8a: Energy gaps of 10-MPmSBs (B3LYP)

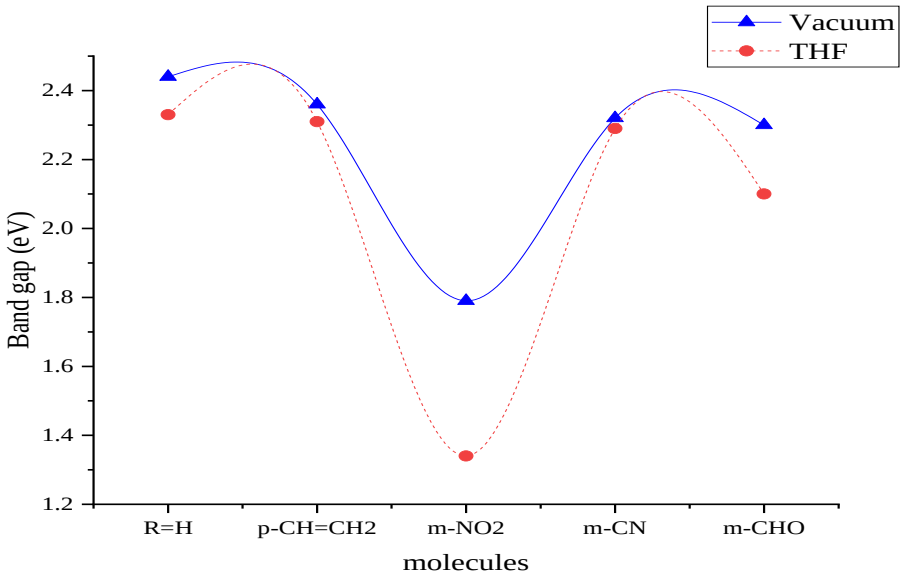

Figure 4.8b: Energy gaps of 10-MPmSBs (BLYP)

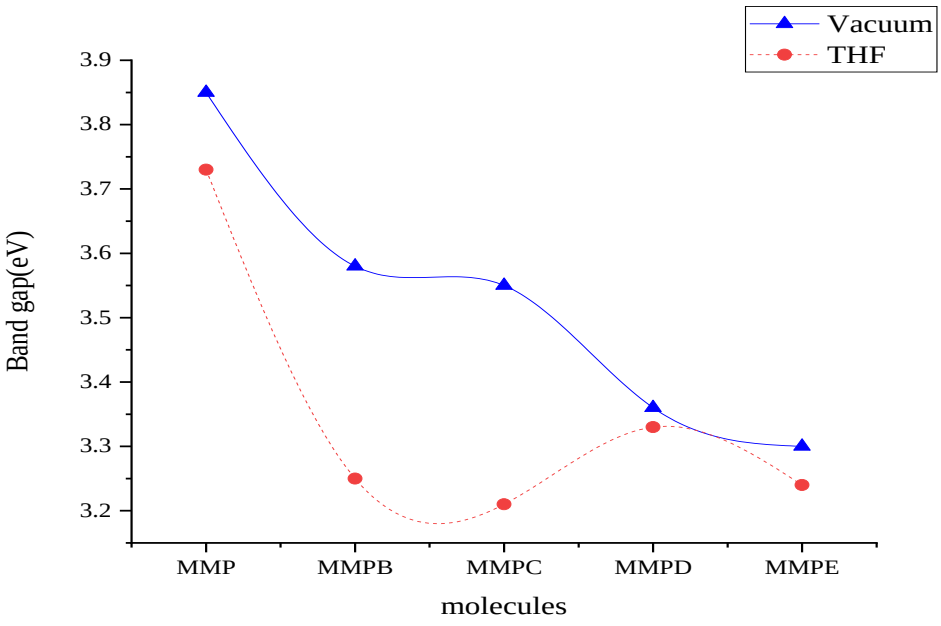

Figure 4.9a: Energy gaps of MMPs (B3LYP)

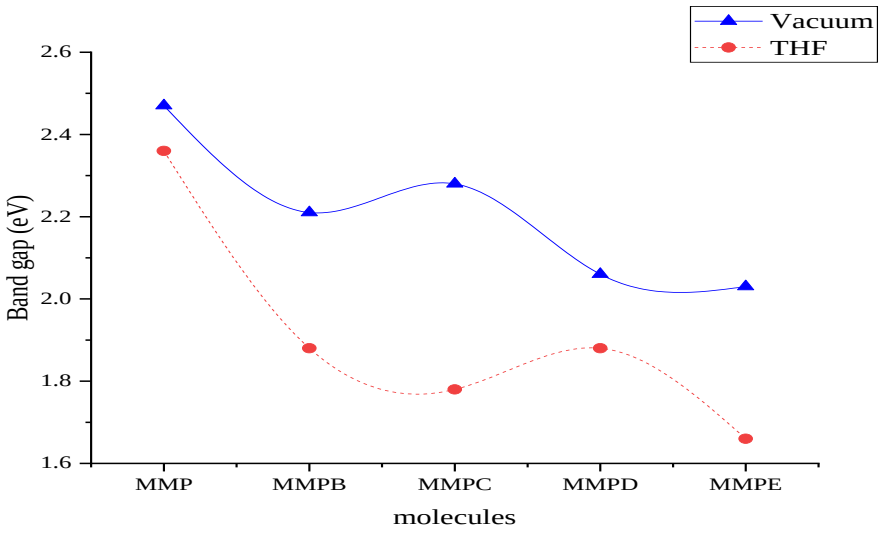

Figure 4.9b: Energy gaps of MMPs (BLYP)

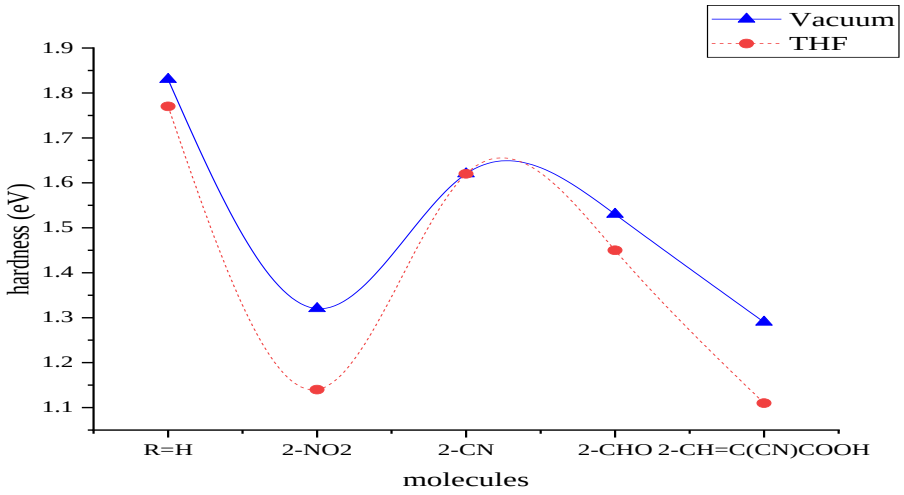

Figure 4.10a: Hardness of 10-OTBPs (B3LYP)

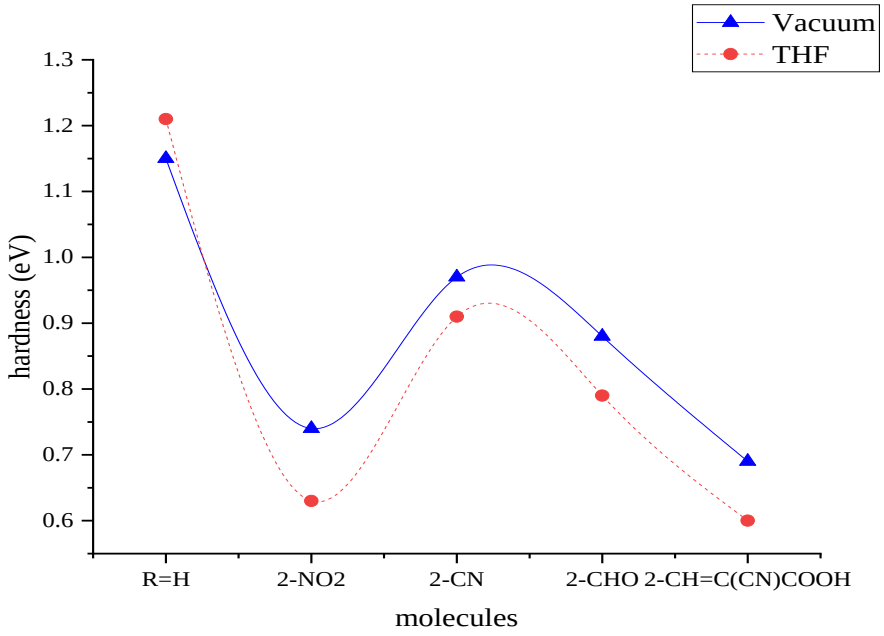

Figure 4.10b: Hardness of 10-OTBPs with (BLYP)

Table 4.17. Frontier molecular energies and reactivity descriptors of 10-OTBPs with B3LYP/6-31G* (vacuum) and THF

Molecules	E_{LUMO}(eV)	E_{HOMO}(eV)	I(eV)	A(eV)	E_g(eV)	η(eV)	S (eV^{-1})	χ (eV)	ω (eV)
			VACUUM						
R=H	-1.17	-4.82	4.82	1.17	3.65(2.89)	1.83	0.55	2.99	2.46
***2*-NO_2**	-2.80	-5.54	5.54	2.80	2.64	1.32	0.75	4.17	6.59
***2*-CN**	-2.15	-5.39	5.39	2.15	3.24	1.62	0.62	3.77	4.39
***2*-CHO**	-2.21	-5.27	5.27	2.21	3.06(2.48)	1.53	0.65	3.74	4.57
***2*-CH=C(CN)COOH**	-2.84	-5.41	5.41	2.84	2.57	1.29	0.78	4.13	6.62
			THF						
R=H	-1.22	-4.76	4.76	1.22	3.54(2.86)	1.77	0.56	2.99	2.53
***2*-NO_2**	-2.73	-5.01	5.01	2.73	2.28	1.14	0.88	3.87	6.57
***2*-CN**	-2.02	-5.12	5.12	2.02	3.11	1.62	0.62	3.57	4.09
***2*-CHO**	-2.11	-5.00	5.00	2.11	2.89(2.46)	1.45	0.69	3.56	4.37
***2*-CH=C(CN)COOH**	-2.73	-4.94	4.94	2.73	2.21	1.11	0.90	3.84	6.65

Experimental results in brackets (Zebiao *et al.*, 2015)

Table 4.18. Frontier molecular energies and reactivity descriptors of 10-OTBPs with BLYP/6-31G* (vacuum) and THF

Molecules	E_{LUMO}(eV)	E_{HOMO}(eV)	I(eV)	A(eV)	E_g(eV)	η(eV)	S (eV^{-1})	χ (eV)	ω (eV)
			VACUUM						
R=H	-1.65	-3.94	3.94	1.65	2.29(2.89)	1.15	0.87	2.79	3.41
***2*-NO_2**	-3.22	-4.70	4.70	3.22	1.48	0.74	1.35	3.96	10.59
***2*-CN**	-2.59	-4.53	4.53	2.59	1.94	0.97	1.03	3.56	6.53
***2*-CHO**	-2.68	-4.44	4.44	2.68	1.76(2.48)	0.88	1.14	3.56	7.20
***2*-CH=C(CN)COOH**	-3.22	-4.60	4.60	3.22	1.38	0.69	1.45	3.91	11.08
			THF						
R=H	-1.66	-4.08	4.08	1.66	2.42(2.86)	1.21	0.83	2.87	3.40
***2*-NO_2**	-3.09	-4.34	4.34	3.09	1.25	0.63	1.59	3.72	11.04
***2*-CN**	-2.41	-4.22	4.22	2.41	1.81	0.91	1.10	3.32	6.07
***2*-CHO**	-2.55	-4.14	4.14	2.55	1.59(2.46)	0.79	1.28	3.35	7.04
***2*-CH=C(CN)COOH**	-3.09	-4.29	4.29	3.09	1.20	0.60	1.60	3.69	11.35

Experimental results in brackets (Zebiao *et al.*, 2015)

Table 4.19. Frontier molecular energies and reactivity descriptors of 10-MTBPs with B3LYP/6-31G* (vacuum) and THF

Molecules	E_{LUMO}(eV)	E_{HOMO}(eV)	I(eV)	A(eV)	E_g(eV)	η(eV)	S (eV^{-1})	χ (eV)	ω (eV)
				VACUUM					
R=H	-1.10	-4.97	4.97	1.10	3.87	1.94	0.52	3.04	2.38
***2*-NO_2**	-2.79	-5.69	5.69	2.79	2.90	1.45	0.69	4.24	6.19
***2*-CN**	-2.13	-5.54	5.54	2.13	3.41	1.71	0.59	3.84	4.31
***2*-CHO**	-2.20	-5.43	5.43	2.20	3.23	1.62	0.62	3.82	4.51
***2*-CH=C(CN)COOH**	-2.85	-5.56	5.56	2.85	2.71	1.36	0.74	4.21	6.53
				THF					
R=H	-1.15	-4.96	4.96	1.15	3.81	1.91	0.53	3.01	2.45
***2*-NO_2**	-2.72	-5.25	5.25	2.72	2.53	1.27	0.79	3.99	6.28
***2*-CN**	-1.97	-5.19	5.19	1.97	3.22	1.61	0.62	3.58	3.98
***2*-CHO**	-2.10	-5.14	5.14	2.10	3.04	1.52	0.66	3.62	4.31
***2*-CH=C(CN)COOH**	-2.77	-5.21	5.21	2.77	2.44	1.22	0.82	3.99	6.53

Table 4.20. Frontier molecular energies and reactivity descriptors of 10-MTBPs with BLYP/6-31G* (vacuum) and THF

Molecules	E_{LUMO}(eV)	E_{HOMO}(eV)	I(eV)	A(eV)	E_g(eV)	η(eV)	S (eV^{-1})	χ (eV)	ω (eV)
			VACUUM						
R=H	-1.60	-4.06	4.06	1.60	2.46	1.23	0.81	2.83	3.27
***2*-NO_2**	-3.23	-4.82	4.82	3.23	1.59	0.80	1.26	4.03	10.19
***2*-CN**	-2.58	-4.66	4.66	2.58	2.08	1.04	0.96	3.62	6.30
***2*-CHO**	-2.68	-4.57	4.57	2.68	1.89	0.95	1.06	3.63	6.95
***2*-CH=C(CN)COOH**	-3.22	-4.73	4.73	3.22	1.51	0.76	1.33	3.98	10.46
			THF						
R=H	-1.63	-4.05	4.05	1.63	2.42	1.21	0.83	2.84	3.33
***2*-NO_2**	-3.09	-4.38	4.38	3.09	1.29	0.65	1.55	3.74	10.84
***2*-CN**	-2.41	-4.30	4.30	2.41	1.89	0.95	1.06	3.36	5.96
***2*-CHO**	-2.55	-4.26	4.26	2.55	1.71	0.86	1.17	3.41	6.78
***2*-CH=C(CN)COOH**	-3.09	-4.38	4.38	3.09	1.29	0.65	1.55	3.74	10.84

Table 4.21. Frontier molecular energies and reactivity descriptors of 10-MP*m*SBs with B3LYP/6-31G* (vacuum) and THF

Molecules	E_{LUMO}(eV)	E_{HOMO}(eV)	I(eV)	A(eV)	E_g(eV)	η(eV)	S (eV^{-1})	χ (eV)	ω (eV)
			VACUUM						
R=H	-1.36	-5.26	5.26	1.36	3.90	1.95	0.51	3.31	2.81
***p*-CH=CH$_2$**	-1.42	-5.26	5.26	1.42	3.84	1.92	0.52	3.34	2.91
***m*-NO$_2$**	-2.18	-5.41	5.41	2.18	3.23	1.62	0.62	3.79	4.46
***m*-CN**	-1.66	-5.41	5.41	1.66	3.75	1.88	0.53	3.54	3.33
***m*-CHO**	-1.66	-5.39	5.39	1.66	3.73	1.87	0.54	3.53	3.33
			THF						
R=H	-1.41	-5.19	5.19	1.41	3.78	1.89	0.53	3.30	2.88
***p*-CH=CH$_2$**	-1.43	-5.19	5.19	1.43	3.76	1.88	0.53	3.31	2.91
***m*-NO$_2$**	-2.42	-5.23	5.23	2.42	2.81	1.41	0.72	3.83	5.21
***m*-CN**	-1.50	-5.23	5.23	1.50	3.73	1.87	0.54	3.37	3.04
***m*-CHO**	-1.64	-5.22	5.22	1.64	3.58	1.79	0.56	3.43	3.29

Table 4.22. Frontier molecular energies and reactivity descriptors of 10-MP*m*SBs with BLYP/6-31G* (vacuum) and THF

Molecules	E_{LUMO}(eV)	E_{HOMO}(eV)	I(eV)	A(eV)	E_g(eV)	η(eV)	S (eV^{-1})	χ (eV)	ω (eV)
			VACUUM						
R=H	-1.90	-4.34	4.34	1.90	2.44	1.22	0.82	3.12	3.99
***p*-CH=CH$_2$**	-1.96	-4.32	4.32	1.96	2.36	1.18	0.85	3.14	4.18
***m*-NO$_2$**	-2.72	-4.51	4.51	2.72	1.79	0.89	1.12	3.62	7.30
***m*-CN**	-2.18	-4.50	4.50	2.18	2.32	1.16	0.86	3.34	4.81
***m*-CHO**	-2.18	-4.48	4.48	2.18	2.30	1.15	0.87	3.33	4.82
			THF						
R=H	-1.93	-4.26	4.26	1.93	2.33	1.17	0.86	3.09	4.11
***p*-CH=CH$_2$**	-1.96	-4.27	4.27	1.96	2.31	1.16	0.87	3.12	4.20
***m*-NO$_2$**	-2.96	-4.30	4.30	2.96	1.34	0.67	1.49	3.63	9.83
***m*-CN**	-2.01	-4.30	4.30	2.01	2.29	1.15	0.87	3.16	4.35
***m*-CHO**	-2.19	-4.29	4.29	2.19	2.10	1.05	0.95	3.24	4.99

Table 4.23: Frontier molecular energies and reactivity descriptors of MMPs with B3LYP/6-31G* (vacuum) and THF

Molecules	E_{LUMO}(eV)	E_{HOMO}(eV)	I(eV)	A(eV)	E_g(eV)	η(eV)	S (eV^{-1})	χ (eV)	ω (eV)
				VACUUM					
A-$COCH_3$, D-SCH3, MMP	-1.94	-5.79	5.79	1.94	3.85(2.27)	1.93	0.52	3.87	3.88
A-NO_2, D-SCH_3	-2.44	-6.02	6.02	2.44	3.58	1.79	0.56	4.23	4.99
A-NO_2, D-NH_2	-2.25	-5.8	5.80	2.25	3.55	1.78	0.56	4.03	4.56
A-CH=C(CN)COOH, D-SCH_3	-2.72	-6.08	6.08	2.72	3.36	1.68	0.59	4.40	5.76
A-CH=C(CN)COOH, D-NH_2	-2.57	-5.87	5.87	2.57	3.30	1.65	0.61	4.22	5.39
				THF					
A-$COCH_3$, D-SCH3, MMP	-1.93	-5.66	5.66	1.93	3.73	1.87	0.54	3.79	3.86
A-NO_2, D-SCH_3	-2.50	-5.75	5.75	2.50	3.25	1.63	0.62	4.13	5.24
A-NO_2, D-NH_2	-2.25	-5.46	5.46	2.25	3.21	1.61	0.62	3.86	4.63
A-CH=C(CN)COOH, D-SCH_3	-2.51	-5.84	5.84	2.51	3.33	1.67	0.60	4.18	5.23
A-CH=C(CN)COOH, D-NH_2	-2.14	-5.38	5.38	2.14	3.24	1.62	0.62	3.76	4.36

Experimental results in bracket (D'Silva *et al.*, 2012).

Table 4.24: Frontier molecular energies and reactivity descriptors of MMP with BLYP/6-31G* (vacuum) and THF

Molecules	E_{LUMO}(eV)	E_{HOMO}(eV)	I(eV)	A(eV)	E_g(eV)	η(eV)	S (eV^{-1})	χ (eV)	ω (eV)
				VACUUM					
A-$COCH_3$, D-SCH3, MMP	-2.41	-4.88	4.88	2.41	2.47(2.27)	1.24	0.81	3.65	5.38
A-NO_2, D-SCH_3	-2.90	-5.11	5.11	2.90	2.21	1.11	0.90	4.01	7.26
A-NO_2, D-NH_2	-2.51	-4.79	4.79	2.41	2.28	1.14	0.88	3.65	5.84
A-CH=C(CN)COOH, D-SCH_3	-3.12	-5.18	5.18	3.12	2.06	1.03	0.97	4.15	8.36
A-CH=C(CN)COOH, D-NH_2	-2.95	-4.98	4.98	2.95	2.03	1.02	0.99	3.97	7.74
				THF					
A-$COCH_3$, D-SCH3, MMP	-2.39	-4.75	4.75	2.39	2.36	1.18	0.85	3.57	5.40
A-NO_2, D-SCH_3	-2.95	-4.83	4.83	2.95	1.88	0.94	1.06	3.89	8.05
A-NO_2, D-NH_2	-2.73	-4.51	4.51	2.73	1.78	0.89	1.12	3.62	7.36
A-CH=C(CN)COOH, D-SCH_3	-2.96	-4.84	4.84	2.96	1.88	0.94	1.06	3.09	8.09
A-CH=C(CN)COOH, D-NH_2	-2.85	-4.51	4.51	2.85	1.66	0.83	1.20	3.68	8.16

Experimental results in bracket (D'Silva *et al.*, 2012).

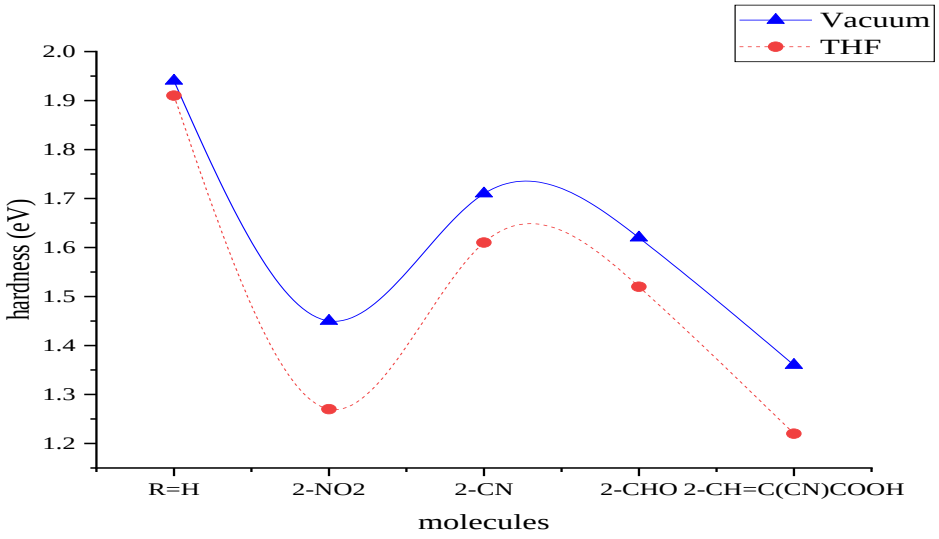

Figure 4.11a: Hardness of 10-MTBPs (B3LYP)

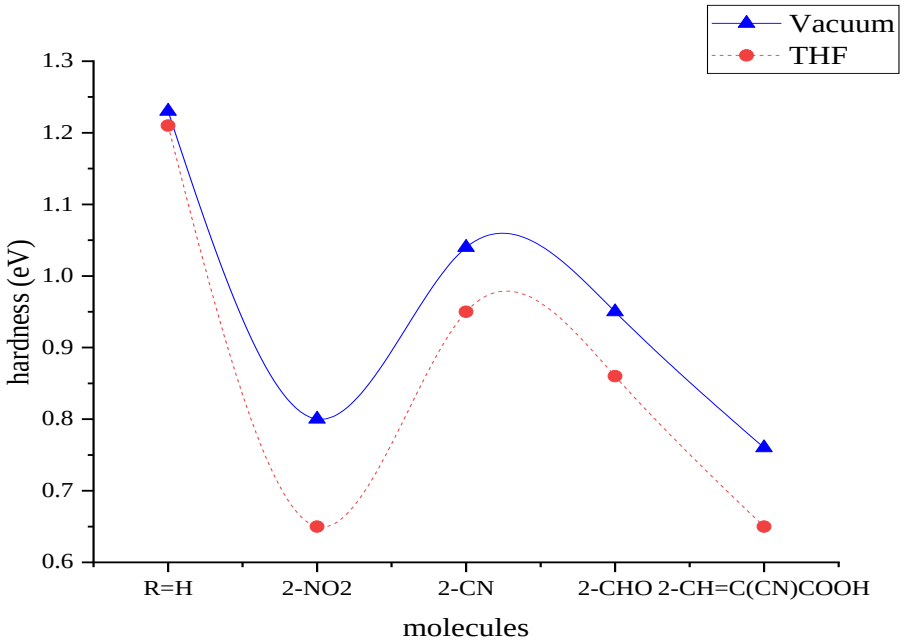

Figure 4.11b: Hardness of 10-MTBPs (BLYP)

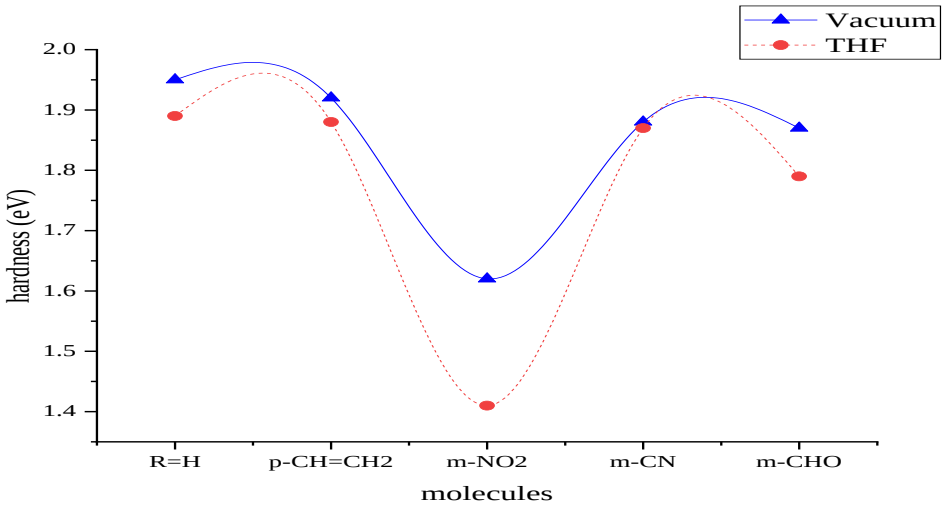

Figure 4.12a: Hardness of 10-MPmSBs (B3LYP)

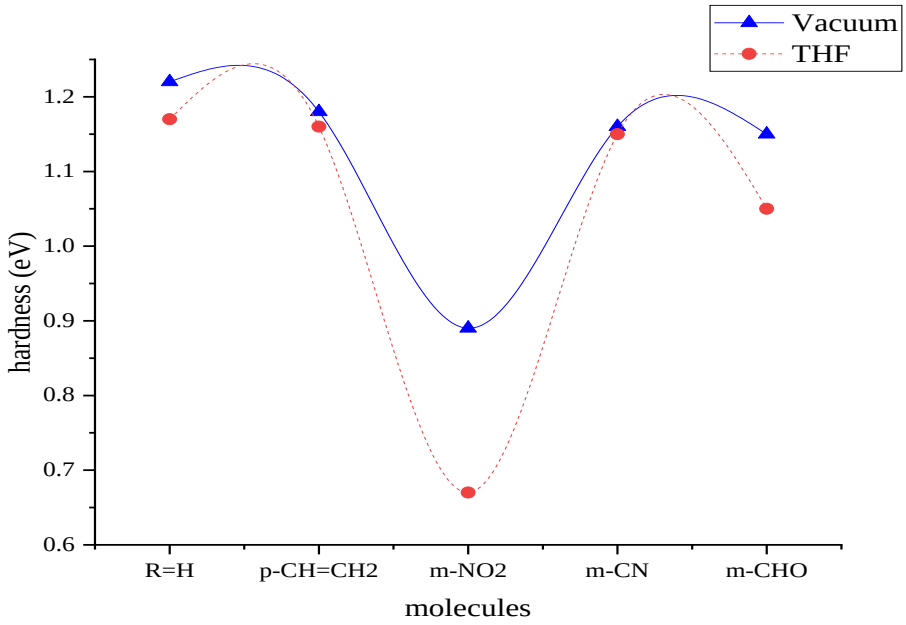

Figure 4.12b: Hardness of 10-MPmSBs (BLYP)

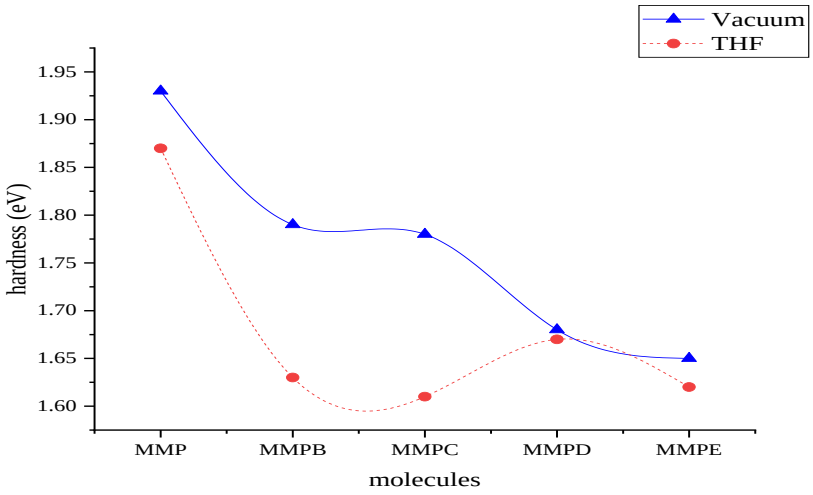

Figure 4.13a: Hardness of MMPs (B3LYP/6-31G*)

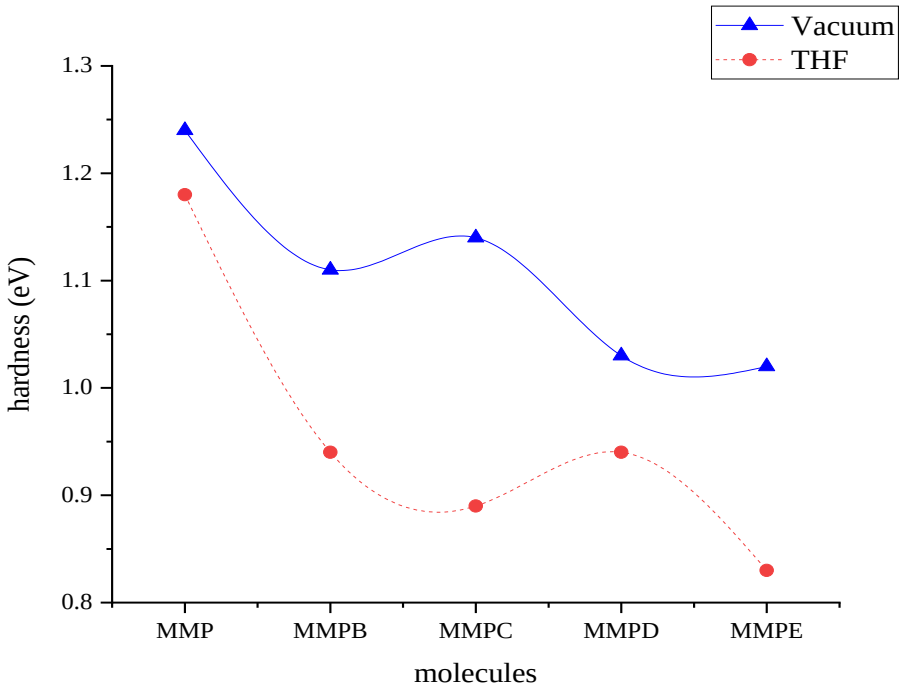

Figure 4.13b: Hardness for MMPs (BLYP)

4.2.3 Chemical Softness (S)

Softness is inversely proportional to the chemical hardness of a molecule as in eqs. 2.25 and 2.26. Molecules with low hardness values (i. e low E_g) are therefore, expected to have high softness values. The possession of low hardness, low energy gap and high softness value is an indication that the substituted derivatives of 10-OTBP, 10-MTBP, 10-MP*m*SB and MMP are more reactive than their unsubstituted analogues. The substituted analogues seem to possess better NLO activities than their unsubstituted ones with their reduction in BLA, lower E_g and η values (they are therefore, expected to be softer than their unsubstituted derivatives) All results are presented on Tables 4.17-4.24 and Figs. 4.14-4.17.

The B3LYP results for the studied systems show that, for 10-OTBP, 1b and 1e have the highest softness of 0.74 eV^{-1} and 0.78 eV^{-1} respectively as against 0.55 eV^{-1} of unsubstituted 10-OTBP in vacuum. The same trend was observed in THF, as 1b and 1e have the highest softness of 0.88 eV^{-1} and 0.90 eV^{-1} respectively as against 0.56 eV^{-1} of unsubstituted 10-OTBP. The BLYP results replicated the same trend for gas phase and in THF. The results for the studied systems show that 1b and 1e have the highest softness of 1.35 eV^{-1} and 1.45 eV^{-1} respectively as against 0.87 eV^{-1} of unsubstituted 10-MTBP in vacuum. The same trend was observed in THF, as 1b and 1e have the highest softness, of 1.59 eV^{-1} and 1.60 eV^{-1} as against 0.83 eV^{-1} of unsubstituted 10-OTBP. Figs. 4.14.

The B3LYP results for the studied systems show that 2b and 2e have the highest softness of 0.69 eV^{-1} and 0.74 eV^{-1} respectively as against 0.52 eV^{-1} of unsubstituted 10-MTBP in vacuum. The same trend is observed in THF, as 2b and 2e have the highest softness of 0.79 eV^{-1} and 0.82 eV^{-1} respectively as against 0.53 eV^{-1} of unsubstituted 10-MTBP. The BLYP results replicated the same trend for gas phase and in the solvent. The results for the studied systems show that 2b and 2e have the highest softness of 1.26 eV^{-1} and 1.33 eV^{-1} respectively as against 0.81 eV^{-1} of unsubstituted 10-MTBP in vacuum. The same trend is observed in THF, as 2b and 2e have the highest softness, both of 1.55 eV^{-1} as against 0.83 eV^{-1} of unsubstituted 10-MTBP. Figs. 4.15.

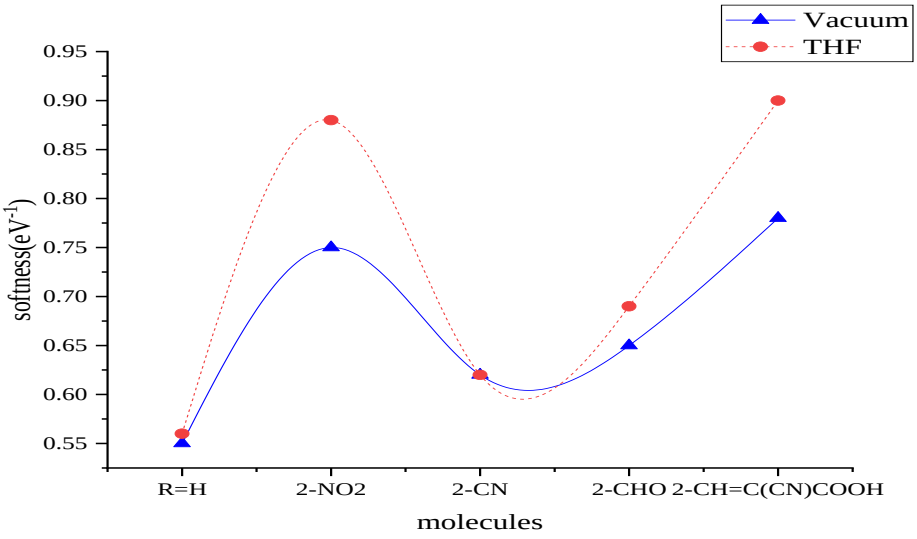

Figure 4.14a: Softness for 10-OTBPs (B3LYP)

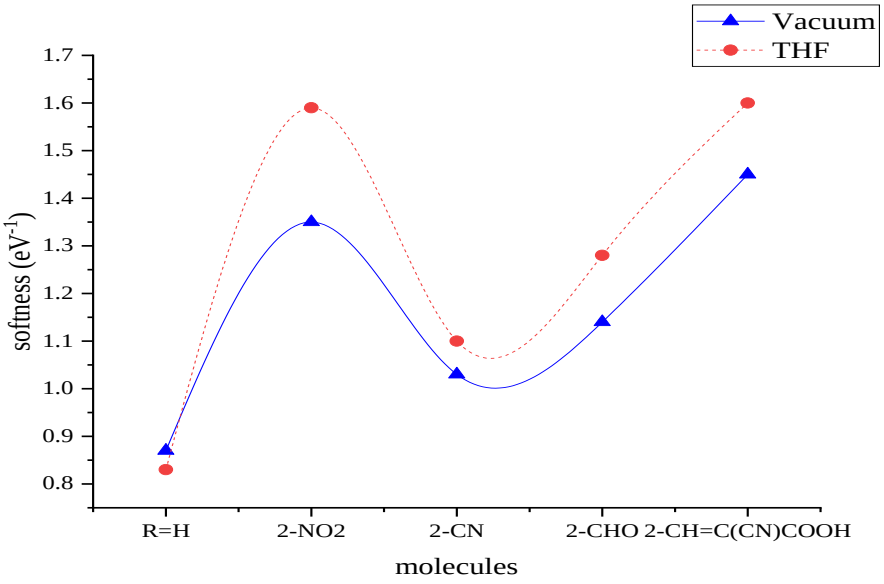

Figure 4.14b: Softness of 10-OTBPs (BLYP)

The B3LYP results for the studied systems show that 3c has the highest softness of 0.62 eV^{-1} as against 0.51 eV^{-1} of unsubstituted 10-MP*m*SB in vacuum. The same trend is observed in THF, as 3c has the highest softness of 0.72 eV^{-1} as against 0.53 eV^{-1} of unsubstituted 10-MP*m*SB. The BLYP results for the studied systems are shows that 3c has the highest softness of 1.12 eV^{-1} as against 0.82 eV^{-1} of unsubstituted 10-MP*m*SB in vacuum. The same trend is observed in THF, as 3c has the highest softness of 1.49 eV^{-1} as against 0.86 eV^{-1} of unsubstituted 10-MP*m*SB. Figs. 4.16.

The B3LYP results for MMP show that 4e is the softest (0.61 eV^{-1}), while MMP has a value of 0.52 eV^{-1}. Other substituted derivatives are softer than MMP. The same trend was observed in THF, all substituted derivatives have higher softness values. The BLYP results for MMP show that 4e is the softest (0.99 eV^{-1}), while MMP has a value of 0.81 eV^{-1}. Other substituted derivatives are softer than MMP. The same trend was observed in THF, all substituted derivatives have higher softness values. The hardness or softness of a molecule is characterized by the value of the energy gap. Hard molecules are less reactive than soft molecules because the larger the gap between the LUMO and HOMO orbital energies, the more difficult for intermolecular charge transfer to take place. Figures 4.10-4.12 show the graphical illustration of the softness of the compounds, the softest molecules are those that are easily polarized. Figs. 4.17. That is why the trend is similar for both E_g values and hardness, while the reverse trend was observed in S values; this is because S is an inverse of η.

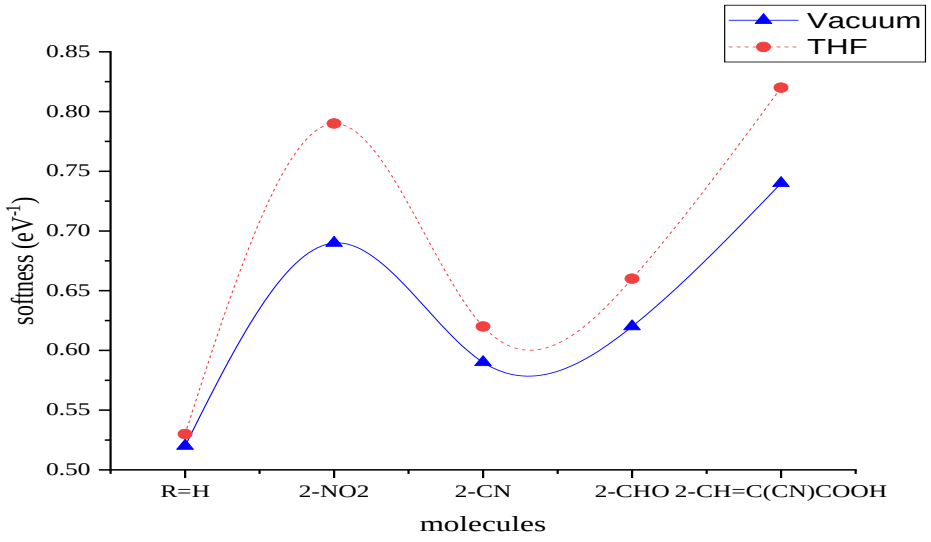

Figure 4.15a: Softness for 10-MTBPs (B3LYP)

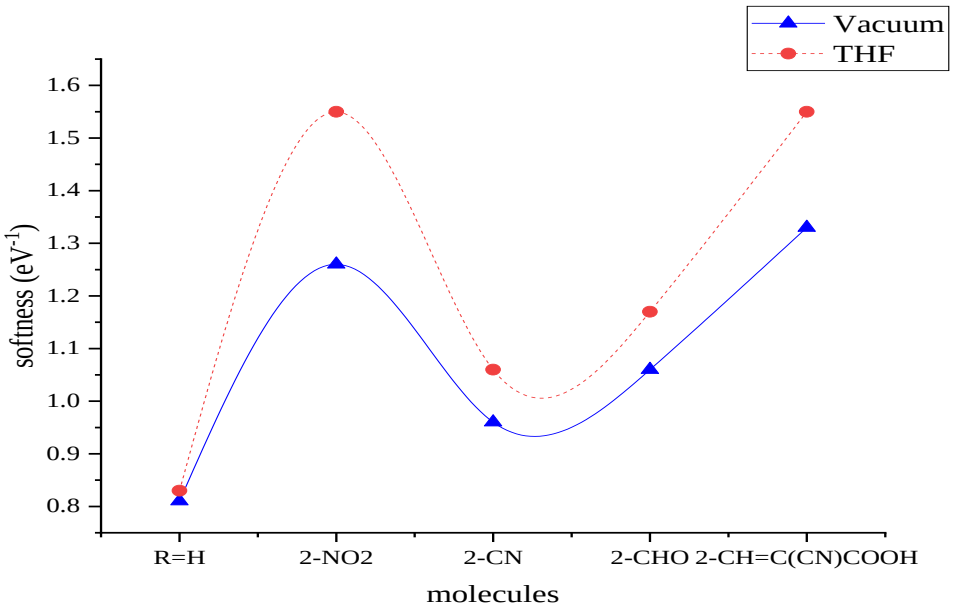

Figure 4.15b: Softness for 10-MTBPs (BLYP)

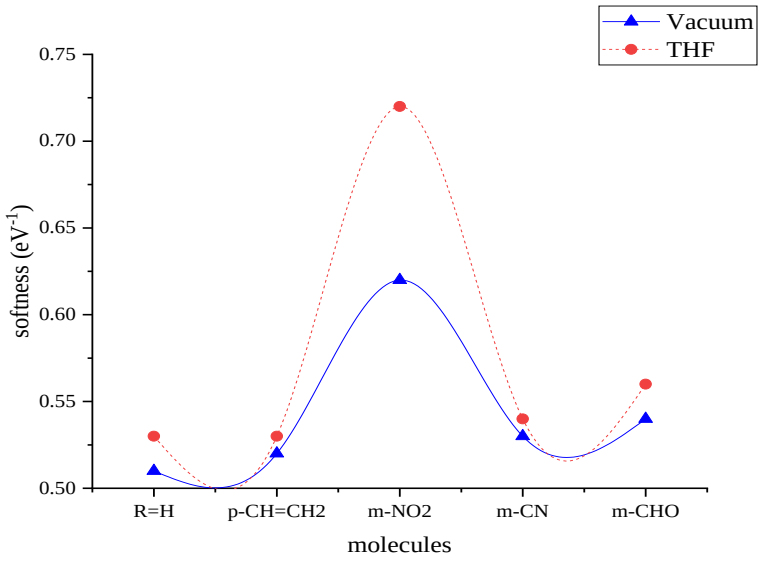

Figure 4.16a: Softness for 10-MPmSBs (B3LYP)

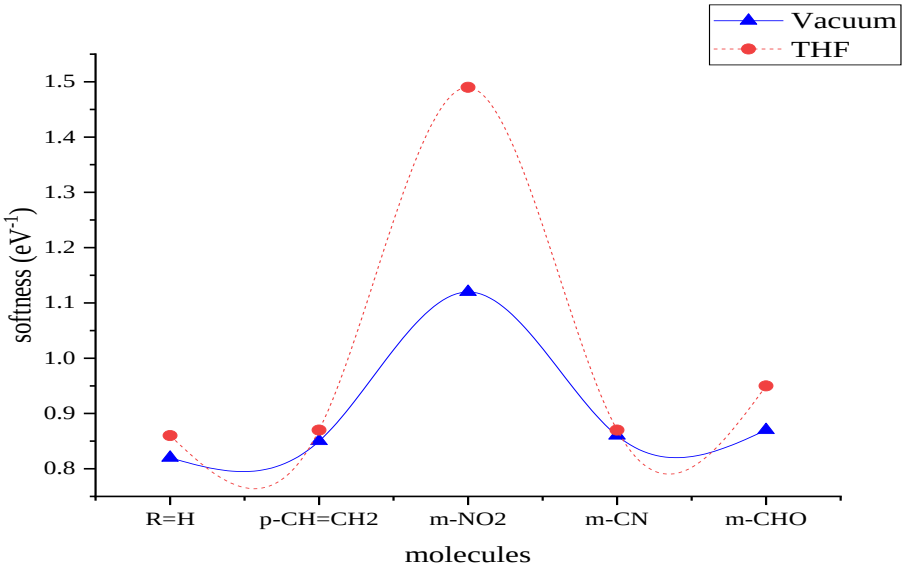

Figure 4.16b: Softness for 10-MPmSBs (BLYP)

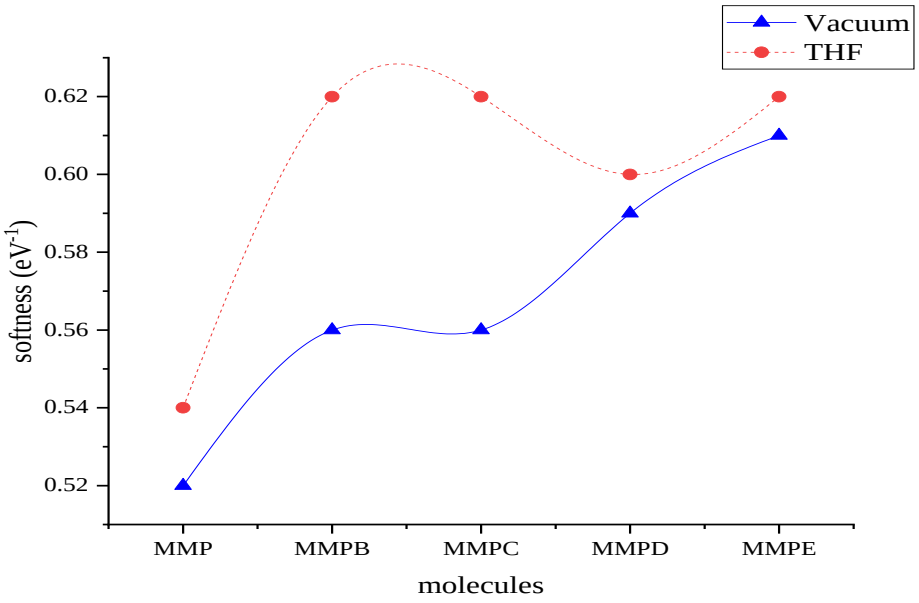

Figure 4.17a: Softness of MMPs (B3LYP)

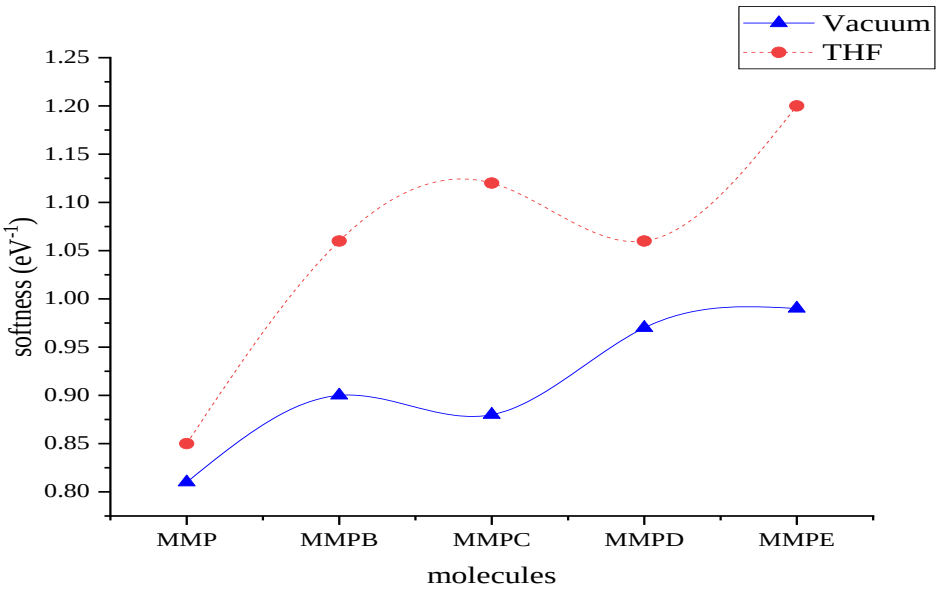

Figure 4.17b: Softness of MMPs (BLYP)

4.2.4 Electronegativity (χ) and Global Electrophilicity (ω)

The χ values of 10-OTBP for B3LYP ranged from 2.99 – 4.17 eV, the unsubstituted molecule has a value of 2.99 eV while being 4.17 eV for 1b in vacuum, 1e also have a high value of 4.13 eV. The unsubstituted molecule has a χ value of 2.99 eV, while being 3.87 eV for 1b and 3.84 eV for 1e in THF. The BLYP χ values for 10-OTBP ranged from 2.79 – 3.96 eV, with the unsubstituted molecule having a value of 2.79 eV while being 3.96 eV for 1b in vacuum, 1e also have a high value of 3.91 eV. The unsubstituted molecule has a χ value of 2.87 eV, while being 3.72 eV for 1b and 3.69 eV for 1e in THF. Figs. 4.18.

The χ values of 10-MTBP for B3LYP ranged from 3.04 – 4.24 eV, with the unsubstituted molecule having a value of 3.04 eV while being 4.24 eV for 2b in vacuum, 2e also have a high value of 4.21 eV. The unsubstituted molecule has a χ value of 3.01 eV, while being 3.99 eV for both 2e and 2b in THF. The BLYP χ values for 10-MTBP ranged from 2.83 – 4.03 eV, with the unsubstituted molecule having a value of 2.83 eV while being 4.03 eV for 2b in vacuum, 2e also have a high value of 3.98 eV. The unsubstituted molecule has a χ value of 2.84 eV, while being 3.74 eV for both 2e and 2b in THF. Figs. 4.19.

The χ values of 10-MP*m*SB for B3LYP ranged from 3.31 – 3.74 eV, with the unsubstituted molecule having a value of 3.31 eV while being 3.74 eV for 3c in vacuum. The unsubstituted molecule also has a χ value of 3.30 eV, while being 3.83 eV for 3c in THF. The χ values of 10-MP*m*SB for BLYP ranged from 3.12 – 3.62 eV, with the unsubstituted molecule having a value of 3.12 eV while being 3.62 eV for 3c in vacuum. The unsubstituted molecule also has a χ value of 3.09 eV, while being 3.63 eV for 3c in THF. Figs. 4.20.

The χ values of MMPs for B3LYP ranged from 3.87 – 4.40 eV, with MMP having a value of 3.87 eV while being 4.40 eV for 4d (vacuum). MMP gave 3.79 eV while it was 4.18 eV for 4d in THF. These values did not follow similar trend with E_g values because it is not from difference between E_{HOMO} and E_{LUMO} rather, it is derived from their sum. The χ values of MMP for BLYP ranged from 3.65 – 4.15 eV, with the unsubstituted molecule having a value of 3.65 eV while being 4.15 eV for 4d in vacuum. MMP has a χ value of 3.57 eV, while being 3.89 eV for 4b in THF. Figs. 4.21. From their higher χ values, the substituted derivatives have better character which attracts bond electrons than the reference molecules.

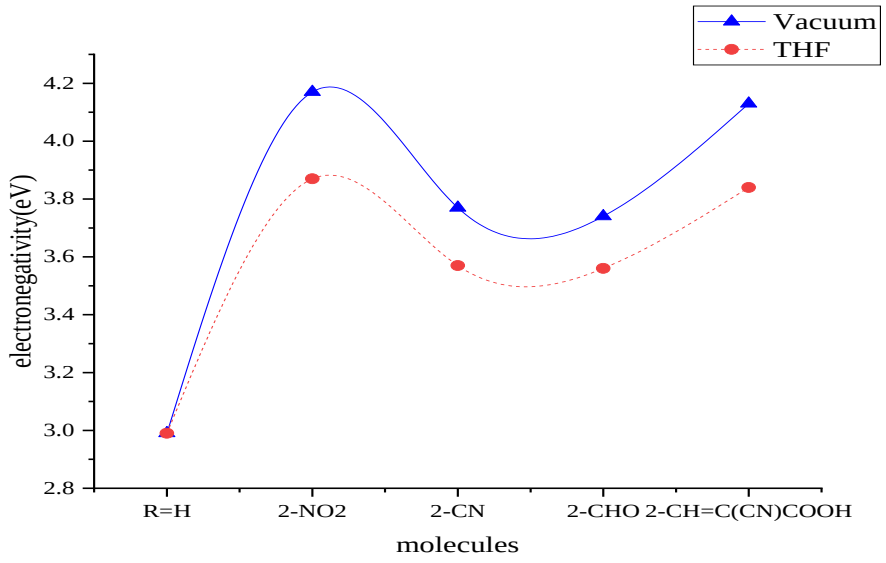

Figure 4.18a: Electronegativity of 10-OTBPs with (B3LYP)

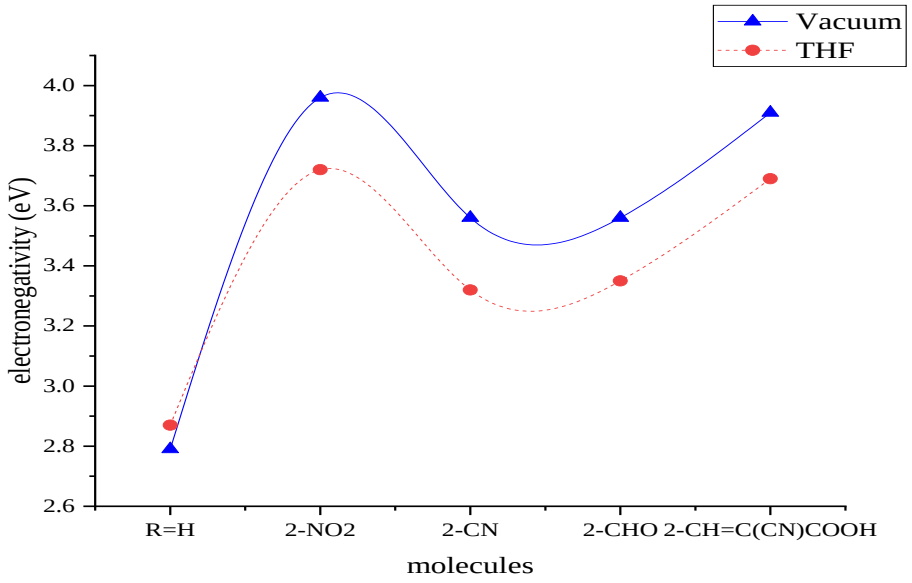

Figure 4.18b: Electronegativity of 10-OTBPs (BLYP)

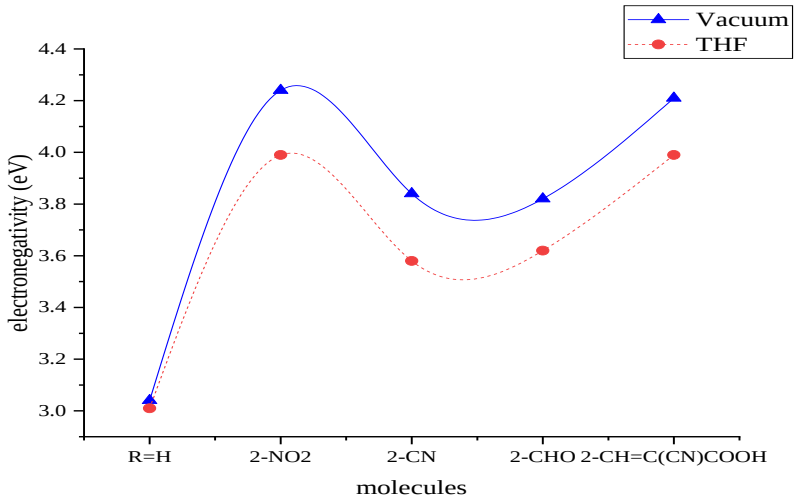

Figure 4.19a: Electronegativity of 10-MTBPs (B3LYP)

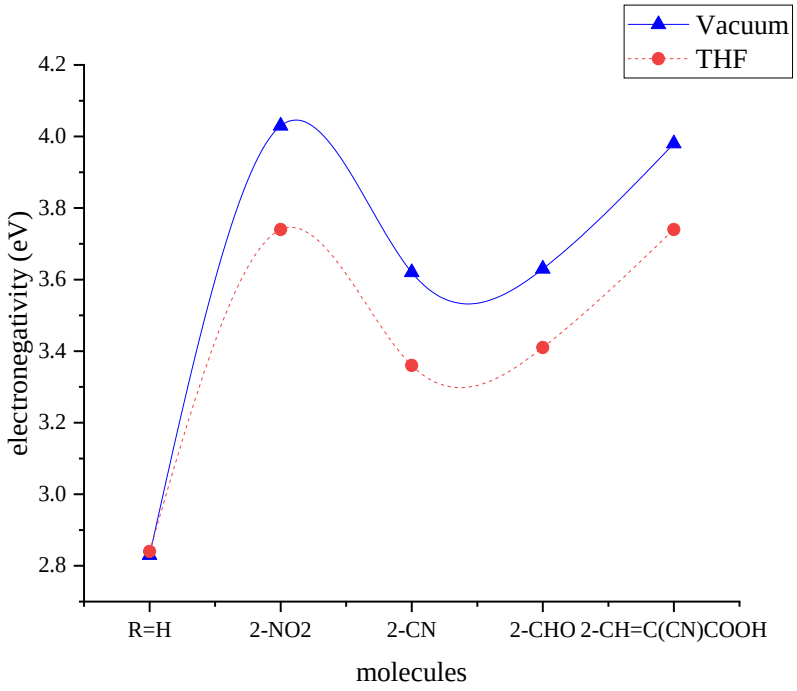

Figure 4.19b: Electronegativity of 10-MTBPs (BLYP)

The C^P values are just the negative values of χ. The values definitely follow the same trend.

The B3LYP ω values for 10-OTBP ranged from 2.46 – 6.62 eV, with the unsubstituted molecule having a value of 2.46 eV while being 6.62 eV for 1e in vacuum, 1b also has high value (6.59 eV). The unsubstituted molecule has a ω value of 2.53 eV, while being 6.65 eV for 1e in THF, 1b also has high value (6.57 eV) in THF. The ω values of 10-MTBP for BLYP ranged from 3.41 – 11.08 eV, with the unsubstituted molecule having a value of 3.41 eV while being 11.08 eV for 1e in vacuum, 1b also has high value (10.59 eV). The unsubstituted molecule has a ω value of 3.40 eV, while being 11.35 eV for 1e and 11.04 eV for 1b in THF. Figs. 4.22.

The ω values of 10-MTBP for B3LYP ranged from 2.38 – 6.53 eV, with the unsubstituted molecule having a value of 2.38 eV while being 2.53 eV for 2e (vacuum), 2b has high value (6.19 eV). The unsubstituted molecule has a ω value of 2.45 eV, while being 6.53 eV for 2e (THF), 2b has high value (6.28 eV). The ω values of 10-MTBP for BLYP ranged from 3.27 – 10.46 eV, with the unsubstituted molecule having a value of 3.27 eV while being 10.46 eV for 2e (vacuum), 2b has high value (10.19 eV). The unsubstituted molecule has a ω value of 3.33 eV, while being 10.84 eV for both 2b and 2e in THF. Figs. 4.23.

The ω values of 10-MP*m*SB for B3LYP ranged from 2.81 – 4.46 eV, with the unsubstituted molecule having a value of 2.81 eV while being 4.46 eV for 3c in vacuum. The unsubstituted molecule has a ω value of 2.88 eV, while being 5.21 eV for 3c in THF. The ω values of 10-MP*m*SB for BLYP ranged from 3.99 – 7.30 eV, with the unsubstituted molecule having a value of 3.99 eV while being 7.30 eV for 3c in vacuum. The unsubstituted molecule has a ω value of 4.11 eV, while being 9.83 eV for 3c in THF. Figs. 4.24.

The ω values of MMPs for B3LYP ranged from 3.88 – 5.76 eV, with MMP having a value of 3.88 eV while being 5.76 eV for 4d in vacuum. MMP gave 3.86 eV while being 5.24 eV for 4b in THF. These values, for BLYP ranged from 5.38 – 8.36 eV, with MMP having a value of 5.38 eV while being 8.36 eV for 4d in vacuum. MMP gave 5.40 eV, while it gave 8.16 eV for 4e in THF. Figs. 4.25.

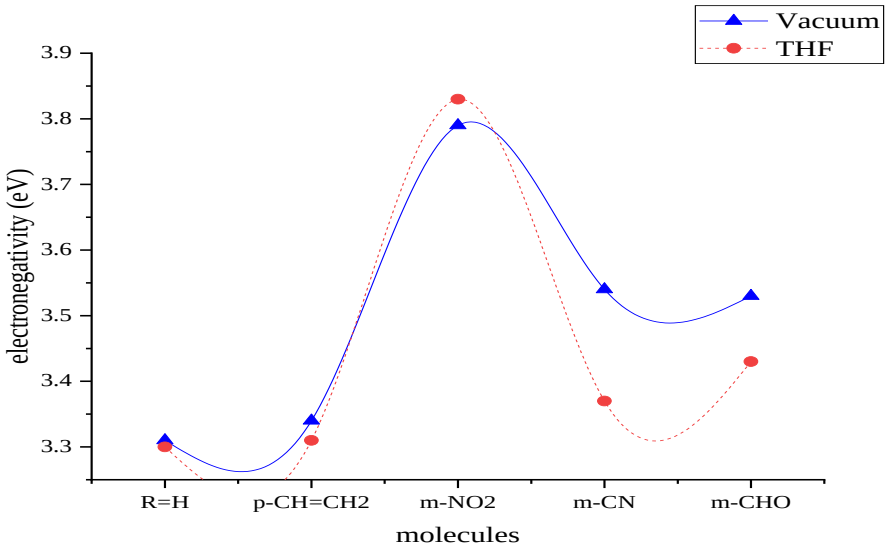

Figure 4.20a: Electronegativity of 10-MPmSBs (B3LYP)

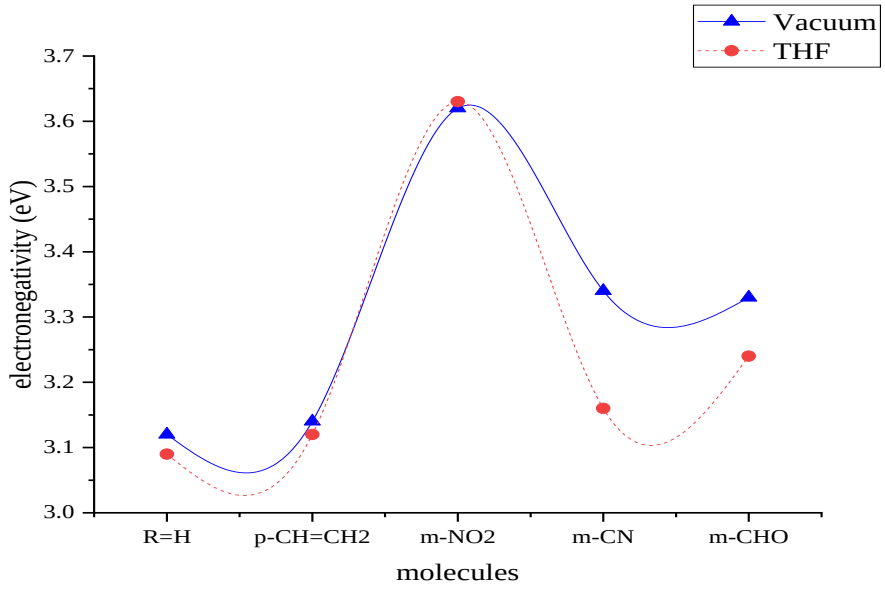

Figure 4.20b: Electronegativity of 10-MPmSBs (BLYP)

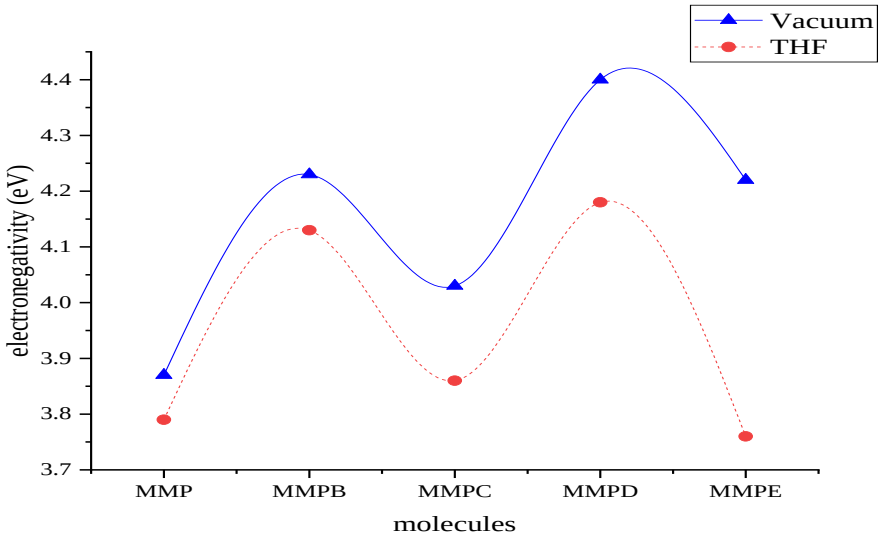

Figure 4.21a: Electronegativity of MMPs (B3LYP)

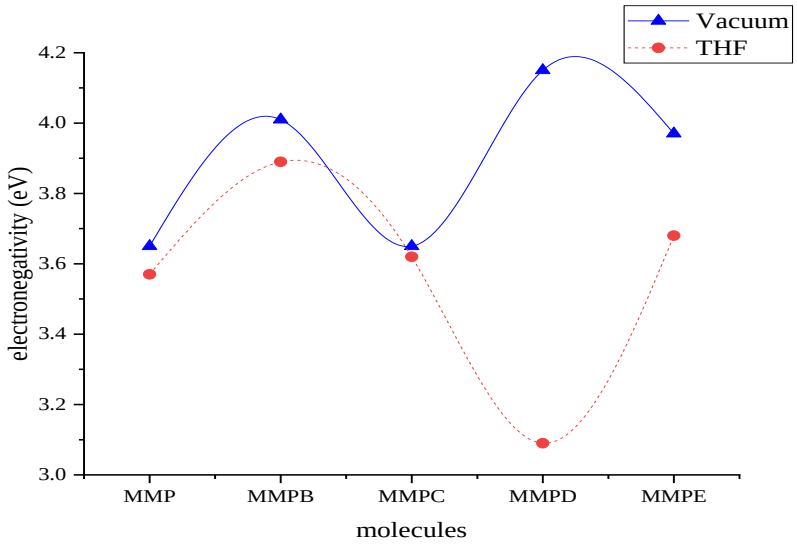

Figure 4.21b: Electronegativity of MMPs (BLYP)

The ω values of the molecules under study increased upon substitution as compared to the unsubstituted analogues, Figs. 4.22-4.25. This is expected as the ω value depends on both χ values and E_g values. Higher global electrophilicity indices possessed by the substituted derivatives are indicative that they possess better reactivities, the substituted derivatives are therefore, expected to generate instantaneous dipoles more readily than their unsubstituted analogues. This further suggests that the substituted analogues have the potentials to be better NLO candidates than MMP.

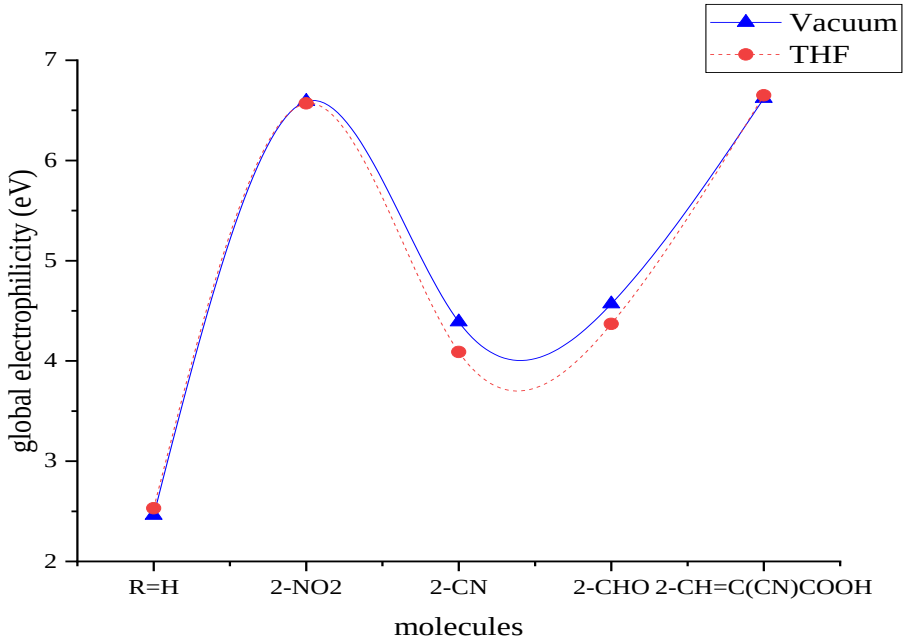

Figure 4.22a: Global electrophilicity index of 10-OTBPs (B3LYP)

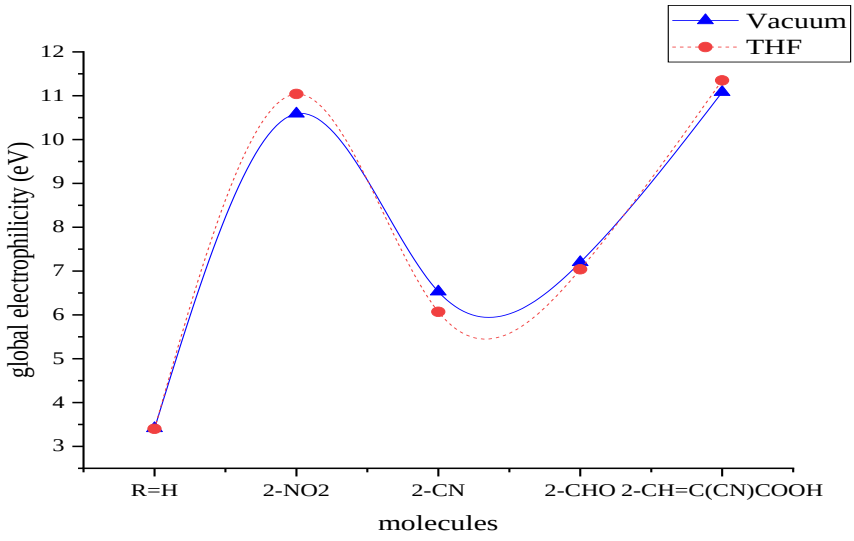

Figure 4.22b: Global electrophilicity index of 10-OTBPs (BLYP)

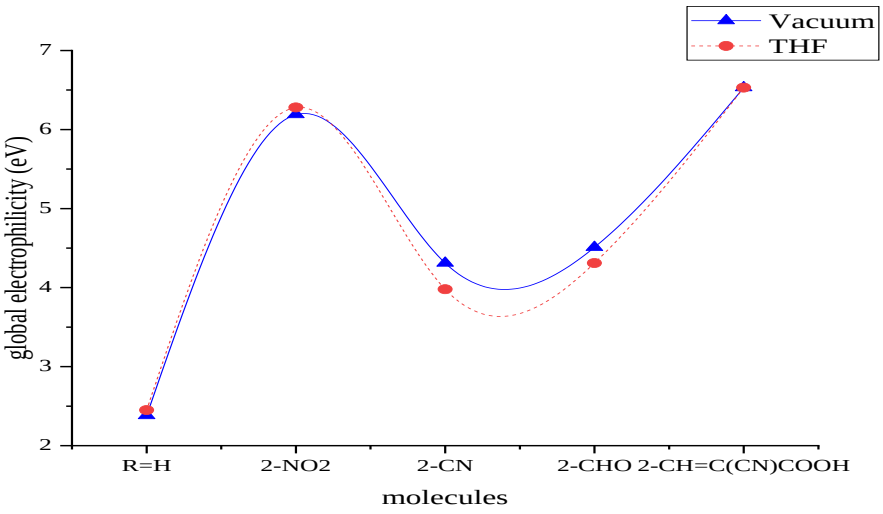

Figure 4.23a: Global electrophilicity index of 10-MTBPs (B3LYP)

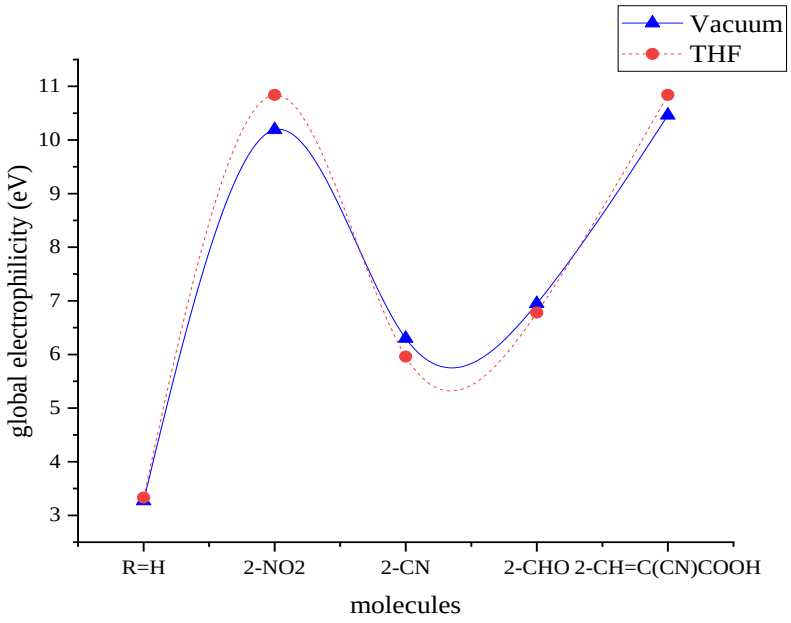

Figure 4.23b: Global electrophilicity index of 10-MTBPs (BLYP)

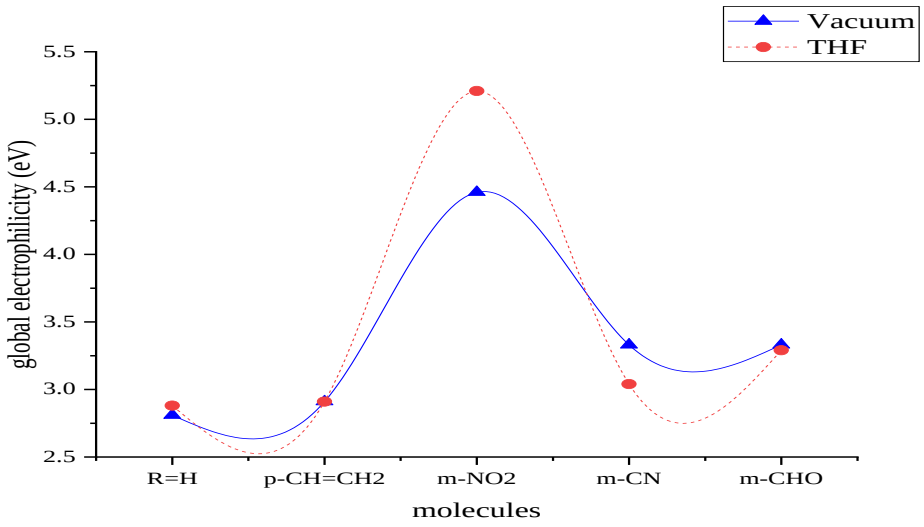

Figure 4.24a: Global electrophilicity index of 10-MPmSBs (B3LYP)

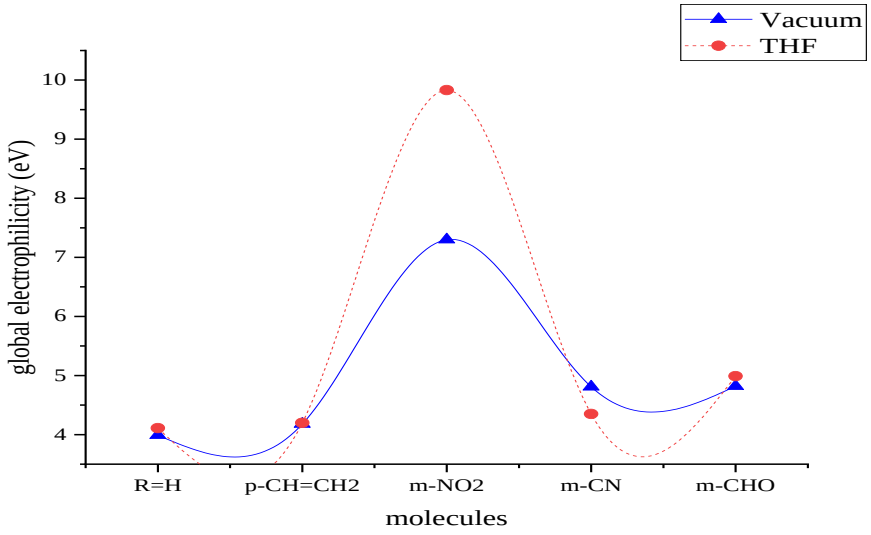

Figure 4.24b: Global electrophilicity index of 10-MPmSBs (BLYP)

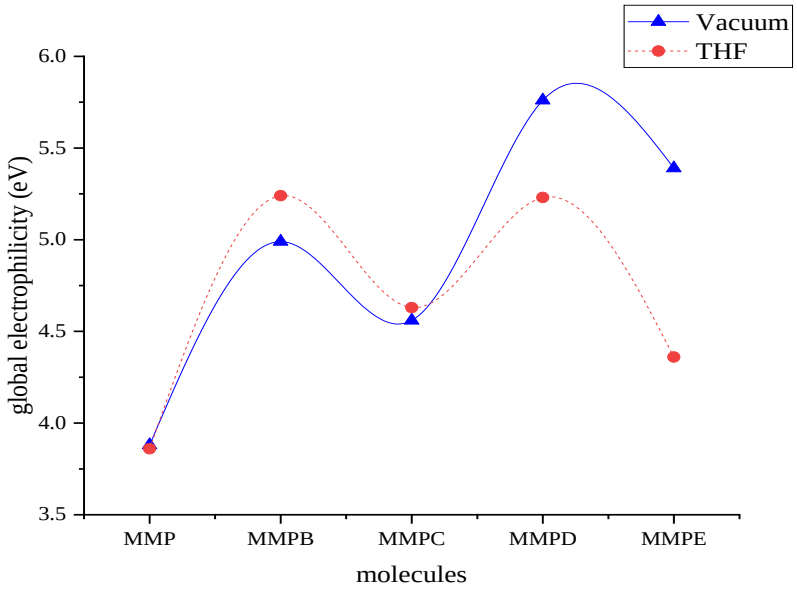

Figure 4.25a: Global electrophilicity index of MMPs with (B3LYP)

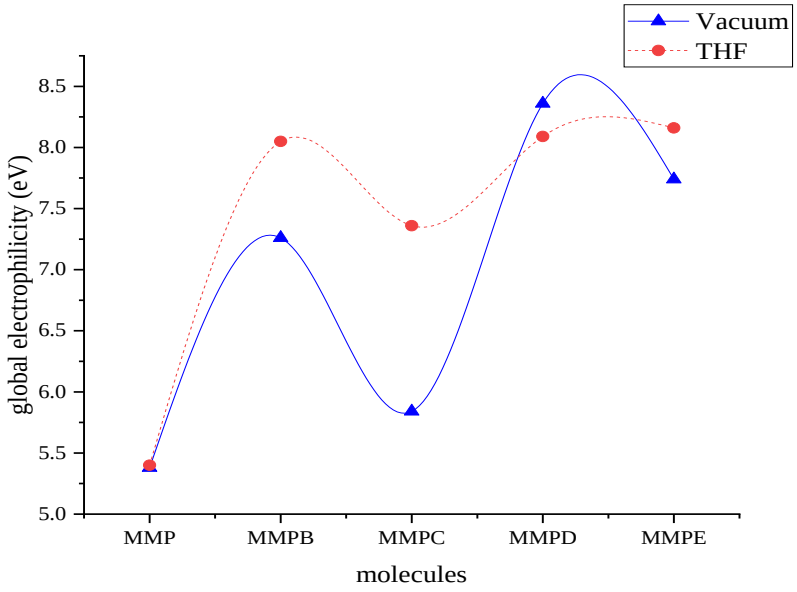

Figure 4.25b: Global electrophilicity index of MMPs (BLYP)

4.2.5 Structural and Solvent Dependence on Polarizability (α)

The B3LYP α values of 10-OTBP on Table 4.25 ranged from 80.37 – 89.90 cm^2V^{-1}, with the unsubstituted having a value of 80.37 cm^2V^{-1} while being 89.90 cm^2V^{-1} for 1e (vacuum), followed by 1b (84.07 cm^2V^{-1}). The unsubstituted has a value of 80.41 cm^2V^{-1} while being 90.00 $cm^2V^{-1}$for 1e (THF), followed by 1b (84.11 cm^2V^{-1}). The BLYP α values of 10-MTBP on Table 4.26 ranged from 81.08 – 94.45 cm^2V^{-1}, with the unsubstituted having a value of 81.08 cm^2V^{-1} while being 94.45 cm^2V^{-1} for 1e (vacuum), followed by 1b having a value of 84.82 cm^2V^{-1}. The unsubstituted has a value of 81.11 cm^2V^{-1} while being 94.53 cm^2V^{-1} for 1e (THF), followed by 1b having 84.90 cm^2V^{-1}. Figs. 4.26.

The B3LYP α values of 10-MTBP on Tables 4.27 ranged from 69.88 – 82.98 cm^2V^{-1}, with the unsubstituted having a value of 69.88 cm^2V^{-1} while being 82.98 $cm^2V^{-1}$for 2e (vacuum), followed by 2b of 73.60 cm^2V^{-1}. The unsubstituted has a value of 69.89 cm^2V^{-1} while being 83.05 cm^2V^{-1} for 2e (THF), followed by 2b of 73.69 cm^2V^{-1}. The BLYP α values of 10-MTBP on Table 4.28 ranged from 70.49 – 83.67 cm^2V^{-1}, with the unsubstituted having a value of 70.49 cm^2V^{-1} while being 83.67 $cm^2V^{-1}$for 2e (vacuum), followed by 2b with 74.25 cm^2V^{-1}. The unsubstituted has a value of 70.50 cm^2V^{-1} while being 83.68 cm^2V^{-1} for 2e (THF), followed by 2b with 74.33 cm^2V^{-1}. Figs. 4.27.

The α values of 10-MP*m*SB for B3LYP on Table 4.29 ranged from 67.17 – 69.81 cm^2V^{-1}, with the unsubstituted having a value of 67.17 cm^2V^{-1} while being 69.81 cm^2V^{-1} for 3b (vacuum), followed by 3c with a value of 69.06 cm^2V^{-1}. The unsubstituted has a value of 67.21 cm^2V^{-1} while being 69.84 cm^2V^{-1} for 3b (THF), followed by 3c with a value of 69.18 cm^2V^{-1}. The values for BLYP on Table 4.30 ranged from 67.77 – 70.45 cm^2V^{-1}, with the unsubstituted having a value of 67.77 cm^2V^{-1} while being 70.45 cm^2V^{-1} for 3b (vacuum), followed by 3c with a value of 69.70 cm^2V^{-1}. The unsubstituted has a value of 67.81 cm^2V^{-1} while being 70.46 cm^2V^{-1} for 3b (THF), followed by 3c with a value of 69.82 cm^2V^{-1}. Figs. 4.28.

The α values of MMPs for B3LYP on Table 4.31 ranged from 59.63 – 66.98 cm^2V^{-1}, with MMP having a value of 59.63 cm^2V^{-1} while being 66.98 cm^2V^{-1} for 4d (vacuum). MMP gave 60.85 cm^2V^{-1} while being 67.12 cm^2V^{-1} for 4d (THF). The values for BLYP on Table

4.32 ranged from 59.63 – 68.33 cm^2V^{-1}, with MMP having a value of 59.63 cm^2V^{-1} while being 68.33 cm^2V^{-1} for 4d (vacuum). MMP gave 60.39 cm^2V^{-1} while being 69.21 cm^2V^{-1} for 4d (THF). In all, the substituted derivatives all increased the α values, with *A*-CH=C(CN)COOH, D-SCH_3 (4d) and *A*-NO_2, D-SCH_3 (4b) analogues having the highest values owing to their large molecular sizes. Figs. 4.29.

The polarizabilities of all the studied molecules increase with decreasing E_g as different substituent groups were added this may be due to the different size and planarity. There is a slight increase in the polarizability values in THF. –NO_2 and -CH=C(CN)COOH substituted derivatives have proven to be the best candidates from all the investigated systems because of their lower E_g and α values. This is a consequence of the withdrawing power of the nitro group and the higher size and longer conjugation of the cyano acrylic group. The substituted molecules undergo drastic changes in their geometries as compared with the reference analogues as a result of steric and inductive effects, this consequently altered the BLAs, E_gs, intra-molecular charge transfer and polarizabilities. This is expected as it has been established earlier in literature.

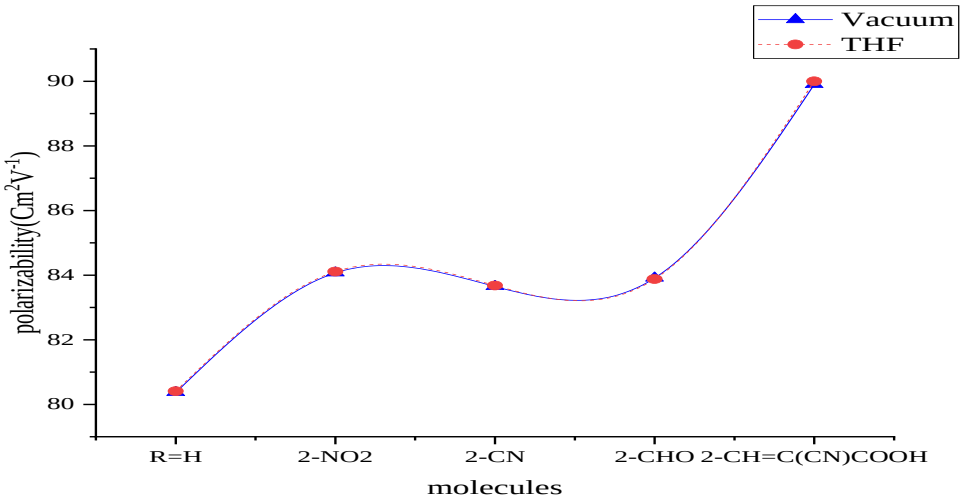

Figure 4.26a: Polarizabilities of 10-OTBPs (B3LYP)

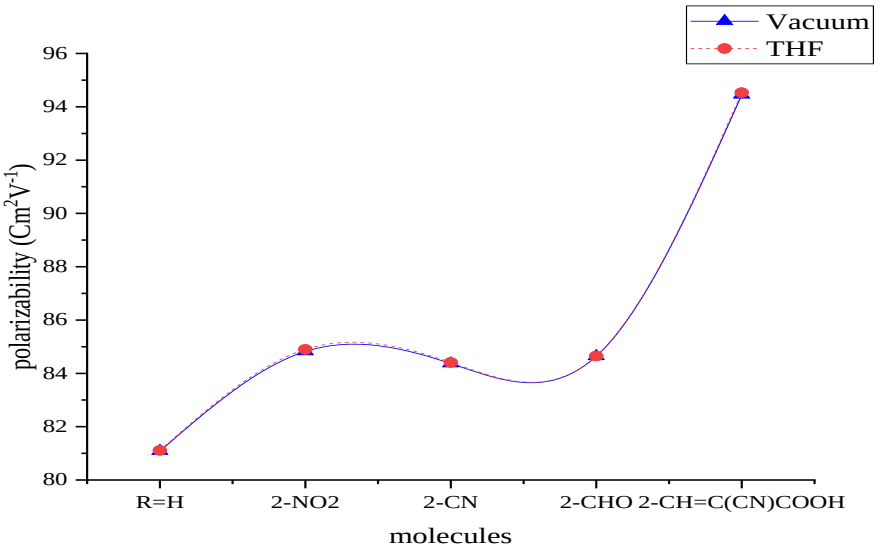

Figure 4.26b: Polarizabiltiies of 10-OTBPs (BLYP)

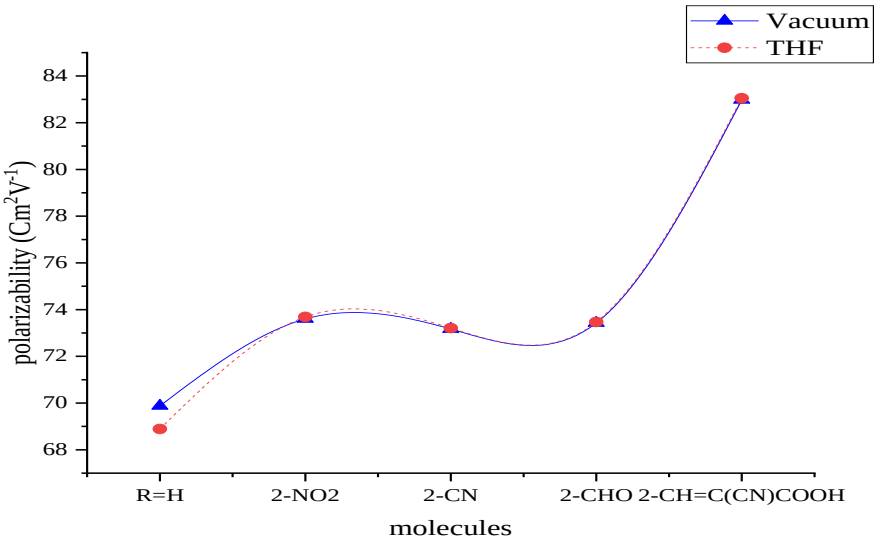

Figure 4.27a: Polarizabilities of 10-MTBPs (B3LYP)

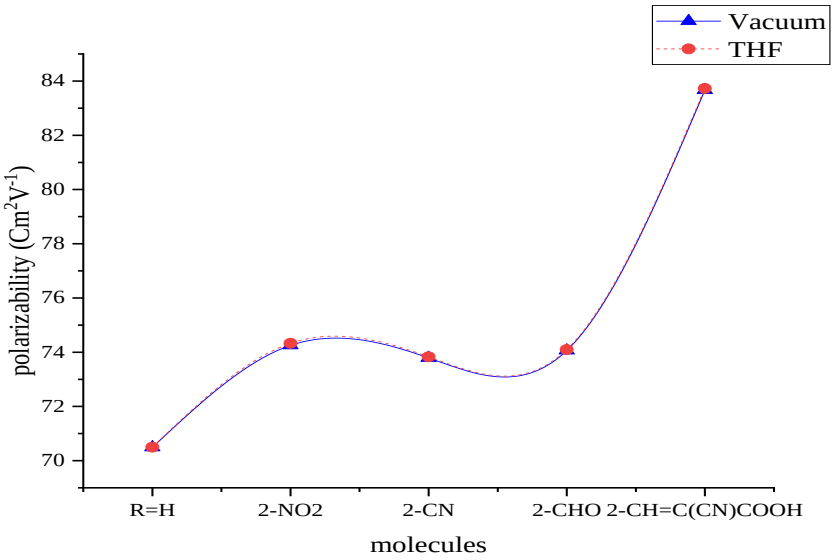

Figure 4.27b: Polarizabilities of 10-MTBPs (BLYP)

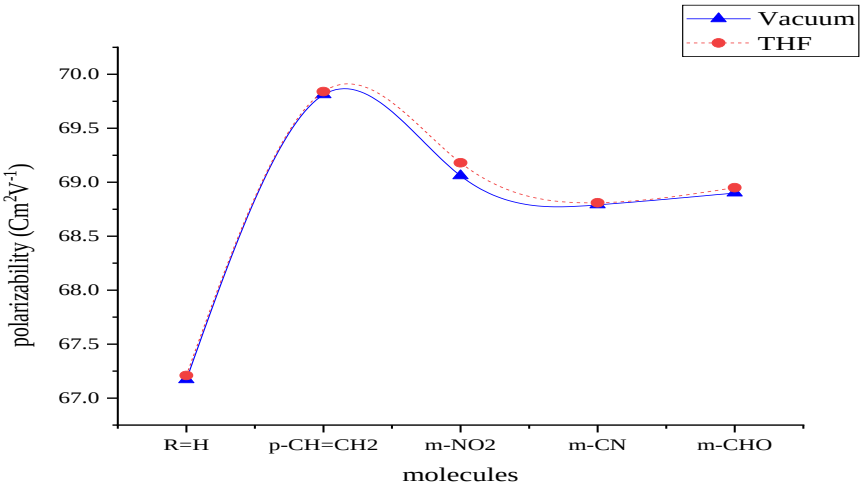

Figure 4.28a: Polarizabilities of 10-MPmSBs (B3LYP)

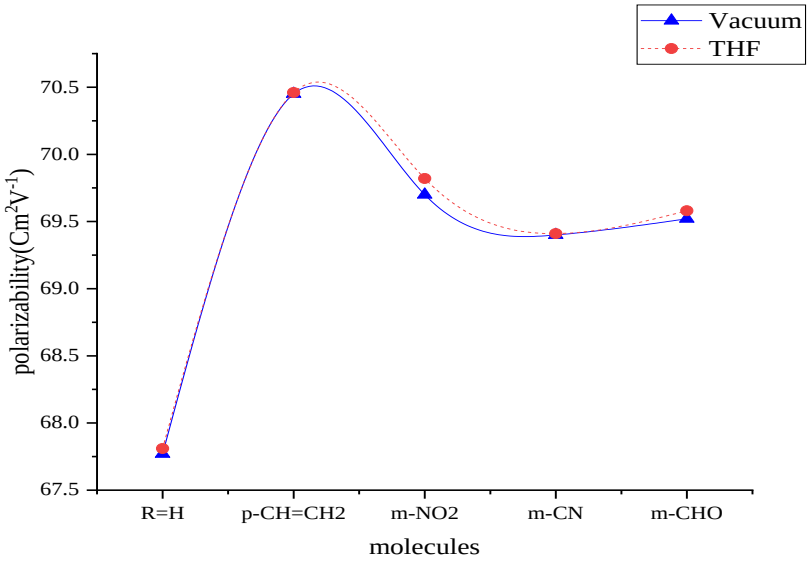

Figure 4.28b: Polarizabilities of 10-MPmSBs (BLYP)

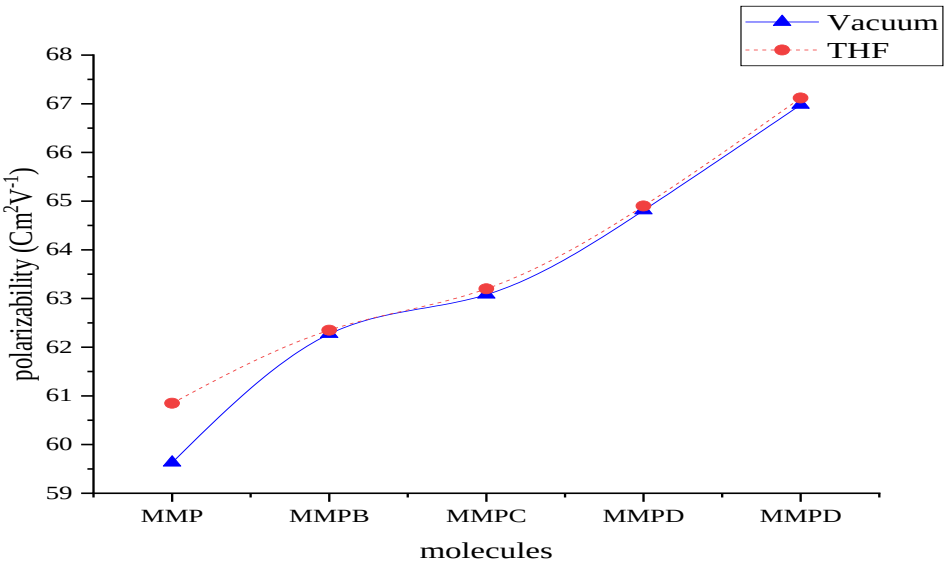

Figure 4.29a: Polarizabilities of MMPs (B3LYP)

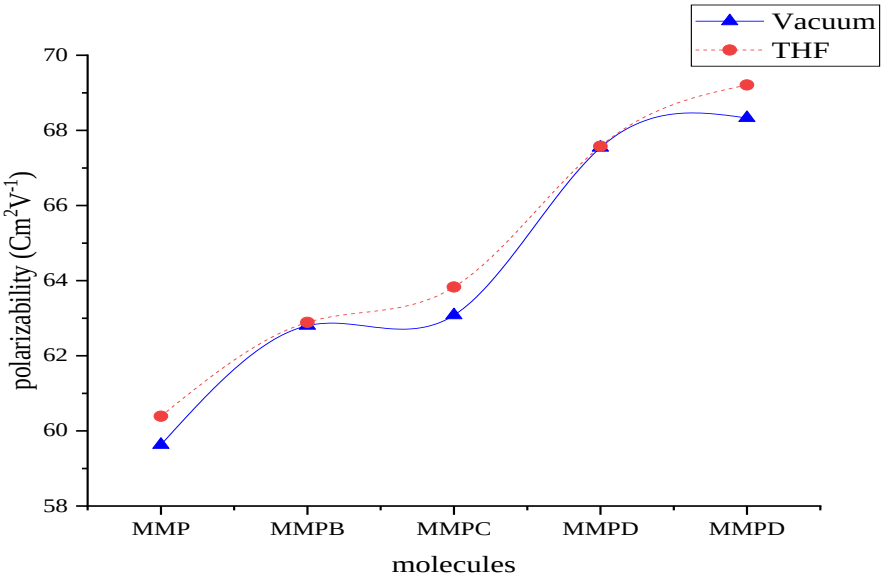

Figure 4.29b: Polarizabilities of MMPs (BLYP)

Table 4.25. The electronic and NLO properties of 10-OTBPs with B3LYP/6-31G* (vacuum) and THF

Molecules	μ (D)	$\alpha(cm^2V^{-1})$	$\beta(x10^{-30}$ esu)	λ_{max} (nm)	*f*	E_{ex}(eV)
			VACUUM			
R=H	2.15	80.37	1.09	293(294)	0.94	4.22
***2*-NO_2**	6.58	84.07	4.67	360	0.42	3.44
***2*-CN**	5.94	83.65	3.88	317	0.75	3.91
***2*-CHO**	6.42	83.91	3.68	328(328)	0.39	3.77
***2*-CH=C(CN)COOH**	9.87	89.90	5.13	378	1.53	3.22
			THF			
R=H	2.97	80.41	1.11	295(292)	0.65	4.35
***2*-NO_2**	8.34	84.11	5.35	361	0.61	3.48
***2*-CN**	7.65	83.68	4.39	340	0.64	3.84
***2*-CHO**	7.22	83.88	4.12	325(324)	0.33	3.71
***2*-CH=C(CN)COOH**	11.67	90.00	7.29	380	1.11	3.15

Experimental results in brackets (Zebiao *et al.*, 2015*)*

Table 4.26. The electronic and NLO properties of 10-OTBPs with BLYP/6-31G* (vacuum) and THF

Molecules	μ (D)	α(cm^2V^{-1})	β(x10^{-30} esu)	λ_{max} (nm)	*f*	E_{ex}(eV)
			VACUUM			
R=H	2.17	81.08	1.04	362(294)	0.26	3.42
***2*-NO_2**	6.76	84.82	4.36	429	0.28	2.89
***2*-CN**	4.04	84.37	3.87	419	0.11	2.96
***2*-CHO**	6.53	84.64	3.01	444(328)	0.66	2.79
***2*-CH=C(CN)COOH**	8.79	94.45	5.76	470	0.80	2.66
			THF			
R=H	3.27	81.11	1.07	368(294)	0.34	3.40
***2*-NO_2**	8.71	84.90	5.31	457	0.26	2.75
***2*-CN**	7.88	84.41	4.36	423	0.21	2.78
***2*-CHO**	8.04	84.65	4.15	413(328)	0.66	2.64
***2*-CH=C(CN)COOH**	13.01	94.53	6.91	492	0.83	2.53

Experimental results in brackets (Zebiao *et al.*, 2015*)*

Table 4.27. The electronic and NLO properties of 10-MTBPs with B3LYP/6-31G* (vacuum) and THF

Molecules	μ (D)	α(cm^2V^{-1})	β(x10^{-30} esu)	λ_{max} (nm)	*f*	E_{ex}(eV)
			VACUUM			
R=H	1.31	69.88	0.62	285	0.70	4.35
***2*-NO_2**	6.07	73.60	4.49	351	0.52	3.52
***2*-CN**	5.64	73.17	3.59	308	0.69	4.01
***2*-CHO**	5.80	73.43	3.66	318	0.56	3.89
***2*-CH=C(CN)COOH**	7.87	82.98	5.40	365	1.60	3.39
			THF			
R=H	1.97	68.89	0.63	285	0.62	4.35
***2*-NO_2**	7.79	73.69	6.15	354	0.53	3.54
***2*-CN**	7.82	73.21	4.57	318	0.41	3.91
***2*-CHO**	7.45	73.47	4.49	339	0.63	3.68
***2*-CH=C(CN)COOH**	11.71	83.05	7.04	382	1.20	3.29

Table 4.28. The electronic and NLO properties of 10-MTBPs with BLYP/6-31G* (vacuum) and THF

Molecules	μ (D)	α(cm^2V^{-1})	β($x10^{-30}$ esu)	λ_{max} (nm)	*f*	E_{ex}(eV)
			VACUUM			
R=H	1.35	70.49	0.58	357	0.79	3.47
***2*-NO_2**	5.72	74.25	4.32	420	0.57	2.95
***2*-CN**	5.47	73.79	3.33	412	0.74	3.01
***2*-CHO**	5.35	74.06	3.69	440	0.63	2.26
***2*-CH=C(CN)COOH**	8.25	83.67	4.81	450	1.03	2.75
			THF			
R=H	2.05	70.50	0.59	355	0.78	3.49
***2*-NO_2**	7.98	74.33	6.11	453	0.50	2.74
***2*-CN**	7.87	73.83	4.57	424	0.70	2.92
***2*-CHO**	7.85	74.10	4.69	454	0.66	2.73
***2*-CH=C(CN)COOH**	12.87	83.73	7.56	485	0.81	2.55

Table 4.29. The electronic and NLO properties of 10-MP*m*SBs with B3LYP/6-31G* (vacuum) and THF

Molecules	μ (D)	α(cm^2V^{-1})	β($x10^{-30}$ esu)	λ_{max} (nm)	*f*	E_{ex}(eV)
			VACUUM			
R=H	4.44	67.17	1.49	276	0.27	4.49
p-CH=CH_2	4.42	69.81	1.71	286	0.11	4.34
***m*-NO_2**	7.46	69.06	3.00	377	0.17	3.29
***m*-CN**	7.39	68.79	1.96	377	0.16	3.28
***m*-CHO**	4.81	68.90	1.85	379	0.16	3.27
			THF			
R=H	5.87	67.21	1.84	280	0.43	4.43
p-CH=CH_2	5.79	69.84	1.99	283	0.71	4.38
***m*-NO_2**	10.55	69.18	4.43	376	0.19	3.29
***m*-CN**	9.70	68.81	2.84	377	0.17	3.29
***m*-CHO**	6.00	68.95	2.94	377	0.11	3.29

Table 4.30. The electronic and NLO properties of 10-MP*m*SBs with BLYP/6-31G* (vacuum) and THF

Molecules	μ (D)	α(cm^2V^{-1})	β(x10^{-30} esu)	λ_{max} (nm)	*f*	E_{ex}(eV)
			VACUUM			
R=H	4.57	67.77	1.51	346	0.07	3.58
p-CH=CH_2	4.63	70.45	1.74	367	0.09	3.38
***m*-NO_2**	7.71	69.7	3.04	468	0.12	2.65
***m*-CN**	7.61	69.4	2.09	426	0.16	2.91
***m*-CHO**	5.25	69.52	2.29	464	0.09	2.67
			THF			
R=H	6.27	67.81	1.90	333	0.16	3.72
p-CH=CH_2	6.23	70.46	2.12	347	0.17	3.57
***m*-NO_2**	11.12	69.82	4.63	462	0.16	2.68
***m*-CN**	10.17	69.41	3.77	457	0.14	2.72
***m*-CHO**	6.75	69.58	3.32	467	0.12	2.66

Table 4.31. The electronic and NLO properties of MMPs with B3LYP/6-31G* (vacuum) and THF

Molecules	μ (D)	α(cm^2V^{-1})	β($x10^{-30}$ esu)	λ_{max} (nm)	*f*	E_{ex}(eV)
			VACUUM			
A-$COCH_3$, D-SCH_3, MMP	4.60	59.63	2.44	344(<400)	0.65	3.61
A-NO_2, D-SCH_3	7.45	62.27	3.84	370	0.79	3.36
A-NO_2, D-NH_2	10.10	63.08	4.78	369	0.73	3.36
A-CH=C(CN)COOH, D-SCH_3	11.49	64.81	8.98	397	0.96	3.13
A-CH=C(CN)COOH, D-NH_2	13.65	66.98	9.67	399	0.92	3.10
			THF			
A-$COCH_3$, D-SCH_3, MMP	5.53	60.85	2.85	350	1.16	3.55
A-NO_2, D-SCH_3	9.11	62.35	4.62	408	0.55	3.04
A-NO_2, D-NH_2	12.96	63.20	6.13	440	0.39	2.81
A-CH=C(CN)COOH, D-SCH_3	14.11	64.90	11.15	420	0.73	2.91
A-CH=C(CN)COOH, D-NH_2	14.40	67.12	12.33	451	0.78	2.74

Experimental results in bracket (D'Silva *et al.*, 2012).

Table 4.32. The electronic and NLO properties of MMP with BLYP/6-31G* (vacuum) and THF

Molecules	μ (D)	α(cm^2V^{-1})	β($x10^{-30}$ esu)	λ_{max} (nm)	*f*	E_{ex}(eV)
			VACUUM			
A-$COCH_3$, D-SCH3, MMP	5.05	59.63	2.61	412(<400)	0.25, 0.68	3.24, 3.01
A-NO_2, D-SCH_3	7.99	62.80	4.03	389,496	0.55, 0.27	3.18, 2.50
A-NO_2, D-NH_2	10.65	63.08	4.95	360,499	0.64, 0.00	3.44, 2.48
A-CH=C(CN)COOH, D-SCH_3	12.14	67.54	9.34	418,525	0.81, 0.37	2.97, 2.36
A-CH=C(CN)COOH, D-NH_2	14.42	68.33	10.09	411,517	0.78, 0.39	3.01, 2.40
			THF			
A-$COCH_3$, D-SCH3, MMP	6.23	60.39	3.12	376, 437	0.46, 0.53	3.29, 2.84
A-NO_2, D-SCH_3	10.23	62.89	5.05	409, 579	0.53, 0.23	3.03, 2.14
A-NO_2, D-NH_2	14.21	63.83	6.65	378, 696	0.79, 0.00	3.28, 1.78
A-CH=C(CN)COOH, D-SCH_3	15.59	67.58	12.15	418, 577	1.05, 0.34	2.97, 2.15
A-CH=C(CN)COOH, D-NH_2	20.60	69.21	14.34	420, 598	0.91, 0.42	2.95, 2.07

Experimental results in bracket (D'Silva *et al.*, 2012).

4.2.6 Structural and Solvent Dependence on Dipole Moment (μ)

The B3LYP μ values of 10-OTBP on Table 4.25 ranged from 2.15 - 9.87 D, with the unsubstituted having a value of 2.15 D while being 7.87 D for 1e (vacuum), followed by 1b with a value of 6.58 D. The unsubstituted has a value of 2.97 D while being 11.67 D for 1e (THF), followed by 1b (8.34 D). The BLYP μ values of 10-OTBP on Table 4.26 ranged from 2.17 – 8.79 D, with the unsubstituted having a value of 2.17 D while being 8.79 D for 2e (vacuum) followed by 1b with a value of 6.76 D. The unsubstituted has a value of 3.27 D while being 13.01 D for 1e (THF), followed by 1b (8.71 D). Figs.4.30.

The B3LYP μ values of 10-MTBP on Table 4.27 ranged from 1.31 - 7.87 D, with the unsubstituted having a value of 1.31 D while being 7.87 D for 2e (vacuum), followed by 2b (6.07 D). The unsubstituted has a value of 1.97 D while being 11.71 D for 2e (THF), with 2c (7.82 D) after 2e. The ranged from 1.35 – 8.25 D on Table 4.28 with BLYP, with the unsubstituted having a value of 1.35 D while being 8.25 D for 2e (vacuum), followed by 2b (5.85 D). The unsubstituted has a value of 2.05 D while being 13.66 D for 2e (THF), followed by 2b (7.98 D). Figs. 4.31.

The B3LYP μ values of 10-MP*m*SB on Table 4.29 ranged from 4.44 - 7.46 D, with the unsubstituted having a value of 4.44 D while being 7.46 D for 3c in vacuum. The unsubstituted has a value of 5.87 D while being 10.55 D for 3c in THF. The BLYP μ values on Table 4.30 ranged from 4.57 – 7.71 D, with the unsubstituted having a value of 4.57 D while being 7.71 D for 3c in vacuum. The unsubstituted molecule has a value of 6.27 D while being 11.12 D for 3c in THF. Figs. 4.32.

The B3LYP μ values of MMPs on Table 4.31 ranged from 4.60 – 13.65 D, with MMP having a value of 4.60 D while being 13.65 D for 4d (vacuum). MMP gave 5.53 D while being 18.40 D for 4d (THF). The BLYP values on Table 4.32 ranged from 5.05 – 14.41 D, with MMP having a value of 5.05 D while being 14.42 D for 4d (vacuum). MMP gave 6.23 D while being 20.20 D for 4d in THF. Figs. 4.33.

The dipole moments, just like with polarizabilities increase with an increase in E_g as different substituent groups were added, this may be due to the different size and planarity. However, it increased significantly in THF. This is an indication that there are changes in

the electronic and geometric structures of the molecules in solution owing to different conFigurations they take in the solvent. $–NO_2$ and -CH=C(CN)COOH substituted derivatives have proven to be the best candidates from all the investigated systems because of their lower E_g and α values.

Molecules possessing higher weight and/or lower energy E_g values are expected possess better ICT and also form instantaneous dipoles more easily than those having higher energy gap values. The results obtained so far have shown than E_g values of the substituted derivatives decrease as compared to their unsubstituted analogues, also, it has been established that they also minimized BLA and higher polarizabilities and now, higher values of dipole moments. These are indicative that the substituted molecules may possess better NLO efficiencies than the unsubstituted dervtives if their second order susceptibilities are higher. To ascertain the NLO efficiency of a molecule, it is necessary to compare their energy gaps with their hyperpolarizability values. A molecule having a lower E_g value has the ability to strengthen the interaction between its frontier orbitals and possesses higher α and β values when compared to another molecule can be said to have better SHG efficiency. The dipole moments are illustrated graphically on Figs. 4.30-4.33.

-CH=C(CN)COOH substituted analogues have proven so far to be the most reactive species of the investigated molecules as well as being the molecules with the best electro-optic response in that they have larger size, lowest E_g values, largest polarizabilities followed by $–NO_2$. To confirm if these molecules are better NLO candidate than the unsubstituted analogues, their SHG efficiencies need to be investigated and this can be done by calculating their second-order susceptibilities, the third-rank tensor component, hyperpolarizabilities using the Kleinman symmetry (Kleinman, 1962) in eqution 2.34.

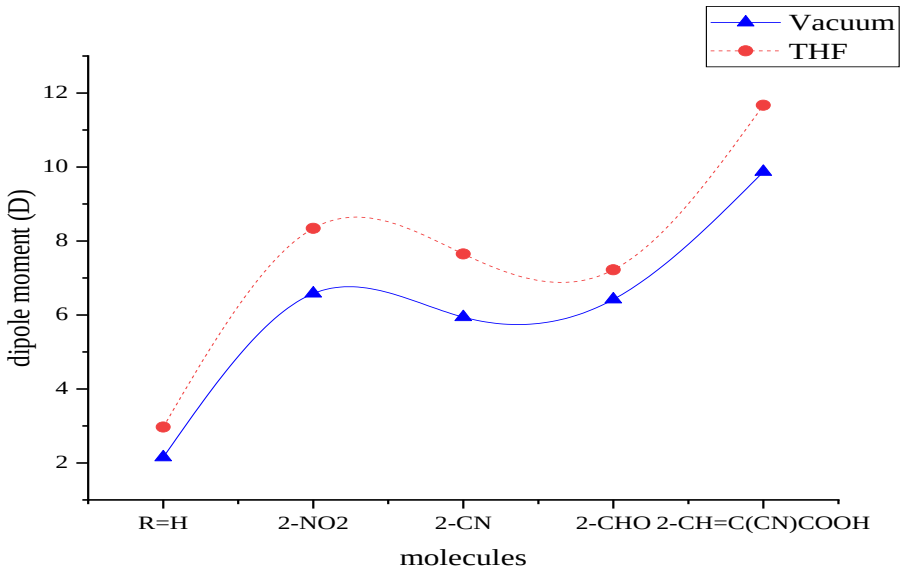

Figure 4.30a: Dipole moments for 10-OTBPs (B3LYP)

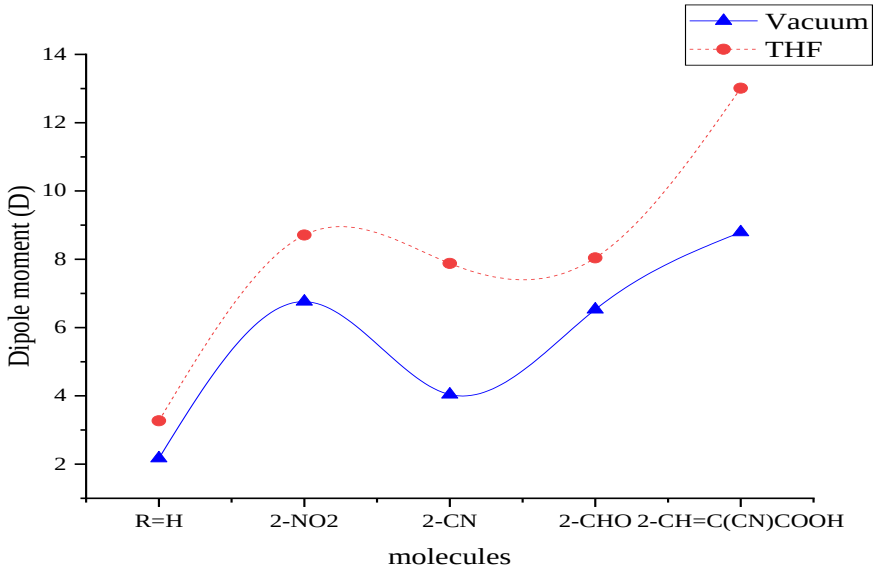

Figure 4.30b: Dipole moments for 10-OTBPs (BLYP)

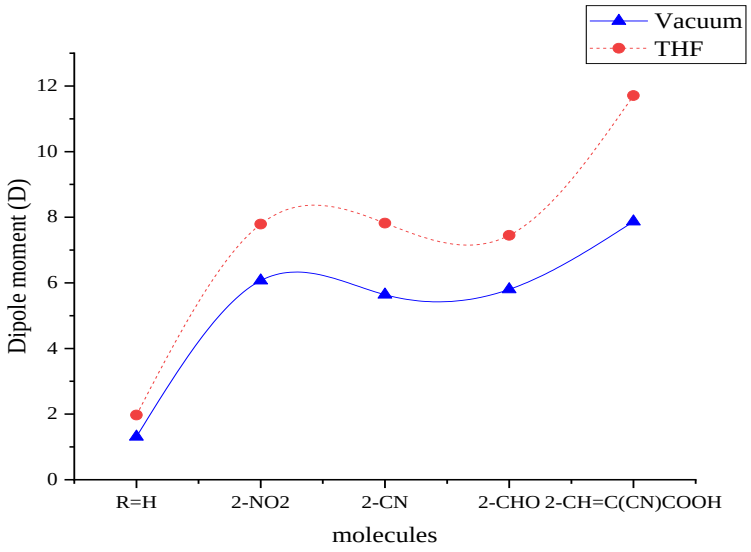

Figure 4.31a: Dipole moments for 10-MTBPs (B3LYP)

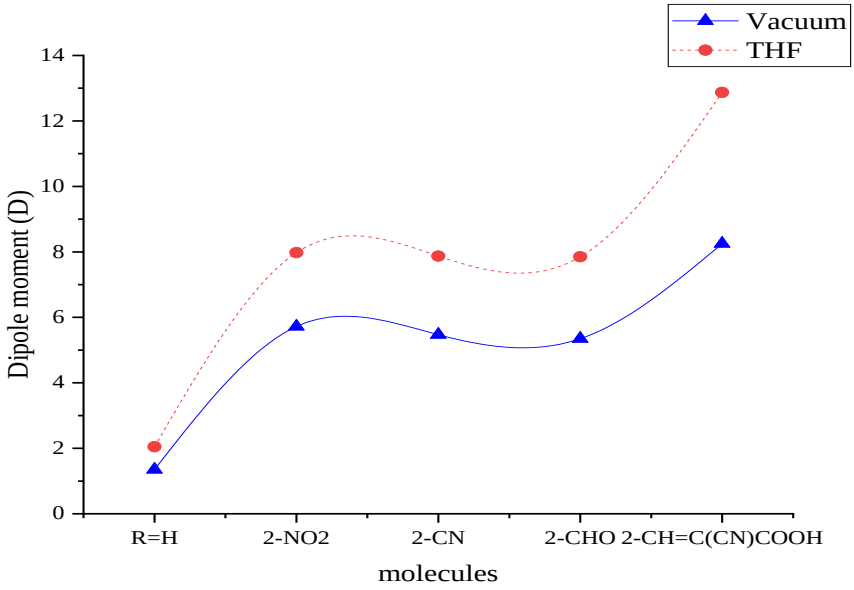

Figure 4.31b: Dipole moments for 10-MTBPs (BLYP)

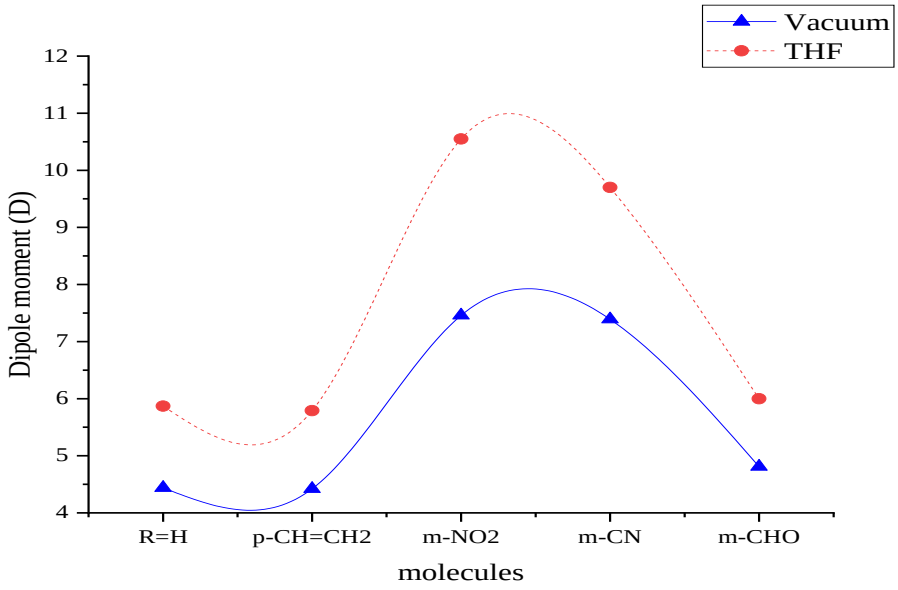

Figure 4.32a: Dipole moments for 10-MPmSBs (B3LYP)

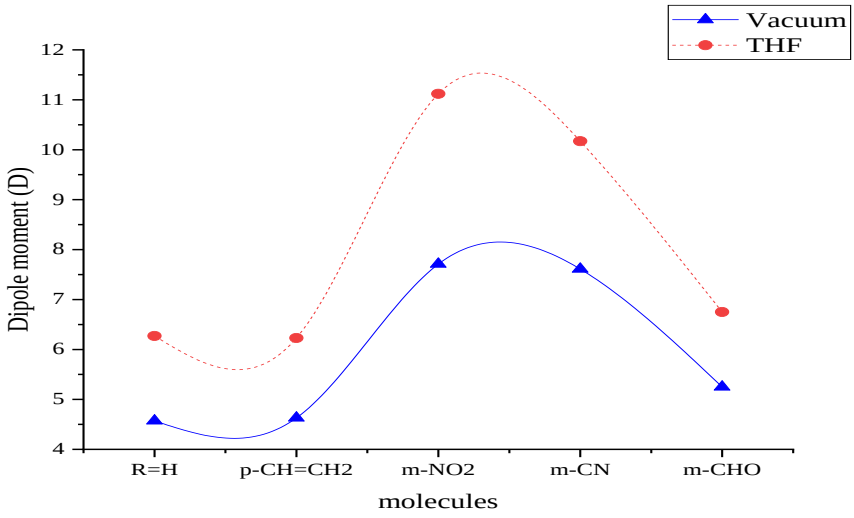

Figure 4.32b: Dipole moments for 10-MPmSBs (BLYP)

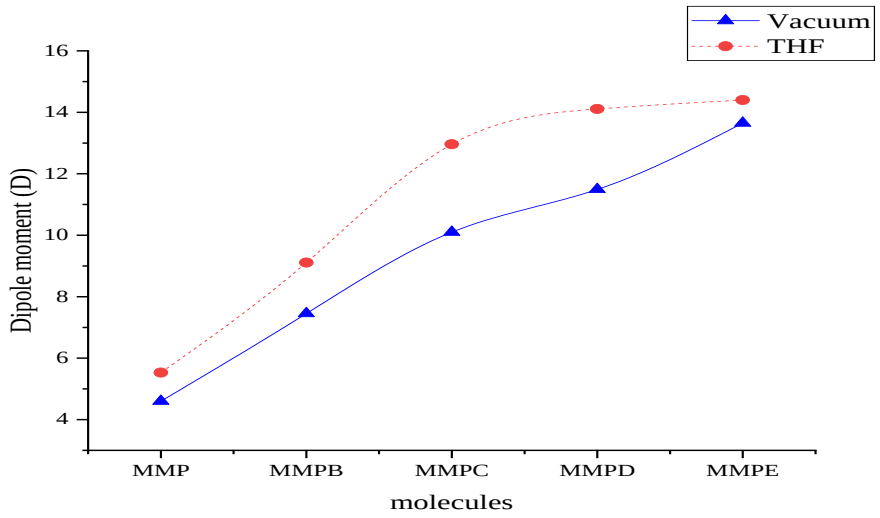

Figure 4.33a: Dipole moments for MMPs (B3LYP)

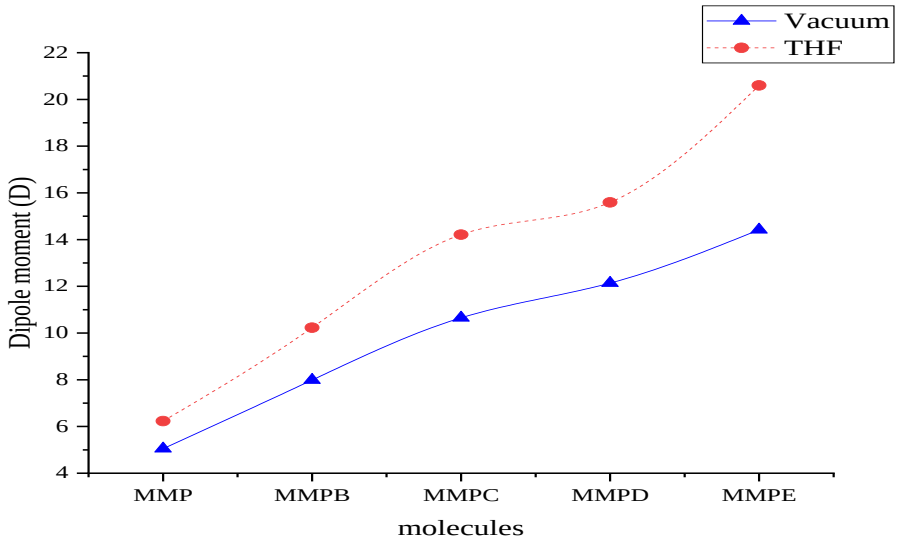

Figure 4.33b: Dipole moments for MMPs (BLYP)

4.2.7 Structural and Solvent Dependence on Molecular First Hyperpolarizability (β)

β values increased as different substituents were added. In the B3LYP/6-31G* results, the β values for 10-OTBP are on Table 4.25 ranged from 1.09 – 5.13 $x10^{-30}$ esu, with 1e giving 5.13 $x10^{-30}$ esu, the highest while the values in THF ranged from 1.11 – 7.29 $x10^{-30}$ esu with all the substituted analogues also increasing significantly these values, with 1e giving 7.29 $x10^{-30}$ esu, the highest. A general observation is that all β values increased in THF as compared with vacuum. In the BLYP/6-31G* results, the β values on Table 4.26 ranged from 1.04 – 5.75 $x10^{-30}$ esu, with 1e giving 5.75 $x10^{-30}$ esu, the highest while the values in THF ranged from 1.07 – 6.91 $x10^{-30}$ esu with all the substituted analogues also increasing significantly these values, with 1e giving 6.91 $x10^{-30}$esu, the highest. A general observation also, is that all β values increased in THF as compared with vacuum. However, solvent has more effect on the dipole moments and hyperpolarizabilities than on polarizabilities, this is what was observed earlier in previous work (Oyeneyin, 2017) on Figs. 4.34.

For 10-MTBP and its substituted derivatives, it is observed on Table 4.27 that β values increased as different substituents were added. In the B3LYP/6-31G* results, the β values on Table 4.27 ranged from 0.62 – 5.40 $x10^{-30}$ esu, with all the substituted analogues increasing significantly these values in vacuum, with 2e giving 5.40 $x10^{-30}$ esu, the highest while the values in THF ranged from 0.63 – 7.04 $x10^{-30}$ esu with all the substituted analogues also increasing significantly these values, with 2e giving 7.04 $x10^{-30}$ esu, the highest. Also, 2b has 6.15 $x10^{-30}$ esu, a high value as well. In the BLYP/6-31G* results, the β values on Table 4.28 ranged from 0.58 – 4.81 $x10^{-30}$esu, with all the substituted analogues increasing significantly these values in vacuum, with 2e giving 4.81 $x10^{-30}$ esu, the highest while the values in THF ranged from 0.59 – 7.56 $x10^{-30}$ esu with all the substituted analogues also increasing significantly these values, with 2e giving 7.56 $x10^{-30}$esu, the highest. 2b also has a high value of 6.11 $x10^{-30}$ esu, a general observation also, is that all β values increased in THF as compared with vacuum. Figs. 4.35.

For 10-MP*m*SB and its substituted derivatives, it is observed on the Table that β values increases as different substituents are added. In the B3LYP/6-31G* results, the β values on Table 4.29 ranged from 1.48 – 3.00 $x10^{-30}$ esu, all the substituted analogues increased these values in the gas phase, 3c giving of 3.00 $x10^{-30}$ esu, the highest while the values in THF

range from 1.84 – 4.43 x 10^{-30} esu with all the substituted analogues also increasing these values, with 3c having a value of 4.43 x10^{-30} esu, the highest, a general observation also, is that all β values increased in THF as compared with vacuum. In the BLYP/6-31G* results, the β values on Table 4.30 ranged from 1.51 – 3.04 x10^{-30} esu, all the substituted analogues increased significantly these values in the gas phase, 3c giving 3.04 x10^{-30} esu, the highest while the values in THF ranged from 1.90 – 4.63 x10^{-30} esu with all the substituted analogues also increasing significantly these values, with 3c giving 4.63 x10^{-30} esu, the highest. A general observation also, is that all β values increased in THF as compared with vacuum. Figs. 4.36.

The first hyperpolarizabilities (β) of MMPs on Tables 4.31 and 4.32. β increased as different substituents were added. In the B3LYP/6-31G* results, the β values range from 2.44 – 9.67 x10^{-30} esu, with all the substituted analogues increasing these values in vacuum, with 4d giving 9.67 x10^{-30} esu, the highest while the values in THF ranged from 2.85 – 12.33 x10^{-30} esu with all the substituted analogues also increasing these values, with 4d giving 12.33 x10^{-30} esu, the highest. In the BLYP/6-31G* results, the β values on Table 4.24 ranged from 2.61 – 10.09 x10^{-30} esu, with all the substituted analogues increasing significantly these values in vacuum, with 4d giving 10.09 x10^{-30} esu, the highest while the values in THF ranged from 3.12 – 14.34 x10^{-30} esu with all the substituted analogues also increasing significantly these values, with 4d giving 14.34 x10^{-30} esu, the highest. Figs. 4.37.

MMP has a B3LYP β value of 2.44 x10^{-30} esu, 3.75 times of urea (0.65 x10^{-30} esu) (Adhikari and Kar, 2012) while the BLYP β value is 2.61 x10^{-30}, 4.02 times that of urea. This is because the D-A conFiguration of MMP allows charge transfer to be enabled in the whole molecule, along the charge transfer axis. This corroborates the fact that the experimental SHG efficiency of MMP was reported to be 4.13 times that of urea crystals (D'Silva *et al.*, 2012), implying that the BLYP (97.34%) correlation predicts the SHG efficiency and second order susceptibility more effectively than the B3LYP (90.8%) correlation. However, all substituted analogues increased β value, confirming that they are better candidates for NLO applications than MMP, with *A*-CH=C(CN)COOH, D-SCH_3 proving the best in that it has the lowest optical/energy gap, highest value of dipole moment, polarizability and hyperpolarizability.

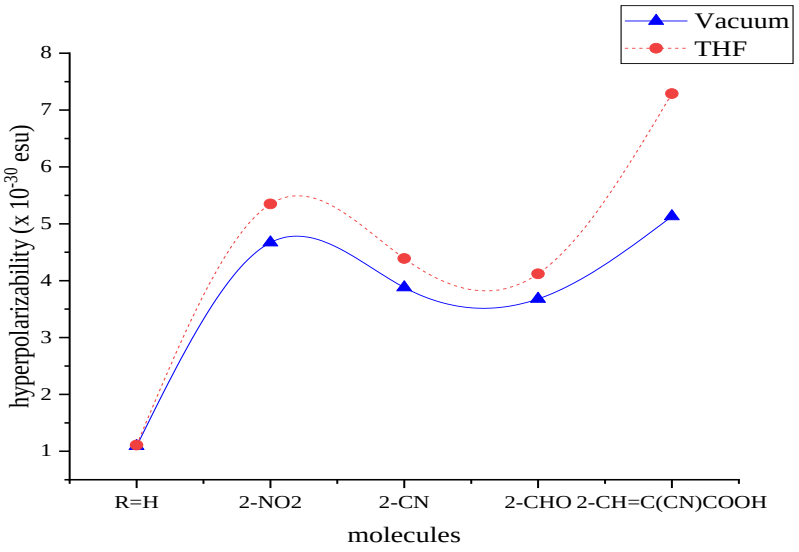

Figure 4.34a: Hyperpolarizabilities for 10-OTBPs (B3LYP)

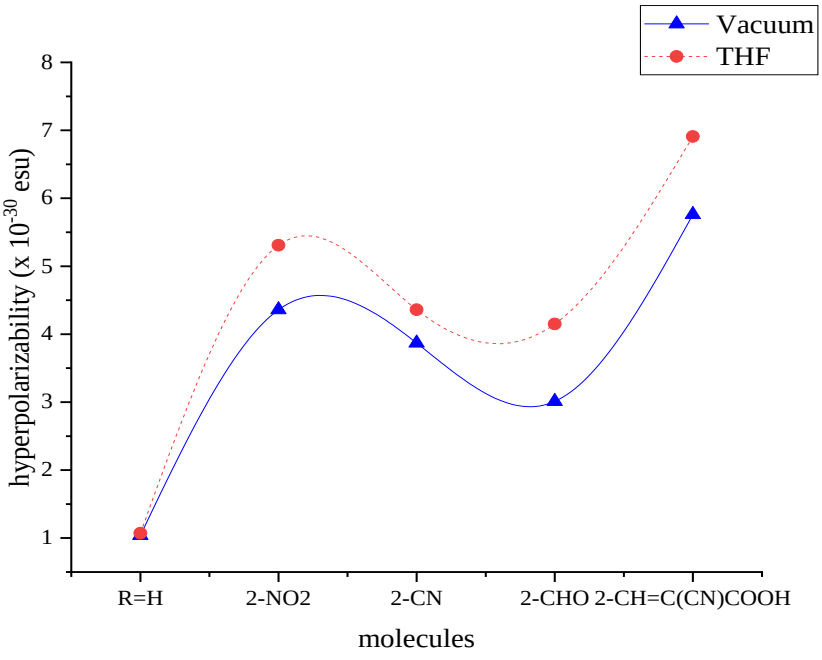

Figure 4.34b: Hyperpolarizabilities for 10-OTBPs (BLYP)

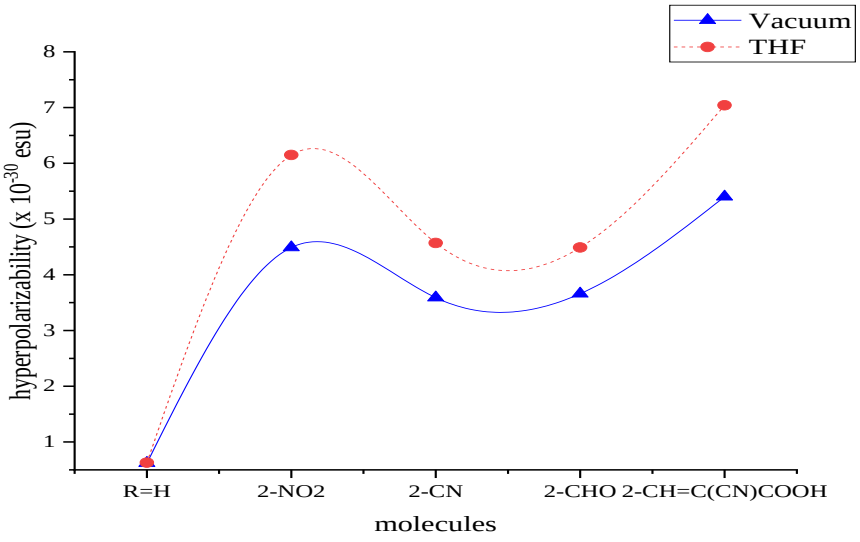

Figure 4.35a: Hyperpolarizabilities for 10-MTBPs (B3LYP)

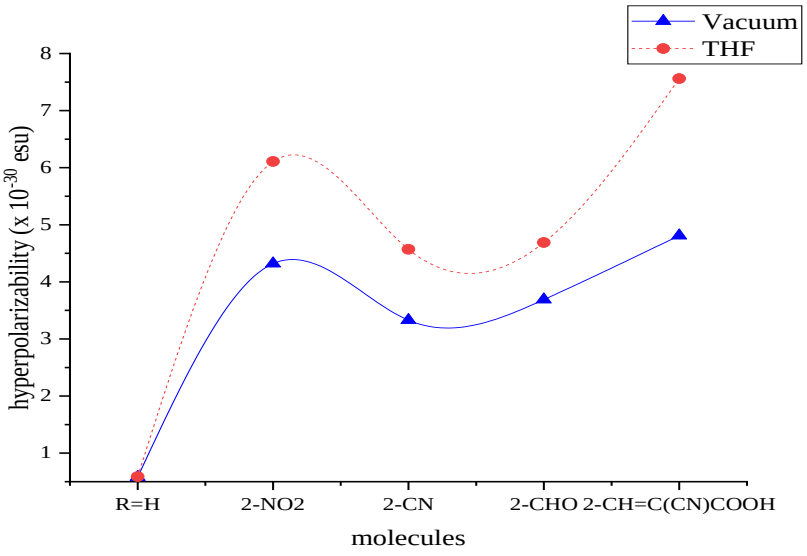

Figure 4.35b: Hyperpolarizabilities for10-MTBPs (BLYP)

The derivatized molecules have shown to be better candidates than unsubstituted ones with the different molecular properties considered so far. For confirmation, the β values also showed that they possess higher β values, implying they possess good second order susceptibilities (χ^2). This is confirming that their nonlinear responses are better. Of all the studied molecules, only unsubstituted 10-MTBP (0.62×10^{-30} esu) has a β value that is smaller than that of urea, all other molecules proved to be better NLO candidates than urea. The substituted derivatives of 10-OTBP, 10-MTBP, 10-MP*m*SB and MMP could be synthesized for NLO applications. The results of the global reactivity descriptors will also be used to investigate the corrosion inhibitive potentials of the molecular systems under study in future works.

High β values of substituted analogues especially for those with $–NO_2$ and -CH=C(CN)COOH substituents further justify the lower E_g values and higher μ values. The results obtained has demonstrated the influence of substituents on NLO properties of the molecular systems. The available experimentally determined E_g and SHG efficiency are well replicated and the observed trend were well predicted. The NLO strength of -CH=C(CN)COOH substituted analogues out-performed others owing to an increase in carbon-chain length as compared to others.

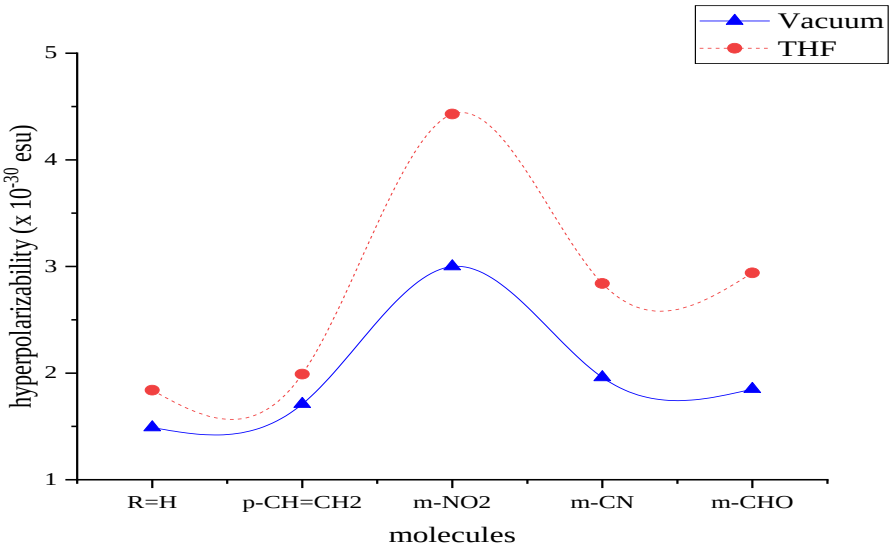

Figure 4.36a: Hyperpolarizabilities of 10-MPmSBs (B3LYP)

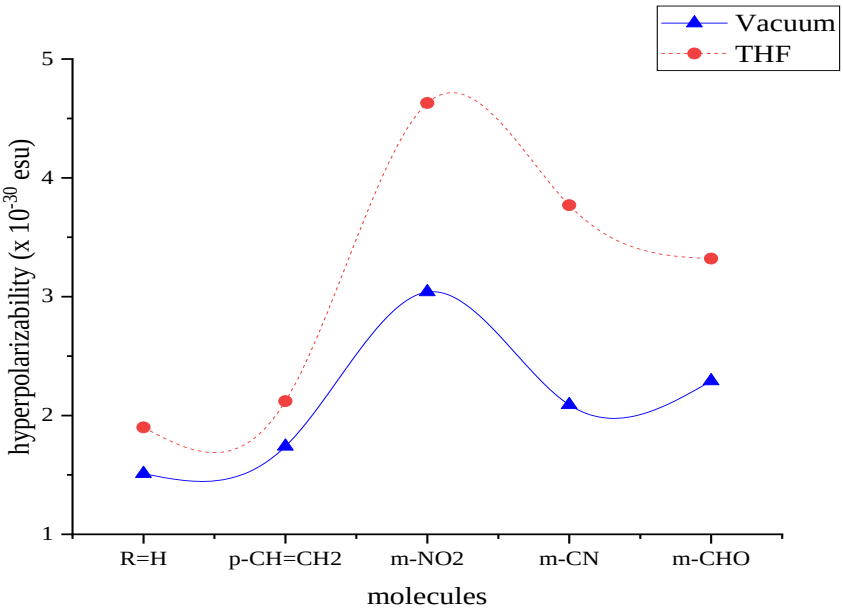

Figure 4.36b: Hyperpolarizabilities of 10-MPmSBs (BLYP)

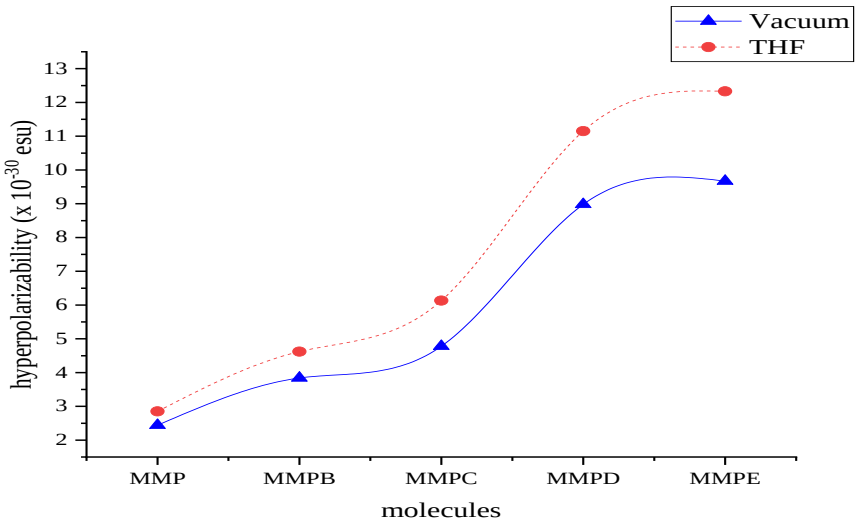

Figure 4.37a: Hyperpolarizabilities for MMPs (B3LYP)

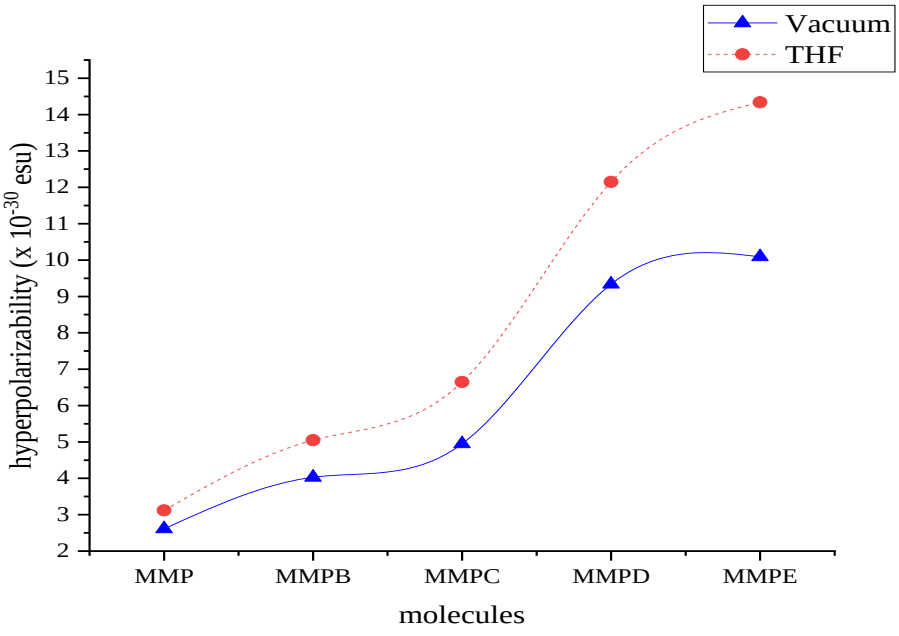

Figure 4.37b: Hyperpolarizabilities for MMPs (BLYP)

4.2.8 Absorption and Electronic Transition

The types of transitions present in a molecule can be gotten by the UV/Vis absorptions. The absorption maxima (λ_{max}), excitation energies (E_{ex}) and oscillator strength (*f*) were calculated using the TD-DFT. There were initially six transitions in all molecules however; only the allowed transitions were considered, hence, the exclusion of others (forbidden), all in appendix A1 – A40.

The λ_{max}, excitation energies and oscillator strengths are presented (Tables 4.25-4.32). It is shown that for 10-OTBP, unsubstituted 1a has absorption at 294 nm (vacuum) with B3LYP, same as in the experiments (Zebiao *et al.,* 2015) and 295 nm (near λ_{exp} of 292 nm (Zebiao *et al.,* 2015) in THF. Their oscillator strengths were strong at 0.94 and 0.65 respectively. They have the same excitation energies of 4.22 eV (vacuum and THF). 1b shifted the absorption to 360 nm in vacuum and 361 nm in THF. Its oscillator strengths were 0.42 and 0.61 respectively while its excitation energies were 3.44 eV (vacuum) and 3.48 eV (THF). 1c red-shifted the absortion to 317 nm (vacuum) and 340 nm (THF). Its oscillator strengths were 0.75 and 0.64 respectively and while its excitation energies were 3.91 eV (vacuum) and 3.84 eV (THF). 1d red-shifted the absorption to 328 nm (vacuum), same as in the experiments (Zebiao *et al.,* 2015). It was 325 nm [THF (experimental value = 324 nm, Zebiao *et al.,* 2015). Its oscillator strengths were 0.29 and 0.33 respectively while its excitation energies were 3.77 eV (vacuum) and 3.71 eV (THF). 1e has absorption at 378 nm (vacuum) and 380 nm (THF), with oscillator strengths of 1.53 and 1.11 respectively. Excitation energies of 3.22 eV (vacuum) and 3.15 eV (THF). 1a had absorption at 362 nm (vacuum), a wide deviation from the experimental value, 368 nm in THF. Its oscillator strengths were 0.26 and 0.34 respectively while its excitation energies were 3.42 in vacuum and 3.40 in THF for BLYP/6-31G* calculation. 1b red-shifted the absorption to 429 nm in vacuum and 457 nm in THF. Its oscillator strengths were 0.28 and 0.26 respectively while its excitation energies were 2.89 eV (vacuum) and 2.75 eV (THF). 1c took the absorption to 419 nm (vacuum) and 423 (THF). Its oscillator strengths were 0.11 and 0.21 respectively while its excitation energies were 2.96 eV (vacuum) and 2.78 eV (THF). 1d had absorption at 444 nm (vacuum), also deviated from experimental value and 413 nm in THF. Its oscillator strengths were the same (0.66) while its excitation energies were 2.79 eV

(vacuum) and 2.64 eV (THF). 1e had absorption at 470 nm (vacuum) and 492 nm (THF). Its oscillator strengths were 0.80 and 0.83 respectively while its excitation energies were 2.66 eV (vacuum) and 2.53 eV (THF). The B3LYP results are very close to the available experimental results, however, there is a deviation from the experimental results with BLYP method. It is therefore suggested that when molecules with similar architectures are considered, the B3LYP should be employed. All these are on appendix A1 – A10.

In Tables 4.27 and 4.28, it is shown that for 10-MTBP, 2a gave 285 nm (vacuum and THF). Its oscillator strengths were 0.70 and 0.63 respectively while its excitation energies were the same in vacuum and in THF (4.35 eV) for B3LYP/6-31G* calculation. This is due to π-π* transition, the n-π* transition was at 369 nm in vacuum and 374 nm in THF. 2b red-shifted the absorption to 352 nm and 350 nm in vacuum and in THF respectively. Its oscillator strengths were 0.30 and 0.56 respectively while its excitation energies were 3.53 eV (vacuum) and 3.54 eV (THF), π-π* transition, n-π* transition occurred at 483 nm and 547 nm in vacuum and THF respectively. 2c gave 308 nm (vacuum) and 318 nm (THF). Its oscillator strengths were 0.69 and 0.49 respectively while its excitation energies were 4.01 eV (vacuum) and 3.91 eV (THF), π-π* transition, n-π* transition occurred at 414 nm and 439 nm in vacuum and THF respectively. 2d gave 318 nm (vacuum) and 337 nm (THF). Its oscillator strengths were 0.56 and 0.63 respectively while its excitation energies were 3.89 eV (vacuum) and 3.68 eV (THF), π-π* transition, n-π* transition occurred at 434 nm and 459 nm in vacuum and THF respectively. 2e gave 365 nm (vacuum) and 380 nm (THF), with oscillator strengths of 1.60 and 1.20 respectively while its excitation energies were 3.39 eV (vacuum) and 3.17 eV (THF), π-π* transition, n-π* transition occurred at 515 nm and 572 nm in vacuum and THF respectively. 2a gave 357 nm (vacuum) and 355 nm (THF). Its oscillator strengths were 0.79 and 0.78 respectively. The excitation energies were 3.47 eV (vacuum) and 3.49 eV (THF) for BLYP. 2b took the absorption to 420 nm (vacuum) and 453 nm (THF). Its oscillator strengths were 0.57 and 0.50 respectively while its excitation energies were 2.95 eV (vacuum) and 2.74 eV (THF). 2c gave 412 nm (vacuum) and 424 nm (THF). Its oscillator strengths were 0.74 and 0.70 respectively while its excitation energies were 3.01 eV (vacuum) and 2.93 eV (THF). 2d gave 440 nm (vacuum) and 454 nm (THF). Its oscillator strengths were 0.63 and 0.66 respectively while its excitation energies were 2.81 eV (vacuum) and 2.73 eV (THF). 2e gave 450 nm (vacuum) and 468 nm (THF), with

oscillator strengths of 1.03 and 1.23 respectively. The excitation energies were 2.75 eV (vacuum) and 2.65 eV (THF).

In Tables 4.29 and 4.30, λ_{max}, excitation energies and oscillator strengths are recorded. It is shown that for 10-MP*m*SB, 3a had absorption at 276 nm (vacuum) and 280 nm (THF). Its oscillator strengths were 0.27 and 0.43. Its excitation energies were 4.49 eV in vacuum and 4.43 eV in THF with B3LYP. Upon substitution with $–CH=CH_2$, 3b, absorption shifted to 286 nm (vacuum) and 283 nm (THF). Its oscillator strengths were 0.11 and 0.71 respectively. The excitation energies were 4.34 eV (vacuum) and 4.38 eV (THF). $–NO_2$, 3c red-shifted to 360 nm (vacuum) and 376 nm (THF). Its oscillator strengths were 0.45 and 0.19 respectively. Its excitation energies were 3.44 eV (vacuum) and 3.29 eV (THF). –CN, 3d also red-shifted to 284 nm (vacuum) and 285 nm (THF). Its oscillator strengths were 0.28 and 0.11 respectively. Its excitation energies were 4.36 eV (vacuum) and 4.33 eV (THF). –CHO, 3e shifted absorption to 379 nm (vacuum) and 377 nm (THF). Its oscillator strengths were 0.16 and 0.11 respectively. Its excitation energies were 3.27 eV (vacuum) and 3.29 eV (THF). 3a has absorption at 346 nm (vacuum) and 344 nm (THF), the oscillator strengths were 0.10 and 0.16 respectively. Its excitation energies were 3.58 eV (vacuum) and 3.72 eV (THF) for BLYP. $–CH=CH_2$, 3b red-shifted the absorption to 367 nm (vacuum) and 347 nm (THF). Its oscillator strengths were 0.19 and 0.17 respectively while its excitation energies were 3.38 eV (vacuum) and 3.57 eV (THF). 3c took absorption to 468 nm (vacuum) and 462 nm (THF). Its oscillator strengths were 0.12 and 0.16 respectively while its excitation energies were 2.65 eV (vacuum) and 2.68 eV (THF). 3d took absorption to 347 nm (vacuum) and 369 nm (THF). Its oscillator strengths were 0.16 and 0.22 respectively. The excitation energies were 3.56 eV (vacuum) and 3.35 eV (THF). 3e has absorption at 464 nm (vacuum) and 467 nm (THF). Its oscillator strengths were 0.10 and 0.12 respectively. The excitation energies were 2.67 eV (vacuum) and 2.66 eV (THF).

In Tables 4.31 and 4.32 λ_{max}, excitation energies and oscillator strengths are recorded. It was observed that for MMP absorbed at (341 nm and 344 nm) in vacuum and 350 nm (THF). Its oscillator strengths were (0.51 and 0.65) and 1.16 respectively. Its excitation energies were [(3.63 eV and 3.61 eV (vacuum)] and 3.55 eV (THF) for B3LYP/6-31G* calculation. The experimental cutoff wavelength was found to be 400 nm (D'Silva *et al.*, 2012). 4b

bathochromically shifted the absorption wavelength to 370 nm in vacuum and 408 nm in THF. Its oscillator strengths were 0.79 and 0.55 respectively. Its excitation energies were 3.36 eV and 3.04 eV respectively. 4c also bathochromically shifted the absorption wavelength to 369 nm in vacuum and 318 nm in THF. Its oscillator strengths were 0.73 and 1.14 respectively. Its excitation energies were 3.36 eV and 3.90 eV respectively. 4d red-shifted the absorption wavelength to (342 nm and 397 nm) in vacuum and (343 nm and 421 nm) in THF with oscillator strength of (0.52 and 0.96) and (0.50 and 0.89) respectively and excitation energies of 3.63 eV and 3.13 eV and (3.61 eV and 2.94 eV) respectively. 4e also red-shifted the absorption wavelength to (338 nm and 399) nm in vacuum and (348 nm and 451 nm) in THF with oscillator strength of (0.52 and 0.92) and (0.91 and 0.78) respectively and excitation energies of (3.67 eV and 3.10 eV) and (3.56 eV and 2.74 eV) respectively.

MMP absorbed at (382 nm and 412 nm) in vacuum and (376 nm and 437 nm) in THF. Its oscillator strengths were (0.25 and 0.68) and (0.46 and 0.53) respectively while its excitation energies were (3.24 eV and 3.01 eV) in vacuum and (3.29 eV and 2.84 eV) in THF for BLYP/6-31G* calculation, closer to the experimental cutoff wavelength. 4b bathochromically shifted the absorption wavelength to (389 nm and 496 nm) in vacuum and (409 nm and 579 nm) in THF with oscillator strength of (0.55 and 0.27) and (0.53 and 0.23) respectively and excitation energies of (3.18 eV and 2.50 eV) and (3.03 eV and 2.14 eV) respectively while 4c absorbed at (360 nm and 499 nm) in vacuum and (378 nm and 696 nm) in THF with oscillator strength of (0.64 and 0.00) and (0.79 and 0.00) respectively and excitation energies of (3.44 eV and 2.48 eV) and (3.28 eV and 1.78 eV) respectively. 4d red-shifted the absorption wavelength to (418 nm and 525 nm) in vacuum and (418 nm and 577 nm) in THF with oscillator strength of (0.81 and 0.37) and (1.05 and 0.34) respectively and excitation energies of (2.97 eV and 2.36 eV) and (2.97 eV and 2.15 eV) respectively. 4e also red-shifted the absorption wavelength to (411 nm and 517 nm) in vacuum and (420 nm and 598 nm) in THF with oscillator strength of (0.78 and 0.39) and (0.91 and 0.42) respectively and excitation energies of (3.01 eV and 2.40 eV) and (2.95 eV and 2.07 eV) respectively.

It clearly showed, from the absorption results and previous ones discussed that the substituted derivatives except for *A*-NO_2, D-NH_2 from MMP derivatives shifted the λ_{max}

bathochromically. The substituted derivatives could be synthesized and incorporated into optical limiting devices.

CHAPTER FIVE

SUMMARY AND CONCLUSION

Organic materials with excellent NLO properties have generated interest due to their low cost of production, ease of fabrication and chemical tunability when compared to their inorganic/organometallic analogues. Material scientists design/create materials that meet certain applications. However, the search for materials with better properties than existing ones is still very important. Theoretical chemistry presents the means of investigating molecular properties of known compounds and seek method(s) corresponding to experimental results. These method(s) can then be used to predict the properties of yet to be synthesized molecules which could be fabricated for potential real life applications by incorporating them into thin films or polymer matrices. Modifying molecular structures could alter molecular properties like polarizability, energy gap, dipole moments, bond lengths and hyperpolarizability which is a measure of the second harmonic generation efficiency. Some phenothiazine based organic molecules were synthesized and studied for light emitting applications (Emese, 2010; Zebiao *et al.*, 2015). Also, 1-[4-({(E)-[4-(methylsulfanyl)phenyl]methylidene}amino) phenyl]ethanone, MMP was synthesized and reported for its NLO behaviour (D'Silva *et al.*, 2012). However, there is need to know the effects of different substituent groups and solvent on their molecular and NLO properties. Therefore, this research work was fashoined to investigate structural and solvent effects on their molecular properties via computational approach.

A systematic study of the NLO properties of 10-OTBP, 10-MTBP, 10-MP*m*SB and MMP and some of their substituted analogues was carried out using quantum mechanical calculations. Since it has been established that NLO properties of molecular systems could be modeled with and without solvent media, all calculations were done in gas phase and in THF within the continuum model. The energies of the LUMO (E_{LUMO}), HOMO (E_{HOMO}), energy/orbital (E_g), bond length alternation (BLA), dihedral angles, dipole moment (μ),

polarizability (α), first hyperpolarizability (β) and UV absorptions (λ_{abs}) were obtained via the Density Functional Theory (DFT) method. The time-dependent density functional theory (TD-DFT) was also used for excited state calculations. Softness (S), chemical hardness (η), chemical potential (C^P), global electrophilicity (ω) and electronegativity (χ) were all calculated from the frontier molecular orbitals (E_{LUMO} and E_{HOMO}).

Results revealed that the substituted derivatives of 10-OTBP, 10-MTBP, 10-MP*m*SB and MMP gave better NLO properties than unsubstituted ones. For instance, experimental E_g for MMP (*A*-$COCH_3$, D-SCH_3, MMP) was found to be 2.27 eV, 2.80 eV and 2.94 eV as obtained by from $\varepsilon_2^{1/2}/\lambda$ versus $(1/\lambda)$ in Tauc's expression (Tauc *et al.,* 1966; D'Silva *et al.,* 2012). The B3LYP E_g value of MMP is 3.85 eV with 6-31G* basis set while its BLYP value is 2.47 eV with 6-31G*. The E_g in BLYP method (2.47 eV) is closer to Tauc's $\varepsilon_2^{1/2}/\lambda$ versus $(1/\lambda)$ method value of 2.27 eV and underestimated the direct and indirect energy gap values of 2.80 eV and 2.94 eV, while being 3.85 eV with B3LYP. As expected, other substituted derivatives possess different E_g values from MMP. This is due to the inductive and mesomeric effects from substituent groups.

Also, MMP has a B3LYP β value of 2.44 $x10^{-30}$ esu, 3.75 times of urea (0.65 $x10^{-30}$ esu) (Adhikari and Kar, 2012) while the BLYP β value is 2.61 $x10^{-30}$, 4.02 times that of urea. This was corroborated with the fact that the experimental SHG efficiency of MMP is 4.13 times urea's SHG efficiency (D'Silva *et al.,* 2012), meaning that the BLYP (97.34%) correlation predicts the SHG efficiency and second order susceptibility more effectively than the B3LYP (90.8%) correlation. However, all substituted analogues increased β value, confirming that they are better candidates for NLO applications than MMP, with *A*-CH=C(CN)COOH, D-SCH_3 proving the best in that it has the lowest optical/energy gap, highest value of dipole moment, polarizability and hyperpolarizability. This is also observed for other molecular systems and their substituted analogues.

For 10-OTBP, 1a with B3LYP method has an abrorptiopn of 294 nm with experimental value also 294 nm (Zebiao *et al.*, 2015) in vacuum while it was 295 nm with experimental value at 292 nm (Zebiao *et al.*, 2015) in THF. $–NO_2$ substituent, 1b bathochromically shifted the absorption to 360 nm (vacuum) and 361 nm (THF). –CN, 1c took the absorption to 317 nm (vacuum) and 340 nm (THF). For –CHO (1d), absorption was at 328 nm (vacuum), just

as in experiments (Zebiao *et al.*, 2015) and 325 nm [(THF (experimental = 324 nm, Zebiao *et al.*, 2015)]. -CH=C(CN)COOH, 1e took absorption to 378 nm (vacuum) and 380 nm (THF). With BLYP method, unsubstituted 10-OTBP, 1a has absorption of 362 nm (vacuum) and 368 nm (THF). $–NO_2$, 1b bathochromically shifted the absorption to 429 nm (vacuum) and 457 nm (THF). –CN (1c) had absorption at 419 nm (vacuum) and 423 nm (THF). –CHO (1d) had absorption at 444 nm (vacuum), also deviated from that in experiments and 413 nm (THF). -CH=C(CN)COOH (1e) had absorption at 470 nm (vacuum) and 492 nm (THF). The B3LYP agreed very well with the available experimental results, however, there is a deviation from the experimental results with BLYP method. It therefore suggests that the hybrid B3LYP methods is better used for predicting the UV/Vis absorptions of 10-OTBP should be employed. This is what was observed in other molecular systems.

Derivatizing the molecules with different substituent groups altered energy gaps. This consequently led to improved reactivities of the molecules. The substituted derivatives have great NLO potentials and are recommended for synthesis. They could be fabricated and incorporated into thin films for use as optical limiters.

REFERENCES

Adhikari, S. and Kar, Tanusree. 2012. Experimental and theoretical studies on physicochemical properties of L-leucine nitrate—a probable nonlinear optical material; *Journal of Crystal Growth*, 356, 4-9.

Alguno, A. C., Chung, W. C., Banaculo, R. V., Vequizo, R. M., Miyata, H., Ignacio, E. W., and Bacala, A. M. 2001. Theoretical study of spectroscopic properties of insulated molecular wires formed by substituted oligothiophenes and cross-linked a-cyclodextrin; *NECTEC Technical Journal,* 2(9), 215-218.

Andriotis, A. N. and Menon, M. 2015. Energy gap engineering via doping: A predictive approach; *Centre for Computational Sciences Faculty Publications, University of Kentucky.*

Angelopoulos, M. 2001. CP in microelectronics; *IBM Journal of Research and Development*, 45(1), 57-75.

Band, Y. B. 1986. Optical properties and applications of reverse saturable absorbers; *Methods of Laser Spectroscopy,* 117-121.

Bankole, O. M. and Nkoyong, T. 2015. Photophysical and nonlinear optical studies of tetraakynyl zincphthalocyanine and its ‘‘clicked’’ analogue; *Journal of Molecular Structure,* 1089, 107-115.

Bass Michael (1994). *Handbook of optics. McGraw-Hill Professional*; 2 edition. ISBN: 978-0-07-047740-7.

Becke, A. D. 1993. Density-functional thermochemistry. III. The role of exact exchange; *The Journal of Chemical Physics,* 98(7), 5648-5652.

Bernier, P., Bidan, G. and Lefrant, S. 1999. Advances in synthetic materials: twenty years of progress in science and technology; *Elsevier, New York*. 98-261.

Bhavitha, K. B., Nair, A. K., Perumbilavil, S., Joseph, S., Kala, M. S., Saha, A., Narayanan, R. A., Hameed, N., Thomas, S., Oluwafemi, O. S., Kalarikkal, Z. 2017. Investigating solvent effects on aggregation behaviour, linear and nonlinear optical properties of silver nanoclusters; *Optical Materials,* 73, 695-705.

Blinder, S. M. 1965. Basic concepts of self-consistent-field theory. *American Journal of Physics.* 33, 431.

Boukabcha, N., Benhalima, N., Rahmani, R., Chouaih, A. and Hamzaoui, F. Theoretical investigation of electrostatic potential and nonlinear optical properties of *m*-nitroacetanilide. *Rasayan Journal of Chemistry.* 8(4), 509-516.

Boyd, R. W. 2003. *Nonlinear Optics*. 2nd Edition. Academic Press: San Diego, CA. 301, 200.

Cammi, R., Mennucci, B. and Tomasi, J. 1998. Solvent effects on linear and nonlinear optical properties of donor−acceptor polyenes: investigation of electronic and vibrational components in terms of structure and charge distribution changes; *Journal of American Chemical Society,* 120(34), 8834-8847.

Chaikin, P. M. and Lubensky, T. C. 2000. Principles of condensed matter physics; *Cambridge: Cambridge University Press.* 195-218.

Chandrasekhar, V., Azhakar, R., Murugesapandian, B., Senapati, T., Bag, P., Pandey, M. D., Maurya, S. K. and Goswami, D. 2010. Synthesis, structure, and two-photon absorption studies of a phosphorus-based tris hydrazone ligand (S)P[N(Me)NdCH-C_6H_3-2-OH-4-N(CH_2CH_3)2]$_3$ and its metal complexes; *Inorgic Chemistry*, 49, 4008–4016.

Chuan-Kui, W., Xiao-Juan, X., Xiao-Ming, H. and Yun, Gao. 2007. Solvent effects on structure and optical properties of D-A azobenzene dye. *Chinese Physics.* 16(11), 3323.

Cornil, J., Gueli, I., Dkhissi, A., Sancho-Garcia, J. C., Hennebicq, E., Calbert, J. P., Lemaur, V., Beljonne, D. and Bredas, J. L. 2003. Electronic and optical properties of polyfluorene and fluorine based copolymers: A quantum chemical characterization; *The Journal of Chemical Physics,* 118(14), 6615-6623.

Cui, Y., Qian, G., Gao, J., Chen, L., Wang, Z. and Wang, M. 2005. Preparation and nonlinear optical properties of inorganic-organic hybrid films with various substituents on chromophores; *The Journal of Physical Chemistry B,* 23295-23299.

D'Silva, E. D., Podagatlapalli, G. K., Rao, S. V. and Dharmaprakash S. M. 2012. Structural, optical and electrical characteristics of a new NLO crystal; *Optics and Laser Technology*, 44, 1689-1697.

Da Silva, R. R., Ramalho, T. C., Santos, J. M. and Figueroa-Vilaar, J. D. 2006. On the limits of highest-occupied molecular orbital driven reactions: the frontier effective-for-reaction molecular orbital concept. *The Journal of Physical Chemistry A.* 110, 1031.

Day, P. N., Nguyen, K. A and Pachter, R. 2005. TDDFT study of one- and two-photon absorption properties: donor−π−acceptor chromophores; *The Journal of Physical Chemistry B,* 109(5), 1803-1814.

Day, P. N., Nguyen, K. A. and Pachter, R. 2006. Calculation of two-photon absorption spectra of donor-pi-acceptor compounds in solution using quadratic response time-dependent density functional theory; *The Journal of Chemical Physics,* 125(9), 094103.

Day, P. N., Nguyen, K. A. and Pachter, R. 2008. Calculation of one-photon and two-photon absorption spectra of porphyrins using time-dependent density functional theory; *Journal of Chemical Theory and Computation*., 4(7), 1094−1106.

Deng, X., Zhang, X., Wang, Y., Song, Y., Liu, S. and L, C. 1999. Intensity threshold in the conversion from reverse saturable absorption to saturable absorption and its application in optical limiting; *Optics Communication,* 168, 207-212.

Dirac, P. A. M. 1930. Note on exchange phenomena in the Thomas atom. *Mathematical proceedings of the Cambridge Philosophical.* 26(3), 376-385.

Drobizhev, M., Makarov, N. S., Stepanenko, Y. and Rebane, A. 2006. Near-infrared two-photon absorption in phthalocyanines: Enhancement of lowest gerade-gerade transition by symmetrical electron-accepting substitution; *The Journal of Chemical Physics*, 124(22), 224701-11.

Emese, G. 2010. Synthesis and characterization of some new heterocyclic aromatic derivatives, precursors for materials with nonlinear optical properties; phd thesis, faculty of chemistry and chemical engineering, Organic Chemistry Department, Babes-Bolyai University, Cluj-Napoca.

Fermi, E. 1927. A statistical method for the determination of some atomic property. Endiconti; *Atti dell Accademia Nazionale dei Lincei*, 6, 602.

Fortunelli, A. and Tomasi, J. 1994. The implementation of density functional theory within the polarizable continuum model for solvation; *Chemical Physics Letters,* 231(1), 34-39.

Ganeev, R., Ryasnyanskiy, A. I. and Usmanov. 2003. Nonlinear refraction and nonlinear absorption of As2S3 aqeous solution; *Optical and Quantum Electronics*, 35(3), 211-219.

Gao, J. and Alhambra, A. 1997. Solvent effects on the bond length alternation and absorption energy of conjugated compounds; *J. Am. Chem. Soc.,* 119, 2962-2963.

Gierschner, J., Cornil, J. and Egelhaaf, H. J. 2007. Optical bandgaps of p-conjugated organic materials at the polymer limit: Experiment and theory, *Advanced Materials*; 19, 173–191.

Hadji, D. and Rahmouni, A. 2015. Theoretical study of nonlinear optical properties of some azo dyes; *Mediterranean Journal of Chemistry*, 4(4), 185-192.

Havinga, E. E., Ten-Hoeve, W. and Wynberg, H. 1993. Alternate donor-acceptor small energy gap semi-conductor polymers; *Synthetic Metals*, 55, 299-306.

Heeger, A. J., Kivelson, S., Schrieffer, J. and Su, W. P. 1988. Solitons in conducting polymers; *Reviews of Modern Physics*, 60, 781.

Henre, J. W. 2003. A Guide to molecular mechanics and quantum chemical calculations. *Wavefunction, Inc.* ISBN 1-890661-18-X.

Hoffmann, R. 1963. An extended Huckel theory. I. hydrocarbons. The *Journal of Chemical Physics.* 39(6), 1397-1412.

Hohenberg, P. and Kohn, W. 1964. Inhomogeneous electron gas, *Phys. Rev.:* 136B, 864–871.

Islam, N. and Lone, H. 2017. Computational studies on optoelectronic and nonlinear properties of octaphyrin derivatives. *Frontiers in Chemistry.* 5, 1-11.

Jacquemin, D. and Adamo, C. 2013. The calculations of excited-state properties with time-dependent density functional theory; *Chemical Society Reviews*, 42(3), 845-856.

Jarrahpour, A. A. and Rezaei, S. 2006. Synthesis of N,N'-bis(a-methylsalicylidene)4,4'-diaminodiphenylmethane as a novel complexing agent, *Molbank*, M456.

Jarrahpour, A. A., Shekarriz, M. and Taslimi, A. 2004**.** Synthesis and antimicrobial activity of some new sugar-based monocyclic β-lactams; *Molecules*, 9, 29-38.

Jarrahpour, A. and Zarei, M. 2009. DMF-dimethyl sulfate as a new reagent for the synthesis of S- lactams**;** *Tetrahedron Letters, 50,* 1568-1570.

Jolly, W. L. 1984. Modern Inorganic Chemistry, *New York: McGraw-Hill.* Chapter 3.

Jordon, G., Kobayashi, T., Blau, W.J., Pfeiffer, S., Horhold, H. H. 2003. Frequency upconversion of 800 nm ultrashort pulses by two-photon absorption in a stilbenoid compound-doped polymer optical fiber; *Advanced Functional Materials*, 13, 751–4.

Kennedy, S.M. and Lytle, F.E. 1986. *p*-Bis(o-methylstyryl)benzene as a power-squared sensor for two-photon absorption measurements between 537 and 694 nm. *Analytical Chemistry*. 58(13), 2643-2647.

Kershaw, S. 1998. In characterization techniques and tabulations for organic nonlinear optical materials; Kuzyk, M. G., Dirk, C. W., Eds.; Marcel Dekker: New York, 1998; Chapter 7.

Kleinman, D. A. 1962. Nonlinear dielectric polarization in optical media; *Physcal Review*, 126(6), 1977-1979.

Kohn, W. and Sham, L. J. 1965. Self-consistent equations including exchange and corrrelation effects; *Physical Review*, 140: A1133.

Koopman, T. 1934. About the assignment of wave functions and eigenvalues to the individual electrons of an atom; *Physica*, 1(1-6), 104-113.

Kroon, R., Lenes, M., Hummelen, J. C., Blom, P. W. M. and De Boer, B. 2008. Small bandgap polymers for organic solar cells (polymer material developments in the last 5 years); *Polymer Reviews*, 48(3), 531-582.

Lasry, J. M., Lions, P. L. 2007. Mean field games; *Japanese Journal of Mathematics*, 2, 229–260.

Li, N., Lu, J., Xia, X., Xu, Q., and Wang, L. 2009. Synthesis of third-order nonlinear optical polyacrylates containing an azobenzene side chain via atom transfer radical polymerization; *Dyes and Pigments,* 80, 73-79.

Lipinski, J. and Bartkowiak, W. 1999. Conformation and solvent dependence of the first and second molecular hyperpolarizabilities of charge-transfer chromophores. Quantum mechanical calculations. *Chemical Physics.* 245(1-3), 263-276.

Machado, D. F. S., Lopes, T. O., Lima, I. T., Filho, D. A. and De Oliviera, H. C. B. 2016. Strong solvent effects on the nonlinear optical properties of z and e isomers from azo-enaminine derivatives; *The Journal of Physical Chemistry C*, 120(31), 17660-17669.

Makarov, N. S., Drobizhev, M., Wicks, G., Makarova E. A., Lukyanets, E. A. and Rebane, A. 2013. Alternative selection rules for one- and two-photon transitions in tribenzotetraazachlorin: Quasi-centrosymmetrical π-conjugation pathway of formally non-centrosymmetrical molecule; The *Journal of Chemical Physics*, 138(21), 214314.

Marder, S. R. 2006. Organic nonlinear optical materials: Where we have been and where we are going; *Chemical Communications*, 2, 131-134.

Marder, S. R., Gorman, C. B., Cheng, L. T. and Teimann, B. G. 1993. Optimizing the optical nonlinearities of organic molecules: Asymmetric cyanines and highly polarized polyenes; *SPIE*, 1775, 19-31.

Marder, S. R., Gorman, C. B., Meyers, F., Perry, J. W., Bourhill, G., Bredas, J. L. and Pierce, B. M. 1994. Unified description of linear and nonlinear polarization in organic polymethine dyes; *Science*, 265, 632-635.

McGraw-Hill Encyclopedia of Science and Technology (5th ed.). McGraw-Hill. 1993.

McQuarrie, D. A. 1997. Quantum Chemistry Soluion Manual; *Univ Science Books*, ISBN 10: 093570213X ISBN 13: 9780935702132.

Meier, U., Bosch, M., Bossshard, C., Pan, F. and Gunter, P. 1998. Parametric interactions in the organic salt 4-N,N-dimethylamino-4'-N'-methylstilbazolium tosylate at telecommunication wavelengths; *Journal of Applied Physics*, 83, 3486.

Mennucci, B., Cammi, R. and Tomasi, J. 1998. Excited states and solvatochromic shifts within a nonequilibrium solvation approach: A new formulation of the integral equation formalism method at the self-consistent field, conFiguration interaction, and multiconFiguration self-consistent field level; *The Journal of Chemical Physics*, 109(7), 2798-2807.

Metcalf, R. L. 1948. The Mode of Action of Organic Insecticides; *National Academies*, Issues 1-5, 44.

Mullekom, H. A. M., Vekemans, J. A. J. M. and Meijer, E. W. 2001. Developments in the chemistry and energy gap engineering of donor–acceptor substituted conjugated polymers; *Materials Science and Engineering Reports, 32(1), 1-40.*

Nag, A. and Goswani, D. 2009. Solvent effect on two-photon absorption and fluorescence of rhodamine dyes; *Journal of Photochemistry and Photobiology A,* 206(2-3), 188.

Natarajan, S., Moovendaran, K., Sundar, J. K. and Ravikumar, K. 2012. Crystal structure of L-histidinium 2-nitrobenzoate; *Journal of amino Acids*, 463183, 1-6.

Ohlow, M. J. and Moosmann, B. 2011. Phenothiazine: the seven lives of pharmacology's first lead structure; *Drug Discovery Today*, 16(3-4), 119-31

Okuno, Y., Yokoyama, S. and Mashiko, S. 2001. Interaction between monomeric units of donor−acceptor-functionalized azobenzene dendrimers: effects on macroscopic conFiguration and first hyperpolarizability; *Journal of Physical Chemistry B*, 105(11), 2163–2169.

Onsager, L. 1936. Electric moments of molecules in liquids; *Journal of American Chemical Society*, 58(8), 1486-1493.

Oyeneyin, O. E. 2017. Structural and solvent dependence of the electronic properties and corrosion inhibitive potentials of 1,3,4-thiadiazole and its substituted derivatives- A theoretical investigation; *Physical Science International Journal*, 16(2), 1-8.

Parker, C. B. 1994. *McGraw Hill Encyclopedia of Physics* (2nd Edition). ISBN: 0-07-051400-3.

Parr, R. G., Szentpaly, L. V. and Liu, Shubin. 1999. Electrophilicity index; *Journal of American Chemical Society*, 121(9), 1922-1924.

Pearson, R. G. 1997. *Chemical Hardness*; Wiley-VCH: Weinhein, 198.

Pearson, R. G. and Parr, R. G. 1983. Absolute hardness – companion parameter to absolute electronegativity; *Journal of American Chemical Society*, 105, 7512– 7516.

Pegu, D. 2012. Solvent effects on nonlinear optical properties of novel *para*-nitroaniline derivatives: A density functional approach; *International Journal of Science and Research*, 3(7), 469-474.

Pople, J. A. and Beveridge, D. L. 1970. Approximate molecular orbital theory. McGraw-Hill, New York, 57, 89

Prasad, P. N. and Williams, D. J. 1991. Introduction to nonlinear optical effects in molecules and polymers; *John Wiley*, New York. 59-260; 272-273.

Ramachandran, K. I., Deepa, G. and Namboori, K. 2008. Computational chemistry and molecular modelling- principles and applications; *Springer-Verlag Berlin Heidelberg*, ISBN-13 978-3-540-77302-3 e-ISBN-13 978-3-540-77304-7.

Raman, N., Mitu, L., Sakthivel, A. and Pandi, M. S. S. 2009. Studies on DNA cleavage and antimicrobial screening of transition metal complexes of 4-aminoantipyrine derivatives of N_2O_2 type: *Journal of the Iranian Chemical Society*, 6, 738-748.

Ravindra, H. J., Chandrashekaran, K., Harrison, W. T. A. and Dharmaprakash, S. M. 2009. Structure and NLO property relationship in a novel chalcone co-crystal; *Applied Physics B*, 94(3), 503-511.

Ribeiro, A., Greca, I. M. 2003. Computer simulations and modeling tools in chemical education: A review of published literature; *Química Nova*, 26, 542-549.

Roncali, J. 1992. Conjugated poly(thiophenes): synthesis, functionalization and applications: *Chemical Reviews*, 92, 711.

Roncali, J. 2007. Molecular engineering of the energy gap of π-conjugated systems: Facing technological applications; *Molecular Rapid Communications,* 28(17), 1761-1775.

Rughooputh, S. D. D. V., Hotta, S., Heeger, A. J. and Wudl, F. 1987. Chromism of soluble polythienylenes; *Journal of Polymer Science B*, 25(5), 1071–1078.

Sanusi, K., Khene, S. and Nyokong, T. 2014. Enhanced optical limiting performance in phthalocyanine-quantum dot nanocomposites by free-carrier absorption mechanism; *Optical Materials*, 37, 572-582.

Saleh, B. E. A. and Teich, M. C. 1991. Fundamentals of Photonics ~Wiley, New York. p. 461-466, 494-503.

Shikarawa, H., Louis, E. J., Macdiarmid, A. G., Chiang, C. K. and Heeger, A. J. 1977. Synthesis of electrically conducting organic polymers: Halogen derivatives of PA, $(CH)_x$; *Journal of the Chemical Society, -Chemical Commun*ications**,** 16, 578-580.

Skyner, R.; McDonagh, J. L., Groom, C. R., van Mourik, T., Mitchell, J. B. O.; Groom, C. R.; Van Mourik, T.; Mitchell, J. B. O. (2015). "A review of methods for the calculation of solution free energies and the modelling of systems in solution"; *Physical Chemistry Chemical Physics*, 17(9), 6174–91.

Sliwa, M., Spangenberg, A., Malfant, I., Lacroix, P. G., Metivier R., Pansu, R. B. and Nakatani, K. 2008. Structural, optical and theoretical studies of a thermochromic organic crystal with reversibly variable second harmonic generation. *Chemistry of Materials.* 20, 4062.

Sokic-Lazic, D. and Minteer, S. 2008. Citric acid cycle bomimic on a carbon electrode; *Biosensors and Bioelectronics*, 24(4), 939-944.

Srinivas, N. K. M., Rao, S. V. and Rao, D. N. 2003. Saturable and reverse saturable absorption of Rhodamine B in methanol and water; *Journal of the Optical Society of America B.*, 20(12), 2470-2479.

Stefan, E., Kenneth, R. G., Pengjie,S., Richard, T. F., Timothy, T. S., Robert, N. B., Prasad, T., Jianguo, M., Lazaro, A. P., Trenton, R. E., Honghua, H., Scott, W., David, J. H., Eric, W. V., Kirk, S. S., and John, R. R. 2011. Donor-acceptor-donor-based π-conjugated oligomers for nonlinear optics and near-ir emission; *Chemistry of Materials*, (*American Chemical Society)*, 23, 3805–3817.

Sunitha, M. S., Adhikari, A. V. and Vishnumurthy, K. A. 2012. Nonlinear optical studies of a d-a type conjugated polymer containing heterocyclic moieties; *International Journal of Applied Physics and Mathematics*, 2(6), 436-438.

Suresh, M. S. and Prakash, V. 2010. Preparation and characterization of Cr(III), Mn(II), Co(III), Ni(II), Cu(II), Zn(II) and Cd(II) chelates of schiffs base derived from vanillin and 4-amino antipyrine; *Journal of the Physical Sciences*, 5(14), 2203-2211.

Targema, M., Obi-Egbedi, N. O. and Adeoye, M. D. 2013. Molecular structure and solvent effects on the dipole moments and polarizabilities of some aniline derivatives; *Computational and Theoretical Chemistry*, 1012, 47–53.

Tauc, J., Grigorovici, R. and Vance, A. 1966. Optical properties and electronic structure of amorphous germanium. *Physica Status Solidi B,* 15, 627–37.

Thomas, H. 1927. The calculation of atomic fields; *Proceedings of the Cambridge Philosophical Society*, 23, 542.

Thorley, K. J., Hales, J. M., Kim, H., Ohira, S., Bredas, J. L., Perry, J. W. and Anderson, H. L. 2013. Cyanine-Like Dyes with Large Bond-Length Alternation; *A Chemistry European Journal.* 19(31), 10061-10418.

Torre, G., Vazquez, P., Agullo-Lopez, F. and Torres, T. 2004. Role of Structural factors in the nonlinear optical properties of phthalocyanines and related compounds; *Chemical Reviews*, 104(9), 3723-3750.

Tripathi, R. N. 2010. Lasers in forensic science; *The Himalayan Physics*, 1(1), 32-33

Tuutila, T., Lipsonen J., Huuskonen J., and Rissanen K. 2009. Chiral donor-π-acceptor azobenzene dyes; *Dyes and Pigments*, 80, 34-40.

Wade, C. W. L., Fritz, A. E., Digianantonio, K. M. and Hartley, S. C. 2012. Push-pull macromolecules: donor-acceptor compounds with paired linearly conjugated or cross-linked pathways; *Journal of Organic Chemistry,* 77, 2285-2298.

Wang, C. T. Chen, S. H., Ma, H. Y. and Qi, C. S. 2003. Protection of copper corrosion by carbazole and N-vinylcarbazole self-assembled films in NaCl solution; *Journal of Applied Electrochem*istry, 33, 179–186.

Weiss, P. 1907. "L'hypothèse du champ moléculaire et la propriété ferromagnétique"; *Journal of Physics: Theories and Applications*, 6(1), 661–690.

Wherret, B. S. 1984. Scaling rules for multiphoton absorption in semiconductors. *Journal of the Optical Society of America B.* 1. p. 67.

Winder, C. and Sariciftci, N. S. 2004. Low bandgap polymers for photon harvesting in bulk heterojunction solar cells; *Journal of Material Chem*istry, 14, 1077-1086.

Young, D. C. 2001. Computational Chemistry- A practical guide for applying real world problems; *Wiley-interscience,* ISBN 0-471-33368-9. 1-319.

Zebiao, T., Xiaoxia, S., Huayin, S. and Hewei, Y. 2015. Synthesis of novel donor-acceptor type molecule based on phenothiazine units for organic light-emitting material; *Asian Journal of Chemistry,* 27(7), 2423-2426.

Zein, S., Delbecq, F. and Simon, D. 2009. A TD-DFT investigation of two-photon absorption of fluorine derivatives; *Physical Chemistry and Chemical Physics*, 11(4), 694-702.

Zhang, L. and Cui, D. 2011. Investigation of second-harmonic generation and molecular orientation in electrostatically self-assembled thin films; *Polymers,* 3, 1297-1309.

Zhang, N., Yuan, D., Tao, X., Shao, Z., Dou, S., Jiang, M. and Xu, D. 1992. New nonlinear optical crystal 3-methoxy-4-hydroxy-benzaldehyde and its phase-matched properties; *Journal of Crystal Growth,* 123(1-2), 255-260.

Zhang, L., Qi, D., Zhao, L., Chen, C., Bian, Y. and Li, W. 2012. Density functional theory study on subtriazaporphyrin derivatives: dipolar/octupolar contribution to the second-order nonlinear optical activity. *The Journal of Physical Chemistry A.* 116(41), 10249-1-256.

APPENDIX A

ELECTRONIC TRANSITIONS OF THE STUDIED SYSTEMS

A1: Electronic Excitation Parameters [wavelengths (λ), Oscillator Strength (*f*), Excitation Energies (E_{ex}) and the Transitions] for 10-OTBP(R=H) with TD-DFT/B3LYP (vacuum) and THF (ε= 7.58)

Number	λ(nm)	E_{ex}(eV)	O.S. *(f)*	Assignment	λ(nm)	E_{ex}(eV)	O.S. *(f)*	Assignment
			VACUUM				**THF**	
1	**395.14**	**3.14**	**0.35**	**HOM→LUM**	**399.23**	**3.11**	**0.39**	**HOM →LUM**
2	331.39	3.74	0.03	HOM→LUM+1	333.56	3.72	0.03	HOM→LUM+1
3	322.51	3.84	0.06	HOM→LUM+3	325.36	3.81	0.10	HOM→LUM+3
4	309.25	4.01	0.05	HOM→LUM+2	312.44	3.97	0.08	HOM→LUM+2
5	**293.51**	**4.22**	**0.94**	**HOM-1→LUM**	**295.15**	**4.34**	**0.65**	**HOM-1→LUM**
6	**277.12**	**4.47**	**0.17**	**HOM-1→LUM**	**277.32**	**4.47**	**0.17**	**HOM-1→LUM**
								HOM→LUM+1

A2: Electronic Excitation Parameters [wavelengths (λ), Oscillator Strength (*f*), Excitation Energies (E_{ex}) and the Transitions] for 10-OTBP(R=H) with TD-DFT/BLYP (vacuum) and THF (ε= 7.58)

Number	λ(nm)	E_{ex}(eV)	O.S. *(f)*	Assignment	λ(nm)	E_{ex}(eV)	O.S. *(f)*	Assignment
			VACUUM				**THF**	
1	**484.57**	**2.56**	**0.31**	**HOM→LUM**	**492.22**	**2.52**	**0.36**	**HOM →LUM**
2	426.93	2.90	0.02	HOM-1→LUM	427.53	2.90	0.02	HOM-1→LUM
				HOM→LUM+1				HOM→LUM+1
3	387.28	3.20	0.00	HOM-2→LUM	395.09	3.14	0.00	HOM-2→LUM
				HOM→LUM+2				HOM→LUM+2
4	367.70	3.37	0.01	HOM→LUM+3	**368.39**	**3.39**	**0.34**	**HOM→LUM+3**
5	**362.47**	**3.42**	**0.26**	**HOM-2→LUM**	**360.98**	**3.44**	**0.34**	**HOM-2→LUM**
				HOM→LUM+2				**HOM→LUM+2**
6	349.30	3.55	0.04	HOM-2→LUM+1	345.01	3.59	0.05	HOM-2→LUM+1
				HOM-1→LUM				HOM-1→LUM

A3: Electronic Excitation Parameters [wavelengths (λ), Oscillator Strength (*f*), Excitation Energies (E_{ex}) and the Transitions] for 10-OTBP(2-NO_2) with TD-DFT/B3LYP (vacuum) and THF (ε= 7.58)

Number	λ(nm)	E_{ex}(eV)	O.S. *(f)*	Assignment	λ(nm)	E_{ex}(eV)	O.S. *(f)*	Assignment
			VACUUM				**THF**	
1	**514.22**	**2.41**	**0.56**	**HOM→LUM**	**580.24**	**2.14**	**0.71**	**HOM→LUM**
2	467.57	2.66	0.04	HOM→LUM+1	523.56	2.37	0.04	HOM→LUM+1
3	**360.08**	**3.44**	**0.42**	HOM-1→LUM	**392.21**	**3.16**	**0.42**	**HOM-1→LUM**
4	348.14	3.56	0.00	HOM→LUM+2 HOM→LUM+4	375.42	3.30	0.00	HOM→LUM+2 HOM→LUM+4
5	344.03	3.60	0.00	HOM-2→LUM HOM-1→LUM+1	**361.43**	**3.48**	**0.61**	**HOM-2→LUM+1** **HOM+2→LUM+2**
6	336.89	3.68	0.00	HOM-8→LUM+1 HOM-7→LUM	340.19	3.65	0.03	HOM-2→LUM HOM-1→LUM+1

A4: Electronic Excitation Parameters [wavelengths (λ), Oscillator Strength (*f*), Excitation Energies (E_{ex}) and the Transitions] for 10-OTBP(2-NO_2) with TD-DFT/BLYP (vacuum) and THF (ε= 7.58)

Number	λ(nm)	E_{ex}(eV)	O.S. *(f)*	Assignment	λ(nm)	E_{ex}(eV)	O.S. *(f)*	Assignment
			VACUUM				**THF**	
1	**723.22**	**1.71**	**0.41**	**HOM→LUM**	**798.23**	**1.55**	**0.41**	**HOM→LUM**
2	668.79	1.85	0.02	HOM-2→LUM HOM→LUM+1	725.52	1.71	0.03	HOM-2→LUM HOM→LUM+1
3	**494.01**	**2.51**	**0.12**	**HOM-2→LUM+1** **HOM-1→LUM**	**540.62**	**2.29**	**0.11**	**HOM-2→LUM+1** **HOM-1 →LUM**
4	485.08	2.56	0.00	HOM-2→LUM HOM-1→LUM+1	531.18	2.33	0.00	HOM-2→LUM HOM-1→LUM+1
5	429.60	2.89	0.01	HOM-4→LUM	**457.35**	**2.75**	**0.26**	**HOM-1→LUM**
6	**429.03**	**2.89**	**0.28**	**HOM→LUM+2**	434.56	2.86	0.04	HOM→LUM+3

A5: Electronic Excitation Parameters [wavelengths (λ), Oscillator Strength (*f*), Excitation Energies (E_{ex}) and the Transitions] for 10-OTBP(2-CN) with TD-DFT/B3LYP (vacuum) and THF (ε= 7.58)

Number	λ(nm)	E_{ex}(eV)	O.S. *(f)*	Assignment	λ(nm)	E_{ex}(eV)	O.S. *(f)*	Assignment
			VACUUM				**THF**	
1	**440.63**	**2.81**	**0.57**	**HOM→LUM**	**459.65**	**2.72**	**0.62**	**HOM→LUM**
2	383.96	3.23	0.06	HOM→LUM+1	401.97	3.11	0.06	HOM→LUM+1
3	333.23	3.72	0.00	HOM-2→LUM	**340.46**	**3.84**	**0.64**	**HOM-2→LUM**
				HOM→LUM+2				**HOM→LUM+2**
4	**317.44**	**3.91**	**0.75**	**HOM-2→LUM**	**326.96**	**3.91**	**0.73**	**HOM-2→LUM**
				HOM→LUM+2				**HOM-1→LUM+2**
5	313.97	3.95	0.03	HOM→LUM+3	319.05	3.90	0.00	HOM→LUM+3
6	301.28	4.12	0.07	HOM-1→LUM	305.99	4.08	0.04	HOM-2→LUM+1
				HOM-2→LUM+1				HOM-1→LUM

A6: Electronic Excitation Parameters [wavelengths (λ), Oscillator Strength (*f*), Excitation Energies (E_{ex}) and the Transitions] for 10-OTBP(2-CN) with TD-DFT/BLYP (vacuum) and THF (ε= 7.58)

Number	λ(nm)	E_{ex}(eV)	O.S. *(f)*	Assignment	λ(nm)	E_{ex}(eV)	O.S. *(f)*	Assignment
			VACUUM				**THF**	
1	**567.23**	**2.19**	**0.45**	**HOM→LUM**	**601.23**	**1.79**	**0.49**	**HOM →LUM**
2	511.51	2.42	0.03	HOM-1→LUM	540.33	2.23	0.03	HOM-1→LUM
				HOM→LUM+1				HOM→LUM+1
3	**418.65**	**2.96**	**0.11**	**HOM-1→LUM**	**423.00**	**2.78**	**0.21**	**HOM-1→LUM**
				HOM-1→LUM+1				**HOM-1→LUM+1**
4	402.65	3.08	0.01	HOM-2→LUM	414.50	3.01	0.00	HOM-2→LUM
				HOM-1→LUM+1				HOM-1→LUM+1
5	389.23	3.19	0.03	HOM-1→LUM+1	396.50	3.12	0.01	HOM-2→LUM+1
				HOM→LUM+2				HOM→LUM+2
6	369.43	3.36	0.01	HOM→LUM+3	389.11	3.19	0.01	HOM→LUM+3

A7: Electronic Excitation Parameters [wavelengths (λ), Oscillator Strength (*f*), Excitation Energies (E_{ex}) and the Transitions] for 10-OTBP(2-CHO) with TD-DFT/B3LYP (vacuum) and THF (ε= 7.58)

Number	λ(nm)	E_{ex}(eV)	O.S. *(f)*	Assignment	λ(nm)	E_{ex}(eV)	O.S. *(f)*	Assignment
			VACUUM				**THF**	
1	**461.79**	**2.68**	**0.58**	**HOM→LUM**	**489.32**	**2.58**	**0.60**	**HOM→LUM**
2	410.14	3.02	0.05	HOM→LUM+1	438.00	2.94	0.06	HOM→LUM+1
3	348.87	3.55	0.00	HOM-4→LUM	339.01	3.65	0.03	HOM-4→LUM
				HOM-3→LUM+1				HOM-3→LUM+1
4	348.86	3.55	0.00	HOM-4→LUM+1	**324.83**	**3.71**	**0.33**	**HOM-4→LUM+1**
				HOM-3→LUM				**HOM-3→LUM**
5	**338.66**	**3.66**	**0.16**	**HOM-2→LUM**	**346.96**	**3.58**	**0.11**	**HOM-2→LUM**
				HOM→LUM+2				**HOM→LUM+2**
				HOM→LUM+4				**HOM→LUM+4**
6	**328.16**	**3.77**	**0.39**	**HOM-2→LUM**	**334.77**	**3.72**	**0.11**	**HOM-2→LUM**
				HOM→LUM+2				**HOM→LUM+2**

A8: Electronic Excitation Parameters [wavelengths (λ), Oscillator Strength (*f*), Excitation Energies (E_{ex}) and the Transitions] for 10-OTBP(2-CHO) with TD-DFT/BLYP (vacuum) and THF (ε= 7.58)

Number	λ(nm)	E_{ex}(eV)	O.S. *(f)*	Assignment	λ(nm)	E_{ex}(eV)	O.S. *(f)*	Assignment
			VACUUM				**THF**	
1	**617.48**	**2.01**	**0.42**	**HOM→LUM**	**650.51**	**1.78**	**0.44**	**HOM→LUM**
2	565.83	2.19	0.02	HOM→LUM+1	589.53	2.10	0.02	HOM→LUM+1
3	459.91	2.69	0.00	HOM-3→LUM	454.88	2.42	0.03	HOM-3→LUM
				HOM-2→LUM+1				HOM-2→LUM+1
4	459.78	2.69	0.00	HOM-2→LUM	446.11	2.52	0.00	HOM-2→LUM
5	**444.23**	**2.79**	**0.66**	**HOM-4→LUM**	**413.34**	**2.64**	**0.66**	**HOM-4→LUM**
				HOM-3→LUM+1				**HOM-3→LUM+1**
				HOM-1→LUM+1				
6	435.39	2.85	0.01	HOM-4→LUM+1	437.89	2.85	0.00	HOM-4→LUM+1
				HOM-3→LUM				HOM-3→LUM
				HOM-1→LUM				

A9: Electronic Excitation Parameters [wavelengths (λ), Oscillator Strength (*f*), Excitation Energies (E_{ex}) and the Transitions] for 10-OTBP(2-CH=C(CN)COOH) with TD-DFT/B3LYP (vacuum) and THF (ε= 7.58)

Number	λ(nm)	E_{ex}(eV)	O.S. *(f)*	Assignment	λ(nm)	E_{ex}(eV)	O.S. *(f)*	Assignment
			VACUUM				**THF**	
1	**544.21**	**2.28**	**0.77**	**HOM→LUM**	**591.23**	**2.09**	**0.74**	**HOM →LUM**
2	472.33	2.63	0.01	HOM-1→LUM	527.28	2.35	0.01	HOM-1→LUM
				HOM→LUM+1				HOM→LUM+1
3	386.21	3.21	0.00	HOM-2→LUM	405.22	3.06	0.00	HOM-2→LUM
				HOM-1→LUM+1				HOM-1→LUM+1
4	385.56	3.22	0.08	HOM-2→LUM+1	402..21	3.08	0.03	HOM-2→LUM+1
				HOM-1→LUM				HOM-1→LUM
5	**378.22**	**3.22**	**1.53**	**HOM-3→LUM**	**380.47**	**3.15**	**1.11**	**HOM-3→LUM**
				HOM-2→LUM				**HOM-2→LUM**
				HOM-1→LUM+1				**HOM-1→LUM+1**
6	**355.32**	**3.49**	**0.44**	**HOM-1→LUM**	**368.33**	**3.37**	**0.42**	**HOM-1→LUM**
				HOM→LUM+1				**HOM→LUM+1**

A10: Electronic Excitation Parameters [wavelengths (λ), Oscillator Strength (*f*), Excitation Energies (E_{ex}) and the Transitions] for 10-OTBP(2-CH=C(CN)COOH) with TD-DFT/BLYP (vacuum) and THF (ε= 7.58)

Number	λ(nm)	E_{ex}(eV)	O.S. *(f)*	Assignment	λ(nm)	E_{ex}(eV)	O.S. *(f)*	Assignment
			VACUUM				**THF**	
1	**743.32**	**1.67**	**0.43**	**HOM→LUM**	790.11	1.57	0.42	**HOM→LUM**
2	672.40	1.84	0.00	HOM-1→LUM	713.28	1.74	0.02	HOM-1→LUM
				HOM→LUM+1				HOM→LUM+1
3	551.22	2.25	0.00	HOM-2→LUM	555.49	2.23	0.00	HOM-2→LUM
				HOM-1→LUM+1				HOM-1→LUM+1
4	540.76	2.29	0.02	HOM-2→LUM+1	553.21	2.24	0.01	HOM-2→LUM+1
				HOM-1→LUM				HOM-1→LUM
5	**470.48**	**2.66**	**0.80**	**HOM-3→LUM**	**492.44**	**2.53**	**0.83**	**HOM-3→LUM**
				HOM-2→LUM				**HOM-2→LUM**
				HOM-1→LUM+1				**HOM-1→LUM+1**
6	431.19	2.88	0.01	HOM-1→LUM	445.22	2.79	0.00	HOM-1→LUM
				HOM→LUM+3				HOM→LUM+1

A11: Electronic Excitation Parameters [wavelengths (λ), Oscillator Strength (*f*), Excitation Energies (E_{ex}) and the Transitions] for 10-MTBP(R=H) with TD-DFT/B3LYP (vacuum) and THF (ε= 7.58)

Number	λ(nm)	E_{ex}(eV)	O.S. *(f)*	Assignment	λ(nm)	E_{ex}(eV)	O.S. *(f)*	Assignment
			VACUUM				**THF**	
1	**368.79**	**3.36**	**0.35**	**HOM→LUM**	**374.16**	**3.31**	**0.39**	**HOM→LUM**
2	324.31	3.82	0.04	HOM-1→LUM	325.61	3.81	0.04	HOM-1→LUM
				HOM→LUM+1				HOM→LUM+1
3	**316.18**	**3.92**	**0.10**	**HOM-2→LUM**	**319.36**	**3.88**	**0.13**	**HOM-2→LUM**
				HOM→LUM+2				**HOM→LUM+2**
4	303.41	4.09	0.04	HOM→LUM+1	305.36	4.06	0.09	HOM→LUM+3
				HOM→LUM+3				
5	**285.06**	**4.35**	**0.70**	**HOM-2→LUM**	**285.15**	**4.35**	**0.63**	**HOM-2→LUM**
				HOM→LUM+2				**HOM→LUM+2**
6	**272.30**	**4.55**	**0.16**	**HOM-2→LUM+1**	272.48	**4.55**	**0.18**	**HOM-2→LUM+1**
				HOM-1→LUM				**HOM-1→LUM**
				HOM→LUM+1				**HOM→LUM+1**

A12: Electronic Excitation Parameters [wavelengths (λ), Oscillator Strength (*f*), Excitation Energies (E_{ex}) and the Transitions] for 10-MTBP(R=H) with TD-DFT/BLYP in vacuum and THF (ε= 7.58)

Number	λ(nm)	E_{ex}(eV)	O.S. *(f)*	Assignment	λ(nm)	E_{ex}(eV)	O.S. *(f)*	Assignment
			VACUUM				**THF**	
1	**457.85**	**2.71**	**0.28**	**HOM→LUM**	**462.14**	**2.68**	**0.33**	**HOM→LUM**
2	418.08	2.97	0.02	HOM-1→LUM HOM→LUM+1	419.53	2.96	0.02	HOM-1→LUM HOM→LUM+1
3	379.61	3.27	0.02	HOM-2→LUM HOM→LUM+2	383.79	3.23	0.03	HOM-2→LUM HOM→LUM+2
4	361.66	3.43	0.01	HOM→LUM+1 HOM→LUM+3	363.63	3.41	0.01	HOM→LUM+3
5	**356.75**	**3.48**	**0.79**	**H-2→L** **HOM→LUM+2**	**355.51**	**3.49**	**0.78**	**HOM-2→LUM** **HOM→LUM+2**
6	344.86	3.59	0.03	HOM-2→LUM+1 HOM-1→LUM HOM→LUM+1 HOM→LUM+3	341.91	3.63	0.04	HOM-2→LUM+1 HOM-1→LUM HOM→LUM+1

A13: Electronic Excitation Parameters [wavelengths (λ), Oscillator Strength (*f*), Excitation Energies (E_{ex}) and the Transitions] for 10-MTBP(2-NO_2) with TD-DFT/B3LYP in vacuum and THF (ε= 7.58)

Number	λ(nm)	E_{ex}(eV)	O.S. *(f)*	Assignment	λ(nm)	E_{ex}(eV)	O.S. *(f)*	Assignment
			VACUUM				**THF**	
1	**483.37**	**2.57**	**0.52**	**HOM→LUM**	**547.14**	**2.27**	**0.61**	**HOM→LUM**
2	448.78	2.76	0.06	HOM→LUM+1	502.36	2.47	0.06	HOM→LUM+1
3	**351.73**	**3.53**	**0.29**	**HOM-2→LUM**	**382.63**	**3.24**	**0.29**	**HOM-2→LUM**
				HOM→LUM+2				
4	341.09	3.64	0.00	HOM-2→LUM+1	370.82	3.34	0.00	HOM-2→LUM
				HOM-1→LUM				HOM-1→LUM+1
5	336.75	3.68	0.00	HOM-2→LUM+1	**350.12**	**3.54**	**0.56**	**HOM-2→LUM+1**
				HOM-1→LUM				**HOM+2→LUM+2**
6	336.75	3.68	0.00	HOM-2→LUM+1	**342.29**	**3.62**	**0.16**	**HOM-2→LUM**
				HOM-1→LUM				**HOM-1→LUM+1**
				HOM→LUM+1				

A14: Electronic Excitation Parameters [wavelengths (λ), Oscillator Strength (*f*), Excitation Energies (E_{ex}) and the Transitions] for 10-MTBP(2-NO_2) with TD-DFT/BLYP in vacuum and THF (ε= 7.58)

Number	λ(nm)	E_{ex}(eV)	O.S. *(f)*	Assignment	λ(nm)	E_{ex}(eV)	O.S. *(f)*	Assignment
			VACUUM				**THF**	
1	**688.27**	**1.80**	**0.37**	**HOM→LUM**	**777.83**	**1.59**	**0.49**	**HOM→LUM**
2	644.27	1.92	0.02	HOM-2→LUM	718.92	1.72	0.03	HOM-2→LUM
				HOM→LUM+1				HOM→LUM+1
3	487.49	2.54	0.06	HOM-2→LUM+1	**536.62**	**2.31**	**0.11**	**HOM-2→LUM+1**
				HOM-1→LUM				**HOM-1 →LUM**
4	480.45	2.58	0.00	HOM-2→LUM	526.18	2.36	0.00	HOM-2→LUM
				HOM-1→LUM+1				HOM-1→LUM+1
5	426.97	2.90	0.00	HOM-4→LUM	**452.46**	**2.74**	**0.49**	**HOM-5→LUM**
				HOM-3→LUM+1				**HOM-2 →LUM+1**
								HOM-1→LUM
6	**420.01**	**2.95**	**0.57**	**HOM-5→LUM**	424.56	2.92	0.06	HOM-2→LUM
				HOM-2→LUM+1				HOM→LUM+1
				HOM-1→LUM				HOM→LUM+3

A15: Electronic Excitation Parameters [wavelengths (λ), Oscillator Strength (*f*), Excitation Energies (E_{ex}) and the Transitions] for 10-MTBP(2-CN) with TD-DFT/B3LYP in vacuum and THF (ε= 7.58)

Number	λ(nm)	E_{ex}(eV)	O.S. *(f)*	Assignment	λ(nm)	E_{ex}(eV)	O.S. *(f)*	Assignment
			VACUUM				**THF**	
1	**414.56**	**2.99**	**0.55**	**HOM→LUM**	**439.65**	**2.82**	**0.61**	**HOM→LUM**
2	372.94	3.32	0.06	HOM→LUM+1	394.97	3.14	0.07	HOM→LUM+1
3	324.18	3.82	0.00	HOM-2→LUM HOM→LUM+2	330.46	3.75	0.05	HOM-2→LUM HOM→LUM+2
4	**308.82**	**4.01**	**0.69**	**HOM-2→LUM** **HOM→LUM+2**	**316.96**	**3.91**	**0.49**	**HOM-2→LUM** **HOM-1→LUM+2**
5	308.24	4.02	0.01	HOM-2→LUM+1 HOM→LUM+3	313.05	3.96	0.01	HOM-2→LUM+1 HOM-1→LUM HOM→LUM+3
6	297.98	4.16	0.08	HOM-2→LUM+1 HOM-1→LUM HOM→LUM+3	302.50	4.09	0.05	HOM-2→LUM+1 HOM-1→LUM HOM→LUM+3

A16: Electronic Excitation Parameters [wavelengths (λ), Oscillator Strength (*f*), Excitation Energies (E_{ex}) and the Transitions] for 10-MTBP(2-CN) with TD-DFT/BLYP in vacuum and THF (ε= 7.58)

Number	λ(nm)	E_{ex}(eV)	O.S. *(f)*	Assignment	λ(nm)	E_{ex}(eV)	O.S. *(f)*	Assignment
			VACUUM				**THF**	
1	**540.26**	**2.29**	**0.39**	**HOM→LUM**	**582.30**	**2.13**	**0.47**	**HOM→LUM**
2	498.20	2.49	0.07	HOM-1→LUM	530.96	2.34	0.03	HOM-2→LUM
				HOM→LUM+1				HOM→LUM+1
3	**411.86**	**3.01**	**0.74**	**HOM-2→LUM**	**424.00**	**2.92**	**0.70**	**HOM-2→LUM+1**
				HOM-1→LUM+1				**HOM-1→LUM**
				HOM→LUM+2				
4	400.44	3.09	0.01	HOM-2→LUM+1	411.50	3.01	0.00	HOM-2→LUM
				HOM-1→LUM				HOM-1→LUM+1
5	379.56	3.27	0.00	HOM-2→LUM+1	386.59	3.21	0.00	HOM-2→LUM+1
				HOM-1→LUM				HOM→LUM+2
6	362.29	3.42	0.01	HOM→LUM+3	382.51	3.24	0.00	HOM→LUM+3
								HOM-1→LUM+5

A17: Electronic Excitation Parameters [wavelengths (λ), Oscillator Strength (*f*), Excitation Energies (E_{ex}) and the Transitions] for 10-MTBP(2-CHO) with TD-DFT/B3LYP in vacuum and THF (ε= 7.58)

Number	λ(nm)	E_{ex}(eV)	O.S. *(f)*	Assignment	λ(nm)	E_{ex}(eV)	O.S. *(f)*	Assignment
			VACUUM				**THF**	
1	**434.52**	**2.85**	**0.56**	**HOM→LUM**	**459.47**	**2.69**	**0.63**	**HOM→LUM**
2	397.14	3.12	0.06	HOM→LUM+1	418.35	2.96	0.06	HOM→LUM+1
3	348.57	3.56	0.00	HOM-4→LUM HOM-3→LUM+1	339.08	3.66	0.04	HOM-5→LUM HOM-4→LUM+1 HOM-2→LUM
4	348.57	3.56	0.00	HOM-4→LUM+1 HOM-3→LUM	338.83	3.66	0.00	HOM-5→LUM+1 HOM-4→LUM
5	329.99	3.76	0.08	HOM-2→LUM HOM→LUM+2 HOM→LUM+4	**337.76**	**3.67**	**0.11**	**HOM-2→LUM** **HOM→LUM+2** **HOM→LUM+4**
6	**318.01**	**3.89**	**0.29**	**H-2→L** **H→L+2** **H→L+3**	**324.93**	**3.82**	**0.12**	**HOM-2→LUM** **HOM→LUM+3**

A18: Electronic Excitation Parameters [wavelengths (λ), Oscillator Strength (*f*), Excitation Energies (E_{ex}) and the Transitions] for 10-MTBP(2-CHO) with TD-DFT/BLYP in vacuum and THF (ε= 7.58)

Number	λ(nm)	E_{ex}(eV)	O.S. *(f)*	Assignment	λ(nm)	E_{ex}(eV)	O.S. *(f)*	Assignment
			VACUUM				**THF**	
1	**589.29**	**2.10**	**0.38**	**HOM→LUM**	**631.51**	**1.96**	**0.46**	**HOM→LUM**
2	549.78	2.26	0.03	HOM-3→LUM HOM-1→LUM HOM→LUM	584.53	2.12	0.03	HOM-1→LUM HOM→LUM+1
3	455.08	2.72	0.00	HOM-2→LUM HOM-1→LUM+1	**454.88**	**2.73**	**0.66**	**HOM-2→LUM** **HOM-1→LUM+1**
4	455.08	2.72	0.00	HOM-3→LUM HOM-2→LUM+1 HOM-1→LUM	444.73	2.79	0.01	HOM-2→LUM+1 HOM-1→LUM
5	**440.12**	**2.82**	**0.63**	**HOM-4→LUM** **HOM-1→LUM+1**	432.34	2.87	0.00	HOM-4→LUM+1 HOM-3→LUM
6	431.03	2.86	0.01	HOM-4→LUM+1 HOM-3→LUM H-1→L	432.28	2.87	0.00	HOM-4→LUM HOM-3→LUM+1

A19: Electronic Excitation Parameters [wavelengths (λ), Oscillator Strength (*f*), Excitation Energies (E_{ex}) and the Transitions] for 10-MTBP(2-CH=C(CN)COOH) with TD-DFT/B3LYP in vacuum and THF (ε= 7.58)

Number	λ(nm)	E_{ex}(eV)	O.S. *(f)*	Assignment	λ(nm)	E_{ex}(eV)	O.S. *(f)*	Assignment
			VACUUM				**THF**	
1	**515.03**	**2.41**	**0.84**	**HOM→LUM**	**571.83**	**2.17**	**0.95**	**HOM→LUM**
2	474.76	2.61	0.08	HOM-1→LUM HOM→LUM+1	517.18	2.39	0.08	HOM-1→LUM HOM→LUM+1
3	378.53	3.28	0.01	HOM-2→LUM HOM-1→LUM+1	**397.35**	**3.12**	**0.19**	**HOM-2→LUM** **HOM-1→LUM+1**
4	375.03	3.31	0.06	HOM-2→LUM+1 HOM-1→LUM	390.48	3.18	0.03	HOM-2→LUM+1 HOM-1→LUM
5	**365.24**	**3.39**	**1.60**	**HOM-3→LUM** **HOM-2→LUM** **HOM-1→LUM+1**	**379.57**	**3.18**	**1.23**	**HOM-3→LUM** **HOM-2→LUM** **HOM-1→LUM+1**
6	**345.99**	**3.58**	**0.36**	**HOM-3→LUM+1** **HOM-2→LUM+1** **HOM-1→LUM** **HOM→LUM+1**	**359.94**	**3.44**	**0.36**	**H-3→LUM+1** **HOM-2→LUM+1** **HOM-1→LUM** **HOM→LUM+1**

A20: Electronic Excitation Parameters [wavelengths (λ), Oscillator Strength (*f*), Excitation Energies (E_{ex}) and the] for 10-MTBP(2-CH=C(CN)COOH) with TD-DFT/BLYP in vacuum and THF (ε= 7.58)

Number	λ(nm)	E_{ex}(eV)	O.S. *(f)*	Assignment	λ(nm)	E_{ex}(eV)	O.S. *(f)*	Assignment
			VACUUM				**THF**	
1	**721.25**	**1.72**	**0.57**	**HOM→LUM**	**784.54**	**1.58**	**0.65**	**HOM→LUM**
2	676.80	1.83	0.03	HOM-1→LUM	759.00	1.63	0.08	HOM-1→LUM
				HOM→LUM+1				HOM→LUM+1
3	545.36	2.27	0.00	HOM-2→LUM	**542.67**	**2.29**	**0.19**	**HOM-2→LUM**
				HOM-1→LUM+1				**HOM-1→LUM+1**
4	530.76	2.34	0.02	HOM-2→LUM+1	544.78	2.28	0.03	HOM-2→LUM+1
				HOM-1→LUM				H-1→LUM
5	**450.48**	**2.75**	**1.03**	**HOM-3→LUM**	**467.55**	**2.65**	**1.23**	**HOM-3→LUM**
				HOM-2→LUM				**HOM-2→LUM**
				HOM-1→LUM+1				**HOM-1→LUM+1**
6	420.29	2.95	0.09	HOM-3→LUM+1	**431.34**	**2.87**	**0.36**	**HOM-3→LUM+1**
				HOM-2→LUM+1				**HOM-2→LUM+1**
				HOM-1→LUM				**HOM-1→LUM**
				HOM→LUM+3				**HOM→LUM+1**

A21: Electronic Excitation Parameters [wavelengths (λ), Oscillator Strength (*f*), Excitation Energies (E_{ex}) and the Transitions] for 10-MP*m*SB(R=H) with TD-DFT/B3LYP in vacuum and THF (ε= 7.58)

Number	λ(nm)	E_{ex}(eV)	O.S. *(f)*	Assignment	λ(nm)	E_{ex}(eV)	O.S. *(f)*	Assignment
			VACUUM				**THF**	
1	**373.01**	**3.32**	**0.09**	**HOM-1→LUM**	**376.57**	**3.29**	**0.16**	**HOM→LUM**
				HOM+1→LUM				
2	360.19	3.44	0.04	HOM→LUM	352.41	3.52	0.00	HOM-1→LUM
				HOM+1→LUM				
3	306.89	4.04	0.02	HOM-2→LUM	309.05	4.01	0.01	HOM-2→LUM
				HOM→LUM+1				HOM→LUM+1
				HOM→LUM+2				HOM→LUM+2
4	288.84	4.29	0.05	HOM→LUM+1	288.53	4.29	0.04	HOM→LUM+1
				HOM→LUM+2				HOM→LUM+2
5	**275.86**	**4.49**	**0.27**	**HOM-2→LUM**	**279.64**	**4.43**	**0.43**	**HOM-2→LUM**
				HOM→LUM+1				**HOM→LUM+1**
				HOM→LUM+3				**HOM→LUM+4**
6	271.80	4.56	0.02	HOM-3→LUM	**267.50**	**4.63**	**0.25**	**HOM-2→LUM**
				HOM-1→LUM+1				**HOM→LUM+1**
				HOM-1→LUM				**HOM-1→LUM+3**
				HOM→LUM+3				**HOM→LUM+4**

A22: Electronic Excitation Parameters [wavelengths (λ), Oscillator Strength (*f*), Excitation Energies (E_{ex}) and the Transitions] for 10-MP*m*SB(R=H) with TD-DFT/BLYP in vacuum and THF (ε= 7.58)

Number	λ(nm)	E_{ex}(eV)	O.S. *(f)*	Assignment	λ(nm)	E_{ex}(eV)	O.S. *(f)*	Assignment
			VACUUM				**THF**	
1	**457.49**	**2.71**	**0.67**	**HOM-1→LUM** **HOM→LUM**	**464.32**	**2.67**	**0.12**	**HOM→LUM**
2	442.39	2.80	0.03	HOM-1→LUM HOM→LUM	421.37	2.94	0.00	HOM-1→LUM
3	361.75	3.43	0.00	HOM-2→LUM HOM-1→LUM+1 HOM→LUM+1	366.16	3.39	0.00	HOM-2→LUM HOM→LUM+1 HOM→LUM+2
4	350.77	3.53	0.01	HOM-2→LUM HOM+1→LUM+1	**344.43**	**3.59**	**0.10**	**HOM→LUM+1** **HOM→LUM+2**
5	**346.40**	**3.58**	**0.10**	**HOM-1→LUM+2** **HOM+2→LUM+2**	**333.11**	**3.72**	**0.16**	**HOM-2→LUM** **HOM→LUM+1** **HOM→LUM+4**
6	338.71	3.66	0.00	HOM-3→LUM	329.68	3.76	0.02	HOM-2→LUM HOM→LUM+1 HOM-1→LUM+3 HOM→LUM+4

A23: Electronic Excitation Parameters [wavelengths (λ), Oscillator Strength (*f*), Excitation Energies (E_{ex}) and the Transitions] for 10-MP*m*SB(*p*-CH=CH_2) with TD-DFT/B3LYP in vacuum and THF (ε= 7.58)

Number	λ(nm)	E_{ex}(eV)	O.S. *(f)*	Assignment	λ(nm)	E_{ex}(eV)	O.S. *(f)*	Assignment
			VACUUM				**THF**	
1	393.08	3.15	0.06	HOM-1→LUM HOM→LUM	**380.70**	**3.26**	**0.16**	**HOM-1→LUM** HOM→LUM
2	**366.32**	**3.38**	**0.11**	HOM-1→LUM HOM→LUM	370.91	3.34	0.03	HOM-1→LUM HOM→LUM
3	308.05	4.02	0.02	HOM-2→LUM HOM-1→LUM+2 HOM→LUM+1 HOM→LUM+2 HOM→LUM+3	310.03	3.99	0.01	HOM-2→LUM HOM→LUM+1 HOM→LUM+2 HOM→LUM+3
4	291.38	4.26	0.08	HOM-2→LUM HOM→LUM+1	307.62	4.03	0.00	HOM-2→LUM+1 HOM→LUM+1
5	287.48	4.31	0.03	HOM-2→LUM HOM→LUM+1 HOM→LUM+3	288.51	4.29	0.05	HOM→LUM+2 HOM→LUM+3
6	**285.83**	**4.34**	**0.11**	**HOM-1→LUM+2** **HOM→LUM+3**	**283.09**	**4.38**	**0.71**	**HOM-2→LUM** **HOM-1→LUM+1** **HOM→LUM+5**

A24: Electronic Excitation Parameters [wavelengths (λ), Oscillator Strength (*f*), Excitation Energies (E_{ex}) and the Transitions] for 10-MP*m*SB(*p*-CH=CH_2) with TD-DFT/BLYP in vacuum and THF (ε= 7.58)

Number	λ(nm)	E_{ex}(eV)	O.S. *(f)*	Assignment	λ(nm)	E_{ex}(eV)	O.S. *(f)*	Assignment
			VACUUM				**THF**	
1	500.02	2.48	0.04	HOM-1→LUM	**474.15**	**2.61**	**0.12**	**HOM-1→LUM**
				HOM→LUM				HOM→LUM
2	**454.49**	**2.73**	**0.93**	**HOM-1→LUM**	459.44	2.69	0.03	HOM-1→LUM
				HOM→LUM				HOM→LUM
3	378.26	3.28	0.011	HOM-1→LUM+1	415.96	2.98	0.00	HOM→LUM+1
				HOM→LUM+1				
				HOM→LUM+2				
4	376.13	3.29	0.00	HOM-1→LUM+1	367.87	3.37	0.01	HOM-2→LUM
				HOM→LUM+2				HOM→LUM+2
5	**367.18**	**3.38**	**0.19**	**HOM-1→LUM+3**	**347.13**	**3.57**	**0.17**	**HOM-2→LUM**
				HOM→LUM+3				**HOM→LUM+2**
								HOM→LUM+3
6	359.20	3.45	0.01	HOM-2→LUM	344.88	3.59	0.01	HOM-1→LUM+2
				HOM-1→LUM+1				
				H-1→L+2				
				HOM→LUM+2				

A25: Electronic Excitation Parameters [wavelengths (λ), Oscillator Strength (*f*), Excitation Energies (E_{ex}) and the Transitions] for 10-MP*m*SB(*m*-NO_2) with TD-DFT/B3LYP in vacuum and THF (ε= 7.58)

Number	λ(nm)	E_{ex}(eV)	O.S. *(f)*	Assignment	λ(nm)	E_{ex}(eV)	O.S. *(f)*	Assignment
			VACUUM				**THF**	
1	420.12	2.95	0.02	HOM-1→LUM HOM→LUM	519.18	2.39	0.00	HOM→LUM
2	393.21	3.15	0.05	HOM-1→LUM HOM→LUM	382.83	3.24	0.03	HOM-1→LUM
3	**360.34**	**3.44**	**0.45**	**HOM→LUM+1** **HOM→LUM+2**	**375.71**	**3.29**	**0.19**	**HOM+1→LUM+1**
4	340.55	3.64	0.00	HOM-1→LUM+1 HOM→LUM+2	358.86	3.45	0.02	HOM-2→LUM
5	324.11	3.83	0.00	HOM-1→LUM+3 HOM→LUM+3	333.67	3.72	0.02	HOM-2→LUM+1 HOM-1→LUM+1
6	300.21	4.13	0.01	HOM-2→LUM HOM-1→LUM+1 HOM-1→LUM+2 HOM→LUM+2	327.01	3.79	0.00	HOM-5→LUM

A26: Electronic Excitation Parameters [wavelengths (λ), Oscillator Strength (*f*), Excitation Energies (E_{ex}) and the Transitions] for 10-MP*m*SB(*m*-NO_2) with TD-DFT/BLYP in vacuum and THF (ε= 7.58)

Number	λ(nm)	E_{ex}(eV)	O.S. *(f)*	Assignment	λ(nm)	E_{ex}(eV)	O.S. *(f)*	Assignment
			VACUUM				**THF**	
1	691.88	1.79	0.00	HOM→LUM	923.64	1.34	0.00	HOM→LUM
2	474.57	2.59	0.01	HOM-2→LUM HOM-1→LUM	546.14	2.27	0.01	HOM-2→LUM HOM-1→LUM
3	**467.79**	**2.65**	**0.12**	**HOM→LUM+1**	519.76	2.39	0.01	HOM-2→LUM HOM-1→LUM
4	447.25	2.77	0.01	HOM-2→LUM HOM-1→LUM	**462.21**	**2.68**	**0.16**	**HOM-2→LUM+1** **HOM→LUM+1**
5	410.23	3.02	0.03	HOM-1→LUM+1	419.64	2.95	0.00	HOM-3→LUM
6	373.20	3.32	0.00	HOM-4→LUM HOM-3→LUM	391.49	3.17	0.02	HOM-1→LUM+1

A27: Electronic Excitation Parameters [wavelengths (λ), Oscillator Strength (*f*), Excitation Energies (E_{ex}) and the Transitions] for 10-MP*m*SB(*m*-CN) with TD-DFT/B3LYP in vacuum and THF (ε= 7.58)

Number	λ(nm)	E_{ex}(eV)	O.S. *(f)*	Assignment	λ(nm)	E_{ex}(eV)	O.S. *(f)*	Assignment
			VACUUM				**THF**	
1	**377.48**	**3.28**	**0.16**	**HOM→LUM**	**377.22**	**3.29**	**0.17**	**HOM→LUM**
2	347.68	3.57	0.03	HOM-1→LUM	355.94	3.48	0.03	HOM→LUM+1
3	326.86	3.79	0.01	HOM→LUM+1	336.16	3.69	0.01	HOM-1→LUM HOM-1→LUM+1
4	311.69	3.98	0.01	HOM-2→LUM HOM→LUM+1 HOM→LUM+2	313.50	3.95	0.01	HOM-2→LUM HOM→LUM+2
5	286.36	4.33	0.08	HOM-2→LUM HOM-1→LUM+1 HOM→LUM+2 HOM→LUM+3	**287.78**	**4.31**	**0.17**	**HOM-2→LUM** **HOM-1→LUM+1** **HOM→LUM+2** **HOM→LUM+3**
6	**284.03**	**4.37**	**0.28**	**HOM-2→LUM** **HOM-1→LUM+1** **HOM→LUM+3**	**285.70**	**4.34**	**0.11**	**HOM-1→LUM+1** **HOM→LUM+3**

A28: Electronic Excitation Parameters [wavelengths (λ), Oscillator Strength (*f*), Excitation Energies (E_{ex}) and the Transitions] for 10-MP*m*SB(*m*-CN) with TD-DFT/BLYP in vacuum and THF (ε= 7.58)

Number	λ(nm)	E_{ex}(eV)	O.S. *(f)*	Assignment	λ(nm)	E_{ex}(eV)	O.S. *(f)*	Assignment
			VACUUM				**THF**	
1	**471.90**	**2.63**	**0.11**	**HOM→LUM**	503.42	2.46	0.01	HOM→LUM
				HOM→LUM+1				HOM→LUM+2
2	426.39	2.91	0.01	HOM→LUM+1	**456.58**	**2.72**	**0.14**	**HOM-2→LUM**
								HOM→LUM
								HOM→LUM+1
3	414.88	2.99	0.03	HOM-1→LUM	394.76	3.14	0.00	HOM-1→LUM
								HOM-1→LUM+1
4	367.07	3.38	0.01	HOM-2→LUM	**369.51**	**3.36**	**0.22**	**HOM-1→LUM**
				HOM→LUM+2				**HOM-1→LUM+1**
								HOM→LUM+2
5	**347.85**	**3.56**	**0.16**	**HOM-2→LUM**	360.70	3.44	0.017	HOM-2→LUM+1
				HOM→LUM+2				HOM→LUM+2
6	336.42	3.69	0.01	HOM-3→LUM	352.80	3.51	0.00	HOM→LUM+3
				HOM-1→LUM+1				HOM→LUM+4
				HOM-1→LUM+2				

A29: Electronic Excitation Parameters [wavelengths (λ), Oscillator Strength (*f*), Excitation Energies (E_{ex}) and the Transitions] for 10-MP*m*SB(*m*-CHO) with TD-DFT/B3LYP in vacuum and THF (ε= 7.58)

Number	λ(nm)	E_{ex}(eV)	O.S. *(f)*	Assignment	λ(nm)	E_{ex}(eV)	O.S. *(f)*	Assignment
			VACUUM				**THF**	
1	**379.67**	**3.27**	**0.16**	**HOM→LUM** **HOM→LUM+1**	389.24	3.19	0.07	HOM→LUM
2	360.21	3.44	0.00	HOM→LUM HOM→LUM+1	**376.54**	**3.29**	**0.11**	**H→LUM+1**
3	350.72	3.54	0.01	HOM-1→LUM HOM-1→LUM+1 HOM→LUM+1	343.45	3.61	0.00	HOM-1→LUM HOM-1→LUM+1
4	333.40	3.72	0.00	HOM-3→LUM HOM-3→LUM+1	328.31	3.78	0.00	HOM-4→LUM HOM-3→LUM
5	308.57	4.02	0.05	HOM-1→LUM HOM-1→LUM+1	312.22	3.97	0.06	HOM-1→LUM HOM-1→LUM+1
6	306.92	4.04	0.01	HOM-2→LUM HOM-2→LUM+1 HOM→LUM+2 HOM→LUM+3	307.89	4.03	0.00	HOM-2→LUM HOM-2→LUM+1 HOM→LUM+2 HOM→LUM+3

A30: Electronic Excitation Parameters [wavelengths (λ), Oscillator Strength (*f*), Excitation Energies (E_{ex}) and the Transitions] for 10-MP*m*SB(*m*-CHO) with TD-DFT/BLYP in vacuum and THF (ε= 7.58)

Number	λ(nm)	E_{ex}(eV)	O.S. *(f)*	Assignment	λ(nm)	E_{ex}(eV)	O.S. *(f)*	Assignment
			VACUUM				**THF**	
1	521.60	2.38	0.02	HOM→LUM HOM→LUM+1	586.27	2.11	0.01	HOM→LUM
2	**463.64**	**2.67**	**0.10**	**HOM→LUM** **HOM→LUM+1**	**467.07**	**2.65**	**0.12**	**HOM→LUM+1**
3	423.52	2.93	0.00	HOM-1→LUM HOM-1→LUM+1	407.32	3.04	0.00	HOM-1→LUM HOM-1→LUM+1
4	399.56	3.10	0.01	HOM-2→LUM HOM-2→LUM+1	404.34	3.07	0.00	HOM-2→LUM HOM-1→LUM+1
5	386.83	3.21	0.03	HOM-1→LUM+1 HOM-1→LUM HOM-1→LUM+1	390.19	3.18	0.03	HOM-2→LUM HOM-1→LUM HOM-1→LUM+1
6	374.92	3.31	0.01	HOM-3→LUM HOM-3→LUM+1 HOM-2→LUM+1	371.57	3.34	0.01	HOM-3→LUM HOM-3→LUM+1

A31: Electronic Excitation Parameters [wavelengths (λ), Oscillator Strength (*f*), Excitation Energies (E_{ex}) and the Transitions] for MMP (*A*-$COCH_3$, D-SCH_3) with TD-DFT/B3LYP (vacuum) and THF (ε= 7.58)

Number	λ(nm)	E_{ex}(eV)	O.S. *(f)*	Assignment	λ(nm)	E_{ex}(eV)	O.S. *(f)*	Assignment
			VACUUM				**THF**	
1	**343.62**	**3.61**	**0.65**	**HOM→LUM** **HOM+2→LUM**	**349.45**	**3.55**	**1.16**	**HOM+2→LUM**
2	**340.94**	**3.64**	**0.51**	**HOM→LUM**	334.76	3.70	0.01	HOM-2→LUM
3	314.97	3.94	0.04	HOM+1→LUM HOM+2→LUM	315.67	3.93	0.03	HOM+1→LUM
4	280.81	4.42	0.01	HOM-1→LUM HOM+2→LUM+3	279.43	4.44	0.01	HOM-1→LUM HOM+1→LUM+3
5	275.35	4.50	0.00	HOM-2→LUM	278.67	4.45	0.01	HOM-2→LUM
6	**263.79**	**4.70**	**0.12**	**HOM-4→LUM** **HOM+2→LUM+1**	**269.29**	**4.60**	**0.12**	**HOM-4→LUM** **HOM-2→LUM** **HOM+2→LUM+2**

A32: Electronic Excitation Parameters [wavelengths (λ), Oscillator Strength (*f*), Excitation Energies (E_{ex}) and the Transitions] for MMP (*A*-$COCH_3$, D-SCH_3) with TD-DFT/BLYP (vacuum) and THF (ε= 7.58)

Number	λ(nm)	E_{ex}(eV)	O.S. *(f)*	Assignment	λ(nm)	E_{ex}(eV)	O.S. *(f)*	Assignment
			VACUUM				**THF**	
1	471.93	2.63	0.00	HOM→LUM	445.99	2.78	0.00	HOM+1→LUM
2	**411.81**	**3.01**	**0.68**	**HOM+1→LUM**	**436.54**	**2.84**	**0.53**	**HOM→LUM**
								HOM+2→LUM
3	**382.15**	**3.24**	**0.25**	**HOM→LUM**	**376.04**	**3.29**	**0.46**	**HOM-3→LUM**
				HOM+2→LUM				**HOM+2→LUM**
				HOM+2→LUM+1				**HOM+2→LUM+1**
4	344.31	3.60	0.01	HOM+1→LUM+1	334.20	3.71	0.01	HOM+1→LUM+1
5	334.62	3.71	0.01	HOM-2→LUM	330.04	3.76	0.03	HOM-1→LUM
				HOM+2→LUM+3				
6	319.58	3.88	0.06	HOM-4→LUM	327.68	3.78	0.01	HOM-2→LUM
				HOM+2→LUM+1				HOM+2→LUM+2
				HOM+2→LUM+2				

A33: Electronic Excitation Parameters [wavelengths (λ), Oscillator Strength (*f*), Excitation Energies (E_{ex}) and the Transitions] for MMP (*A*-NO_2, D-SCH_3) with TD-DFT/B3LYP in vacuum and THF (ε= 7.58)

Number	λ(nm)	E_{ex}(eV)	O.S. *(f)*	Assignment	λ(nm)	E_{ex}(eV)	O.S. *(f)*	Assignment
			VACUUM				**THF**	
1	**369.57**	**3.35**	**0.79**	**HOM→LUM**	**408.17**	**3.04**	**0.55**	**HOM→LUM**
2	332.18	3.73	0.05	HOM-3→LUM HOM-1→LUM	**335.05**	**3.70**	**0.43**	**HOM-1→LUM**
3	**324.17**	**3.82**	**0.21**	**HOM-4→LUM** **HOM-3→LUM+1** **HOM-1→LUM** **HOM-1→LUM+1**	**328.21**	**3.78**	**0.17**	**HOM→LUM+1**
4	290.07	4.27	0.00	HOM-6→LUM	297.19	4.17	0.00	HOM-2→LUM HOM→LUM+3
5	**285.90**	**4.34**	**0.17**	**HOM-1→LUM** **HOM→LUM+1**	**296.01**	**4.19**	**0.11**	**HOM-3→LUM**
6	284.33	4.3606	0.0377	HOM-3→LUM HOM→LUM+1 HOM-1→LUM+2	**293.28**	**4.23**	**0.12**	**HOM-3→LUM** **HOM-1→LUM** **HOM→LUM+1**

A34: Electronic Excitation Parameters [wavelengths (λ), Oscillator Strength (*f*), Excitation Energies (E_{ex}) and the Transitions] for MMP (*A*-NO_2, D-SCH_3) with TD-DFT/BLYP in vacuum and THF (ε= 7.58)

Number	λ(nm)	E_{ex}(eV)	O.S. *(f)*	Assignment	λ(nm)	E_{ex}(eV)	O.S. *(f)*	Assignment
			VACUUM				**THF**	
1	**495.55**	**2.50**	**0.27**	**HOM→LUM** **HOM+1→LUM**	**579.20**	**2.14**	**0.23**	**HOM→LUM** **HOM+1→LUM**
2	407.98	3.04	0.06	HOM-1→LUM HOM→LUM	**408.59**	**3.03**	**0.53**	**HOM-4→LUM** **HOM-1→LUM** **HOM→LUM**
3	**389.70**	**3.18**	**0.55**	**HOM-4→LUM** **HOM→LUM**	392.18	3.16	0.00	HOM-2→LUM
4	347.90	3.56	0.00	HOM-3→LUM	**388.88**	**3.19**	**0.13**	**HOM-1→LUM**
5	**345.42**	**3.59**	**0.13**	**HOM-4→LUM** **HOM→LUM** **HOM+1→LUM+1**	**357.06**	**3.47**	**0.48**	**HOM-4→LUM** **HOM+1→LUM+1**
6	342.55	3.62	0.05	HOM→LUM HOM+1→LUM+1	349.05	3.55	0.00	HOM-7→LUM HOM-3→LUM HOM→LUM HOM+1→LUM+1

A35: Electronic Excitation Parameters [wavelengths (λ), Oscillator Strength (*f*), Excitation Energies (E_{ex}) and the Transitions] for MMP (*A*-NO_2, D-NH_3) with TD-DFT/B3LYP in vacuum and THF (ε= 7.58)

Number	λ(nm)	E_{ex}(eV)	O.S. *(f)*	Assignment	λ(nm)	E_{ex}(eV)	O.S. *(f)*	Assignment
			VACUUM				**THF**	
1	**368.90**	**3.36**	**0.73**	**HOM→LUM**	440.07	2.82	0.00	HOM→LUM
2	331.10	3.74	0.04	HOM-4→LUM	325.74	3.81	0.00	HOM-5→LUM
				HOM-1→LUM				HOM-4→LUM
3	**319.72**	**3.88**	**0.26**	**HOM-5→LUM**	**317.89**	**3.90**	**1.14**	**HOM-1→LUM**
				HOM-1→LUM				**HOM→LUM+1**
				HOM-1→LUM+1				
4	289.00	4.29	0.00	HOM-6→LUM	297.28	4.17	0.00	HOM-1→LUM+1
5	283.70	4.37	0.02	HOM-3→LUM	286.50	4.33	0.00	HOM-2→LUM
				HOM→LUM+2				
6	277.48	4.47	0.01	HOM-2→LUM	284.97	4.35	0.01	HOM-3→LUM
				HOM-2→LUM+1				HOM-1→LUM+2
				HOM-2→LUM+3				

A36: Electronic Excitation Parameters [wavelengths (λ), Oscillator Strength (*f*), Excitation Energies (E_{ex}) and the Transitions] for MMP (*A*-NO_2, D-NH_2) with TD-DFT/BLYP in vacuum and THF (ε= 7.58)

Number	λ(nm)	E_{ex}(eV)	O.S. *(f)*	Assignment	λ(nm)	E_{ex}(eV)	O.S. *(f)*	Assignment
			VACUUM				**THF**	
1	499.25	2.48	0.00	HOM→LUM	696.36	1.78	0.00	HOM→LUM
2	370.58	3.35	0.00	HOM-2→LUM	396.97	3.12	0.00	HOM-2→LUM
3	364.07	3.41	0.02	HOM-1→LUM+1	**378.22**	**3.28**	**0.79**	**HOM-8→LUM** **HOM-1→LUM** **HOM→LUM+1**
4	**360.14**	**3.44**	**0.64**	**HOM-1→LUM**	371.27	3.34	0.00	HOM-3→LUM
5	336.17	3.69	0.06	HOM-2→LUM+1	347.31	3.57	0.00	HOM→LUM+1 HOM→LUM+2
6	318.26	3.89	0.00	HOM-5→LUM	344.62	3.59	0.00	HOM-1→LUM+1

A37: Electronic Excitation Parameters [wavelengths (λ), Oscillator Strength (*f*), Excitation Energies (E_{ex}) and the Transitions] for MMP (*A*-CH=C(CN)COOH, D-SCH_3) with TD-DFT/B3LYP in vacuum and THF (ε= 7.58)

Number	λ(nm)	E_{ex}(eV)	O.S. *(f)*	Assignment	λ(nm)	E_{ex}(eV)	O.S. *(f)*	Assignment
			VACUUM				**THF**	
1	**396.69**	**3.13**	**0.96**	**HOM→LUM**	**421.11**	**2.95**	**0.89**	**HOM→LUM**
2	**342.02**	**3.63**	**0.52**	**HOM-1→LUM**	**343.97**	**3.61**	**0.50**	**HOM-2→LUM**
3	303.74	4.08	0.01	HOM-6→LUM HOM-3→LUM	304.22	4.08	0.00	HOM-1→LUM HOM→LUM+1
4	295.77	4.19	0.05	HOM-1→LUM HOM→LUM	295.22	4.20	0.00	HOM-3→LUM
5	289.42	4.28	0.01	HOM→LUM+2	288.21	4.30	0.00	HOM→LUM+1 HOM→LUM+2
6	287.87	4.31	0.07	HOM-1→LUM HOM+1→LUM+3	295.00	4.21	0.00	HOM-1→LUM+1

A38: Electronic Excitation Parameters [wavelengths (λ), Oscillator Strength (*f*), Excitation Energies (E_{ex}) and the Transitions] for MMP (*A*-CH=C(CN)COOH, D-SCH_3) with TD-DFT/BLYP in vacuum and THF (ε= 7.58)

Number	λ(nm)	E_{ex}(eV)	O.S. *(f)*	Assignment	λ(nm)	E_{ex}(eV)	O.S. *(f)*	Assignment
			VACUUM				**THF**	
1	**525.21**	**2.36**	**0.37**	**HOM→LUM**	**576.83**	**2.15**	**0.34**	**HOM+1→LUM**
2	**418.03**	**2.97**	**0.81**	**HOM→LUM**	**418.16**	**2.97**	**1.05**	**HOM-4→LUM**
								HOM-1→LUM
								HOM→LUM
								HOM-4→LUM+1
3	**399.17**	**3.11**	**0.16**	**HOM-1→LUM**	389.26	3.19	0.00	HOM-2→LUM
4	371.38	3.34	0.02	HOM-5→LUM	374.75	3.31	0.05	HOM-5→LUM
				HOM-3→LUM				HOM-3→LUM
				HOM-1→LUM+1				HOM-1→LUM
								HOM→LUM+1
5	360.51	3.44	0.00	HOM-3→LUM	363.67	3.41	0.17	HOM-6→LUM
								HOM-1→LUM+1
								HOM→LUM+1
6	**345.03**	**3.59**	**0.22**	**HOM→LUM**	**353.12**	**3.51**	**0.19**	**HOM-6→LUM**
				HOM→LUM+1				**HOM-4→LUM**
				HOM+1→LUM+1				**HOM-1→LUM+1**

A39: Electronic Excitation Parameters [wavelengths (λ), Oscillator Strength (*f*), Excitation Energies (E_{ex}) and the Transitions] for MMP (*A*-CH=C(CN)COOH, D-NH_2) with TD-DFT/B3LYP in vacuum and THF (ε= 7.58)

Number	λ(nm)	E_{ex}(eV)	O.S. *(f)*	Assignment	λ(nm)	E_{ex}(eV)	O.S. *(f)*	Assignment
			VACUUM				**THF**	
1	**399.63**	**3.10**	**0.92**	**HOM→LUM**	**451.77**	**2.74**	**0.78**	**HOM→LUM**
2	**337.63**	**3.67**	**0.52**	**HOM-1→LUM**	**348.49**	**3.56**	**0.91**	**HOM-1→LUM**
				HOM→LUM+1				**HOM→LUM+1**
3	302.05	4.10	0.01	HOM-3→LUM	303.22	4.09	0.00	HOM-2→LUM
4	289.36	4.28	0.00	HOM-4→LUM	301.95	4.11	0.04	HOM-3→LUM
				HOM-1→LUM				
				HOM→LUM+2				
5	288.85	4.29	0.09	HOM-1→LUM+1	**295.00**	**4.20**	**0.36**	**HOM-4→LUM**
				HOM→LUM+1				**HOM-1→LUM**
								HOM→LUM+1
6	285.51	4.34	0.00	HOM-4→LUM	287.00	4.32	0.02	HOM-4→LUM
				HOM→LUM+3				
				HOM+1→LUM+1				
				HOM+1→LUM+4				

A40: Electronic Excitation Parameters [wavelengths (λ), Oscillator Strength (*f*), Excitation Energies (E_{ex}) and the Transitions] for MMP (*A*-CH=C(CN)COOH, D-NH_2) with TD-DFT/BLYP in vacuum and THF (ε= 7.58)

Number	λ(nm)	E_{ex}(eV)	O.S. *(f)*	Assignment	λ(nm)	E_{ex}(eV)	O.S. *(f)*	Assignment
			VACUUM				**THF**	
1	**516.50**	**2.40**	**0.39**	**HOM+1→LUM**	**598.08**	**2.07**	**0.42**	**HOM+1→LUM**
2	**411.29**	**3.01**	**0.78**	**HOM→LUM**	**419.82**	**2.95**	**0.91**	**HOM→LUM**
				HOM+1→LUM				**HOM+1→LUM**
				HOM+1→LUM+1				**HOM+1→LUM+1**
3	393.74	3.15	0.04	HOM-1→LUM	394.51	3.14	0.00	HOM-1→LUM
4	**364.21**	**3.40**	**0.18**	**HOM-2→LUM**	**372.08**	**3.33**	**0.20**	**HOM-2→LUM**
5	359.79	3.45	0.00	HOM-3→LUM	**360.21**	**3.44**	**0.49**	**HOM-4→LUM**
								HOM-3→LUM
6	339.05	3.66	0.01	HOM-4→LUM	349.55	3.55	0.08	HOM-4→LUM
				HOM+1→LUM+2				HOM-2→LUM